NADC-77-107-30

AD A060206

DDC FILE COPY

LIFT SYSTEM INDUCED AERODYNAMICS OF V/STOL AIRCRAFT IN A MOVING DECK ENVIRONMENT

VOLUME I TECHNICAL DISCUSSION

McDonnell Aircraft Company
McDonnell Douglas Corporation
P.O. Box 516
St. Louis MO. 63166

DDC
OCT 23 1978
F

29 September 1978

Final Report for Period 30 September 1977 - 29 September 1978

Approved for Public Release Distribution Unlimited

Prepared for
NAVAL AIR DEVELOPMENT CENTER
WARMINSTER, PENNSYLVANIA 18974

78 10 12 00

SECURITY CLASSIFICATION OF THIS PAGE (When Data Entered)

REPORT DOCUMENTATION PAGE

READ INSTRUCTIONS BEFORE COMPLETING FORM

1. REPORT NUMBER
NADC-77-107-30

2. GOVT ACCESSION NO.

3. RECIPIENT'S CATALOG NUMBER

4. TITLE (and Subtitle)
Lift System Induced Aerodynamics of V/STOL Aircraft In a Moving Deck Environment
Volume I - Technical Discussion

5. TYPE OF REPORT & PERIOD COVERED
Final Technical Report
30 Sep 1977 - 29 Sep 1978

6. PERFORMING ORG. REPORT NUMBER
N/A

7. AUTHOR(s)
James H. Kamman
Charles L. Hall

8. CONTRACT OR GRANT NUMBER(s)
N62269-77-C-0365

9. PERFORMING ORGANIZATION NAME AND ADDRESS
McDonnell Aircraft Company
P.O. Box 516
St. Louis, Missouri 63166

10. PROGRAM ELEMENT, PROJECT, TASK AREA & WORK UNIT NUMBERS

11. CONTROLLING OFFICE NAME AND ADDRESS
Naval Air Development Center
Warminster, Pennsylvania 18974

12. REPORT DATE
29 September 1978

13. NUMBER OF PAGES
174

14. MONITORING AGENCY NAME & ADDRESS (if different from Controlling Office)

15. SECURITY CLASS (of this report)
Unclassified

15a. DECLASSIFICATION/DOWNGRADING SCHEDULE

16. DISTRIBUTION STATEMENT (of this Report)
Unlimited

17. DISTRIBUTION STATEMENT (of the abstract entered in Block 20, if different from Report)
Unlimited

18. SUPPLEMENTARY NOTES

19. KEY WORDS (Continue on reverse side if necessary and identify by block number)
V/STOL
Ground Effects
Suckdown
Fountain Forces
Ship Motion Effects

20. ABSTRACT (Continue on reverse side if necessary and identify by block number)

The propulsive lift system induced aerodynamics of multi-jet V/STOL aircraft configurations were experimentally evaluated over a moving deck and at static hover conditions. Several model configurations representative of advanced subsonic and supersonic V/STOL aircraft were tested.

Dynamic jet-induced force and moment data were obtained for heaving, pitching, and rolling motions of a simulated seaborne landing platform over a range

DD FORM 1 JAN 73 1473 EDITION OF 1 NOV 65 IS OBSOLETE

SECURITY CLASSIFICATION OF THIS PAGE

20. (Cont'd)
of heights, amplitudes, and frequencies. Configuration effects were assessed at both static hover and deck motion conditions, including the effects of wing height, fuselage contouring, lift improvement devices, and nozzle arrangement. In addition, tests were performed to separate the effects of deck motion on the fountain impingement forces. Empirical procedures were defined to aid in predicting the dynamic jet-induced forces and moment variations with deck motion.

Configuration design and model testing guidelines for V/STOL aircraft are described. Recommendations are also made for further research to provide additional information required to develop generalized prediction procedures.

FOREWORD

An investigation was conducted for the Naval Air Development Center (NADC) by McDonnell Aircraft Company (MCAIR) to assess the propulsive lift system induced aerodynamics of V/STOL aircraft over a moving deck. The study was performed under Navy contract N62269-77-C-0365 with Mr. M. M. Walters of NADC as contract monitor. The MCAIR efforts in this program were accomplished under the direction of Mr. J. H. Kamman with Mr. C. L. Hall as principal investigator, both of the MCAIR Propulsion Department.

The authors are particularly indebted to Mr. J. D. Flood for his effort involved in the test program preparations and to Mr. K. P. Connolly for his assistance during the data reduction and report preparation. Special acknowledgements are due Mr. H. Sams, Dr. E. D. Spong, and Mr. R. E. Owen for their contributions.

This report consists of two volumes. The test program description, data analyses results, conclusions and recommendations are presented in Volume I. Appendix A, Test Run Summary, Appendix B, Static Induced Aerodynamic Data, and Appendix C, Induced Aerodynamic Data in Time and Frequency Domains are given in Volume II.

A

TABLE OF CONTENTS

SECTION		PAGE
1.	INTRODUCTION	1
2.	MODELS AND TEST FACILITY	3
	2.1 Subsonic V/STOL Models	3
	2.2 Supersonic V/STOL Model	6
	2.3 Model Instrumentation	12
	2.4 Test Facilities	23
3.	TEST PROGRAM	34
	3.1 Test Variables	34
	3.2 Test Procedures	40
4.	DATA REDUCTION AND REPEATABILITY	44
	4.1 Static Hover Data Reduction	44
	4.2 Dynamic Data Reduction	45
	4.3 Data Repeatability	46
5.	DISCUSSION OF RESULTS	50
	5.1 Static Hover Data	50
	5.1.1 Subsonic V/STOL Configuration	50
	5.1.2 Supersonic V/STOL Configuration	74
	5.2 Dynamic Deck Motion Effects	88
	5.2.1 Dynamic Jet-Induced Force and Moment Data	100
	5.2.2 Frequency Content and Phase Relationships of the Dynamic Data	118
	5.3 Empirical Prediction Procedures	130
	5.3.1 Prediction of Deck Motion Effects from Static Hover Data	134
	5.3.2 Predicton Procedures for Three Jet Subsonic Configuration	147
	5.3.3 Suggested Approach to the Development of Improved Prediction Procedures	166
6.	CONCLUSIONS AND RECOMMENDATIONS	170
	6.1 Conclusions	170
	6.2 Recommendations	172

TABLE OF CONTENTS (Continued)

Section	Page
7. REFERENCES	174
VOLUME II	
APPENDIX A - TEST RUN SUMMARY	A-1
APPENDIX B - INDUCED AERODYNAMIC DATA AT STATIC HOVER CONDITIONS . .	B-1
APPENDIX C - INDUCED AERODYNAMIC DATA IN TIME AND FREQUENCY DOMAINS FOR DYNAMIC DECK MOTION CONDITIONS.	C-1

LIST OF ILLUSTRATIONS

Figure No.		Page
2-1	Subsonic V/STOL Fully Contoured 3-D Model	4
2-2	Subsonic V/STOL 2-D Planform Model	5
2-3	Advanced Subsonic V/STOL Configuration	6
2-4	Subsonic V/STOL Model Detail Dimensions	7
2-5	Subsonic V/STOL Semi-Contoured Planform Model	8
2-6	Subsonic V/STOL 3-D Model with Lids and Pods Installed.	9
2-7	Subsonic V/STOL 3-D Model with Complex Nozzles	10
2-8	Subsonic V/STOL 3-Jet Inner Region Plate	11
2-9	Advanced Supersonic V/STOL Designs	13
2-10	Supersonic V/STOL Model Configurations	15
2-11	Supersonic V/STOL Models.	16
2-12	Supersonic V/STOL Model Detail Dimensions	20
2-13	V/STOL Model/Facility Instrumentation	21
2-14	Model Balance	22
2-15	V/STOL Jet Interaction Test Apparatus	24
2-16	Propulsion Subsystem Test Facility.	25
2-17	Control Console for Exhaust Flows in the JITA	26
2-18	Data Acquisition Console in the PSTF	27
2-19	On-Line Oscillograph Strip Chart Recorders	29
2-20	Hewlett-Packard 5451B Fourier Transform Analyzer for Dynamic Data Reduction.	30
2-21	Deck Motion Test Apparatus	31
2-22	Deck Motion Control Console	33
3-1	Test Variables.	34
3-2	Subsonic V/STOL Model Configuration Variables	36

LIST OF ILLUSTRATIONS (Continued)

Figure No.		Page
3-3	Supersonic V/STOL Model Configuration Variables	37
3-4	Configuration Summary	38
3-5	Test Program Summary.	39
3-6	Ship Motion Predictions Based on Reference 2	40
3-7	Electronic Control System	42
3-8	Sample Deck Motion Output Waveforms	43
4-1	Model Natural Resonance Frequencies	45
4-2	Dynamic Data Reduction Functions	47
4-3	Data Repeatability at Static Hover Conditions	48
4-4	Dynamic Data Repeatability	49
5-1	Subsonic V/STOL Static Height Effects	52
5-2	3-D Subsonic V/STOL Static Pitch Effects	54
5-3	3-D Subsonic V/STOL Static Roll Effects	56
5-4	Effect of Deck Size	59
5-5	Subsonic V/STOL Contouring Effects	60
5-6	Subsonic V/STOL With Lift Improvement Devices	62
5-7	Subsonic V/STOL Roll Effects on Induced Lift with LID's Installed	63
5-8	Subsonic V/STOL Roll Effects on Induced Rolling Moment With LID's Installed	65
5-9	Subsonic V/STOL With Wing Pods	67
5-10	Subsonic V/STOL Wing Height Effects	69
5-11	Subsonic V/STOL Nozzle Arrangement Effects	70
5-12	Subsonic V/STOL Complex Nozzle Effects	71
5-13	Subsonic V/STOL Nozzle Pressure Ratio Effects	72

LIST OF ILLUSTRATIONS (Continued)

Figure No.		Page
5-14	Subsonic V/STOL Thrust Bias Effects	73
5-15	3 Jet Supersonic V/STOL Static Height Effects	75
5-16	3 Jet Supersonic V/STOL Static Pitch Effects	76
5-17	3 Jet Supersonic V/STOL Static Roll Effects	78
5-18	Supersonic V/STOL Contouring Effects	81
5-19	3 Jet Supersonic V/STOL Thrust Bias Effects	82
5-20	Supersonic V/STOL Number of Nozzles Effect	83
5-21	Supersonic V/STOL With Lift Improvement Devices	84
5-22	Supersonic V/STOL Roll Effects on Induced Lift with LID's Installed	85
5-23	Supersonic V/STOL Roll Effects on Induced Rolling Moment With LID's Installed	86
5-24	Supersonic V/STOL Wing Height Effects	87
5-25	4 Jet Supersonic V/STOL Static Height Effects	89
5-26	4 Jet Supersonic V/STOL Static Pitch Effects	90
5-27	4 Jet Supersonic V/STOL Static Roll Effects	92
5-28	2 Jet Supersonic V/STOL Static Height Effects	94
5-29	2 Jet Supersonic V/STOL Thrust Bias Effects	95
5-30	2 Jet Supersonic V/STOL Static Pitch Effects	96
5-31	2 Jet Supersonic V/STOL Static Roll Effects	98
5-32	Induced Lift on Fully-Contoured Subsonic V/STOL For Heaving Deck	101
5-33	Induced Lift on Inner Region Plate For Heaving Deck Motion	103
5-34	Subsonic V/STOL Heave Frequency Effects	104
5-35	Subsonic V/STOL Heave Amplitude Effects	105

LIST OF ILLUSTRATIONS (Continued)

Figure No.		Page
5-36	Subsonic V/STOL Induced Lift For Rolling Deck	106
5-37	Subsonic V/STOL Induced Rolling Moment For Rolling Deck	107
5-38	Subsonic V/STOL Height Effects For Rolling Deck . . .	108
5-39	Subsonic V/STOL Induced Lift For Pitching Deck	110
5-40	Subsonic V/STOL Induced Pitching Moment For Pitching Deck	111
5-41	Subsonic V/STOL Height Effects For Pitching Deck . . .	112
5-42	Subsonic V/STOL Induced Lift For Heaving and Rolling Deck	114
5-43	Subsonic V/STOL Induced Lift For Heaving and Pitching Deck	115
5-44	Subsonic V/STOL Induced Lift For Pitching and Rolling Deck	116
5-45	Subsonic V/STOL Induced Lift For Heaving, Pitching and Rolling Deck	117
5-46	Subsonic V/STOL Induced Lift For Dynamic Vertical Takeoff and Landing Simulation	119
5-47	Planform Configuration Effects For Heaving Deck . . .	120
5-48	Subsonic V/STOL LID Effects For Heaving Deck	121
5-49	Subsonic V/STOL Fuselage Contouring Effects For Heaving Deck	122
5-50	Subsonic V/STOL Induced Lift PSD Response to Heaving Deck	124
5-51	Subsonic V/STOL Induced Lift PSD Response with Frequency Variations	125
5-52	Subsonic V/STOL Induced Lift PSD Response With Amplitude Variations	127
5-53	Response Phase Angle With Height Variations For Heaving Deck	129

LIST OF ILLUSTRATIONS (Continued)

Figure No.		Page
5-54	Response Phase Angle With Height Variations for Rolling Deck	131
5-55	Amplitude and Phase Angle Frequency Response to Heaving Deck	132
5-56	Amplitude and Phase Angle Frequency Response to Rolling Deck	133
5-57	Subsonic V/STOL Static To Dynamic Data Comparison In Time Domain For Heaving Deck	136
5-58	Subsonic V/STOL Static to Dynamic Data Comparison In Physical Domain For Heaving Deck	137
5-59	Subsonic V/STOL Static To Dynamic Induced Lift Data Comparison For Pitching Deck	138
5-60	Subsonic V/STOL Static To Dynamic Induced Pitching Moment Data Comparison For Pitching Deck	139
5-61	Subsonic V/STOL Static To Dynamic Induced Lift and Induced Rolling Moment Comparison For Rolling Deck	140
5-62	Supersonic V/STOL Static to Dynamic Induced Lift Data Comparison For Heaving Deck	142
5-63	Supersonic V/STOL Static To Dynamic Induced Lift Data Comparison For Pitching Deck	143
5-64	Supersonic V/STOL Static To Dynamic Induced Pitching Moment Data Comparison For Pitching Deck	144
5-65	Supersonic V/STOL Static To Dynamic Induced Lift and Induced Rolling Moment Comparison For Rolling Deck	145
5-66	Subsonic V/STOL Static To Dynamic Induced Lift and Induced Rolling Moment Data Comparison For Heaving and Rolling Deck	146
5-67	Subsonic V/STOL Static To Dynamic Induced Lift Data Comparison For Pitching and Rolling Deck	148
5-68	Subsonic V/STOL Static To Dynamic Induced Lift Data Comparison For Pitching and Rolling Deck Out of Phase	149
5-69	Fourier Series Fit of Induced Lift Variations For Heaving Deck	151

LIST OF ILLUSTRATIONS (Continued)

Figure No.		Page
5-70	Fourier Series Fit of Induced Lift Variations For Pitching Deck	153
5-71	Fourier Series Fit of Induced Pitching Moment Variations for Pitching Deck	155
5-72	Fourier Series Fit of Induced Lift Variations For Rolling Deck	157
5-73	Fourier Series Fit of Induced Rolling Moment Variations For Rolling Deck	159
5-74	Fourier Series Fit of Induced Lift Variations For Heaving Deck at Various Frequencies	161
5-75	Induced Lift Variation For Heaving Deck Based on Inner Region Model	167
5-76	Induced Lift Variation for Rolling Deck Based on Inner Region Model	168

LIST OF ABBREVIATIONS, ACRONYMS, AND SYMBOLS

AC	Auto Correlation statistical function
A_n	Fourier series coefficient of cosine function for complex periodic data
A_T	Total combined exit area of all nozzles
b	Wing span, inches or cm.
B_n	Fourier series coefficient of sine function for complex periodic data
c	Mean aerodynamic chord length, inches or cm.
CC	Cross correlation statistical function
CFAS	Non-dimensionalized induced axial force coefficient based on static gross thrust
CFNS	Non-dimensionalized induced lift coefficient based on static gross thrust
CFYS	Non-dimensionalized induced side force coefficient based on static gross thrust
CPMS	Non-dimensionalized induced pitching moment coefficient based on static gross thrust
CRMS	Non-dimensionalized induced rolling moment coefficient based on static gross thrust
CSD	Cross power spectral density statistical function
CYMS	Non-dimensionalized induced yawing moment coefficient based on static gross thrust
D_j	Exit diameter of each nozzle, inches or cm.
D_{je}	Equivalent nozzle exit diameter based on the total areas of all nozzles, inches or cm
D_{Ref}	Nozzle reference dimension = 4.024 inches (10.221 cm)
f	Frequency, Hz
FA	Induced axial force
F_G	Total static gross thrust of the nozzle exhaust flow
$F_{G_{FRONT}}/F_{G_{TOTAL}}$	Tarust bias ratio

ΔFY	Induced side force
FS	Full scale
H	Model nozzle height above the deck, or the distance of the nozzle exit plane above the neutral point of the moving deck, inches or cm
h	Heaving amplitude, inches or cm
Hz	Hertz, cycles per second
JITA	Jet Interaction Test Apparatus
ΔL	Induced lift force acting on the airframe
MS	Model scale
NPR	Nozzle pressure ratio, P_{t_j}/P_{amb}
P_a	Ambient pressure
ΔPM	Induced pitching moment, in-lb_f or kg-cm
PSD	Power Spectral Density statistical function
PSTF	Propulsion Subsystem Test Facility
P_{t_j}	Nozzle exhaust total pressure, lb_f/in^2 or kg/m^2
ΔRM	Induced rolling moment, in-lb_f or kg-cm
R_x	Auto correlation statistical function
R_{xy}	Cross correlation statistical function
ΔYM	Induced yawing moment, in-lb_f or kg-cm
t	Time, seconds
T	Period of one cycle, seconds
T_{T_j}	Nozzle total temperature, °R
α	Deck pitch angle, degrees
γ	Deck roll angle, degrees
τ	Lag time, seconds
ϕ	Phase angle between pitch and roll or other combined deck motions, degrees

SUMMARY

In ground effect, the propulsive lift system induced aerodynamics experienced by V/STOL aircraft can significantly degrade the aircraft lift capability as well as the stability and control. In addition, for operations at sea, the ship motion will cause fluctuations in these induced forces and moments.

To investigate these effects, the induced aerodynamics of multi-jet V/STOL aircraft configurations were experimentally evaluated in the dynamic environment of a moving deck as well as at static hover conditions. A variety of model configurations representative of advanced subsonic and supersonic V/STOL aircraft were tested in the MCAIR Propulsion Subsystem Test Facility utilizing the Jet Interaction Test Apparatus and Deck Motion Simulator.

Dynamic effects were assessed for heaving, pitching, and rolling motions of the deck over a range of deck heights, amplitudes, and frequencies. Further, the dynamic data were analyzed statistically to determine the frequency content and phase relationships between the deck motions and the aerodynamic responses. Several configuration effects were also assessed in the test program including the effects of wing height, fuselage contouring, lift improvement devices, and nozzle arrangement. Empirical procedures were defined to aid in predicting the dynamic jet-induced forces and moments resulting from deck motion. In this effort, comparisons were made between predictions based on static hover data and the actual dynamic response data.

Significant results relating primarily to the effects of deck motion are summarized below:

- The responses of the jet-induced force and moment data to deck motion are of a complex periodic nature at the same and/or multiples of the deck motion frequency.
- The force and moment variations predicted from static hover data can differ significantly from the actual dynamic data particularly for combined motions (e.g., heave and roll).
- Simulation of the model lower surface contouring is important, particularly in the fountain impingement region.
- The induced lift resulting from fountain impingement increases as the deck heaves toward the model.
- The fountain appears to have the largest impact on the force and moment variations with deck motion.

- For a configuration with high suckdown in ground effect, an increase in lift loss occurs when the deck heaves away from the model.
- The deck motion frequency has little effect on the statistical aerodynamic response but can affect the instantaneous response characteristics.
- Properly designed LID's can significantly enhance the induced lift even at substantial deck roll angles.

Configuration design and model testing guidelines for V/STOL aircraft are described based upon the data obtained in this program. Recommendations are also made for further research to extend the empirical data base and to provide additional information required to develop generalized prediction procedures.

1. INTRODUCTION

Operation of V/STOL aircraft from ships, particularly from small non-aviation type ships, such as the DD963 class destroyer, presents problems due to the ship motion and the flowfield conditions in the landing area. In proximity to the landing area, the lift system induced aerodynamics experienced by V/STOL aircraft can significantly degrade the aircraft lift capability as well as the stability and control. The motion of the ship and the wind conditions cause fluctuations in these induced forces and moments, further complicating V/STOL aircraft take-off and recovery operations.

The majority of existing induced aerodynamic data are for static hover conditions and cannot be used to assess the effects of deck motion. Therefore, McDonnell Aircraft Company (MCAIR) conducted an investigation under contract to the Naval Air Development Center (NADC) to parametrically evaluate the jet-induced aerodynamics of typical advanced V/STOL aircraft above a moving platform as well as at static hover conditions. This investigation was performed without the added complexity introduced by wind

A parametric test program was conducted in the MCAIR Propulsion Subsystem Test Facility in February-March 1978, using both fully contoured and simple flat plate planform models representative of subsonic and supersonic V/STOL aircraft configurations. The jet-induced forces and moments acting on the airframe models were measured with a six-component force balance. The MCAIR Deck Motion Test Apparatus was used to simulate both simple one axis deck motions such as heave and complex multi-axis motions such as combined heave and roll. Simple sinusoidal deck motions were used to represent the ship motion.

Tests were performed over a range of deck motion amplitudes and frequencies, representing responses to moderate to rough sea conditions. Configuration variables included wing height, nozzle spacing and arrangement, and model surface contouring. The tests thus provide an extensive data base on jet-induced aerodynamics both for static hover conditions and for dynamic conditions with deck motion.

Following the test program, the force and moment data were analyzed to assess the effects of deck motion, to compare the dynamic and static hover data, and to evaluate the effects of the configuration variables. Statistical

analyses were used to determine the frequency content of the dynamic response data and the phase relationships between the deck motion and the measured response of the models. Parametric data plots were generated to assist in the prediction of the jet-induced forces and moments acting on typical V/STOL planforms. Empirical approaches to the prediction of the dynamic response to deck motion were also defined. In addition, guidelines relating to general V/STOL aircraft design and model testing were derived from the test results.

Descriptions of the models and the test equipment as well as the test program are provided in Sections 2 and 3. The data reduction procedures involved in computing the induced forces and moments are discussed in Section 4 for both static hover and dynamic deck motion conditions. The results are presented in Section 5 and conclusions and recommendations in Section 6. In Volume II, a summary of the test runs is given in Appendix A and the basic static and dynamic induced force and moment data are presented in Appendices B and C.

2. MODELS AND TEST FACILITY

Small scale models representative of both subsonic and supersonic V/STOL aircraft configurations were tested in the Jet Interaction Test Apparatus of the MCAIR Propulsion Subsystem Test Facility. The models, instrumentation, and test equipment used in the measurement of the jet-induced forces and moments are described below.

2.1 SUBSONIC V/STOL MODELS - Two subsonic V/STOL models were tested, a fully contoured 3-D model (Configuration 1) and a 2-D planform model (Configuration 2) as shown in Figures 2-1 and 2-2. These models, approximately 5% scale, have identical planforms to simulate the same advanced full scale vehicle illustrated in Figure 2-3. The aircraft represented has a lift fan in the forward fuselage and two lift/cruise fans mounted above the wings. Detail dimensions for the model are given in Figure 2-4.

The fully contoured model, Configuration 1, can also be configured as a modified planform model with a contoured lower fuselage and wings, as shown in Figure 2-5. This is accomplished by removing the upper fuselage section and adding a simple planform extension to simulate the aft fuselage and tail. The horizontal tail is raised to simulate a high tail. Lift improvement devices (LID's) can be mounted on Configuration 1 consisting of two longitudinal strakes and a lateral fence which are designed to increase the lift in ground effect by trapping the fountain upwash. Wing pods can be installed on each wing to simulate stores. The LID's and pods are illustrated in Figure 2-6. The model, as tested, has simple circular nozzles as shown in Figure 2-1. Yaw vanes can be provided in the rear nozzles and both pitch and yaw vanes in the front nozzle as shown in Figure 2-7.

The 2-D planform subsonic V/STOL model, Configuration 2, was designed in a modular fashion to allow a wide range of parametric testing. With this model, the wings can be mounted in low, mid, and high positions. The 2-D planform tail can be mounted in either a low or raised position.

An inner region plate model was tested to a limited extent to separate the forces acting on the center fuselage region from the total airframe force. This model, shown in Figure 2-8, consists of a simple flat plate comprising the area bounded by the three nozzles.

2.2 SUPERSONIC V/STOL MODEL - The supersonic V/STOL aircraft model, Configuration 3, is a 2-D planform model based on a configuration that has either one or two lift fans in the center fuselage and either one or two lift/cruise jets in the rear, as illustrated by the advanced designs shown in Figure 2-9.

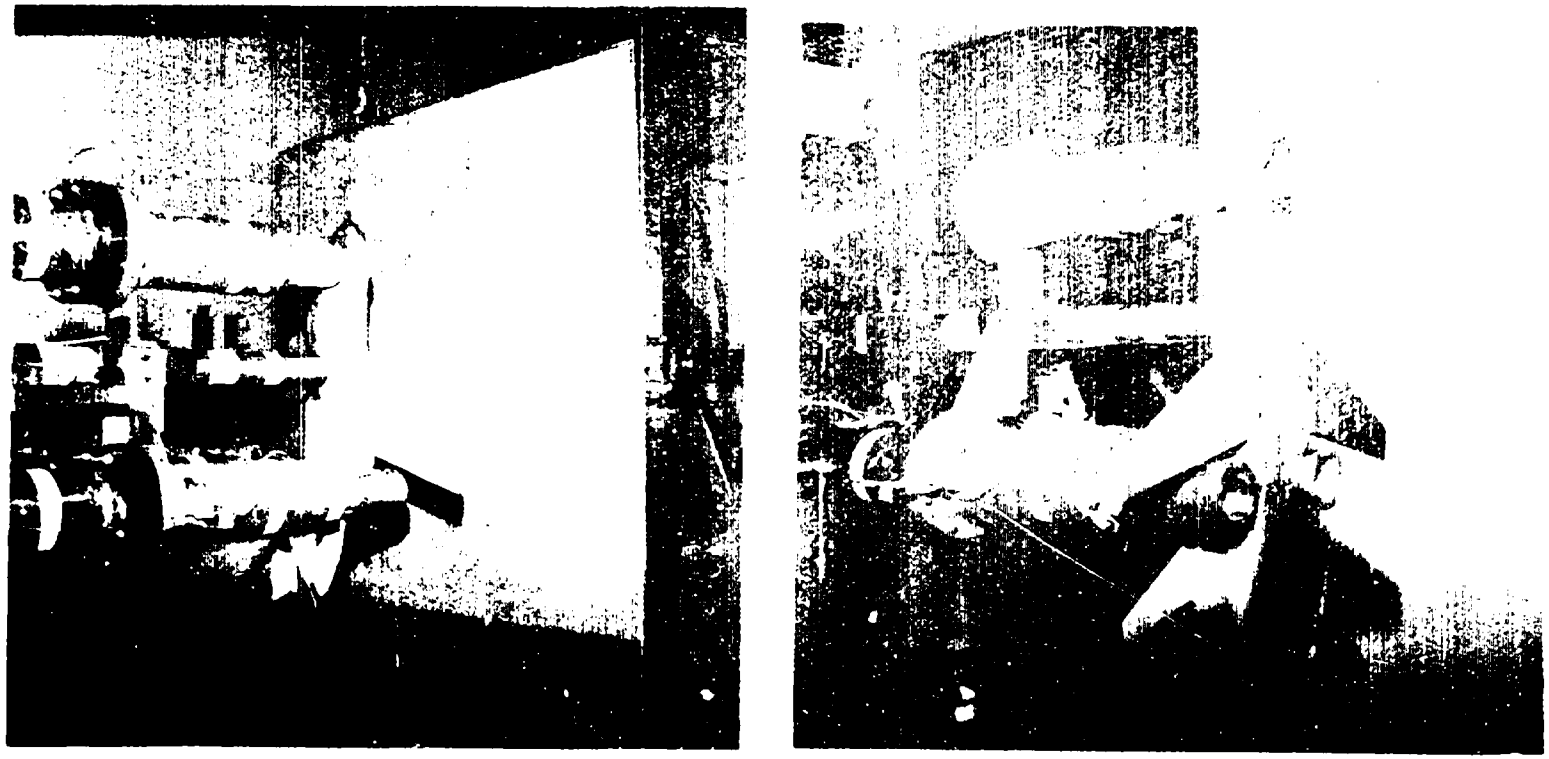

GP78 0726 1

FIGURE 2-1
SUBSONIC V/STOL FULLY CONTOURED 3-D MODEL
Configuration 1

GP78-0729-2

FIGURE 2-2
SUBSONIC V/STOL 2-D PLANFORM MODEL
Configuration 2, Low Wing

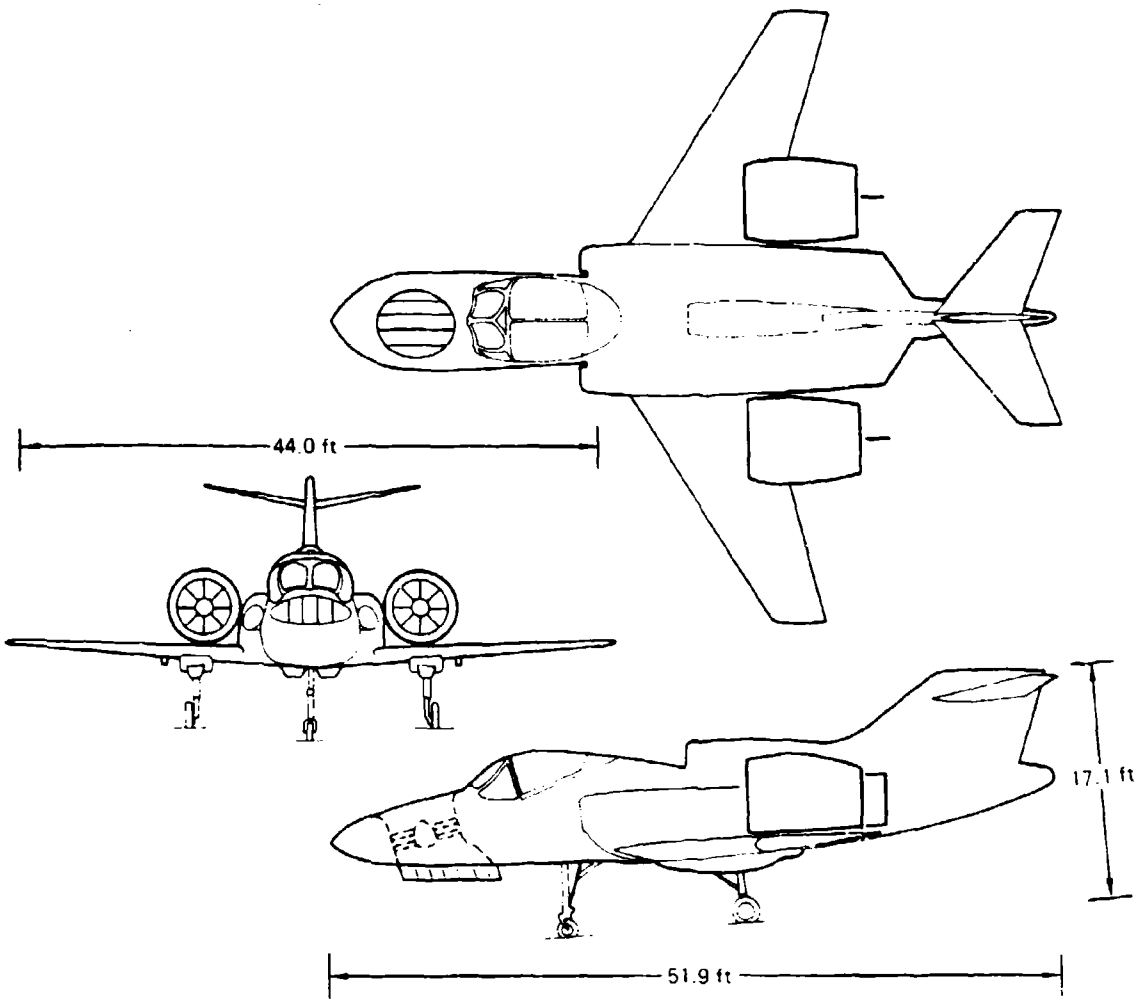

FIGURE 2-3
ADVANCED SUBSONIC V/STOL CONFIGURATION

Parameter	Subsonic V/STOL
Reference Diameter, D_{Ref}	4.024 in. (10.221 cm)
Wing Planform Area, S_W	84.5 in.^{2} (545.4 cm^2
Wing Span, b	21.66 in. (55.02 cm)
Wing Mean Aerodynamic Chord, c	4.13 in. (10.48 cm)
Tail Area, S_T	17.0 in.^{2} (1031.6 cm^2)
Aircraft Planform Area, S_P	159.9 in.^{2} (1031.6 cm^2)
C.G. Location, Measured from Nose Along Fuselage Centerline	12.89 in. (32.74 cm)
Overall Aircraft Length, L	25.52 in. (64.82 cm)

Note: Dimensions given in model scale

2 Jet	3 Jet	Configurations
D_{je} = 3.285 in. (8.344 cm)	D_{je} = 4.024 in. (10.221 cm)	1, 11, 12, 13, 14, 2, 21, 22, 23

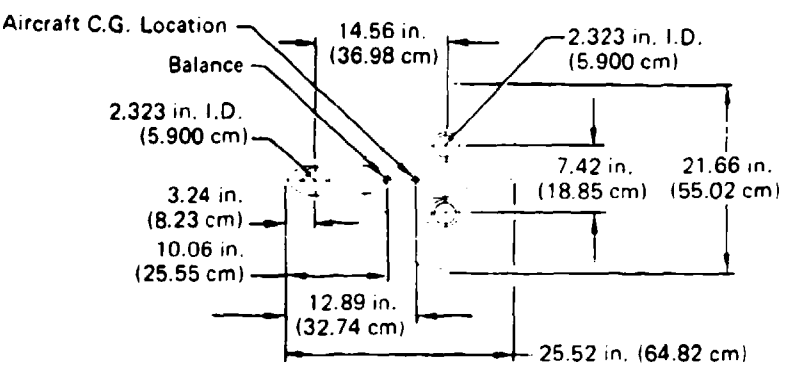

(a) Subsonic V/STOL

GP78 0895 77

FIGURE 2-4
SUBSONIC V/STOL MODEL DETAIL DIMENSIONS

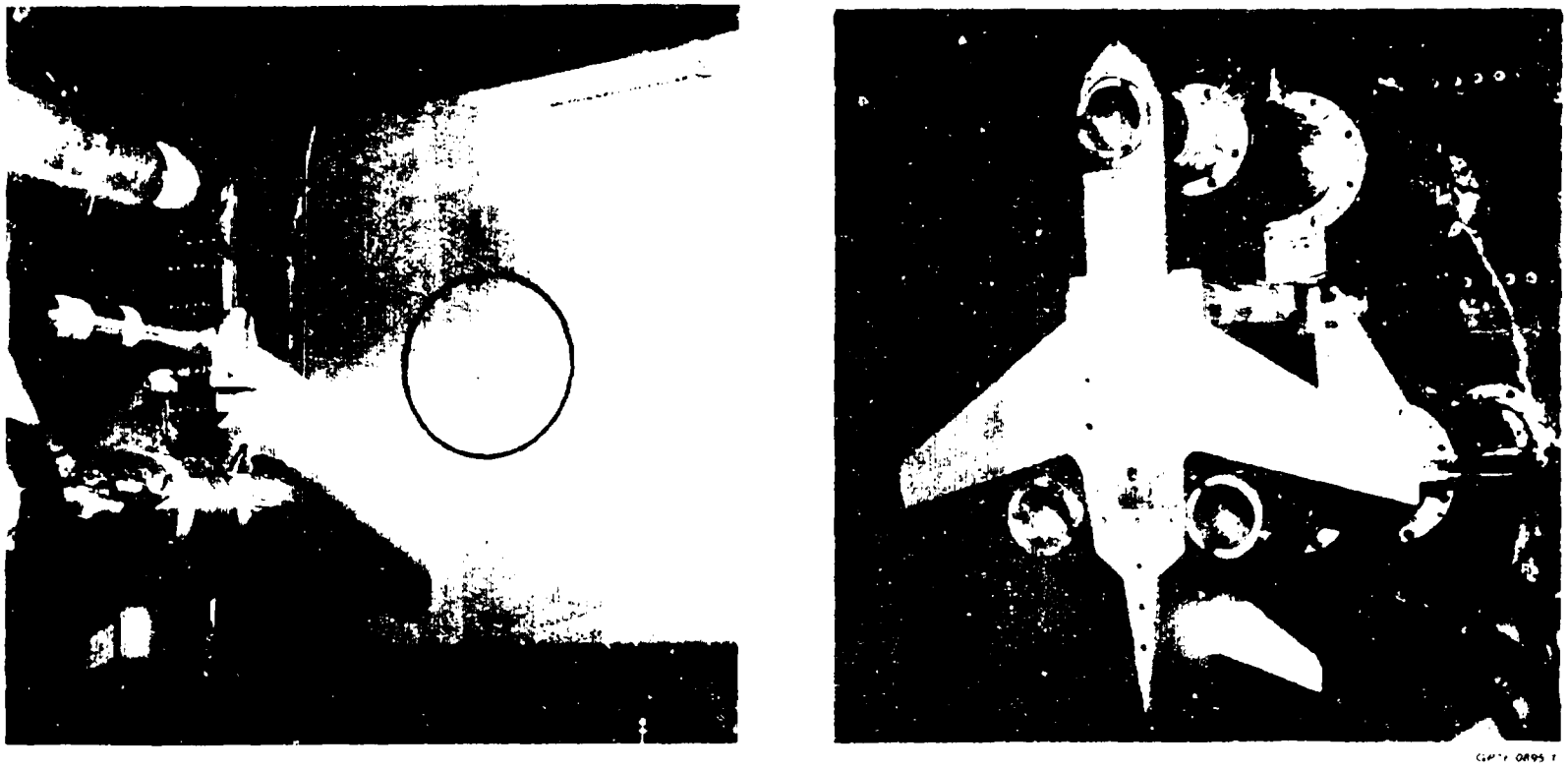

FIGURE 2-5
SUBSONIC V/STOL SEMICONTOURED PLANFORM MODEL
Configuration 14

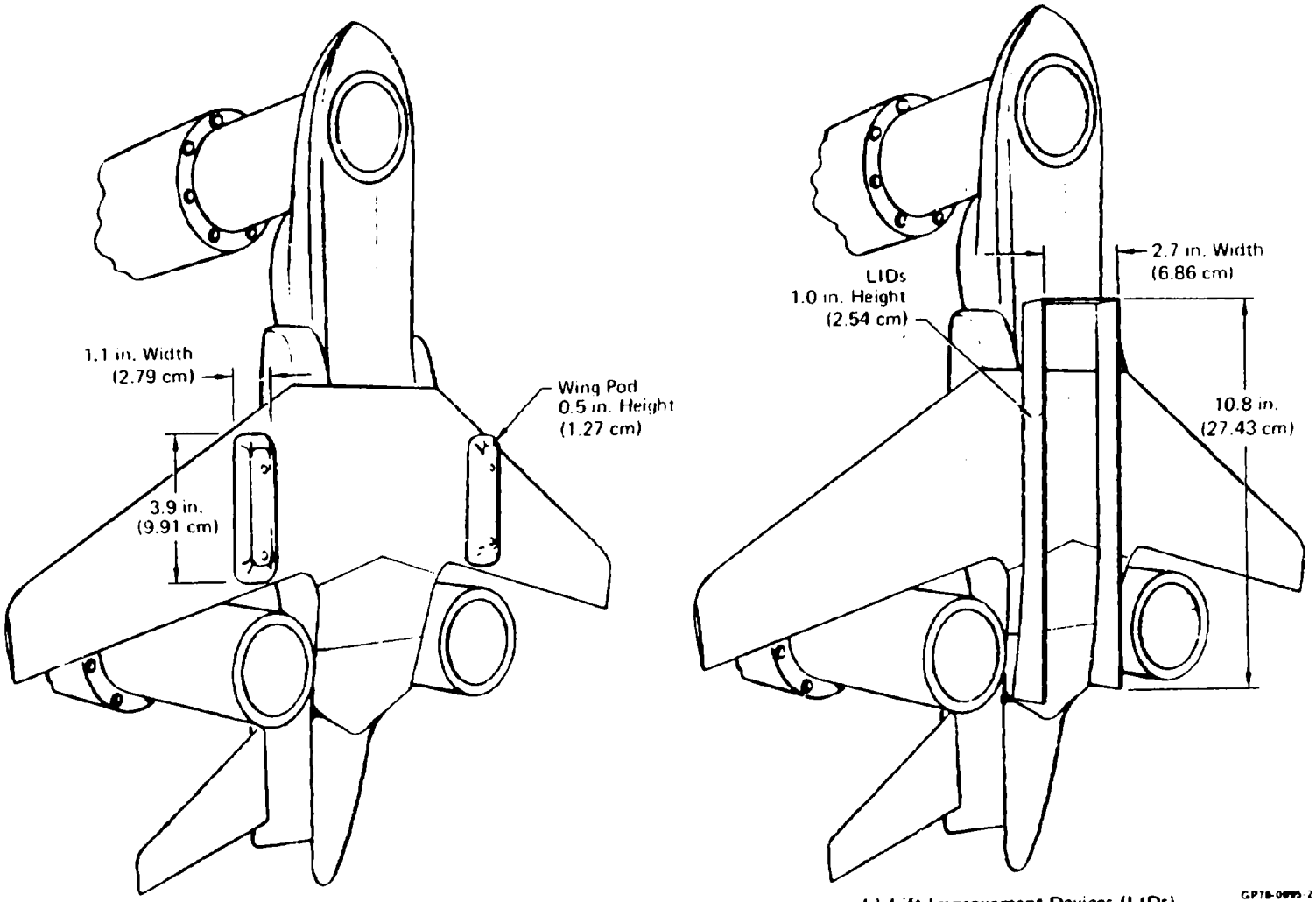

a) Wing Pods Installed

b) Lift Improvement Devices (LIDs) Installed on Lower Fuselage

GP78-0095-2

FIGURE 2-6
SUBSONIC V/STOL 3-D MODEL WITH LIDS AND PODS INSTALLED

GP78 0729 6

FIGURE 2-7
SUBSONIC V/STOL 3-D MODEL WITH COMPLEX NOZZLES
Configuration 12

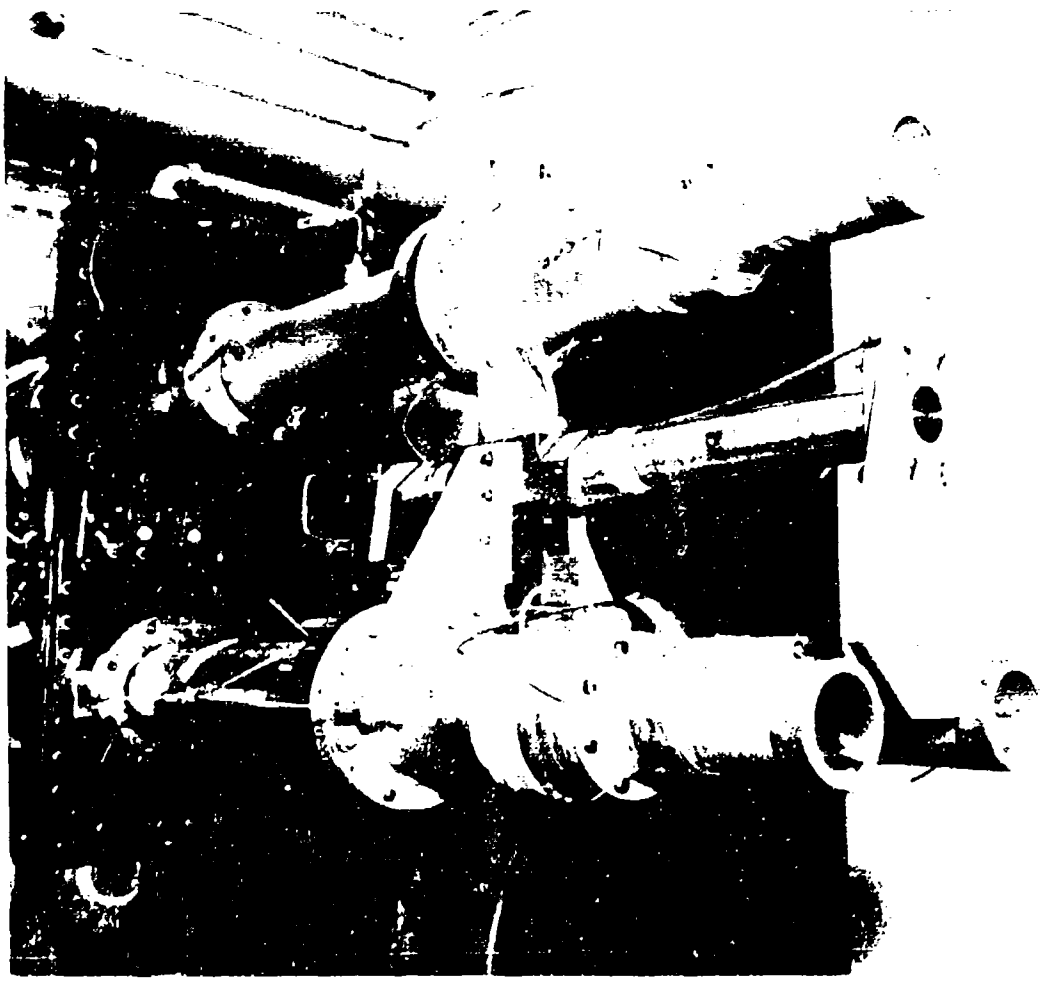

GP78 0729 10

FIGURE 2-8
SUBSONIC V/STOL 3-JET INNER REGION PLATE

As with the planform subsonic model, Configuration 3 was designed in a modular fashion to allow testing with a variety of nozzle arrangements and wing positions, as shown schematically in Figure 2-10. An attachment is provided to simulate contouring on the lower fuselage. The majority of tests with Configuration 3 were conducted with a three nozzle arrangement consisting of a single large diameter nozzle located in the center fuselage and two small diameter nozzles located in the aft end. This nozzle arrangement as well as the other arrangements and configurations are shown in Figure 2-11. In addition to the nominal arrangement, the model can be configured (1) with large diameter nozzles in both the center and aft fuselage and (2) with two transverse medium diameter nozzles in the center and two small diameter nozzles in the rear. The longitudinal spacing between the fore and aft nozzles is variable for both of these alternate nozzle arrangements. Detail model dimensions are provided in Figure 2-12

The wing height on Configuration 3 is adjustable to simulate low, mid, and high positions. LID's can be installed on the nominal three nozzle arrangement. These LID's, shown in Figure 2-11(e), consist of the two longitudinal strakes and a lateral fence.

2.3 MODEL INSTRUMENTATION - The airframe models were supported, as illustrated in Figure 2-13, by a six-component strain gage balance which provides measurements of the jet-induced forces acting on the airframe. A Task Mark XXIII 1.5 inch (3.81 cm) diameter force balance, shown in Figure 2-14, was used due to proven accuracy in previous tests and high frequency response (> 1000 Hz). The balance was positioned to align the axial force gage, which has the lowest force rating (100 lbf), with the lift axis. This provides an accurate measure of the lift forces acting on the airframe (accuracy within 0.25 percent of the maximum rated load).

The jet exhaust flows were simulated with high pressure air at ambient temperature. The nozzles of each of the models were non-metric so as not to transmit any thrust force to the force balance, thus increasing the accuracy of the jet-induced force measurements. A radial clearance of 0.020 inch (0.05 cm) and an active grounding detection system was provided between the outside diameter of the nozzles and the model. Each nozzle was instrumented, as illustrated in Figure 2-13, to determine the nozzle pressure ratio, jet thrust, and mass flow rate. The thrust characteristics of each nozzle were determined in and out of ground effect in the MCAIR Nozzle Thrust Stand. No

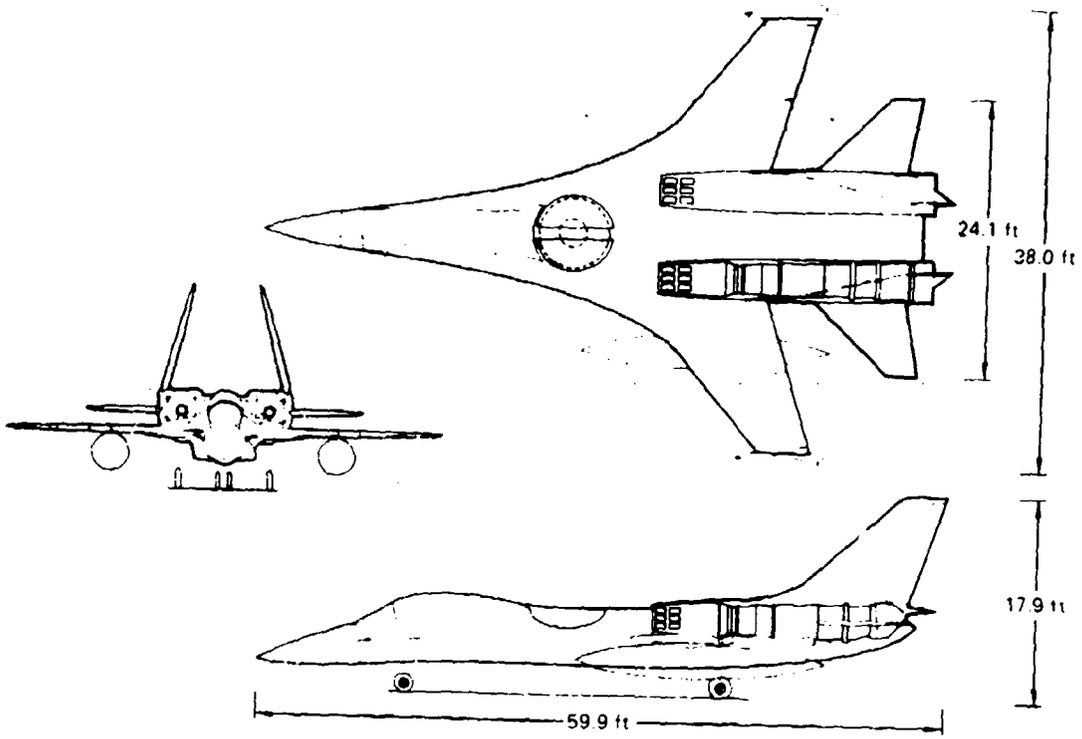

a) Single Lift Fan with Dual Lift/Cruise Jets

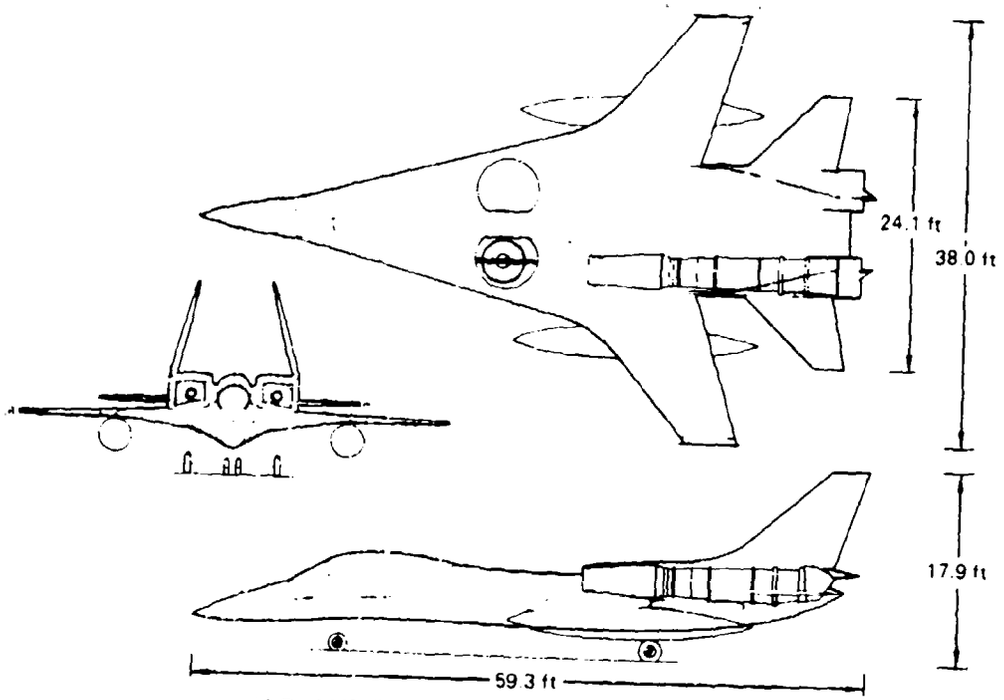

b) Dual Lift Fans with Dual Lift/Cruise Jets

FIGURE 2-9
ADVANCED SUPERSONIC V/STOL DESIGNS

GP78-0895 123

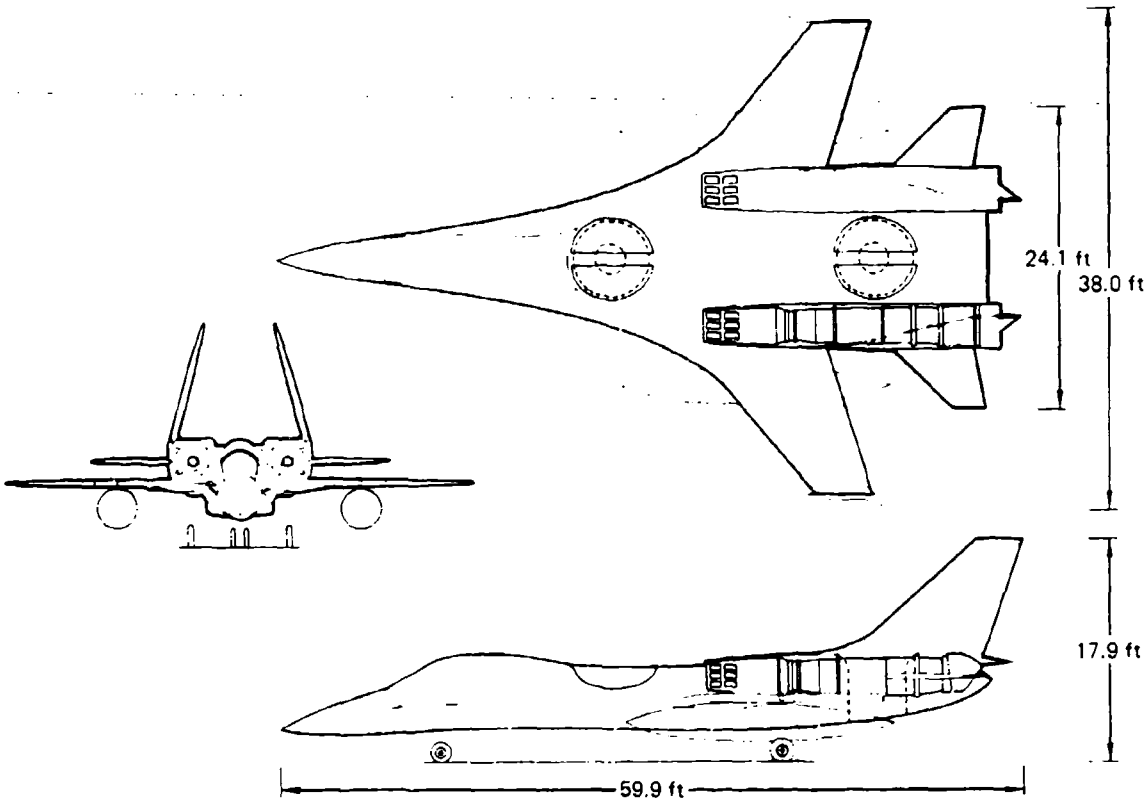

(c) Dual Lift Fans

QP78-0729-29

FIGURE 2-9 (Concluded)
ADVANCED SUPERSONIC V/STOL DESIGNS

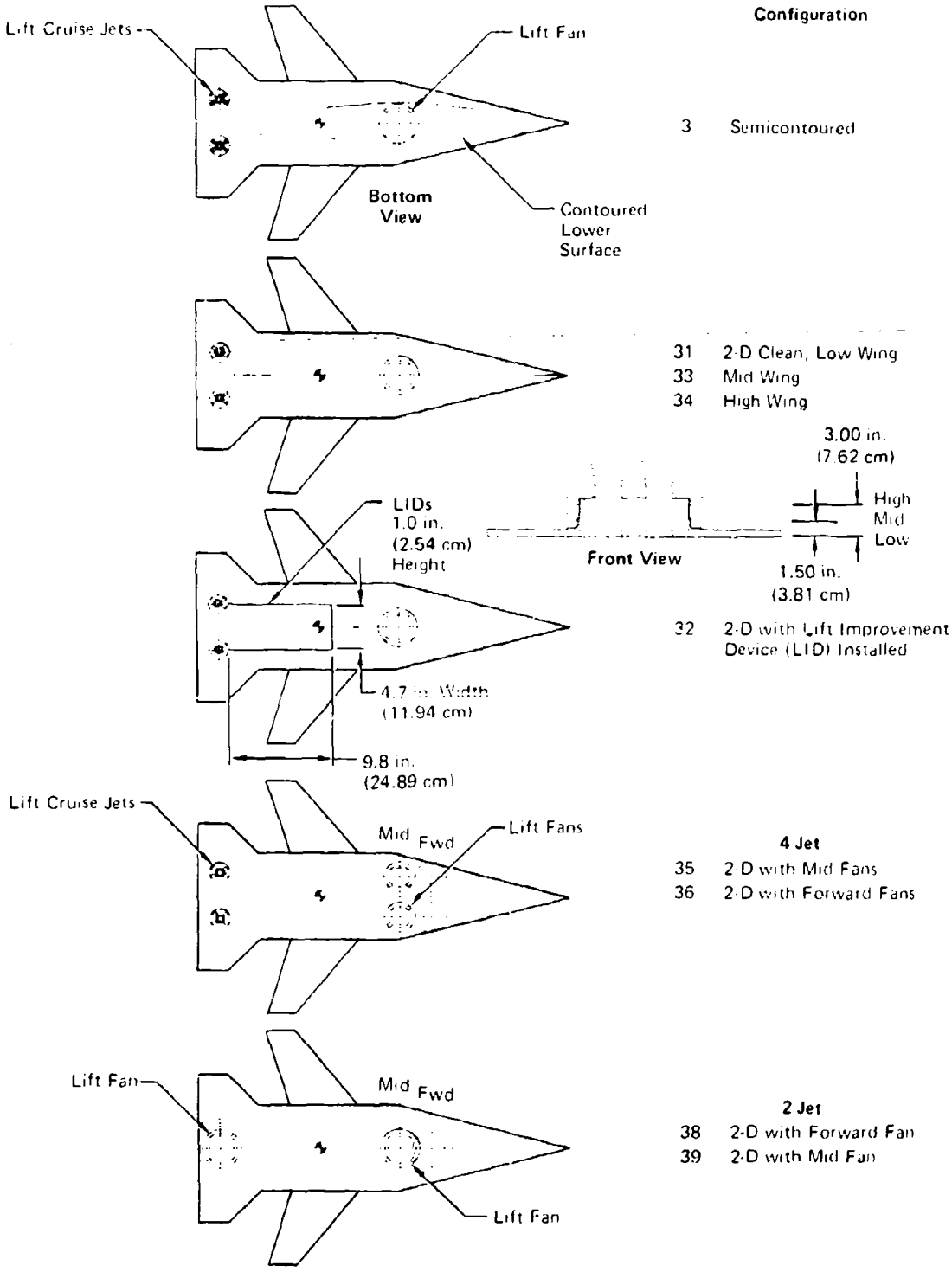

FIGURE 2-10
SUPERSONIC V/STOL MODEL CONFIGURATIONS

GP78-0895-3

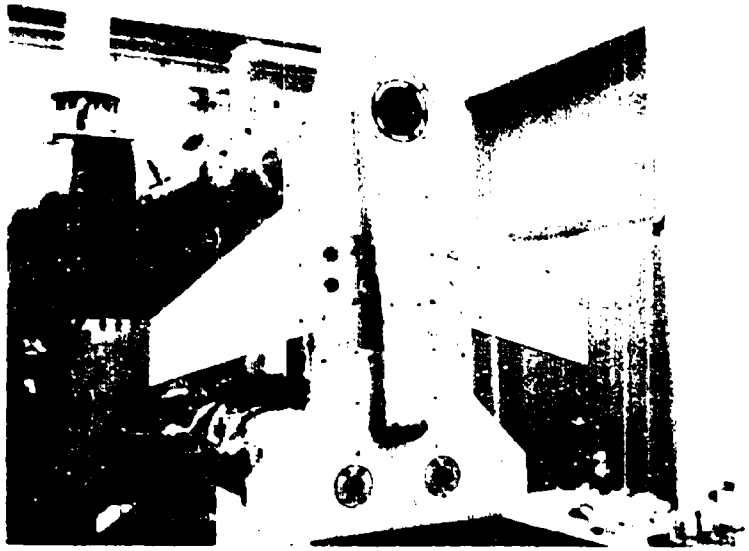

a) Semi-Contoured Lower Fuselage Model (Configuration 3)

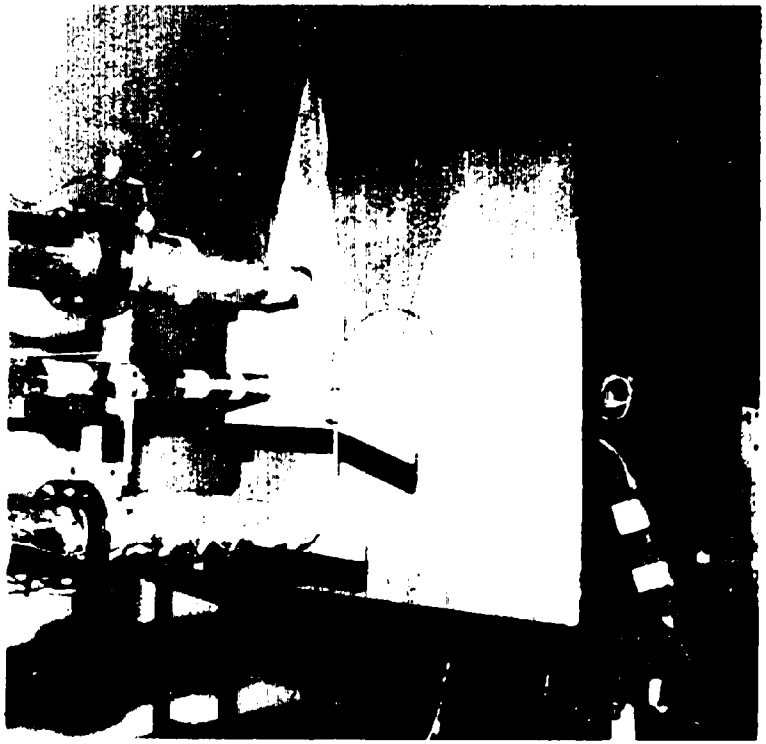

b) Upper Surface of Semi-Contoured Model (Configuration 3)

GP78-0729-9

FIGURE 2-11
SUPERSONIC V/STOL MODELS

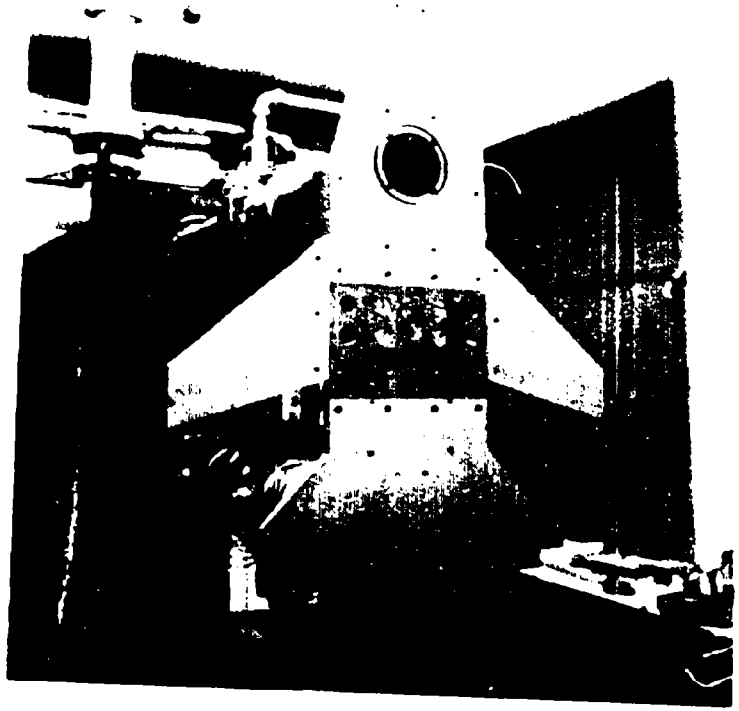

c) 2-D Planform Model (Configuration 31)

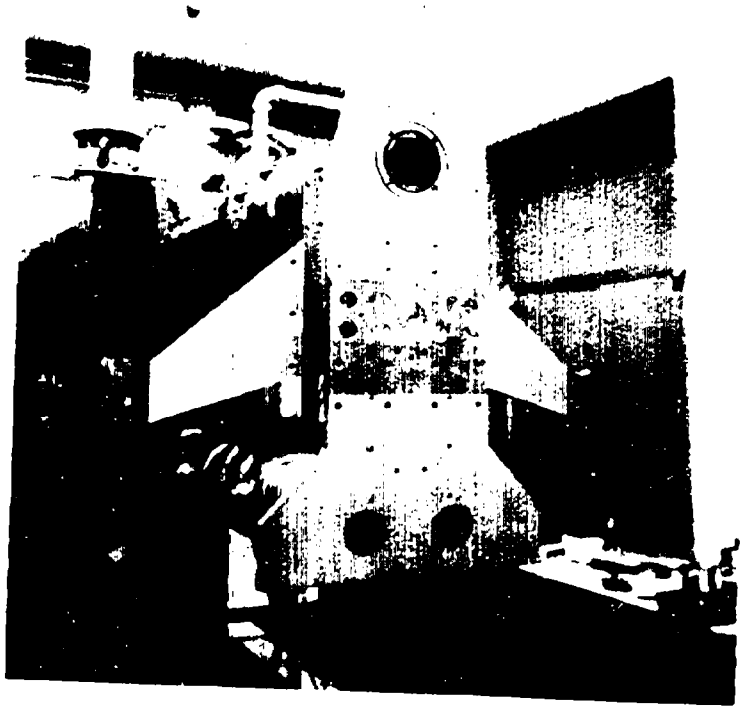

d) 2-D High Wing Model (Configuration 34)

FIGURE 2-11 (Continued)
SUPERSONIC V/STOL MODELS

GP78-0729-10

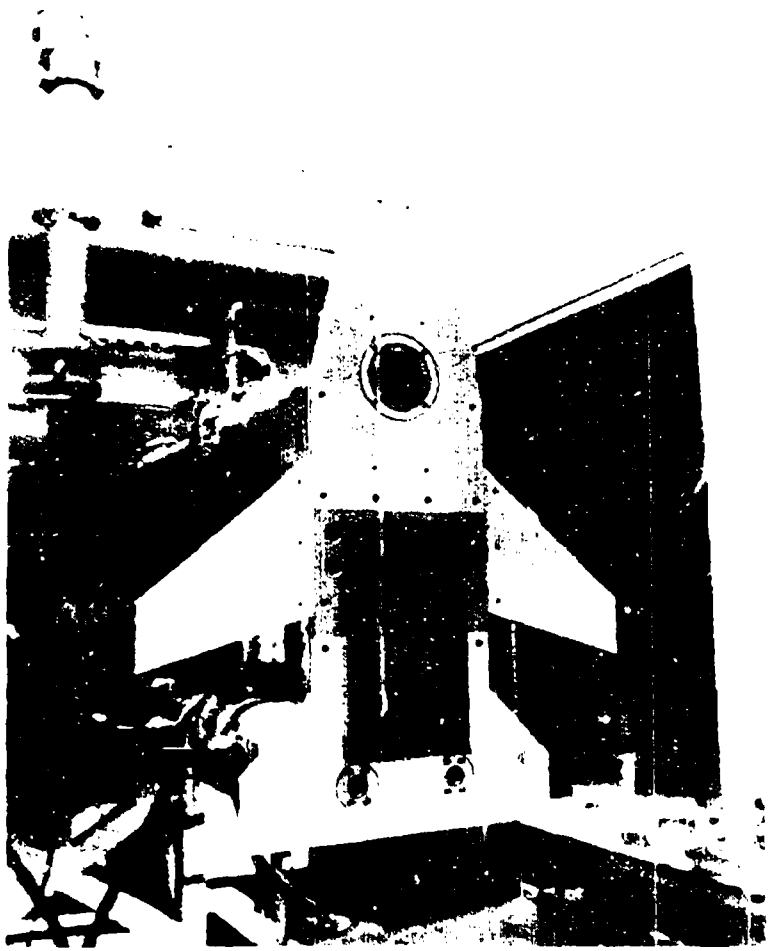

e) 2-D Model with LID Installed
(Configuration 32)

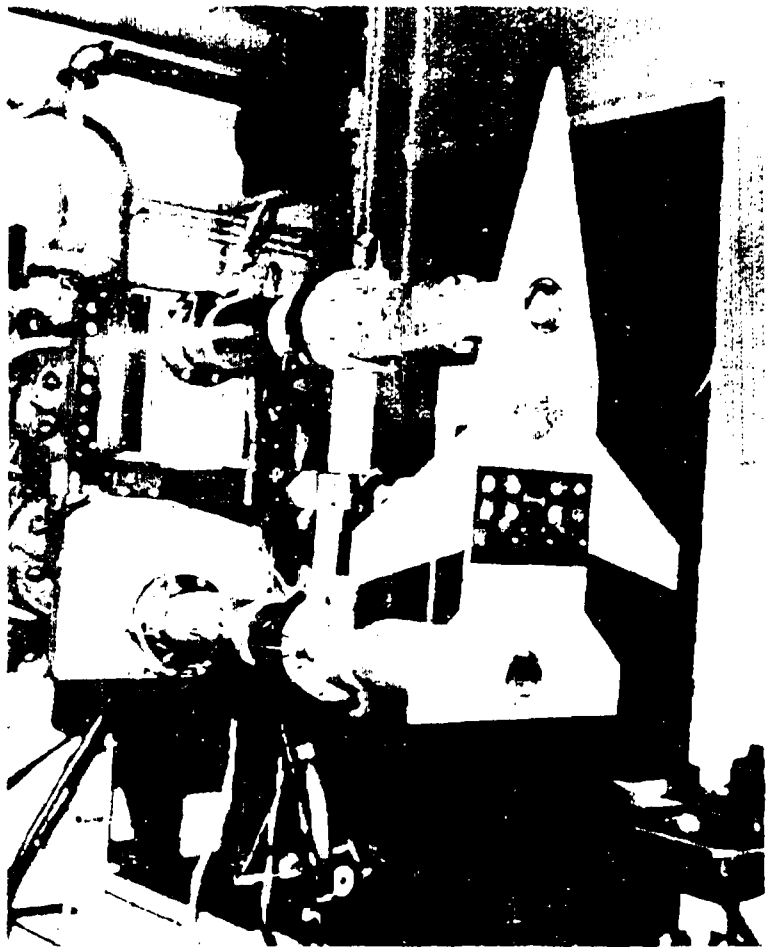

f) 2-D 2-Nozzle Model with Forward and Aft Lift Fans
(Configuration 38)

FIGURE 2-11 (Continued)
SUPERSONIC V/STOL MODELS

GP78 0729-11

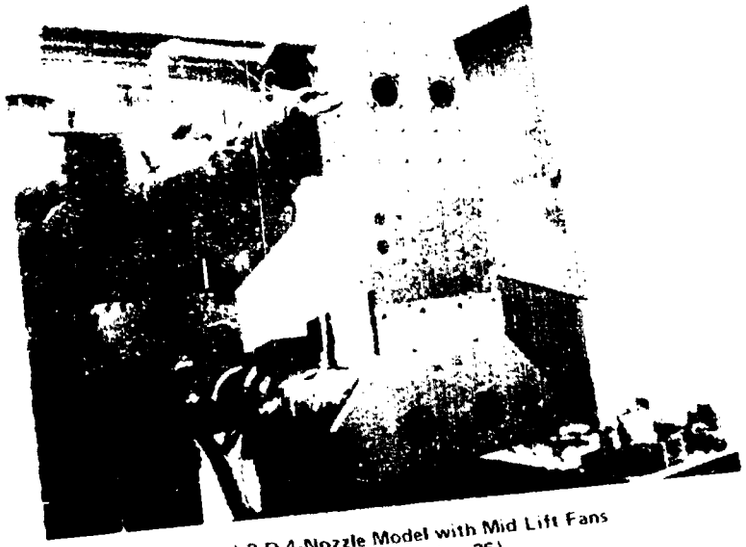

g) 2-D 4-Nozzle Model with Mid Lift Fans
(Configuration 35)

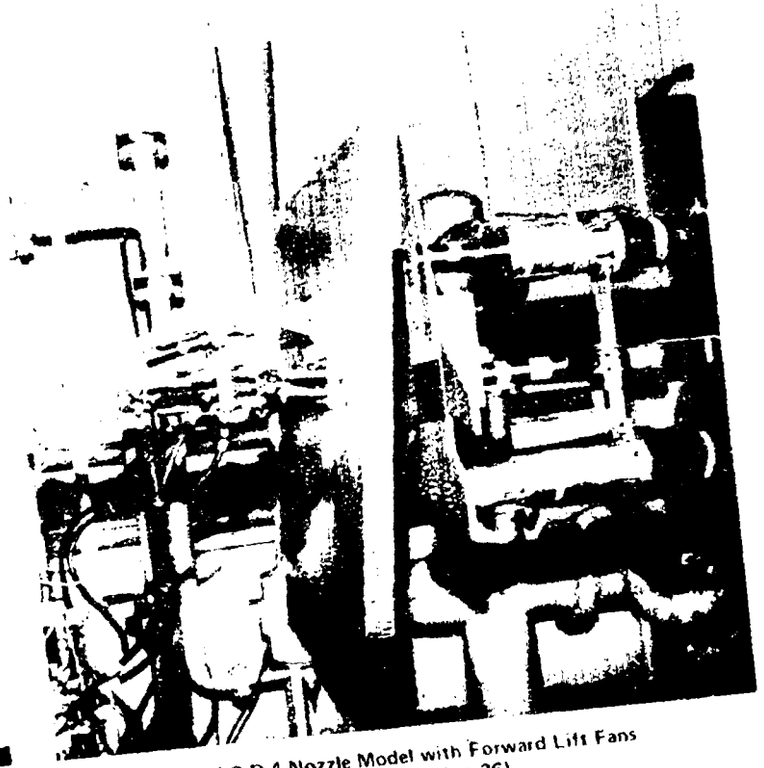

h) 2-D 4-Nozzle Model with Forward Lift Fans
(Configuration 36)

GP78-0729-12

FIGURE 2-11(Concluded)
SUPERSONIC V/STOL MODELS

Parameter	Supersonic V/STOL
Reference Diameter, D_{Ref}	4.024 in. (10.221 cm)
Wing Planform Area, S_W	130.9 in. (844.5 cm^2)
Wing Span, b	22.76 in. (57.81 cm)
Wing Mean Aerodynamic Chord, c	6.24 in. (15.85 cm)
Tail Area S_T	27.9 $in.^2$ (180.0 cm^2)
Aircraft Planform Area, S_P	321.0 $in.^2$ (2071.0 cm^2)
Overall Aircraft Length, L	35.58 in. (90.37 cm)

Note: Dimensions given in model scale

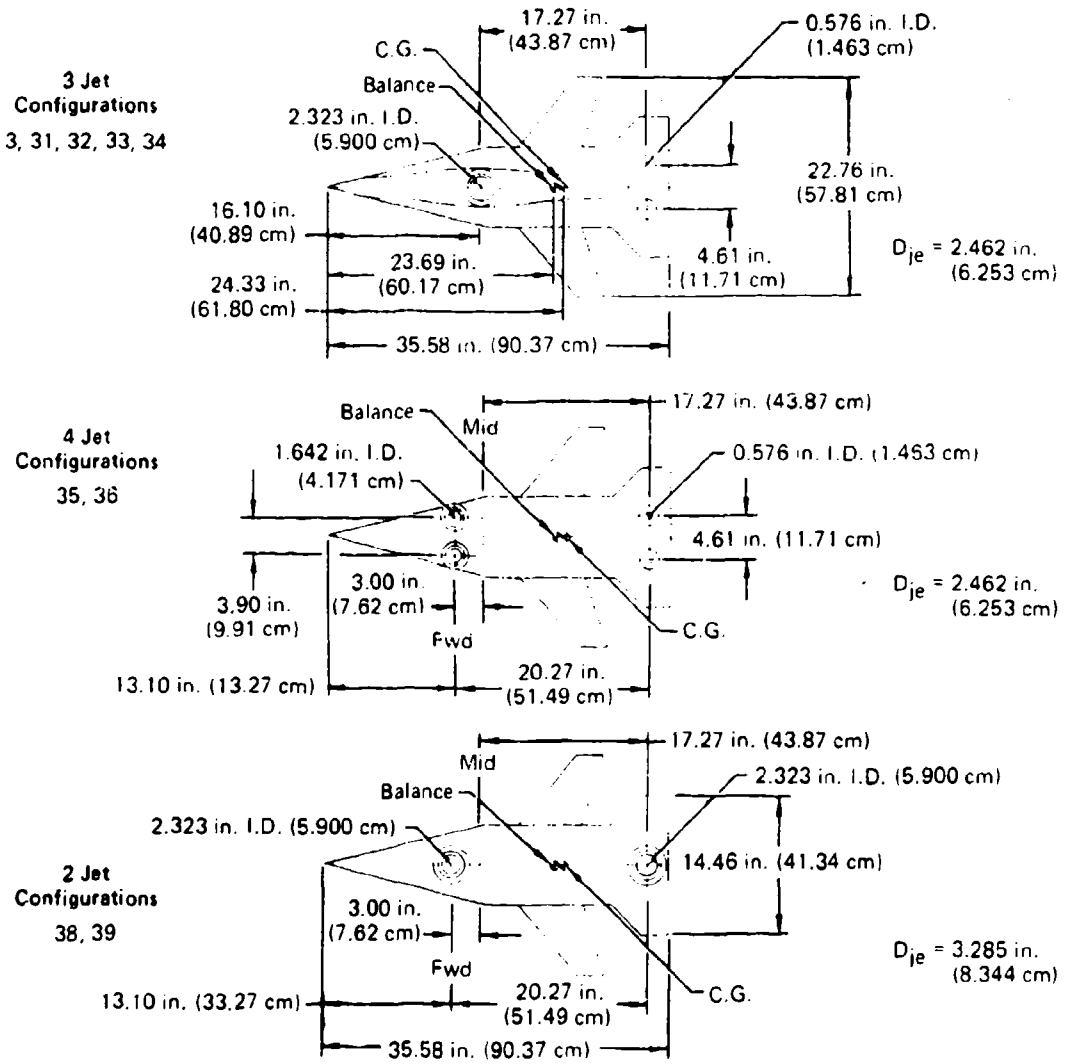

FIGURE 2-12
SUPERSONIC V/STOL MODEL DETAIL DIMENSIONS

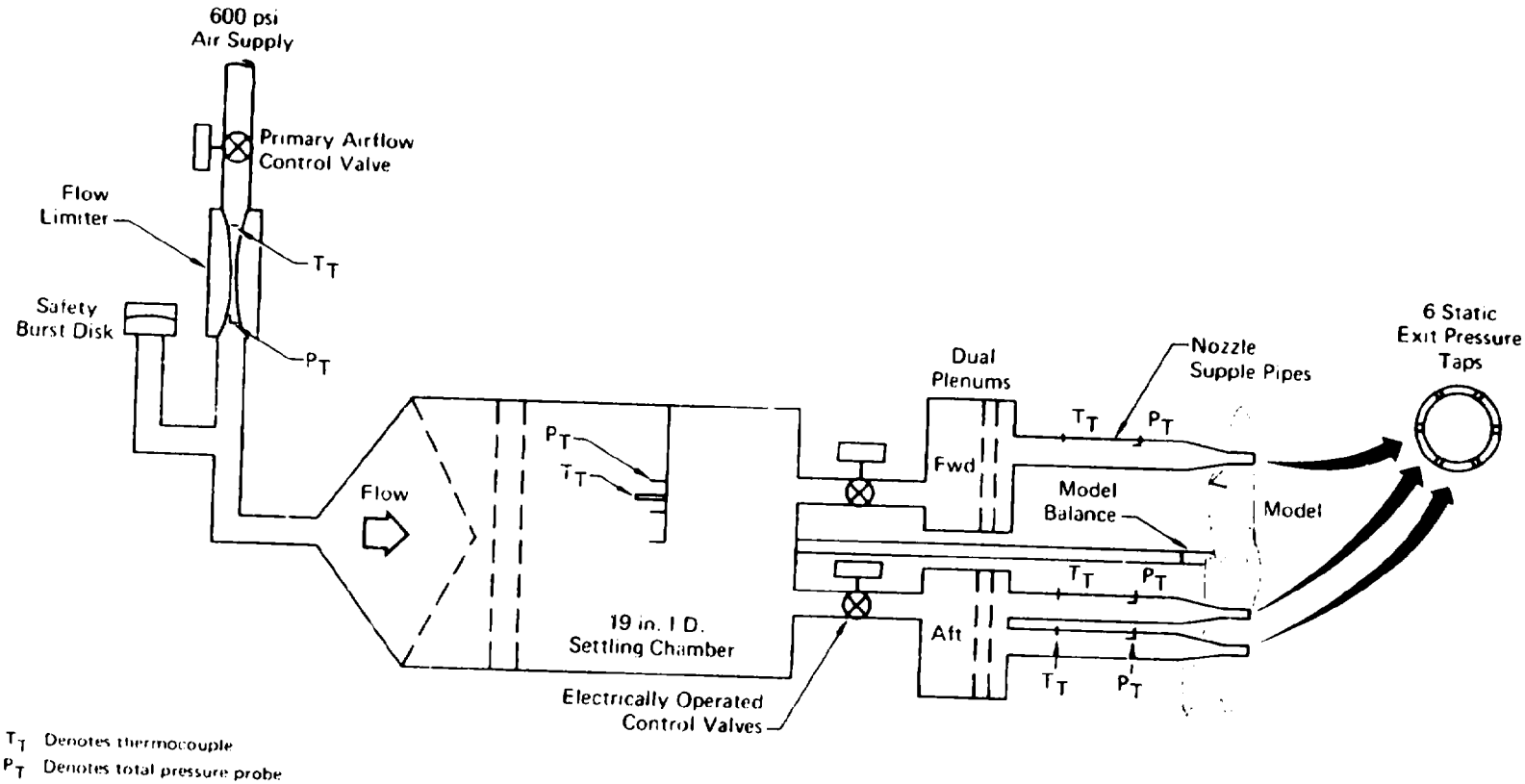

FIGURE 2-13
V/STOL MODEL/FACILITY INSTRUMENTATION

GP78-0729-13

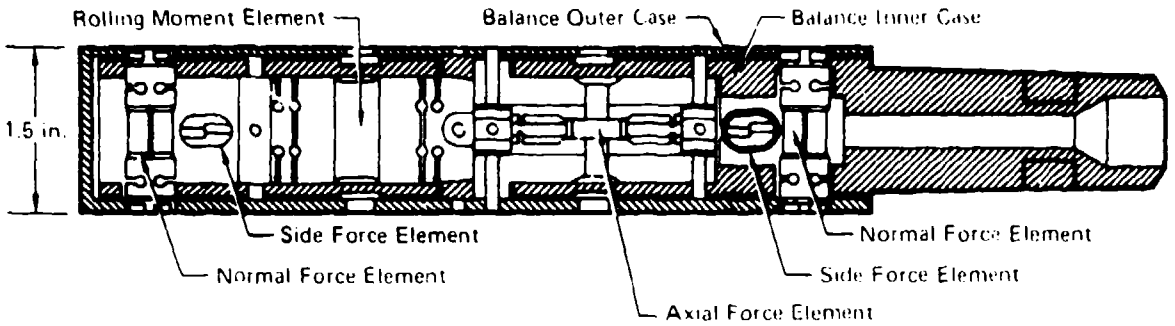

a) Task Mark XXIII Balance Details

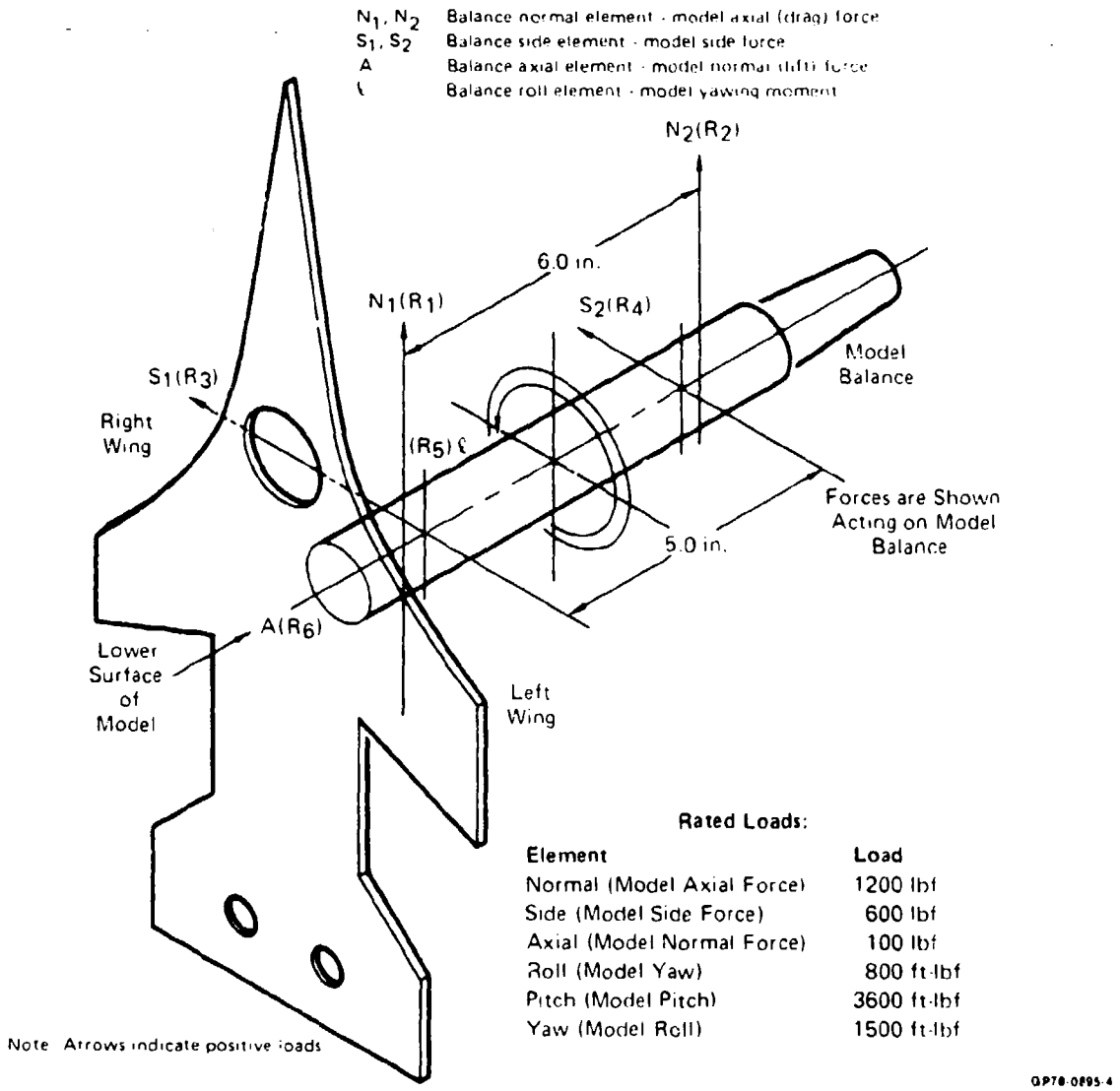

b) Model Balance Installation

FIGURE 2-14
MODEL BALANCE

substantial ground effects on the nozzle thrust were measured except at heights substantially below typical gear heights.

2.4 TEST FACILITIES - The major elements of the test arrangement were the Jet Interaction Test Apparatus, the Data Acquisition/Reduction Systems, and the Deck Motion Test Apparatus.

Jet Interaction Test Apparatus - The MCAIR V/STOL Jet Interaction Test Apparatus (JITA), Figure 2-15, consists of a 19 inch (0.48M) I.D. settling chamber, two independent nozzle plenum chambers, a model support beam, and interchangeable nozzles mounted on the plenums. The JITA is located in a 32 ft. (9.75m) long by 19 ft. (5.79m) wide by 24 ft (7.32m) high test cell, as illustrated in Figure 2-16. The large test cell eliminates any wall effects which might influence the jet-induced aerodynamics. The JITA control console for the model exhaust flows is shown in Figure 2-17.

High pressure air can be supplied continuously from 600 psig tanks at a rate up to 16 lb/sec to the settling chamber for simulating exhaust flows. The air is heated to approximately 100°F. The settling chamber has a conical spreader screen and two normal screens to provide uniform flow conditions to the two nozzle plenum chambers. Nozzle pressure ratios from 1.1 to 7.0 can be tested. The plenums are provided with independently controlled pressure valves to allow testing at different front and rear nozzle pressure ratios. This feature is particularly important for some V/STOL configurations which utilize both lift fans and lift jets.

The force balance is attached to the support beam which is centrally mounted off the settling chamber. The test models are attached to the force balance, which locates them away from the plenums (typically by one wing span), thus minimizing the potential effect of the plenum blockage on the induced flowfield.

Data Acquisition/Reduction Systems - A six-component strain gage balance was used to measure the steady state and transient jet-induced forces. The steady state data, including the nozzle exhaust pressures and temperatures, the ground plane position and attitude, and the balance outputs, were recorded at a rate of two samples per second with a Datum Model 120 Digital Data Acquisition System (DDAS) and are filtered with a 10 Hz filter. The DDAS provides signal conditioning, amplification, and excitation for up to 40 input channels. The data acquisition console is shown in Figure 2-18. The digitized data

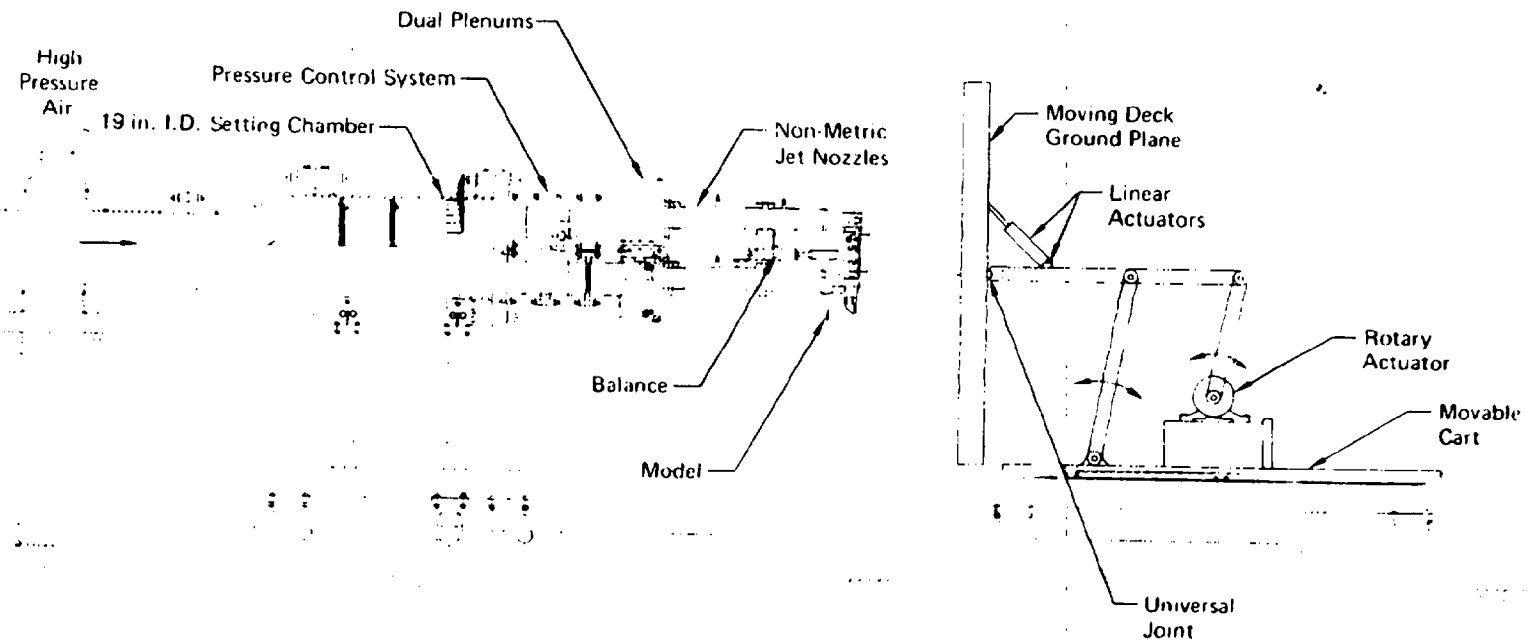

FIGURE 2-15
V/STOL JET INTERACTION TEST APPARATUS
JITA

GP78-0729-15

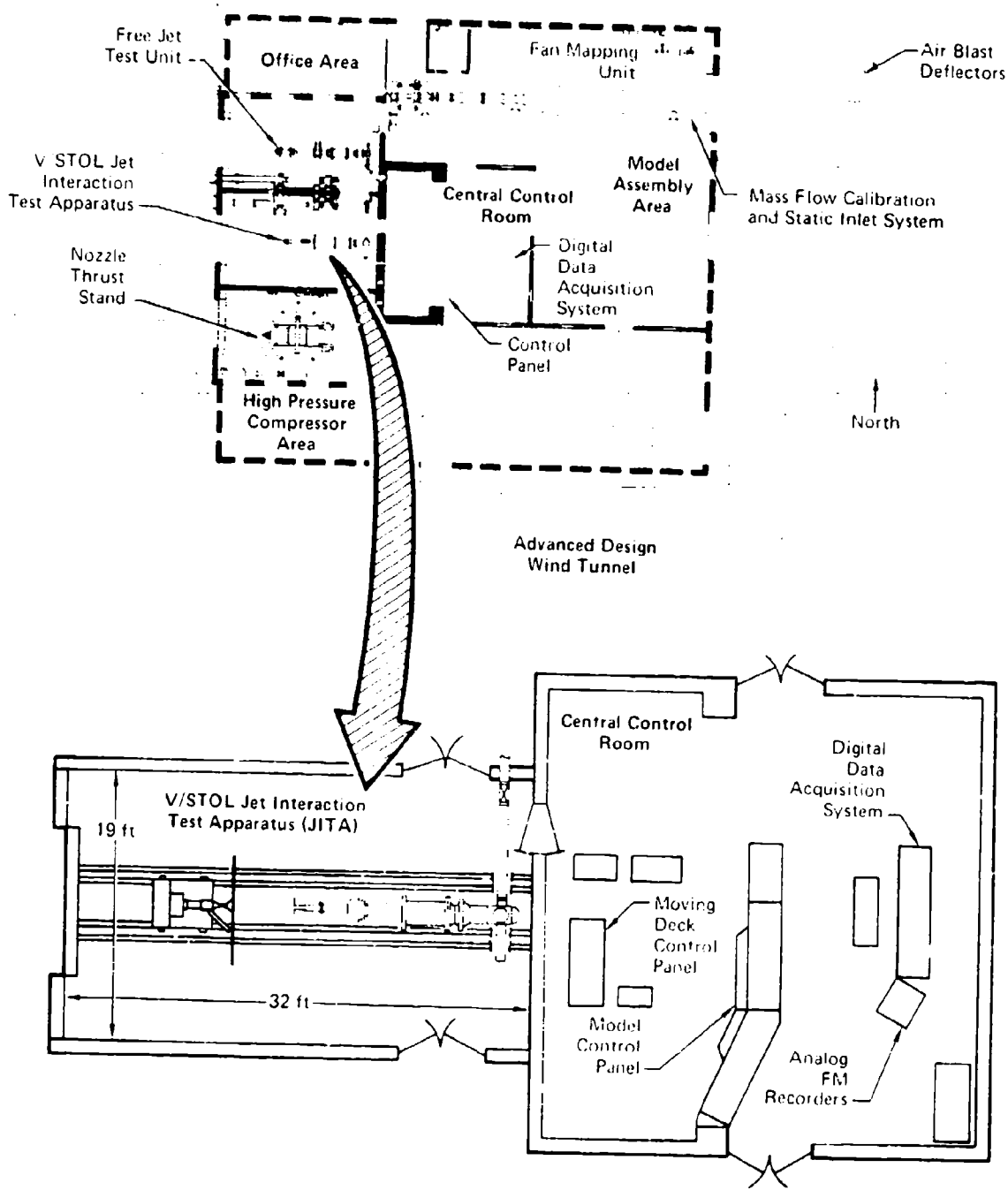

FIGURE 2-16
PROPULSION SUBSYSTEM TEST FACILITY
PSTF

QP73-0729-16

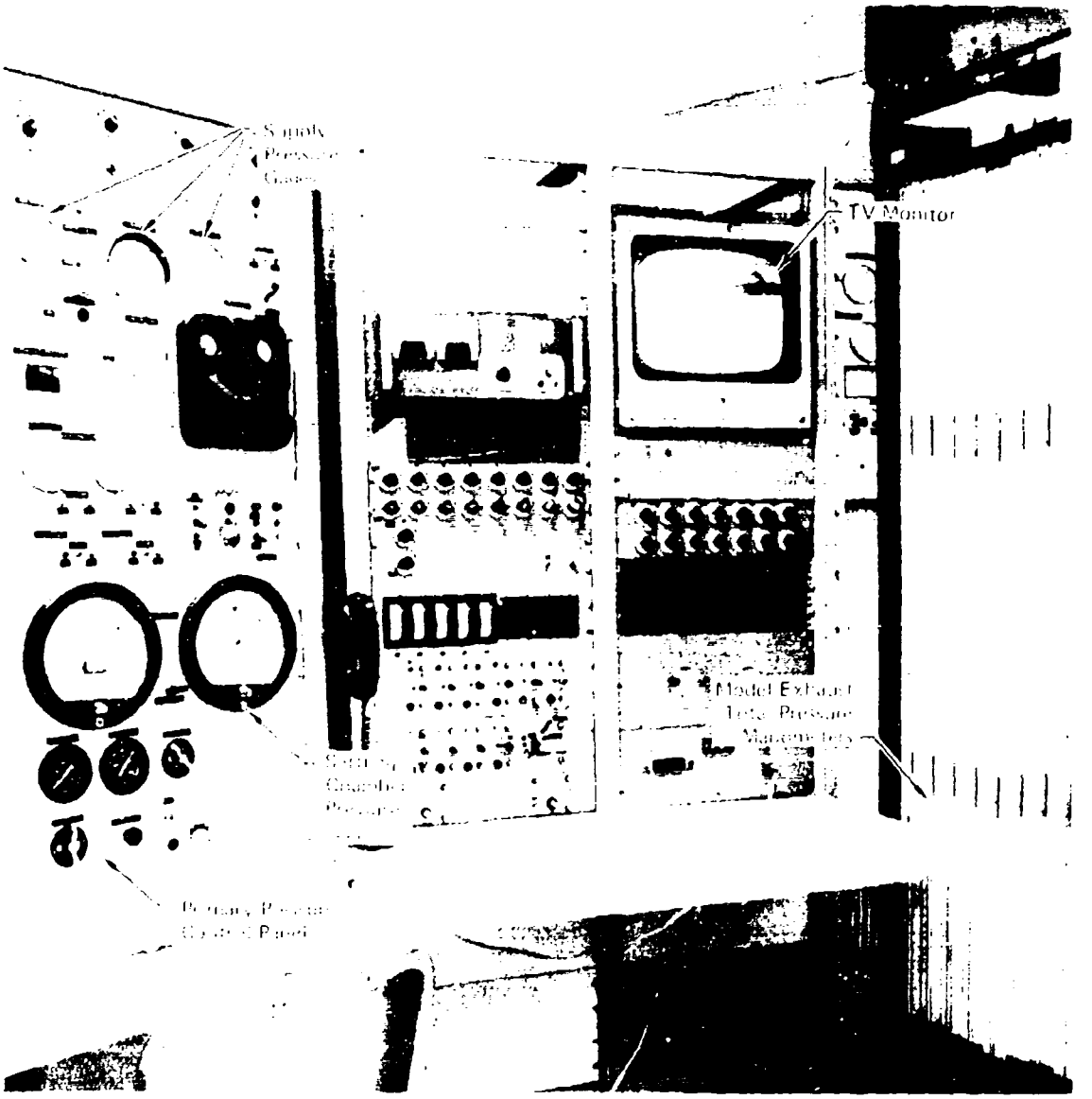

FIGURE 2-17

GP78-0726-17

CONTROL CONSOLE FOR EXHAUST FLOWS IN THE JITA

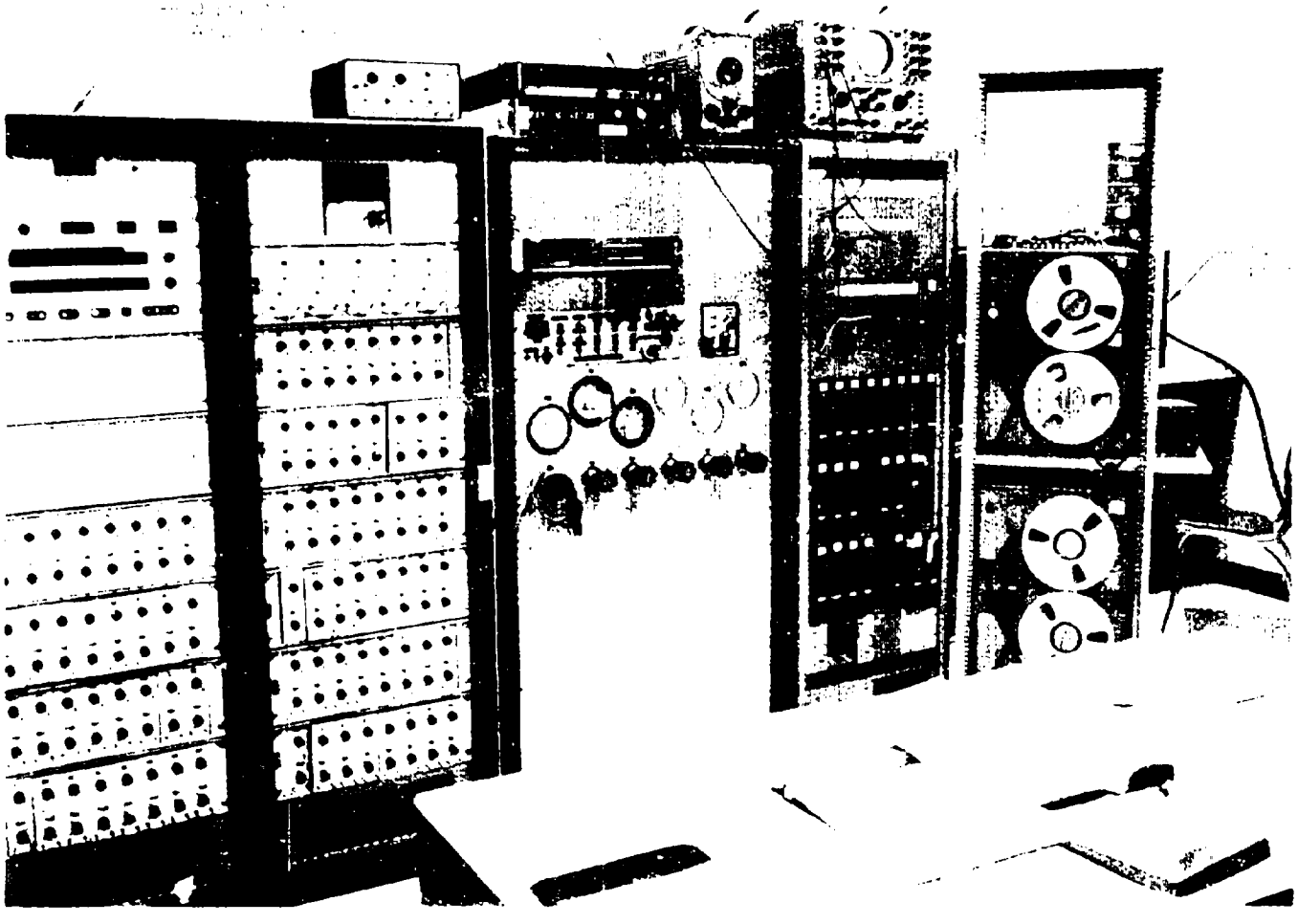

FIGURE 2-18
DATA ACQUISITION CONSOLE IN THE PSTF

were recorded on magnetic tape and reduced on a Scientific Engineering Laboratory Model 86 Digital Computer.

To assess the dynamic jet-induced forces and moments, the force balance analog signals were recorded on a 14 track FM tape, along with the outputs from the three ground plane potentiometers and a computer time code. The balance and potentiometer signals were also recorded on oscillograph strip charts, shown in Figure 2-19, for on-line monitoring. A Hewlett-Packard 5451B Fourier Transform Analyzer, Figure 2-20, was used off-line to digitize the dynamic data and analyze the data statistically. The HP5451B has a built-in analog-to-digital converter and keyboard controlled statistical computations such as power spectral densities and autocorrelations. Time histories of the balance data can also be provided for selected time segments.

Deck Motion Test Apparatus - The moving deck hardware, shown in Figure 2-15 and 2-21, consists of a simulated deck, a hydraulic actuation system, a movable support cart, an electronic control system, and electronic/mechanical safety devices. Two decks are available, one measuring 6 x 6 ft (1.83 x 1.83 m) and the other 3 x 3 ft (0.91 x 0.91 m). The larger deck represents an aircraft carrier (CV) deck while the smaller deck represents the landing platform of a non-aviation type ship such as a DD963 destroyer. The decks have a 2.0 inch (5.08 cm) honeycomb core with 0.04 inch (0.10 cm) aluminum skins. This provides a lightweight structure for the fast movements required for simulated deck motion with small scale models and the rigidity required to avoid bending. The rigid construction has a high natural frequency and negligible deflection under maximum jet thrust loading. The natural frequencies of the deck were verified to be well over 100 Hz by a Spectral Dynamics Corporation Real Time Analyzer. In addition, static loads were applied to the deck at points where jet thrust loads were experienced in the program. The measured deflection at the corner of the deck was .051 inches (0.130 cm) with the maximum jet thrust load, indicating the rigidity of the deck.

The hydraulic actuator system consists of a single rotary actuator for the heaving motion and two linear actuators, located at right angles to one another, for pitch and roll. The drive arm connected to the rotary actuator is attached to the deck through a universal joint. The actuators are powered

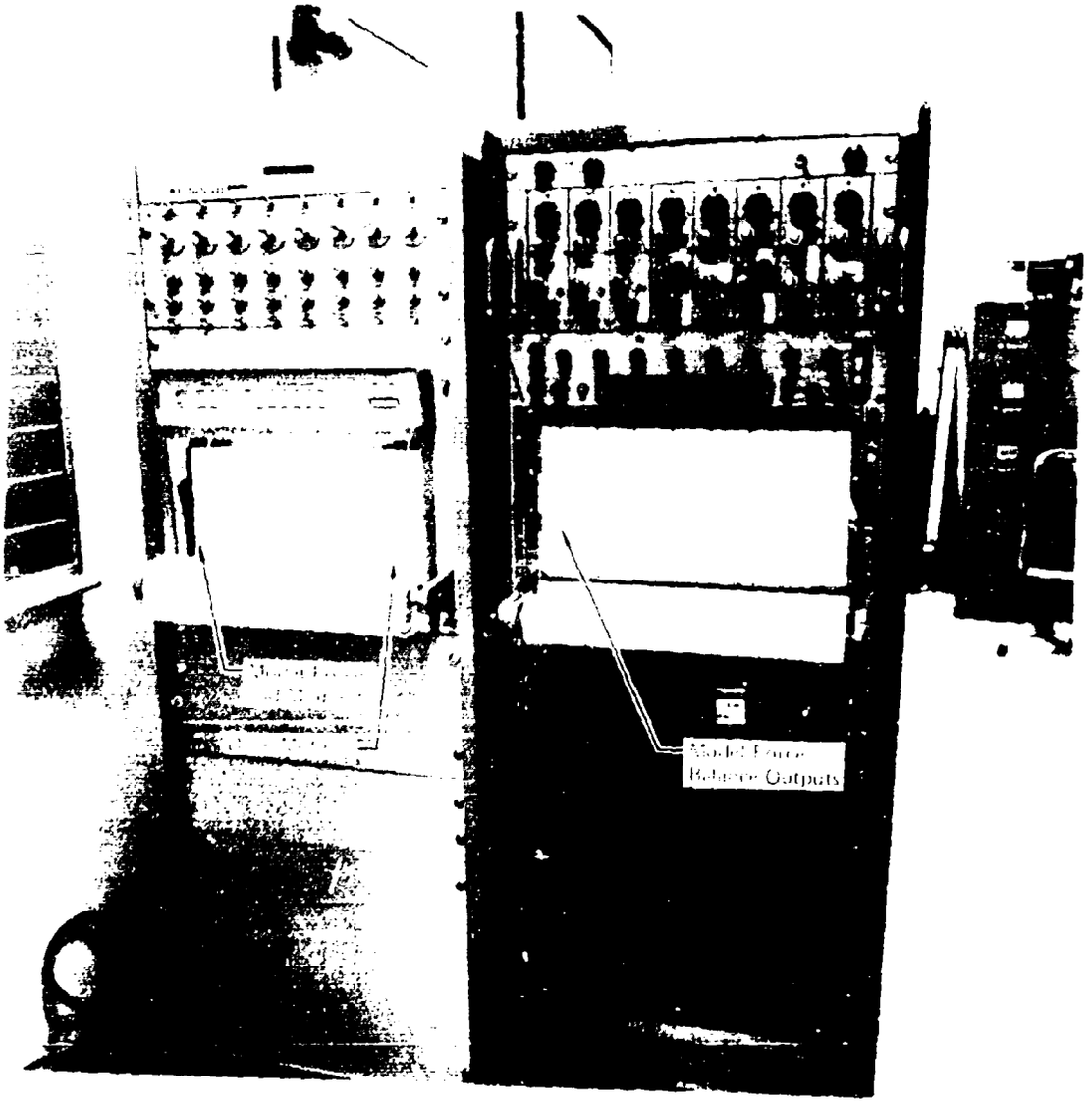

GP78-0729-19

FIGURE 2-19
ON-LINE OSCILLOGRAPH STRIP CHART RECORDERS

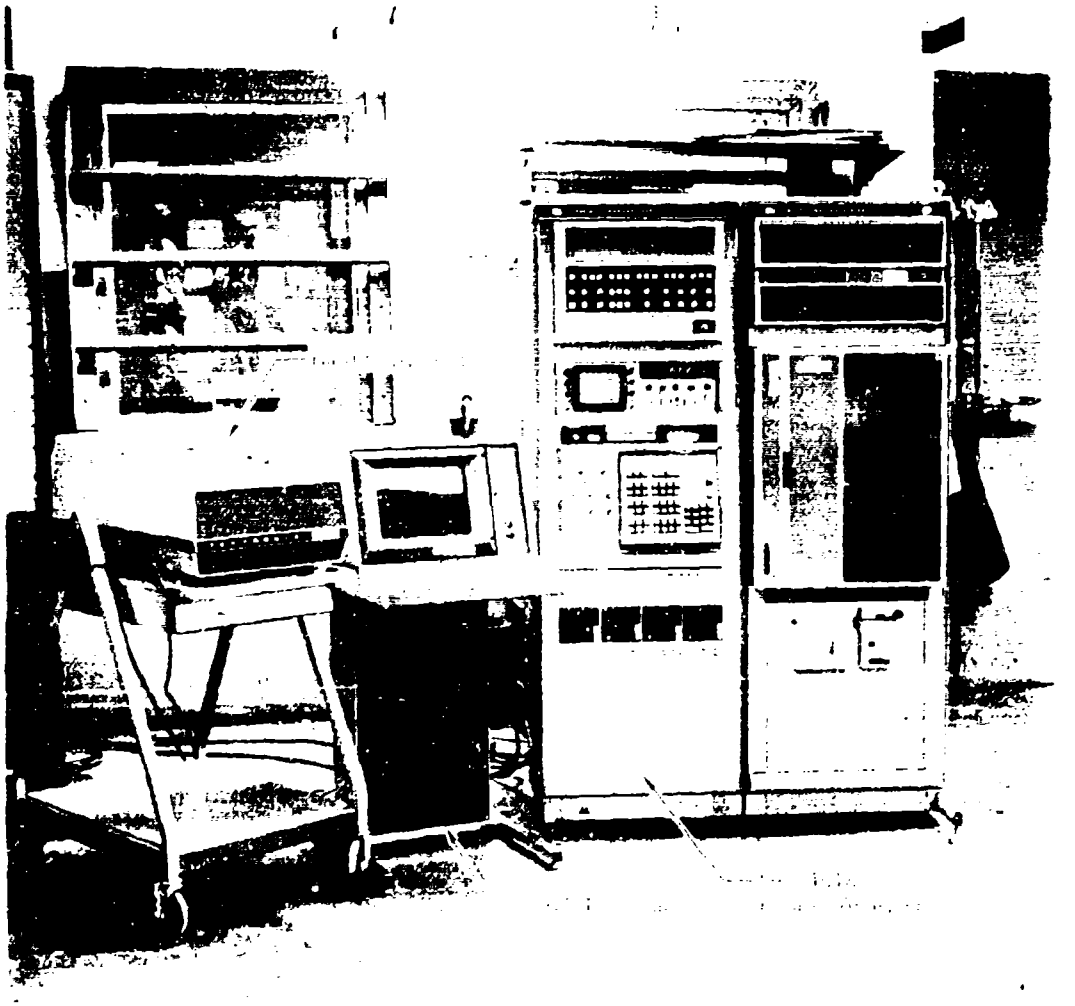

FIGURE 2-20
HEWLETT-PACKARD 5451B FOURIER TRANSFORM ANALYZER
FOR DYNAMIC DATA REDUCTION

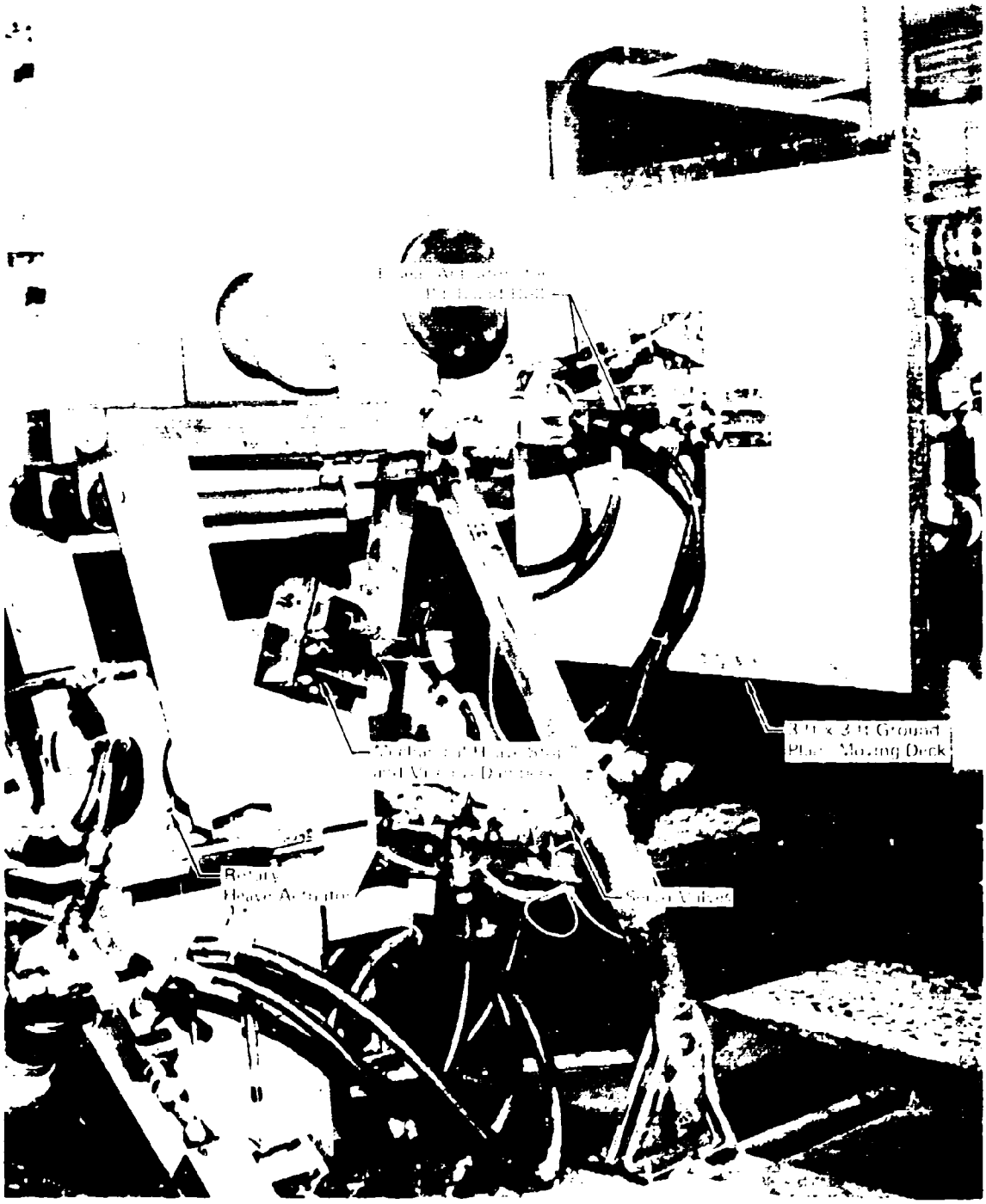

GP'8 0'29-20

FIGURE 2-21
DECK MOTION TEST APPARATUS

by a single 30 GPM, 3000 psi hydraulic pump with variable output pressure and flow rate. The ground plane and actuators are mounted on a movable support cart mounted on a track. During testing, the cart is securely anchored with bolt clamps through I-beams to the floor.

The ranges for the deck motions are as follows:

Heave, ±6 in (15.2 cm) at frequencies up to 3 Hz, with higher frequencies at lower amplitudes.

Translation, ±12 in (30.5 cm) maximum travel from a fixed neutral point. The neutral point can be varied over a 157 in (4bm) range by movement of the cart along the tracks.

Pitch, ±10° at frequencies up to 3 Hz.

Roll, ±15° at frequencies up to 3 Hz.

Derivation of these ranges and frequencies is discussed in Section 3.2.

The deck motion is controlled by an electronic control system consisting of a function generator for command inputs, servovalves for flow control, amplifier circuit boards, and potentiometers for position indication to a closed loop system. The control console is shown in Figure 2-22. The control system provides closed loop feedback position control for accurately repeatable motion, as described in Section 3.2.

The input command signals can be either a sine wave, square wave, ramp function, or sine wave superimposed on a ramp. The latter can be used to simulate take-offs and landings with the moving deck. The deck motion frequency and amplitude are independent variable inputs to the control system for the three degrees of freedom. To improve the static stiffness of the axes, a notch filter and a strain gage torsional load feedback circuit were incorporated into the control system. Lead and lag compensation circuits were used to adjust the phase relationships between multiple axis motions and to reduce position error.

Mechanical stops and microswitches are supplied to prevent the deck from striking the model. Such an impact would cause considerable damage to the model, force balance, and deck apparatus. The microswitches are installed on the pitch and roll actuators to sense an actuator overtravel and provide a signal to the control system which automatically drives the deck away to the neutral point and halts motion. The mechanical stops are designed with viscous dampers and rubber pads to absorb the kinetic energy of the moving deck.

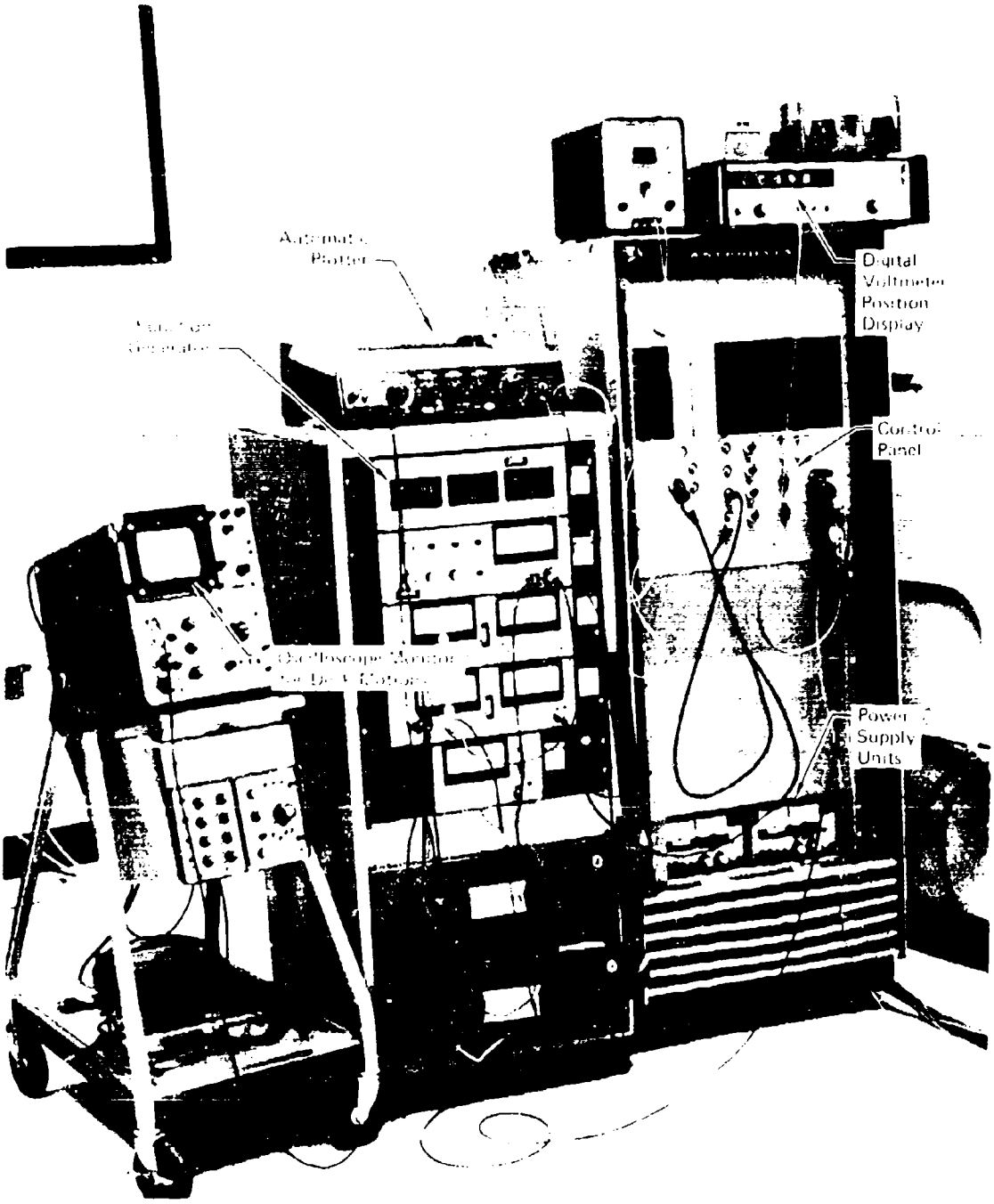

FIGURE 2-22
DECK MOTION CONTROL CONSOLE

GP78-0729-21

3. TEST PROGRAM

The test program was performed in the MCAIR Jet Interaction Test Apparatus. The test variables and ranges investigated, and the test procedures used are described below.

3.1 TEST VARIABLES - The primary test variables consisted of the model height above the deck and the deck heave, pitch, and roll amplitudes and frequencies. Additional test variables included the phase angle between two motions (e.g., between pitch and roll), the deck size, and the nozzle pressure ratios. These test variables are illustrated in Figure 3-1.

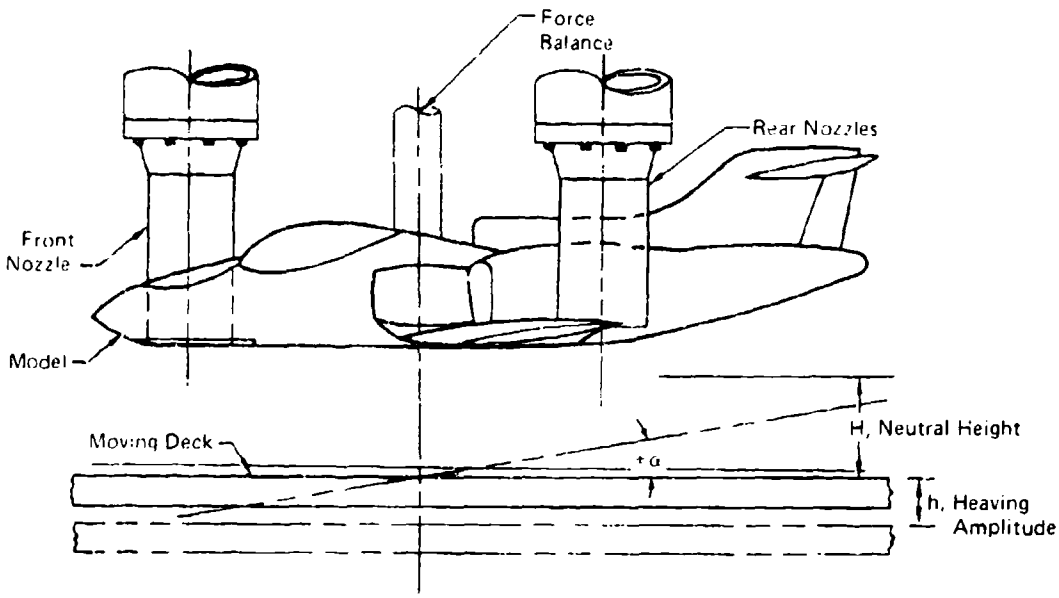

Test Variables	
Parameter	**Ranges**
Model Nozzle Height Above Deck, H/D_{je}	0.5 to 10 (100 cm)
Heaving Amplitude, h/D_{je}	0.5 ro 1.5 (15 cm)
Deck Pitch Angle, α (Aircraft Nose Up - Positive)	0 to $\pm 10^{o}$
Deck Roll Angle, γ (Aircraft Right Wing Down - Positive)	0 to $\pm 15^{o}$
Deck Heave, Pitch, and Roll Frequencies, f_h, f_α, f_γ	0 to 3 Hz
Dynamic Phase Angle, ϕ	0°, 90°
Nozzle Pressure Ratio, P_{t_j}/P_{amb}	1.1 to 4.4
Nozzle Pressure Bias Ratio, $P_{t_{jfront}}/P_{t_{jrear}}$	0 to 1.0
Ground Plane Size	0.91 m x 0.91 m, 1.83 m x 1.83 m

GP78-0895-25

FIGURE 3-1
TEST VARIABLES

Several model configuration variables were investigated for both the subsonic and supersonic V/STOL models. These variables included the degree of fuselage contouring, the number of nozzles and their arrangement, the wing height, and external appendages such as lift improvement devices. These model configuration variables are illustrated in Figures 3-2 and 3-3. The model configurations tested are defined in Figure 3-4. The test program is summarized in Figure 3-5. A detailed run summary is provided in Appendix A in Volume II.

Since the deck motion variables are unique to this program, a discussion of the derivation of the amplitudes and frequencies is felt necessary. The amplitudes and freqeuncies were derived by scaling typical ship responses to selected sea state conditions. The nominal design point was Sea State 3, moderate to rough seas, with significant wave heights of 4 feet (1.22 m) and 15 knot (27.8 km/hr) winds, Reference 1. For landing platforms aboard small ships, such as the DD963 class destroyer or the FF1052 frigate, the maximum full scale motions were estimated to be a heave of ±8 ft. (2.44 m) at a maximum velocity of 8 ft/sec (2.44 m/sec), a roll of ±10° with a period of 8 seconds, and a pitch of ±2° in 4.5 seconds. These amplitudes are in good agreement with computed values obtained from Reference 2. As can be seen from results of the Reference 2 computer program in Figure 3-6, the response of a DD963 class destroyer to typical sea conditions is somewhat random in nature, but at most given periods of time the response can be represented fairly well by a sine wave. The maximum amplitudes for the deck motion simulator were established by the maximum amplitudes indicated in Reference 2 and the tests were performed with constant amplitude, sinusoidal motions. To allow for variations in aircraft and ship headings and speeds, the full scale conditions selected for the design were a heave of ±10 ft (±3.05 m), a roll of ±15°, and a pitch of ±10° all with a period of 8 seconds.

The amplitudes are scaled by the nominal model scale factor. The frequencies, on the other hand, are scaled by the inverse of both the model scale factor and the ratio of the full scale jet velocity to the model jet velocity. This establishes flowfield similarity between the model and full scale conditions. The jet velocities differ only by the ratio of the square root of the

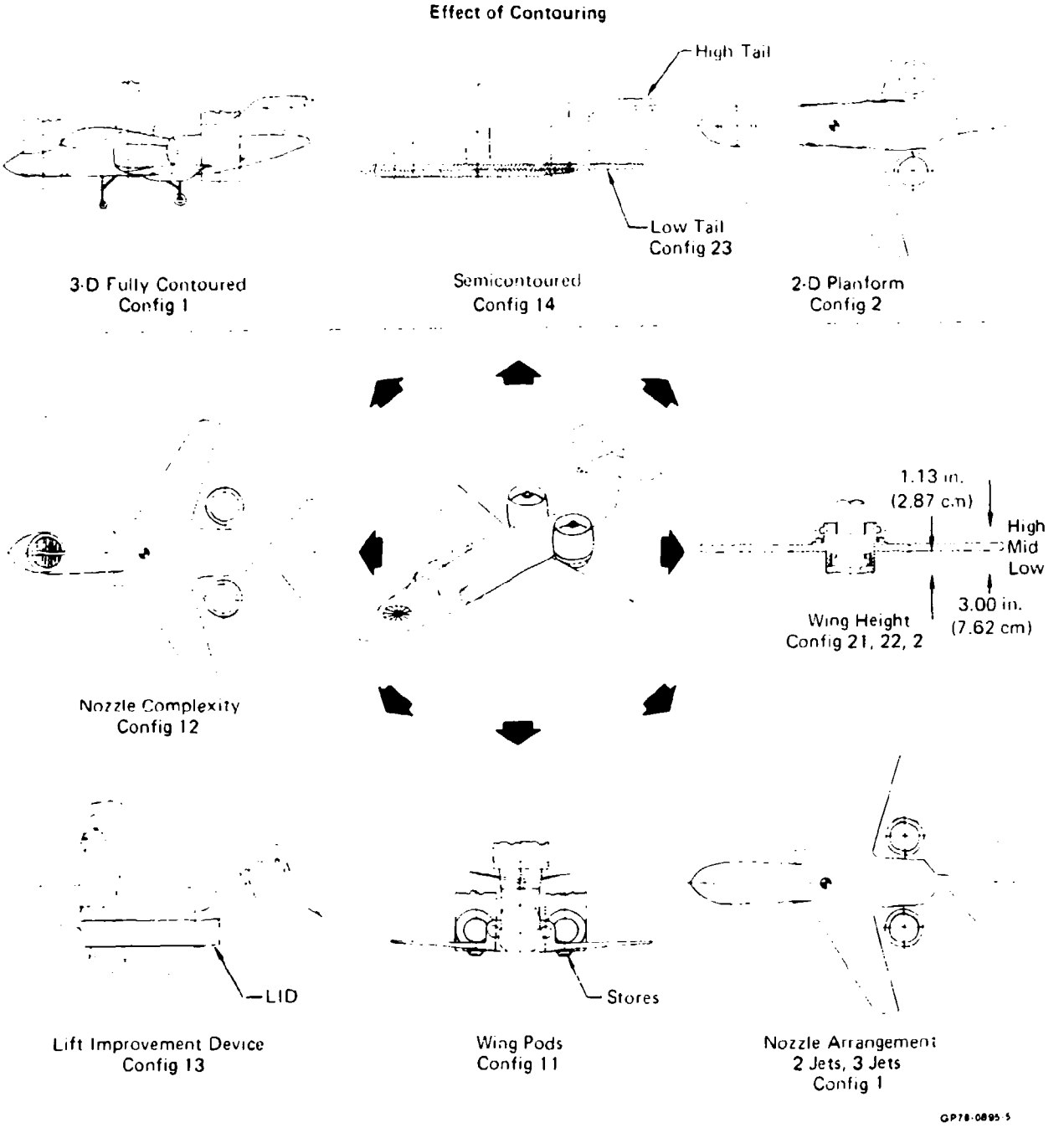

FIGURE 3-2
SUBSONIC V/STOL MODEL CONFIGURATION VARIABLES

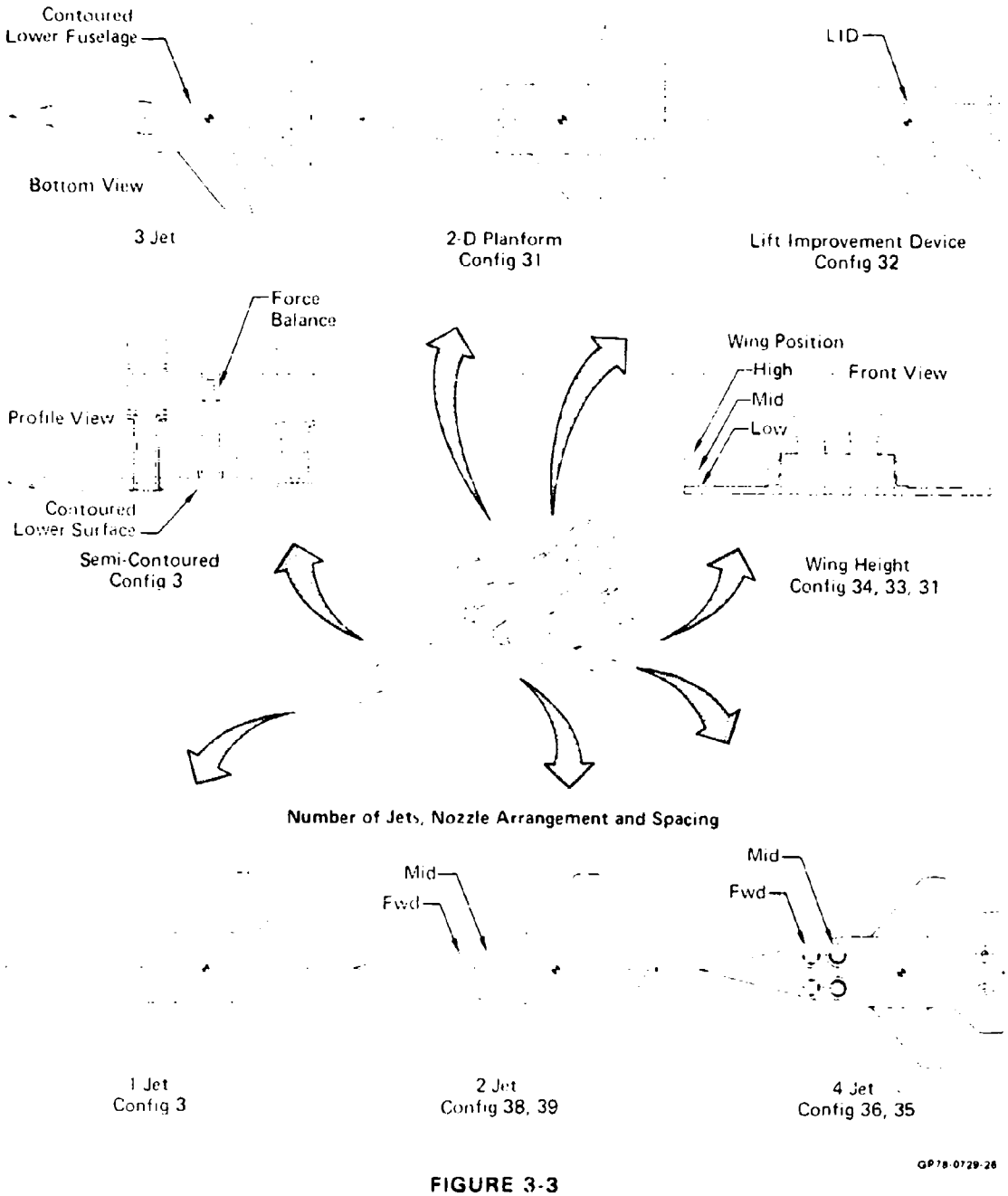

FIGURE 3-3
SUPERSONIC V/STOL MODEL CONFIGURATION VARIABLES

CONFIG. NO.	DESCRIPTION	NOZZLES NO.	NOZZLES TYPE	NOZZLES POSITION	WING	TAIL
Subsonic V/STOL:						
1	3-D Clean	3*	Fan	Mid	Low	High
11	3-D with Wing Pods	3	Fan	Mid	Low	High
12	3-D with Complex Nozzles	3	Fan	Mid	Low	High
13	3-D with 3 Sided LID	3	Fan	Mid	Low	High
14	Semi-Contoured	3	Fan	Mid	Low	High
2	2-D Clean	3	Fan	Mid	Low	High
21	2-D with High Wing	3	Fan	Mid	High	High
22	2-D with Mid Wing	3	Fan	Mid	Mid	High
23	2-D with Low Tail	3	Fan	Mid	Low	Low
4	Inner Region Plate	3	Fan	Mid	-	-
Supersonic V/STOL:						
3	Semi-Contoured	3*	1-Fan, 2-Jet	Mid	Low	Low
31	2-D Clean	3	1-Fan, 2-Jet	Mid	Low	Low
32	2-D with 3 Sided LID	3	1-Fan, 2-Jet	Mid	Low	Low
33	2-D with Mid Wing	3	1-Fan, 2-Jet	Mid	Mid	Low
34	2-D with High Wing	3	1-Fan, 2 Jet	Mid	High	Low
35	2-D Clean	4	2 Fan, 2 Jet	Mid	Low	Low
36	2-D Clean	4	2-Fan, 2-Jet	Forward	Low	Low
38	2-D Clean	2	2 Fan	Forward	Low	Low
39	2-D Clean	2	2 Fan	Mid	Low	Low

* Configuration also tested with only 1 front nozzle or 2 aft nozzles operating

FIGURE 3-4 CONFIGURATION SUMMARY

TEST VARIABLE	CONFIGURATION																		
	SUBSONIC										SUPERSONIC								
	1	11	12	13	14	2	21	22	23	4	3	31	32	33	34	35	36	38	39
HEIGHT	X	X	X	X	X	X	X	X	X	X	X	X	X	X	X	X	X	X	X
PITCH	X	X			X	X					X	X				X	X		X
ROLL	X	X	X	X	X	X	X			X	X	X	X		X	X	X	X	X
HEAVE MOTION	X	X	X	X	X	X	X	X		X	X	X	X	X	X	X	X	X	X
PITCH MOTION	X	X			X	X					X	X				X	X		X
ROLL MOTION	X	X	X	X	X	X	X			X	X	X	X		X	X	X	X	X
HEAVE FREQUENCY	X	X				X					X					X			X
PITCH FREQUENCY	X				X	X					X								
ROLL FREQUENCY	X				X	X					X					X			X
NOZZLE PRESSURE RATIO	X										X								
THRUST BIAS	X										X					X		X	X
FORWARD FAN	X										X								
LIFT CRUISE JETS	X																		
COMBINED MOTIONS	X					X					X								
SIMULATED TAKE-OFFS & LANDINGS	X										X								
GROUND PLANE SIZE	X																		

FIGURE 3-5 TEST PROGRAM SUMMARY

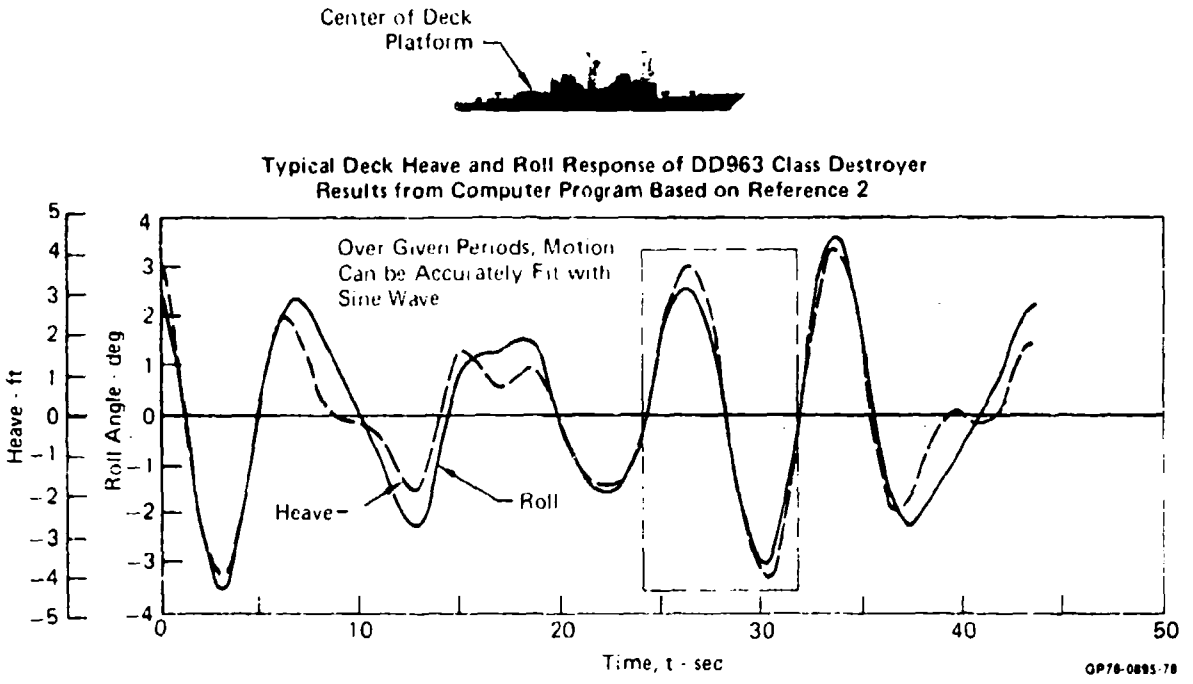

FIGURE 3-6
SHIP MOTION PREDICTIONS BASED ON REFERENCE 2

temperatures. Thus, for typical lift fan nozzle exit conditions where the full scale frequency of the motion may be 1/8 Hz, the model frequency required is:

$$f_{MS} = \frac{1}{\text{Scale Factor}} \cdot \frac{1}{\sqrt{T_{T_j}/T_{T_j}}_{FS}/_{MS}} \cdot f_{FS} = \frac{1}{.05} \frac{1}{\sqrt{700/560}}(1/8) = 2.2 \text{ Hz}$$

Deck motions were therefore nominally tested at 2 Hz with selected tests at 1 Hz and 3 Hz.

3.2 TEST PROCEDURES - The test procedures followed during the program were established to allow efficient integration of the static and dynamic testing.

Static Hover Testing - The jet conditions were first set at the desired nozzle pressure ratio, utilizing the automatic pressure valves and manometer. The deck position was then remotely positioned to the desired height and attitude, based on calibrations of the rotary potentiometer on the heave drive arm and the linear potentiometers on the pitch and roll actuators. Once the deck was properly positioned, the data acquisition cycle was initiated to acquire the force balance data and the pressure data. Static height, pitch, and roll surveys were obtained in discrete increments with the moving deck support cart set at a particular position.

To obtain data over the complete height range, three cart positions were required. Generally, the static and dynamic data were obtained in sequence at each cart position.

Dynamic Deck Motion Testing - Prior to establishing a particular deck motion, static hover data were obtained to provide a record of the test point in the computer printout as well as the nozzle thrust characteristics. These reference data were obtained with the deck at its neutral point. The deck motion was then established utilizing the electronic control system, calibrated potentiometers, peak voltage meters, and a calibrated oscilloscope. The motion in each of the deck's three degrees of freedom was also recorded on an oscillograph recorder for reference and to ensure uniform sinusoidal motion throughout each test run.

The electronic control system, shown schematically in Figure 3-7, was highly reliable and provided excellent control over the deck motion waveform since it was a closed loop system. Disturbances caused by nozzle thrust loads, friction, spurious electrical noise, and induced drag on the deck were essentially eliminated and smooth sinusoidal motions resulted. Examples of the output waveforms for heave, pitch, and roll are given in Figure 3-8.

Once a desired deck motion was established, the dynamic data acquisition cycle was initiated. This involved recording the force balance outputs, the deck motion potentiometer outputs, and a computer time code on two 14 track FM tape recorders. The analog data on the tapes were frequently checked to ensure that no data acquisition problems occurred.

At the beginning of the program, dynamic data were recorded for five minutes to determine the record length required for statistical analyses. Initial analysis revealed that approximately two minutes of data was sufficient. Further post test analyses indicated that since the dynamic induced force and moment data are basically either complex periodic or sinusoidal in nature, acquiring approximately 30 seconds of data would be adequate in future tests.

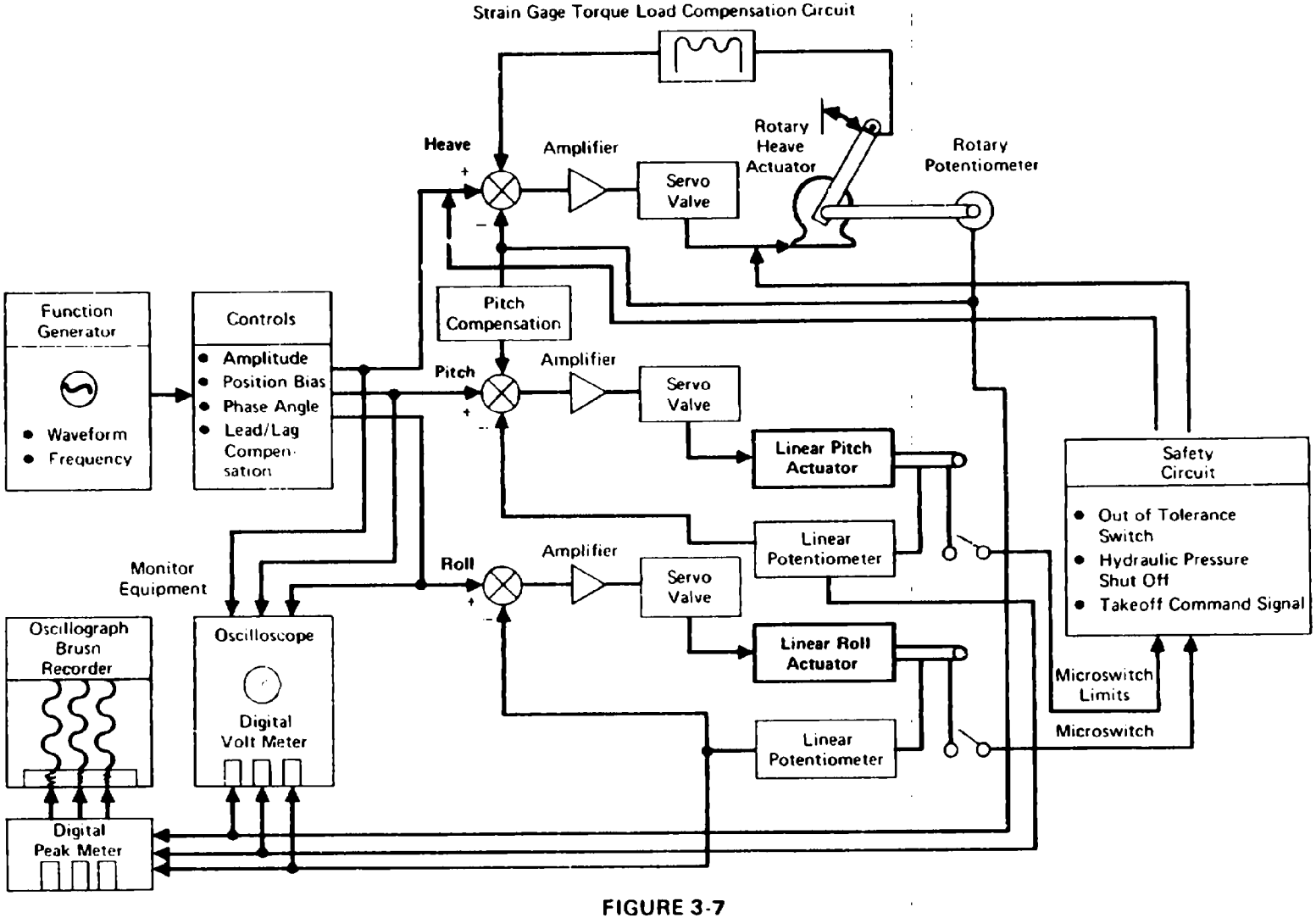

FIGURE 3-7
ELECTRONIC CONTROL SYSTEM

GPTA 0729-22

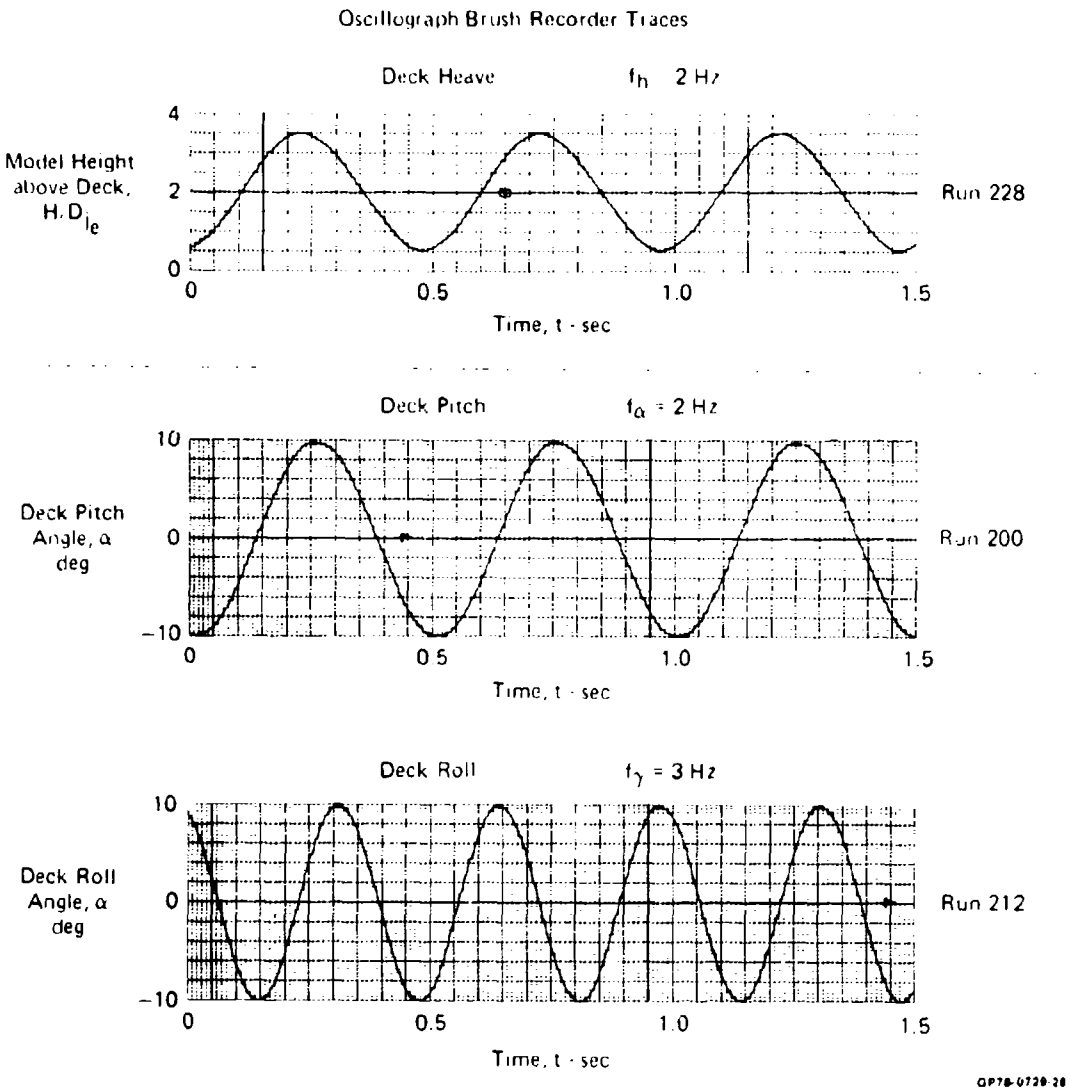

FIGURE 3-8
SAMPLE DECK MOTION OUTPUT WAVEFORMS

4. DATA REDUCTION AND REPEATABILITY

Jet-induced force and moment data were obtained at both static hover conditions and at conditions with deck motion. Due to the different means of acquiring the data at these conditions, significantly different procedures were used for data reduction. These procedures are discussed below.

4.1 STATIC HOVER DATA REDUCTION - For the static hover tests, data were recorded and conditioned as described in Section 3.1 on a Datum Model 120 DDAS. The digitized data were input to a Systems Engineering Laboratory Model 86 computer to calculate the induced forces and moments acting on the airframe. The computer program utilizes a second order force balance calibration consisting of a 6 x 6 coefficient matrix.

The lift was determined directly from the single axial force gage. The axial force and the pitching moment were determined from the two gages aligned parallel to the model centerline. The side force and the rolling moment were determined from the two gages perpendicular to the model centerline. The yawing moment was determined from the moment element gage. All moment computations use a representative center of gravity location for each model.

Following the basic force and moment computations, the results were non-dimensionalized by the thrust determined from the nozzle calibrations and the appropriate dimension as follows:

Induced Lift,

$$CFNS = \frac{\Delta L}{F_G}$$

Induced Axial Force,

$$CFAS = \frac{\Delta FA}{F_G}$$

Induced Pitching Moment,

$$CPMS = \frac{\Delta PM}{F_G \bar{c}}$$

Induced Side Force,

$$CFYS = \frac{\Delta FY}{F_G}$$

Induced Rolling Moment,

$$CRMS = \frac{\Delta RM}{F_G b}$$

Induced Yawing Moment,

$$CYMS = \frac{\Delta YM}{F_G b}$$

The model height above the deck was non-dimensionalized by the equivalent nozzle exit diameter which was computed as follows:

Equivalent Nozzle Diameter, $D_{j_e} = \sqrt{\frac{4\ A_T}{\pi}}$

where $A_T = \frac{\pi}{4} \sum_{j=1}^{K} (D_j)^2$ = Total combined exit area of all nozzles

D_j = Exit diameter of each nozzle

and K = Number of nozzles.

4.2 DYNAMIC DATA REDUCTION - As described in Section 3.1, the dynamic data were recorded in analog form on FM recorders. These data are input on command to a Hewlett-Packard 5451B Fourier Analyzer which digitizes the data to provide time histories or allow statistical computations.

For the dynamic data computations, the same basic equations defined in Section 4.1 were used to compute the induced lift, pitching moment, and rolling moment as functions of time. The balance response was more than adequate to cover the frequency range of interest (0 to approx. 20 Hz). To verify that the natural frequencies of the model/force balance system were above 20 Hz and therefore would not cause spurious signal interactions, a Spectral Dynamics Corporation Real Time Analyzer was used. As can be seen in Figure 4-1, the natural frequencies were above the range of interest.

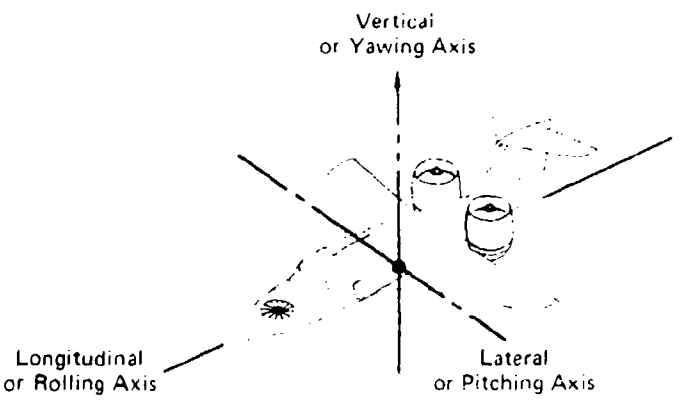

Acceleration Direction	Model Frequencies (Hz)		
	3-D Subsonic V/STOL Configuration 1	2-D Supersonic V/STOL - 3 Jet Configuration 31	2-D Supersonic V/STOL - 2 Jet Configuration 38
1. Vertical (Lift)	149.6	127.0	142.0
2. Lateral (Side)	33.8	25.6	26.4
3. Longitudinal (Axial)	40.4	20.2	20.6
4. Pitch	40.2	27.0	30.2
5. Roll	52.6	25.8	26.6
6. Yaw	25.6	15.6	26.6

QP78-0729-27

FIGURE 4-1
MODEL NATURAL RESONANCE FREQUENCIES

The basic statistical computations primarily utilized in this investigation were the power spectral density (PSD), and the cross power ctral density (CSD) which are defined in Figure 4-2. The auto correlation and the cross correlation were used to a limited extent but are also defined.

4.3 DATA REPEATABILITY - As discussed in Section 3.3, deck position, attitude, and motions were set precisely resulting in repeatable output force and moment data. An example of the repeatability of the static induced lift for the subsonic V/STOL configuration is presented in Figure 4-3. Typical repeatability of the dynamic induced lift data for a heaving deck is shown in Figure 4-4 for the supersonic configuration. Good repeatability is apparent for both the static hover and the dynamic data.

FUNCTION	EQUATION	PURPOSE
Auto Correlation, AC	$R_x(\tau) = \lim_{T\to\infty} \frac{1}{T} \int_0^T x(t)\, x(t+\tau)\, dt$ (time domain)	Describes the general dependence of the values of the data at one time on the values at another time, thus is a measure of the random nature of the characteristic waveforms
Power Spectral Density, PSD Fourier Transform of AC	$G_x(f) = 2 \int_{-\infty}^{\infty} R_x(\tau)\, e^{-j2\pi f\tau}\, d\tau$ (frequency domain)	Describes the general frequency composition and magnitude of the induced aerodynamic data in terms of the spectral density of the mean square value
Cross Correlation, CC	$R_{xy}(\tau) = \lim_{T\to\infty} \frac{1}{T} \int_0^T x(t)\, y(t+\tau)\, dt$ (time domain)	Describes the dependence of the values of set x data on set y data thus defining the degree of causality between the deck motions and the induced forces and moments
Cross Power Spectral Density, CSD Fourier Transform of CC	$G_{xy}(f) = \lvert G_{xy}(f)\rvert\, e^{-j\phi_{xy}(f)}$ where $\lvert G_{xy}(f)\rvert = \sqrt{C_{xy}^2(f) + Q_{xy}^2(f)}$ and $\phi_{xy}(f) = \tan^{-1}\left[\frac{Q_{xy}(f)}{C_{xy}(f)}\right]$ for $C_{xy}(f)$, the real cospectral density function and $Q_{xy}(f)$, the imaginary quadrature spectral density function (frequency domain)	Describes the common frequency composition between two sets of data and indicates the phase angle (i.e. lag time) between the input deck motions and the output induced aerodynamic response

FIGURE 4-2 DYNAMIC DATA REDUCTION FUNCTIONS

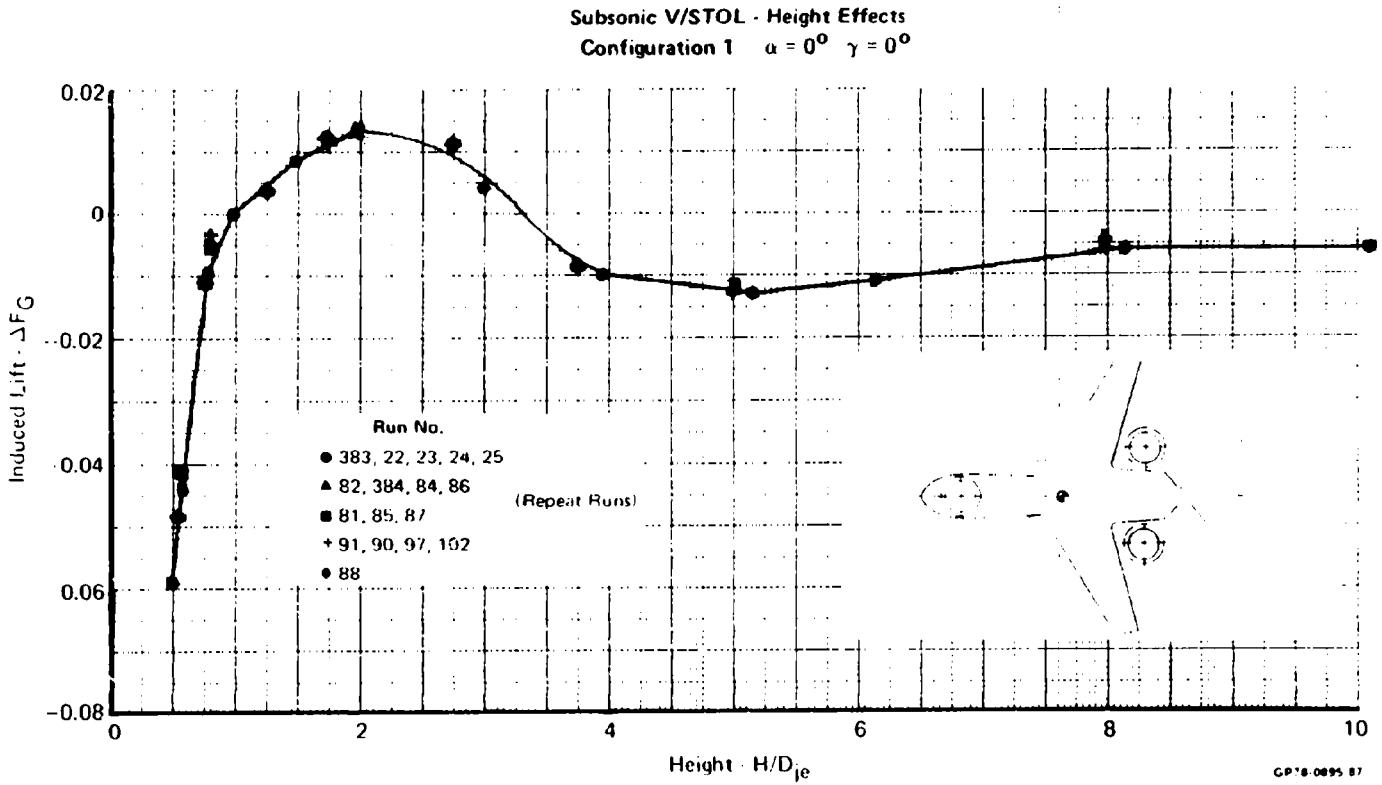

FIGURE 4-3
DATA REPEATABILITY AT STATIC HOVER CONDITIONS

Supersonic V/STOL Contiguration 3

$H/D_{je} = 3.27$ $h/D_{je} = \pm 1.0$ $f_h = 2$ Hz $\alpha = 0^o$ $\gamma = 0^o$

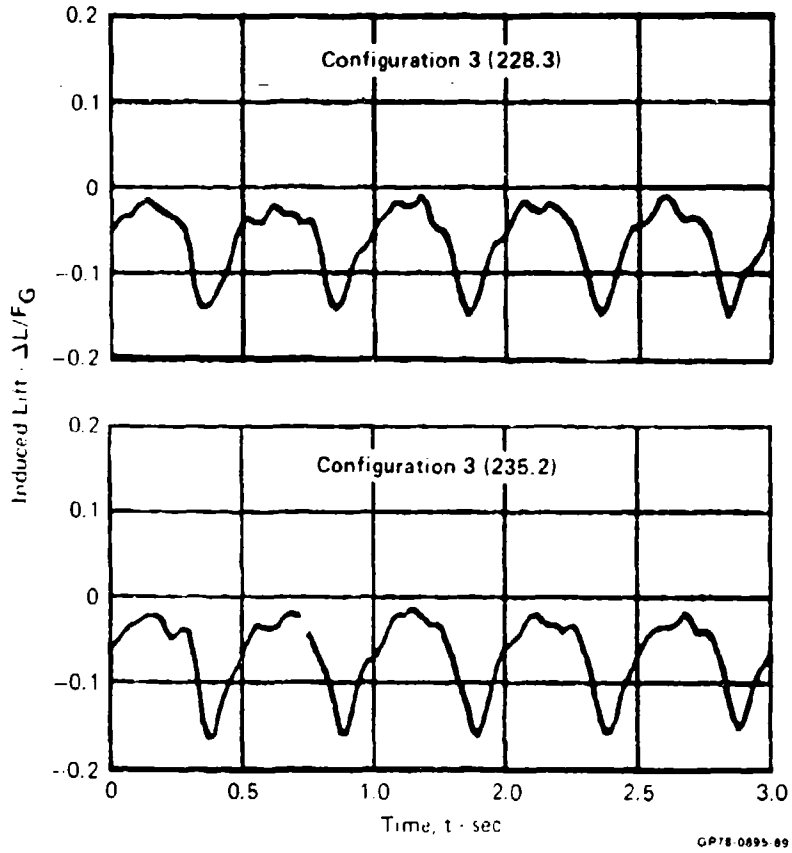

FIGURE 4-4
DYNAMIC DATA REPEATABILITY

5. DISCUSSION OF RESULTS

The jet-induced aerodynamics of V/STOL aircraft in hover over a moving deck were experimentally investigated. The effects of a number of V/STOL aircraft configuration variables applicable to subsonic and supersonic designs were evaluated parametrically, both at static hover and dynamic deck motion conditions. The data obtained at static hover conditions, which are presented in Section 5.1, indicate the general aerodynamic characteristics and serve as a basis of comparison for the data obtained with dynamic deck motion.

The dynamic force and moment data presented in Section 5.2 indicate the effects of deck heave, pitch, and roll on the induced forces and moments. The frequency content and the phase relationships between the sinusoidal deck motions and the aircraft responses are also discussed. Based on the static and dynamic data, V/STOL aircraft design and testing guidelines are defined. Empirical methods of predicting the dynamic response to deck motion are described in Section 5.3.

5.1 STATIC HOVER DATA - The jet-induced aerodynamic data obtained at static hover conditions at fixed heights and deck attitudes provide a significant technology base for evaluating V/STOL aircraft configuration effects as well as for indicating the basic jet induced aerodynamic trends which can be expected with deck motion.

Static hover data are presented for both subsonic and supersonic V/STOL configurations. Emphasis was placed on the induced lift characteristics since this is the critical performance parameter for V/STOL aircraft. However, induced pitching and rolling moment data are also presented as functions of height for the basic configurations and as functions of deck pitch and roll where the variations in the moments become significant. Measurements were also made of induced side force, axial force (drag), and yawing moment, but variations in these parameters were insignificant and are therefore not presented in Volume I. All of the static induced aerodynamic data are presented in plotted form in Appendix B in Volume II of this report.

5.1.1 Subsonic V/STOL Configuration - The basic advanced subsonic V/STOL aircraft configuration, shown in Figure 2-3, represents a three-nozzle, low wing vehicle with a forebody mounted lift fan, and two lift/cruise fans with tilt nacelles mounted over the wing. The configuration variables include model surface contour, nozzle arrangement, lift improvement devices (LID's), stores, wing height and nozzle vectoring vanes. The test variables include

height above the deck, deck pitch and roll angle, deck size, nozzle pressure ratio, and thrust bias.

Effect of Height - The jet-induced aerodynamic lift for the fully contoured (3-D), three nozzle subsonic V/STOL model is shown in Figure 5-1a. Close to the deck, near gear height, ground jet-induced entrainment causes a lift loss of approximately 3 percent of the net thrust. Further away from the deck, at a height of two equivalent nozzle diameters ($H/D_{je} = 2$, approximately 14 ft or 4.3m full scale), the induced lift peaks at about 1.5 percent lift gain. Out of ground effects (above 50 ft or 15.2m full scale), no fountain forms and only a minimal induced lift loss of 0.5 percent results from free-jet flow entrainment over the aircraft surfaces.

The relative strengths of the fountain and suckdown are clearly indicated in Figure 5-1b, where separate measurements of the fountain strength are shown from tests of an inner region plate model (Figure 2-7). Since the fountain upwash flow is concentrated in the inner region, i.e. the area bounded by the three nozzles, the induced lift in this region is representative of the fountain strength. An estimate of the suckdown forces is computed by subtracting the fountain force from the net induced lift measured with the complete airframe model. As shown in Figure 5-1b, this three nozzle arrangement has a moderately strong fountain which results in a peak lift gain of 5 percent at a height of 1.5 nozzle diameters.

Effect of Deck Pitch and Roll Angles - The induced lift and pitching moment for the 3-D model are shown in Figure 5-2 as a function of deck pitch angle. Close to the deck, induced lift and pitching moment vary significantly with pitch angle. Further away, at an H/D_{je} of 5 (35 ft or 10.7m full scale) and above, induced lift and pitching moment are insensitive to pitch angle.

Similarly, close to the ground induced lift and rolling moment vary significantly with deck roll angle, as shown in Figure 5-3. As with pitch, roll angle has little effect at a height of five diameters and above.

Effect of Deck Size - As described in Section 3, two ground planes were used to simulate two different sizes of ship decks, one 3 x 3 ft (0.91 x 0.91m) representing the small landing platform on a DD963 class destroyer and the other 6 x 6 ft (1.83 x 1.83m) representing the landing deck on a conventional aircraft carrier.

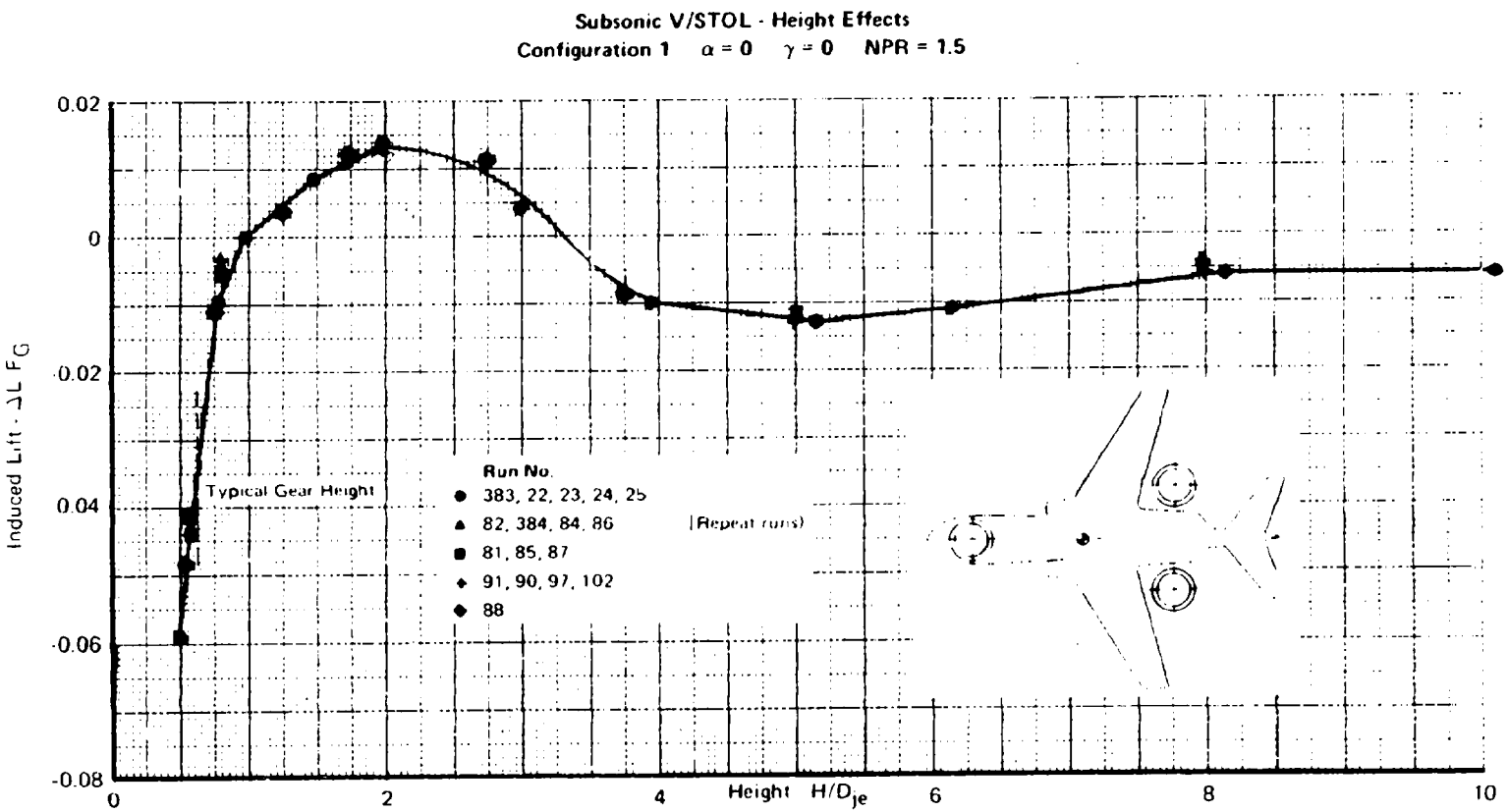

a) Total Induced Lift

FIGURE 5-1
SUBSONIC V/STOL STATIC HEIGHT EFFECTS

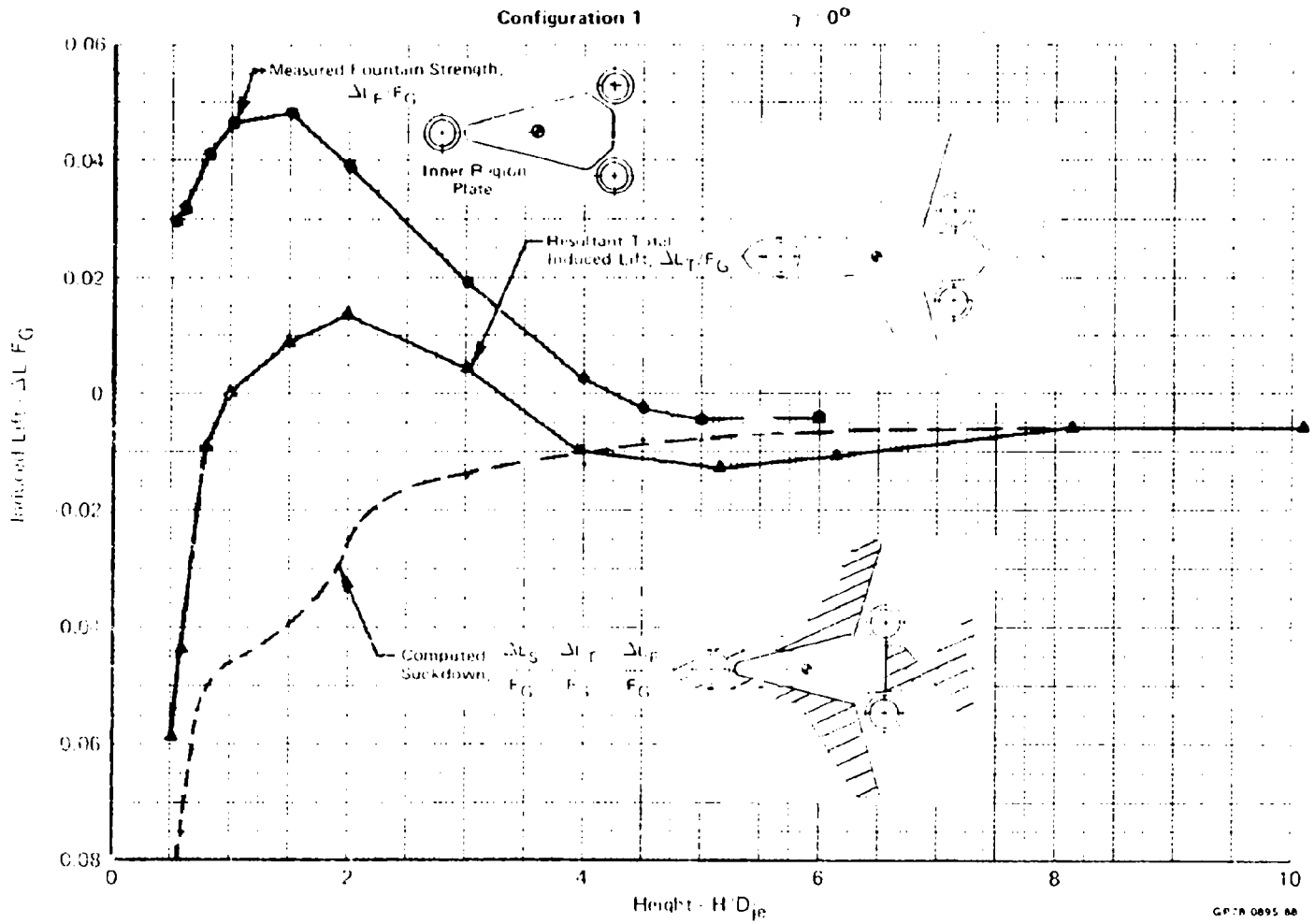

(b) Fountain Strength and Computed Suckdown

FIGURE 5-1 (Concluded)
SUBSONIC V/STOL STATIC HEIGHT EFFECTS

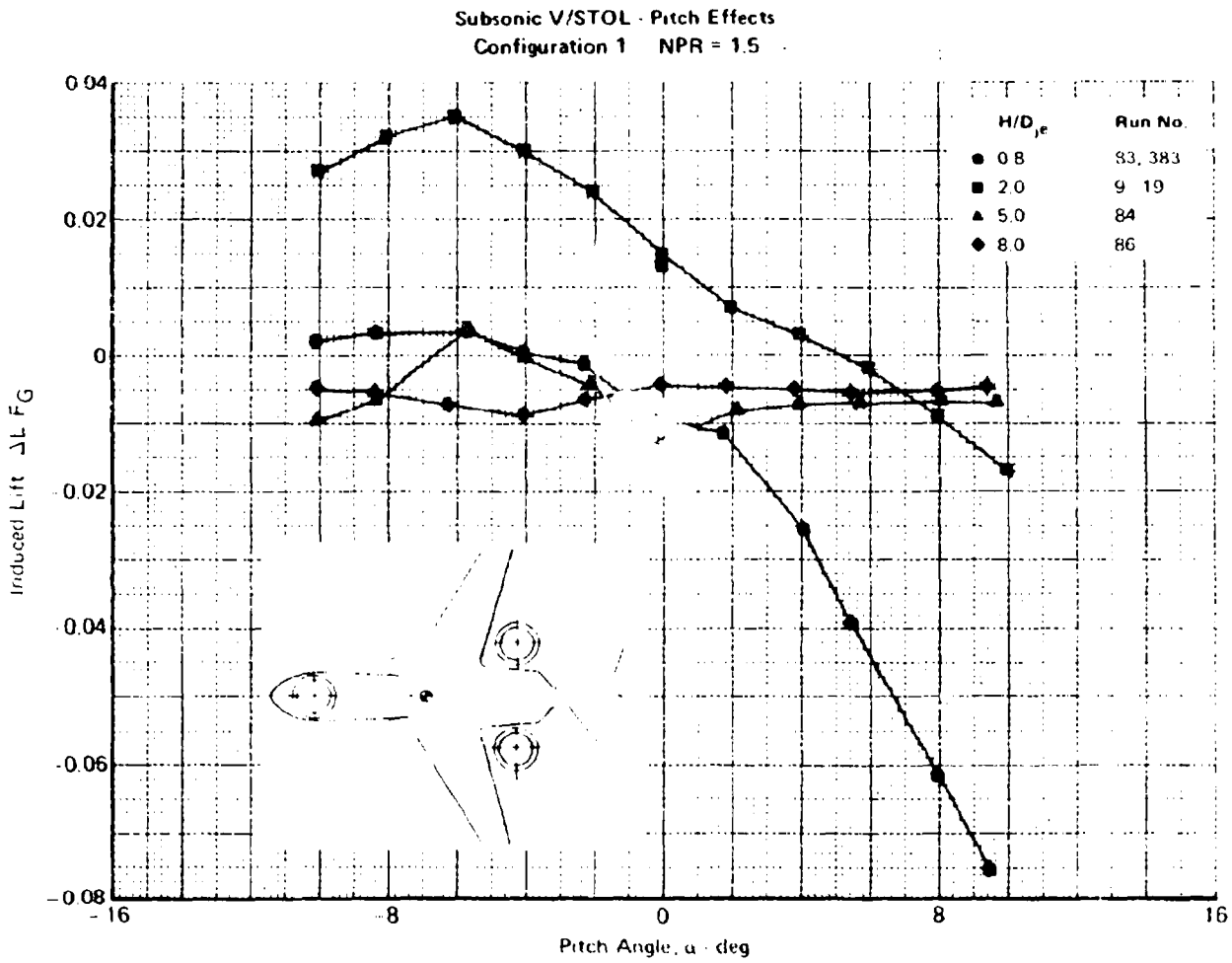

a) Induced Lift

GP78-0895-118

FIGURE 5-2
SUBSONIC V/STOL STATIC PITCH EFFECTS

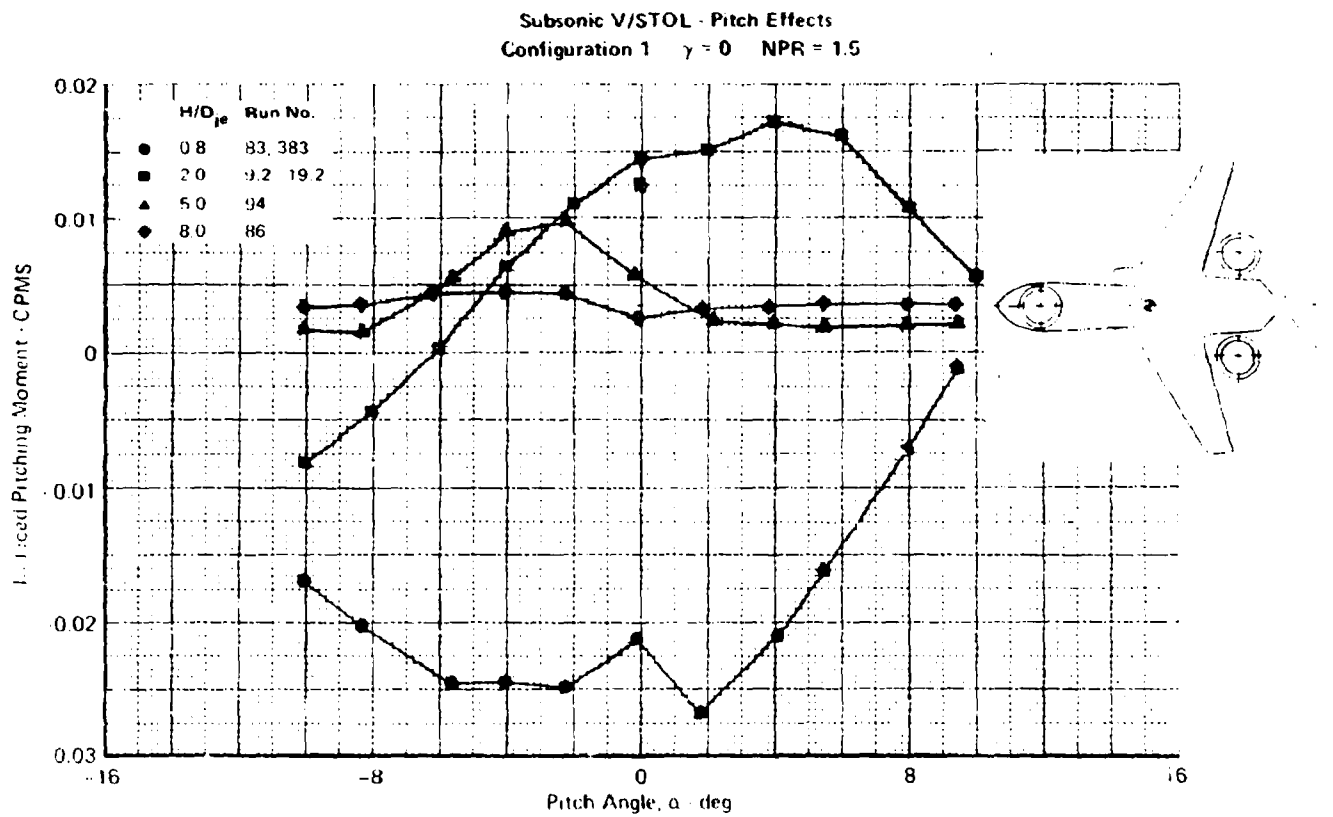

b) Induced Pitching Moment

FIGURE 5-2 (Concluded)
SUBSONIC V/STOL STATIC PITCH EFFECTS

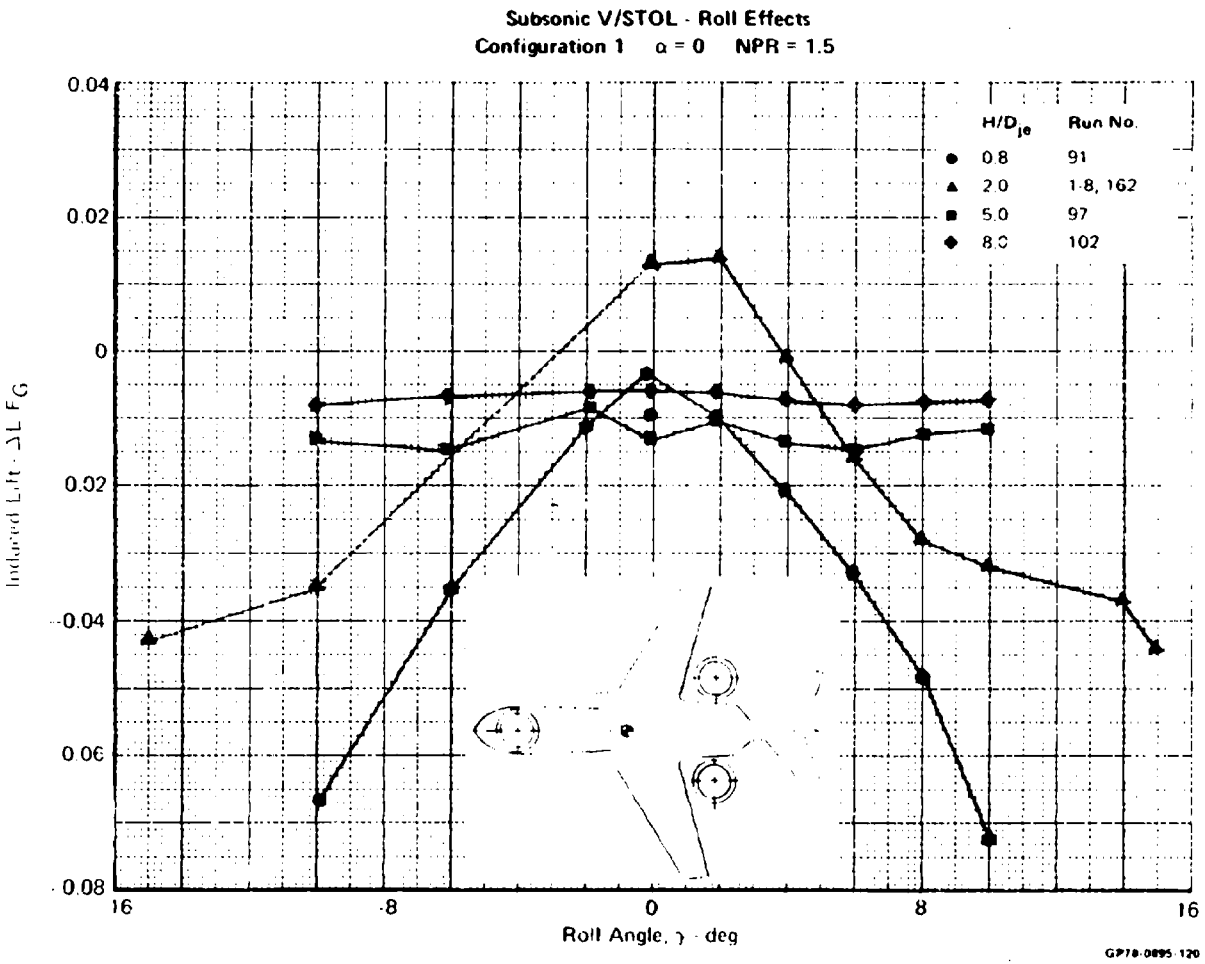

a) Induced Lift

FIGURE 5-3
SUBSONIC V/STOL STATIC ROLL EFFECTS

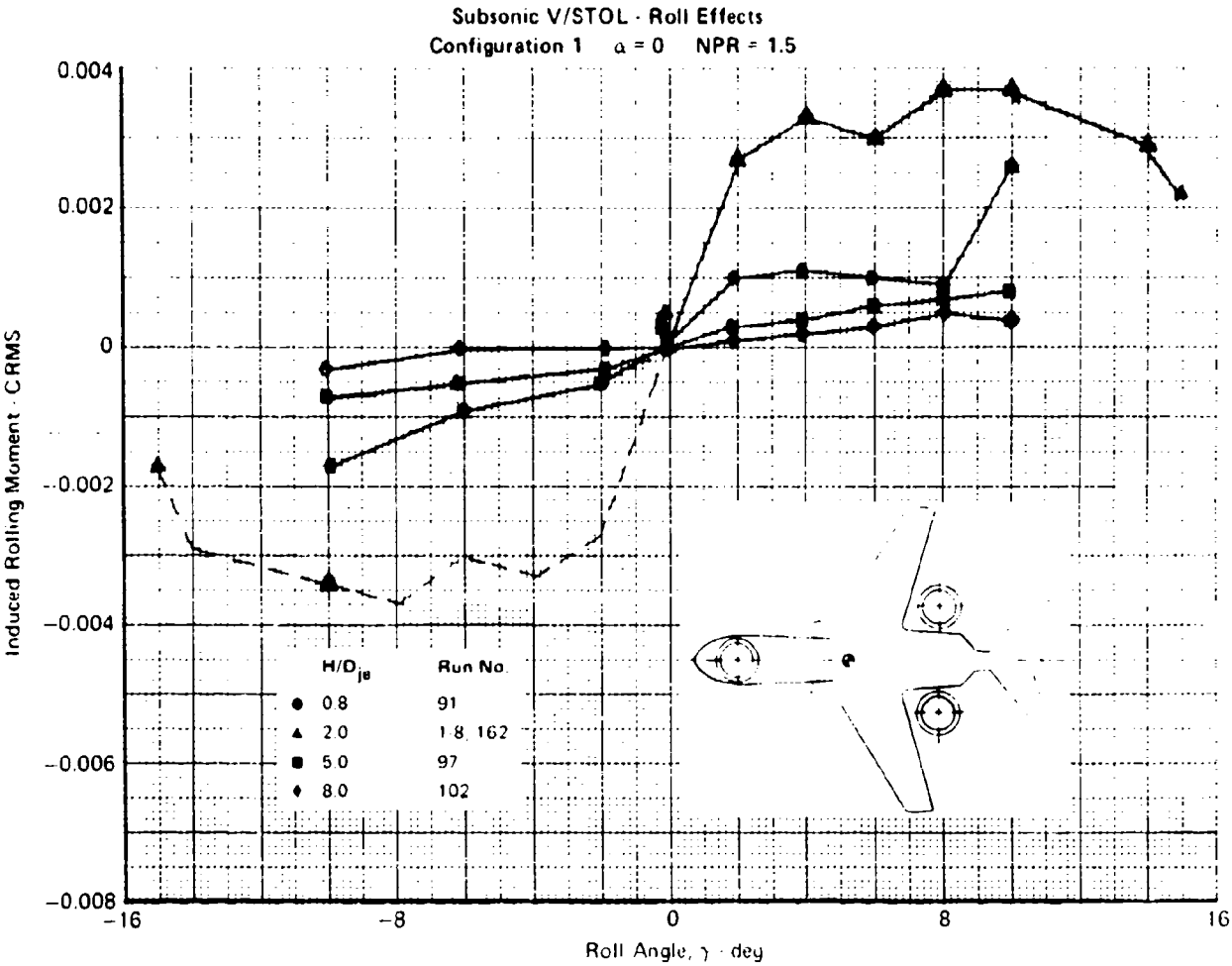

b) Induced Rolling Moment

QP78-0895-121

FIGURE 5-3 (Concluded)
SUBSONIC V/STOL STATIC ROLL EFFECTS

At static hover, the deck size has little effect on the induced lift, as shown in Figure 5-4. This is also the case at various discrete deck roll and pitch angles as well as for the responses to dynamic deck motion. These data are presented in the Appendices B and C in Volume II.

For this program, the aircraft models were centered directly over the deck. Thus, the impinging jet flows and subsequent recirculating flowfields were similar for both deck sizes. Other interactions may be more significant for the small landing platform due to the proximity of the superstructure and the greater likelihood that all of the jets do not impinge directly on the deck surface. Since the small deck offers more potential problems affecting V/STOL operations, the 3 x 3 ft deck was used for the majority of the tests.

Effect of Model Surface Contouring - An important objective of this investigation was to determine the degree of configuration simulation required for jet/lift interaction testing. The subsonic configuration was tested (1) as a fully contoured model, (2) as a semi-contoured half model with contoured lower fuselage and raised tail, and (3) as a simplified 2-D planform model. The results shown in Figure 5-5, indicate the effects of body contour details on the induced lift.

Similar trends are indicated in the data for each of these models, with the peak induced lift occurring at nearly the same height. However, the planform models have a significantly higher induced lift in ground effect. The semi-contoured model has a higher induced lift near gear height, but at 1.5 nozzle diameters and above the results agree with the fully contoured model. A contouring effect is apparent on the planform models up to an H/D_e of 5.

Company funded studies performed on a similar planform model instrumented with numerous surface pressure taps, Reference 3, showed that most of the fountain force is concentrated between the two rear nozzles rather than near the central fountain region. Thus, the increment between the induced lift of the 3-D and planform models is attributed to differences in contouring in the region of fountain impingement. The 3-D model has upward curvature in this region, thus producing a weaker force than on the planform model. The semi-contoured model has a portion of this region contoured and thus provides better agreement with the 3-D model. These results indicate that although a simple planform model can be used in low cost configuration screening tests, some form of contoured model is required for obtaining accurate induced aerodynamic data in ground effect.

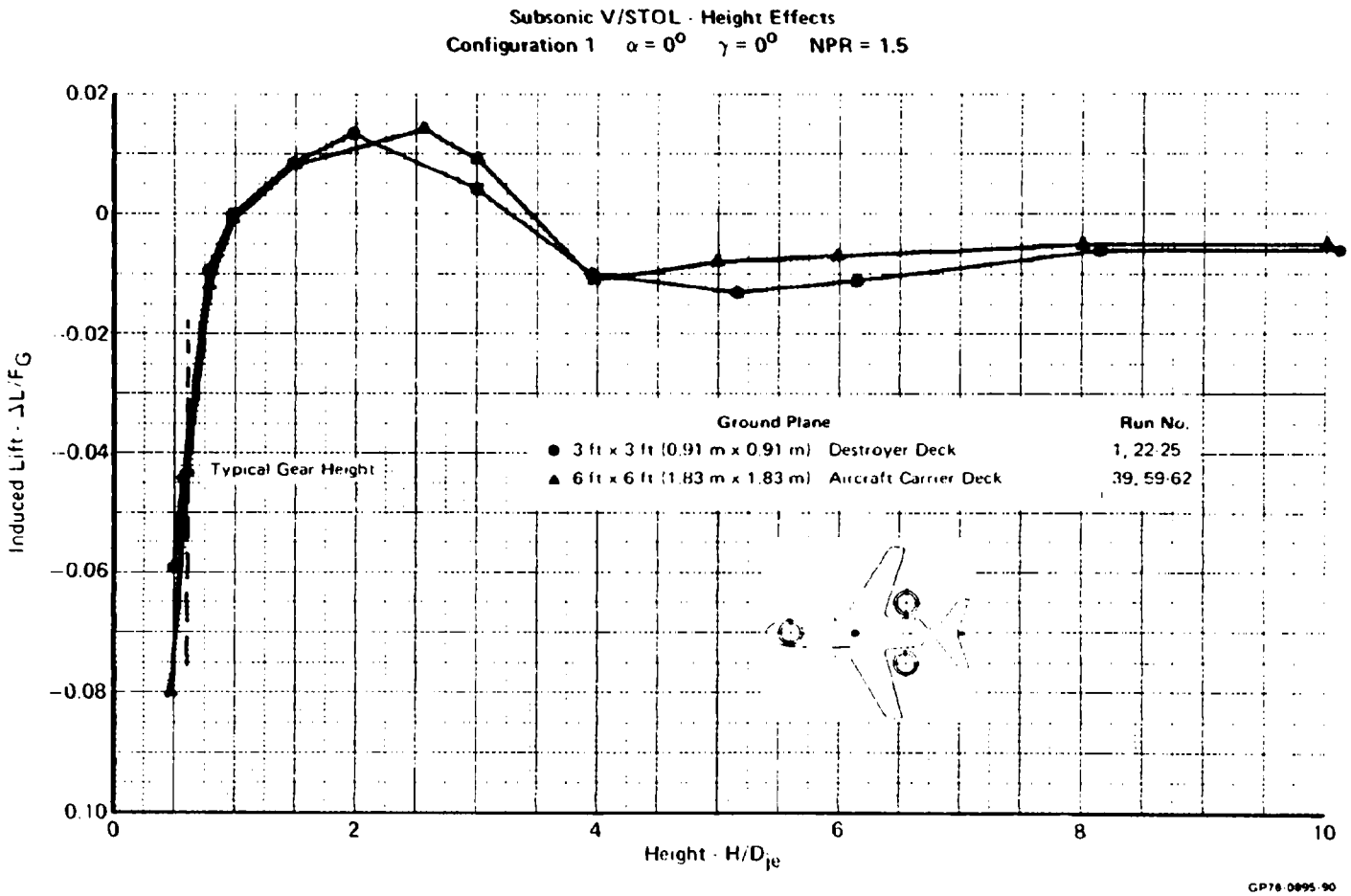

FIGURE 5-4
EFFECT OF DECK SIZE

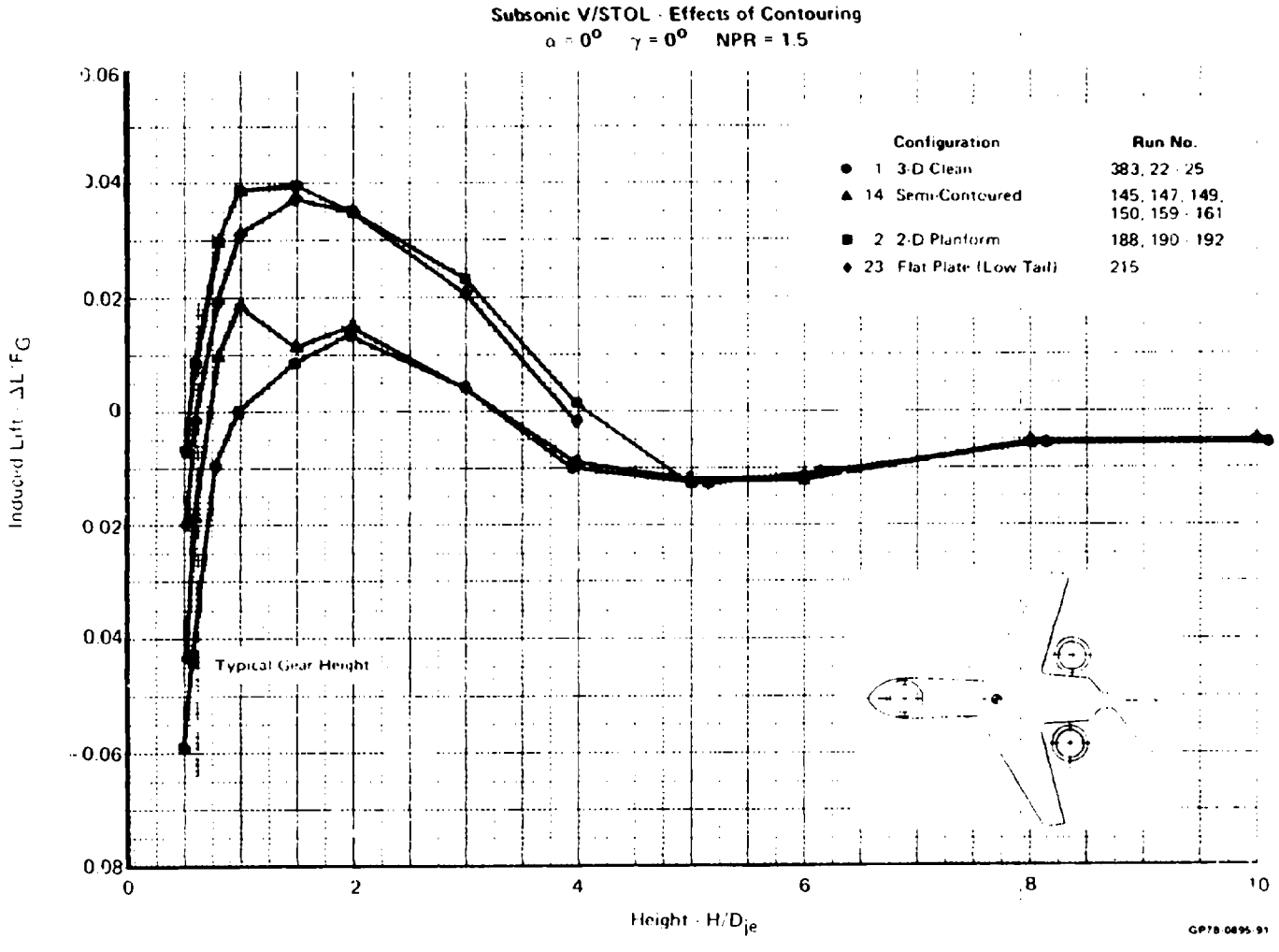

FIGURE 5-5
SUBSONIC V/STOL CONTOURING EFFECTS

On the planform model, testing was conducted with the horizontal tail in the same plane as the wing and fuselage and also in an elevated plane, as on the contoured models. Placing the horizontal tail in the lower plane reduces the induced lift. This is attributed to a slight increase in suckdown on the aft-end due to the proximity of the tail to the rear nozzles. The necessity of placing the wings and tails in the proper plane on a planform model is therefore believed to be dependent on the location of the nozzles relative to these surfaces.

Effect of Lift Improvement Devices and Stores - The fountain upwash momentum can be effectively converted to positive lift on the airframe through the use of properly designed lift improvement devices (LID's) mounted on the lower fuselage, as shown in Figure 5-6. The LID's act to stagnate the impinging fountain flow and redirect it downward, providing an increased lift up to an H/D_{je} of about 2. Near the deck, where lift is especially critical to V/STOL aircraft mission performance, the LID's improve the induced lift dramatically, more than 10 percent. Although a V/STOL aircraft cannot perform a VTO with more payload than it can hover with out of ground effect (OGE), the substantial lift gain can be used to provide rapid acceleration through the ground effects region and to offset any adverse effects, such as result from exhaust gas ingestion. To minimize the drag penalty in wing-borne flight, the lateral fence of the LID could be retractable.

The LID's are also effective even at high roll angles as shown in Figure 5-7. The induced lift remains positive over most of the range indicating that the LID span is sufficient to capture the majority of the fountain. As shown in Figure 5-8, the rolling moment is adversely affected at an $H/D_{je} = 0.8$, presumably due to the impingement of the fountain on the longitudinal strakes.

Pods were installed along the lower wing surfaces to simulate aircraft stores. These improved the induced lift, but only near the deck, as shown in Figure 5-9. The pods trap the fountain upwash flow in a manner similar to LID's, but there is no lateral fence to contain the flow. Also, the pods tested do not extend between the two rear nozzles, where the highest fountain momentum exists.

Effect of Wing Height - Increasing the wing height on the planform model increases the induced lift 2 to 3 percent close to the deck, as shown in Figure 5-10. This is attributed to a reduction in suckdown on the wing surface. It should be noted that the nozzle exit plane remained constant in

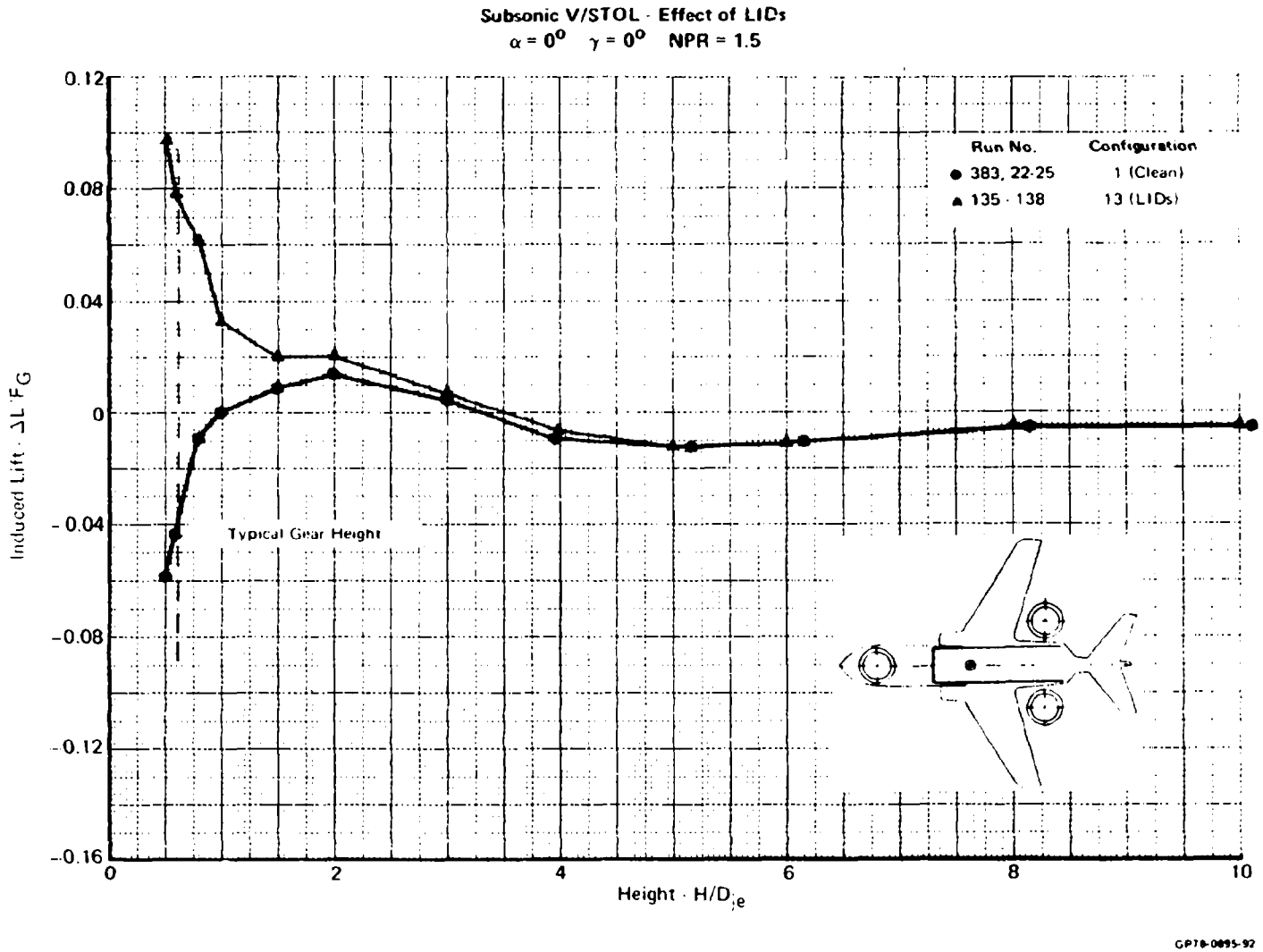

FIGURE 5-6
SUBSONIC V/STOL WITH LIFT IMPROVEMENT DEVICES

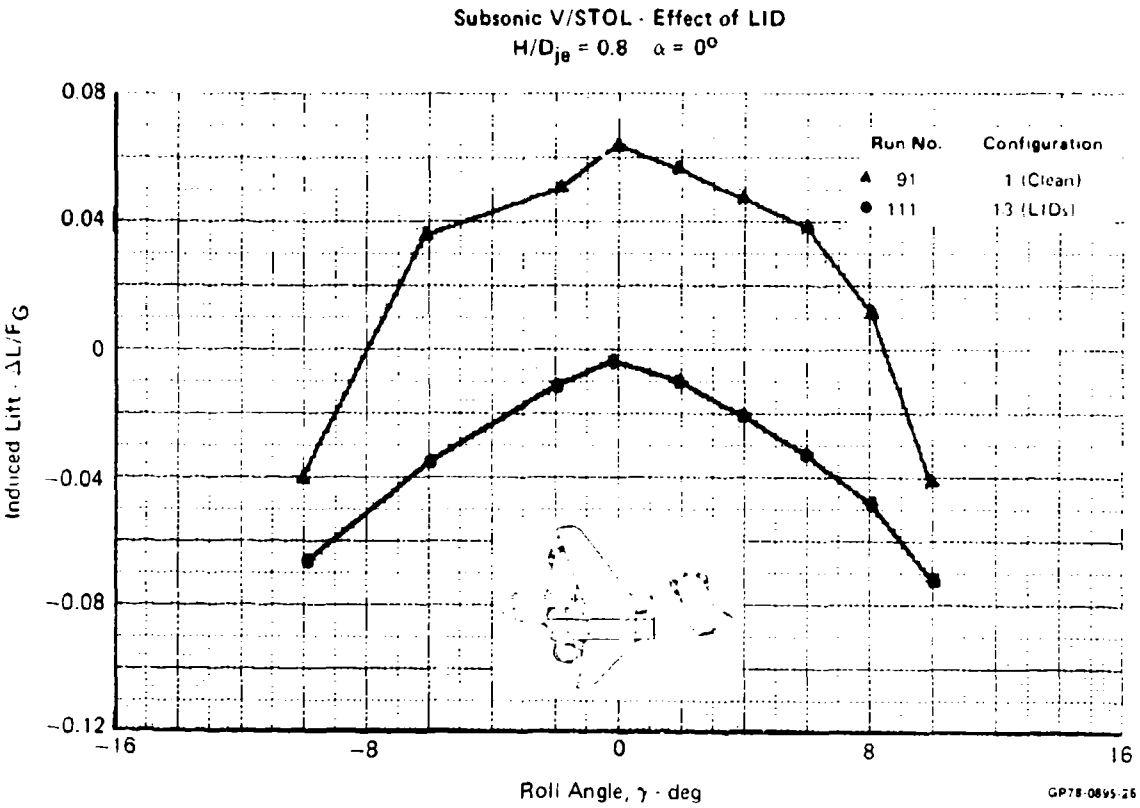

(a) $H/D_{je} = 0.8$

FIGURE 5-7
SUBSONIC V/STOL ROLL EFFECTS ON INDUCED LIFT WITH LIFT IMPROVEMENT DEVICES INSTALLED

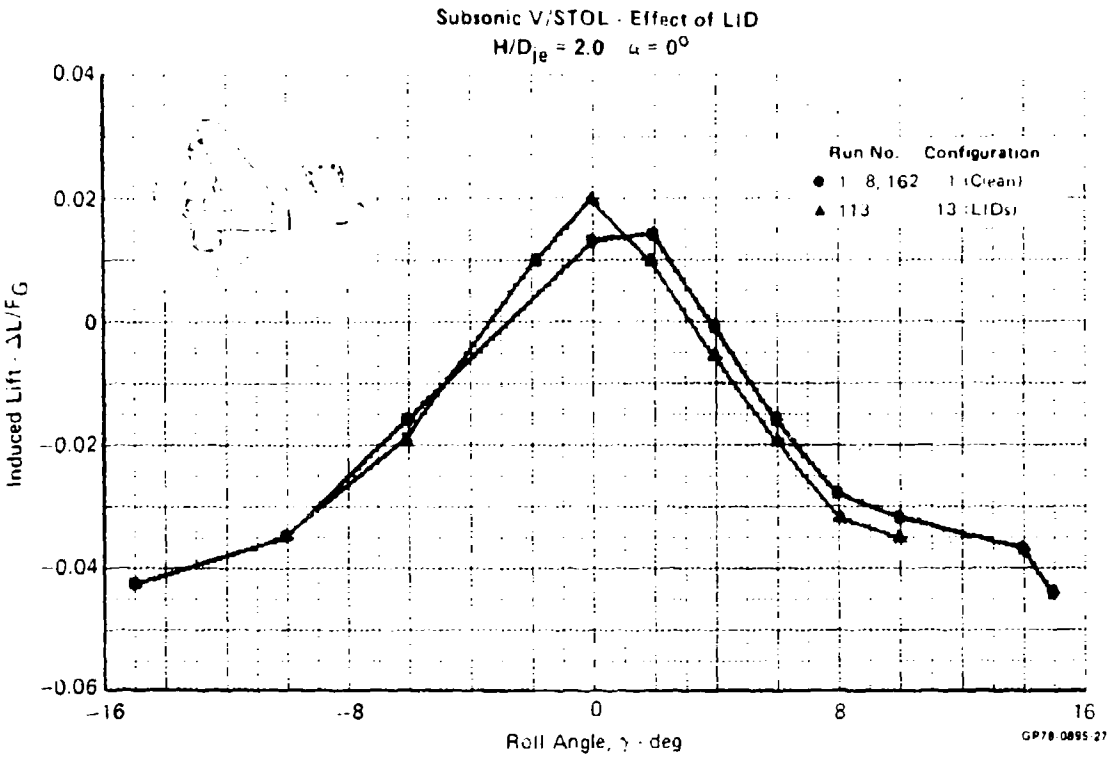

(b) H/D$_{je}$ = 2.0

FIGURE 5-7 (Concluded)
SUBSONIC V/STOL ROLL EFFECTS ON INDUCED LIFT WITH LIFT IMPROVEMENT DEVICES INSTALLED

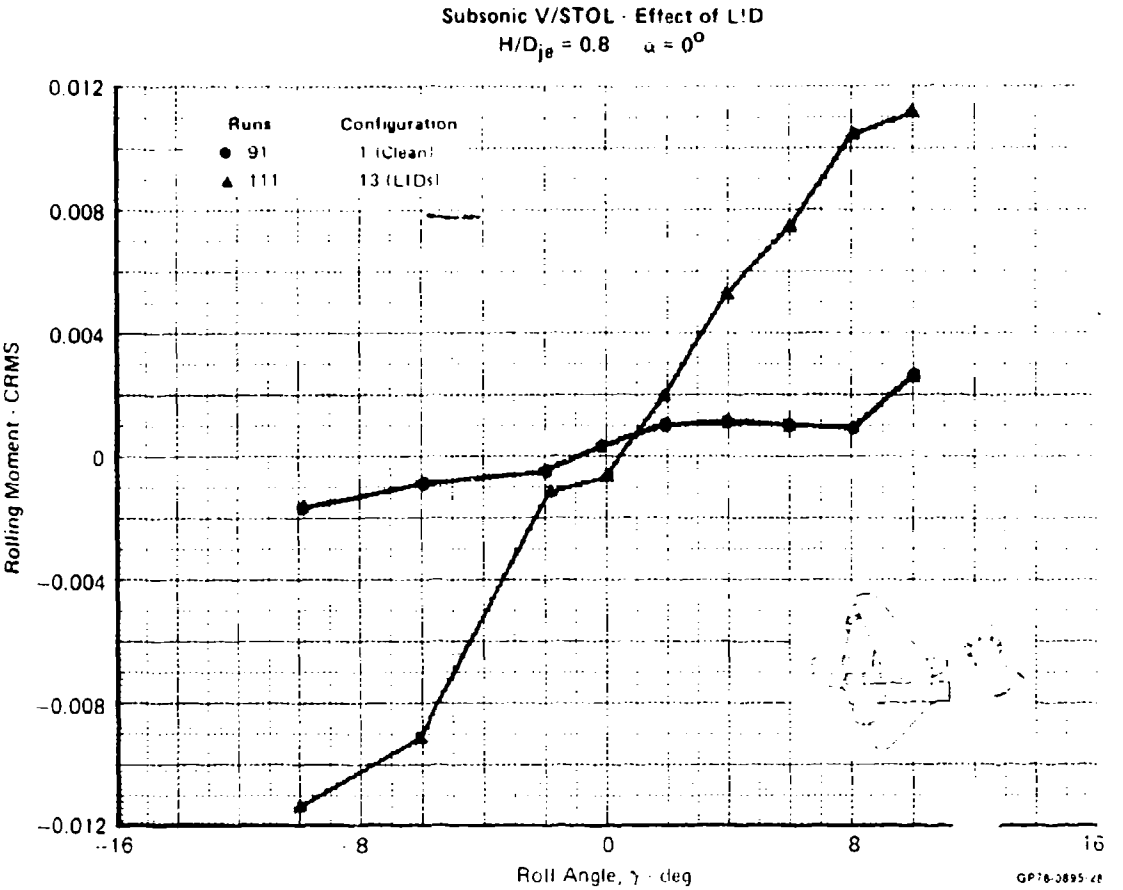

(a) $H/D_{je} = 0.8$

FIGURE 5-8
SUBSONIC V/STOL ROLL EFFECTS ON INDUCED ROLLING MOMENT WITH LIFT IMPROVEMENT DEVICES INSTALLED

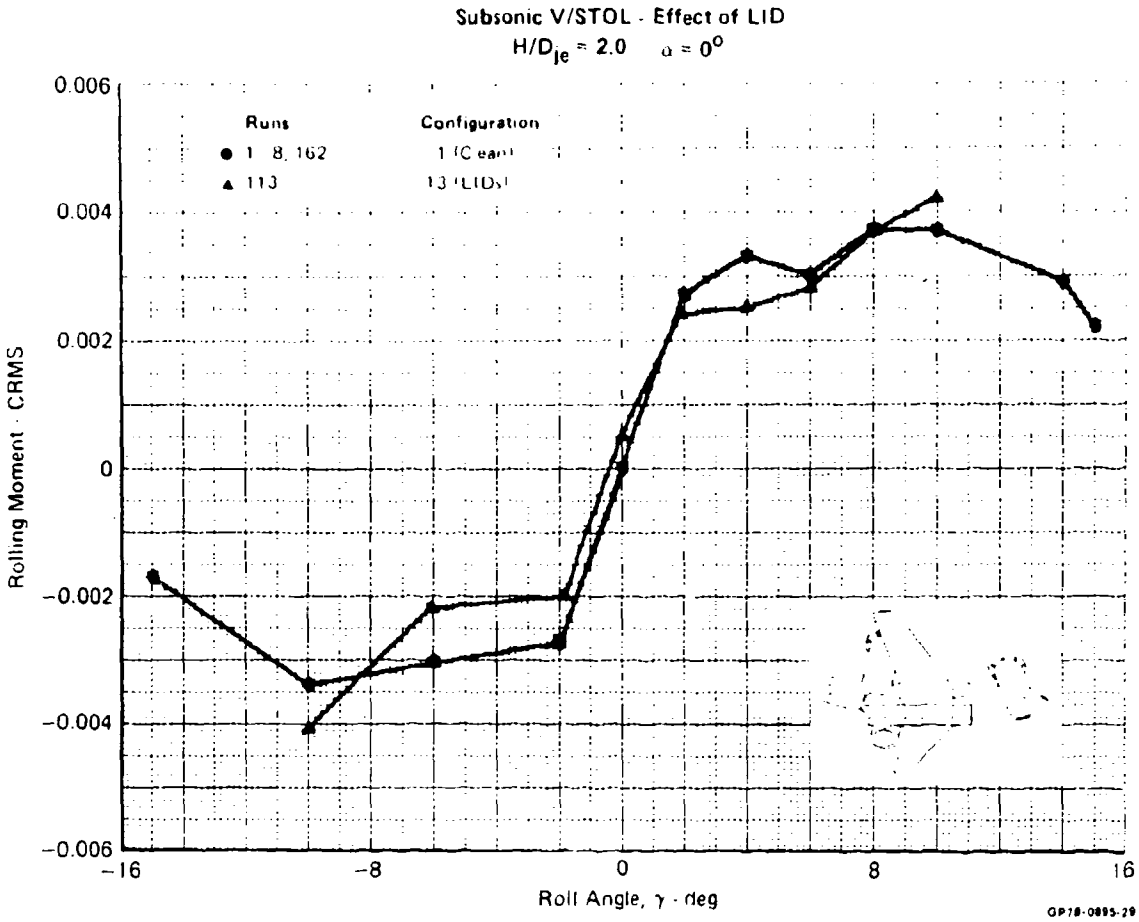

(b) $H/D_{je} = 2.0$

FIGURE 5-8(Concluded)
SUBSONIC V/STOL ROLL EFFECTS ON INDUCED ROLLING MOMENT WITH LIFT IMPROVEMENT DEVICES INSTALLED

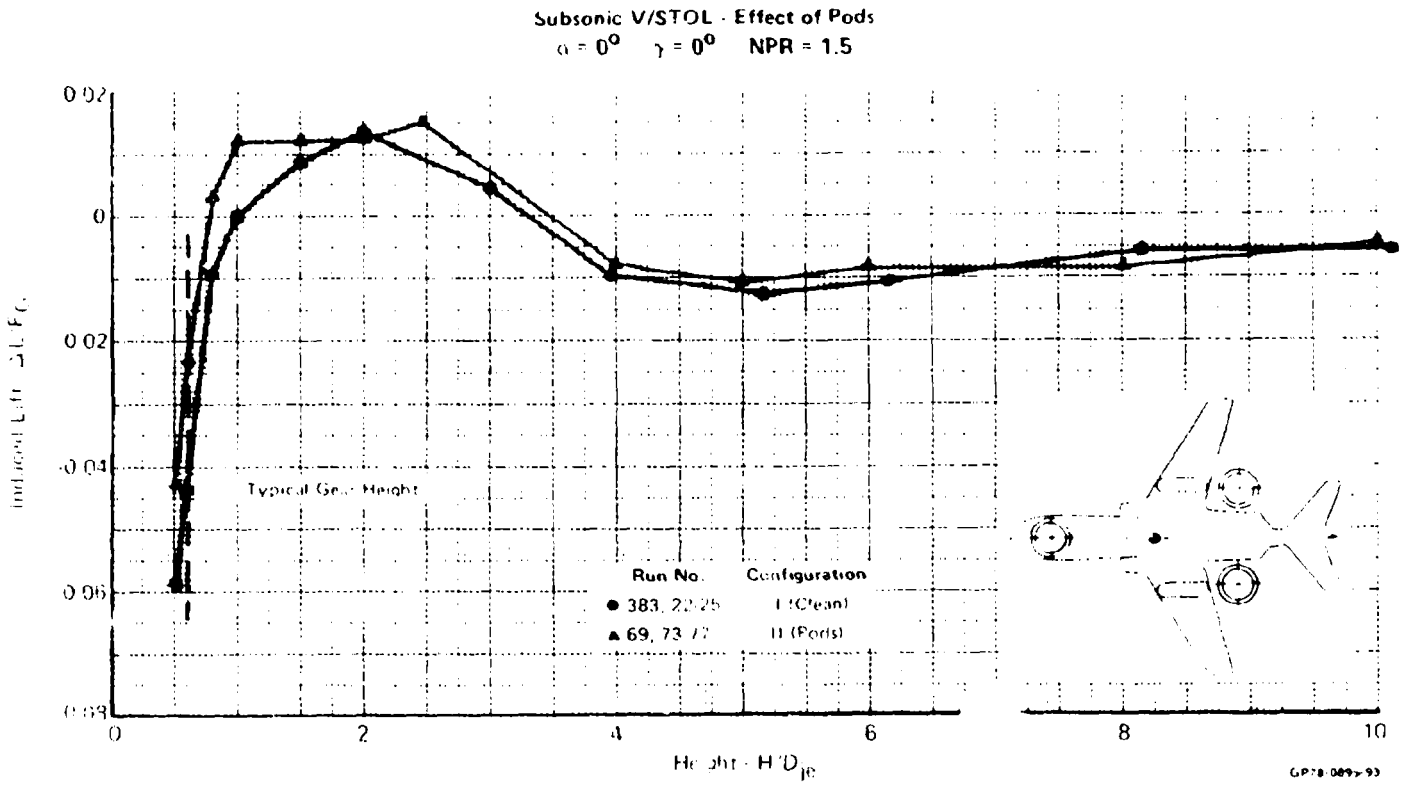

FIGURE 5-9

SUBSONIC V/STOL WITH WING PODS

the same plane as the low wing for these tests. Out of ground proximity, the wing height had no effect.

Effect of Nozzle Arrangement - The number and arrangement of nozzles has a pronounced effect on induced lift, as shown in Figure 5-11 for the 3-D model. When only one jet (the forward lift fan) is operating, no fountain forms and the induced lift consists only of suckdown, resulting in an 8.5 percent lift loss at gear height. For the two-jet configuration, representing a dual tilt nacelle design, increased suckdown occurs, which overcomes the weak fountain formed between the jets. This results in a lift loss of 10 percent of the thrust at gear height. On the three-jet configuration, a fairly strong fountain forms which results in a lift loss of only 3 percent at gear height and a peak lift gain of nearly 2 percent at an H/D_{je} of 2.

Effect of Nozzle Simulation and Operation - Accurate simulation of the nozzle geometry, the airframe geometry near the nozzle exits, and the exhaust flow conditions is particularly important in order to provide realistic results, since flow entrainment is strongest in the region of high jet velocities. The effects on the induced lift of adding pitch and yaw vanes and a hub centerbody to the front nozzle and yaw vanes to the rear nozzles are presented in Figure 5-12. The complex nozzles were found to reduce the induced lift near the deck by as much as 2 percent. From the company funded study on a similar model that was pressure instrumented (Reference 3), the louvers and vanes were found to alter the flowfield stagnation areas, thus inhibiting flow into the inner region and reducing fountain strength.

Increasing the nozzle pressure ratio (NPR) from a typical lift fan value of 1.1 with subsonic nozzle flow to a direct lift jet condition with choked flow, NPR of 2.0, reduces the induced lift near the ground approximately 1 percent, as shown in Figure 5-13. No effect is seen OGE. The effect of nozzle pressure ratio indicates that testing with the proper full scale nozzle exit Mach number and exhaust momentum is required to obtain an accurate simulation of the recirculating flowfield and the induced aerodynamics. The majority of the tests with the subsonic configuration were conducted with a NPR of 1.3, representing an advanced lift fan propulsion system.

The induced lift is extremely sensitive to the thrust split between the forward (lift fan) and aft (lift/cruise fan) nozzles, as shown in Figure 5-14. A split with somewhat greater than 50 percent of the thrust provided by the forebody lift fan appears to be optimum compared to the nominal design value of 33 percent.

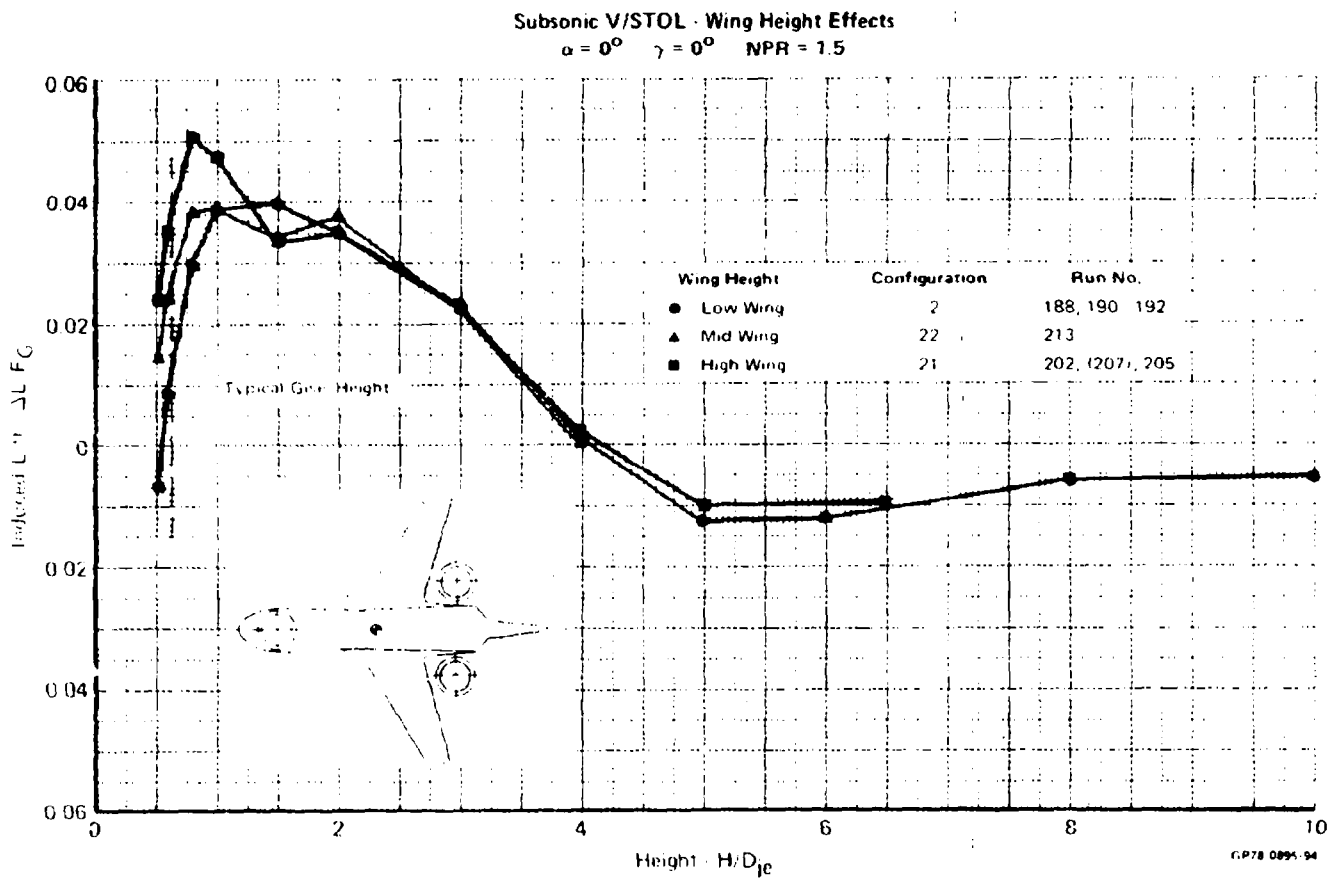

FIGURE 5-10
SUBSONIC V/STOL WING HEIGHT EFFECTS

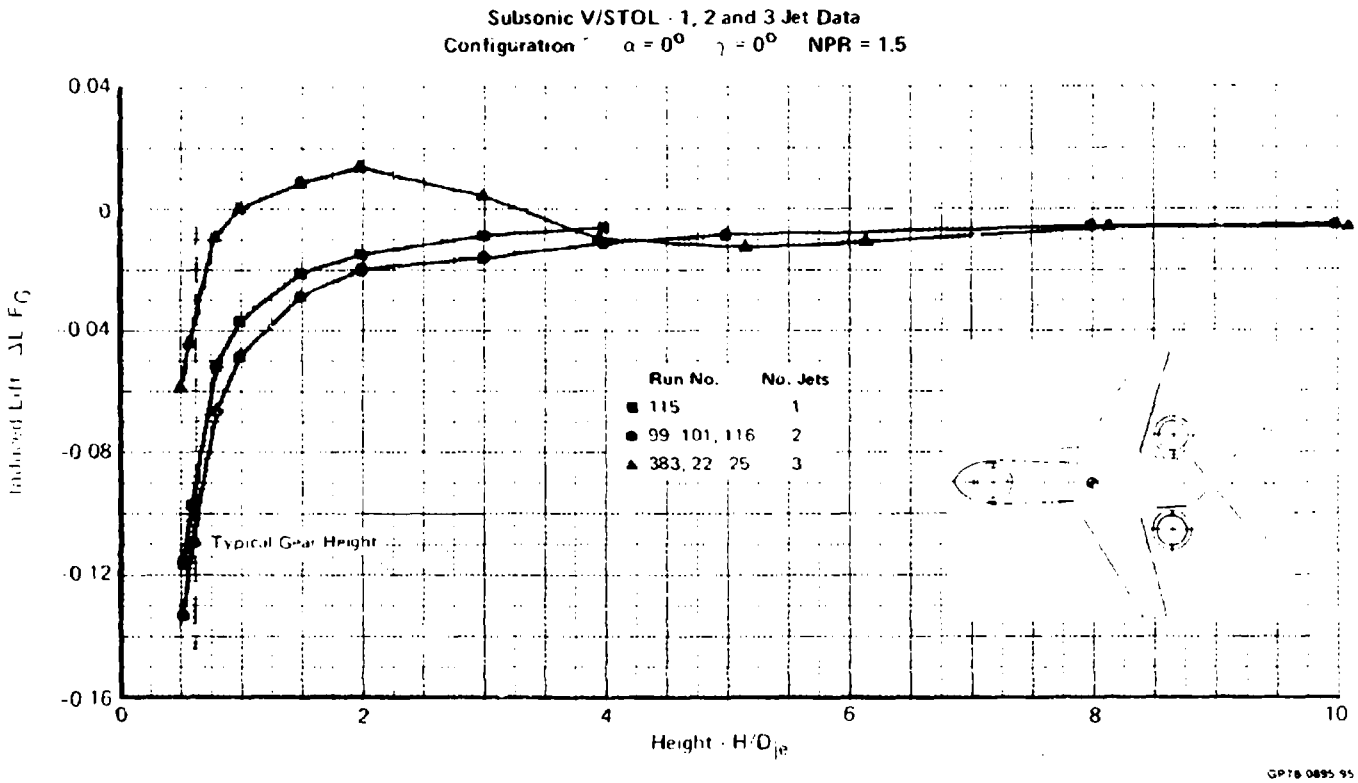

FIGURE 5-11
SUBSONIC V/STOL NOZZLE ARRANGEMENT EFFECTS

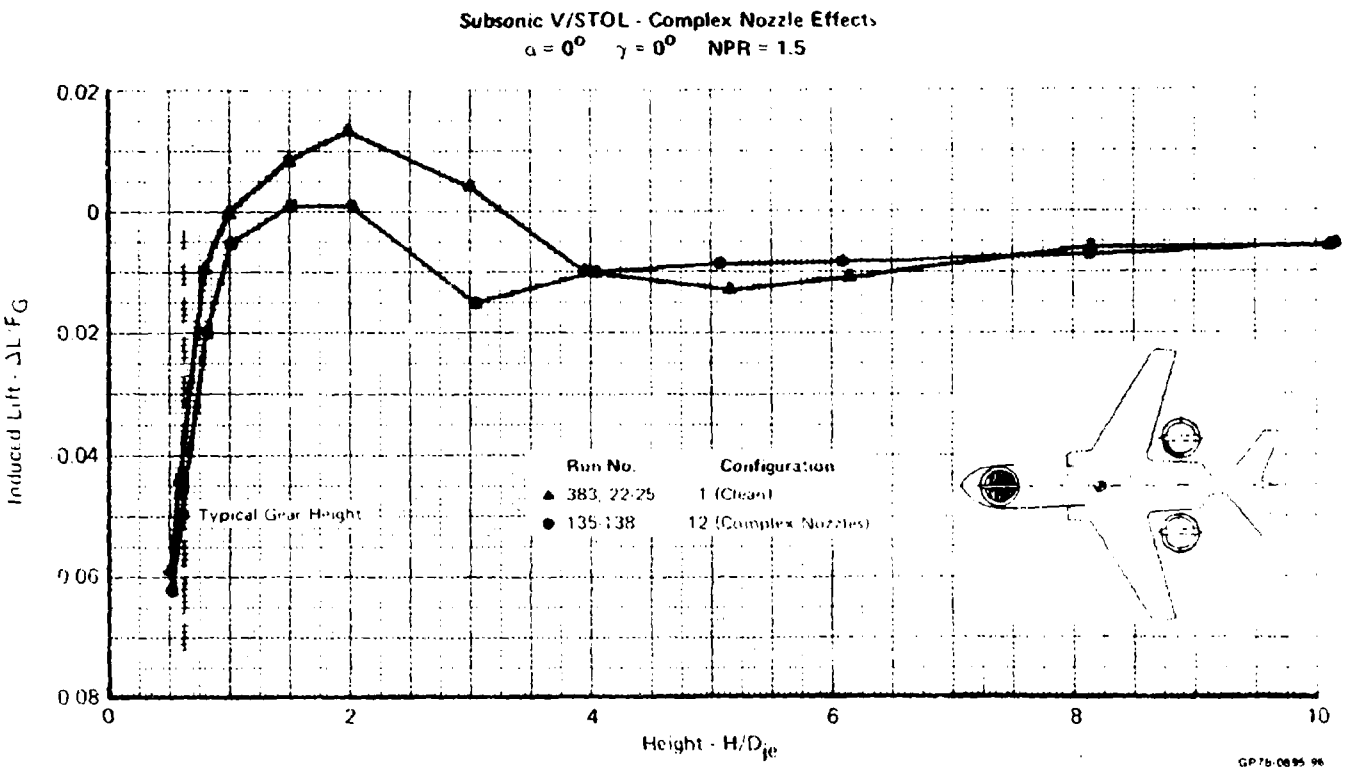

FIGURE 5-12
SUBSONIC V/STOL COMPLEX NOZZLE EFFECTS

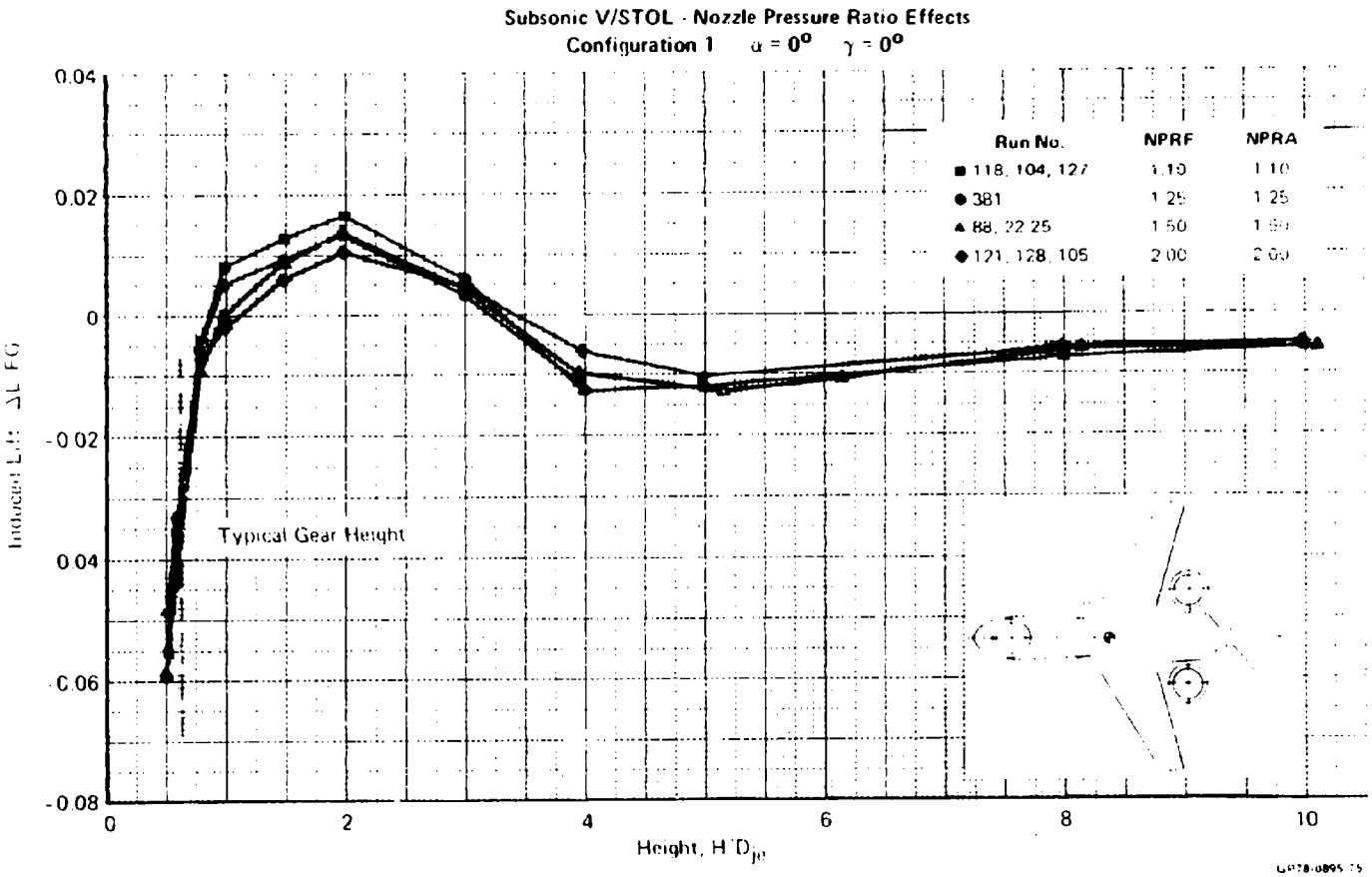

FIGURE 5-13
SUBSONIC V/STOL NOZZLE PRESSURE RATIO EFFECTS

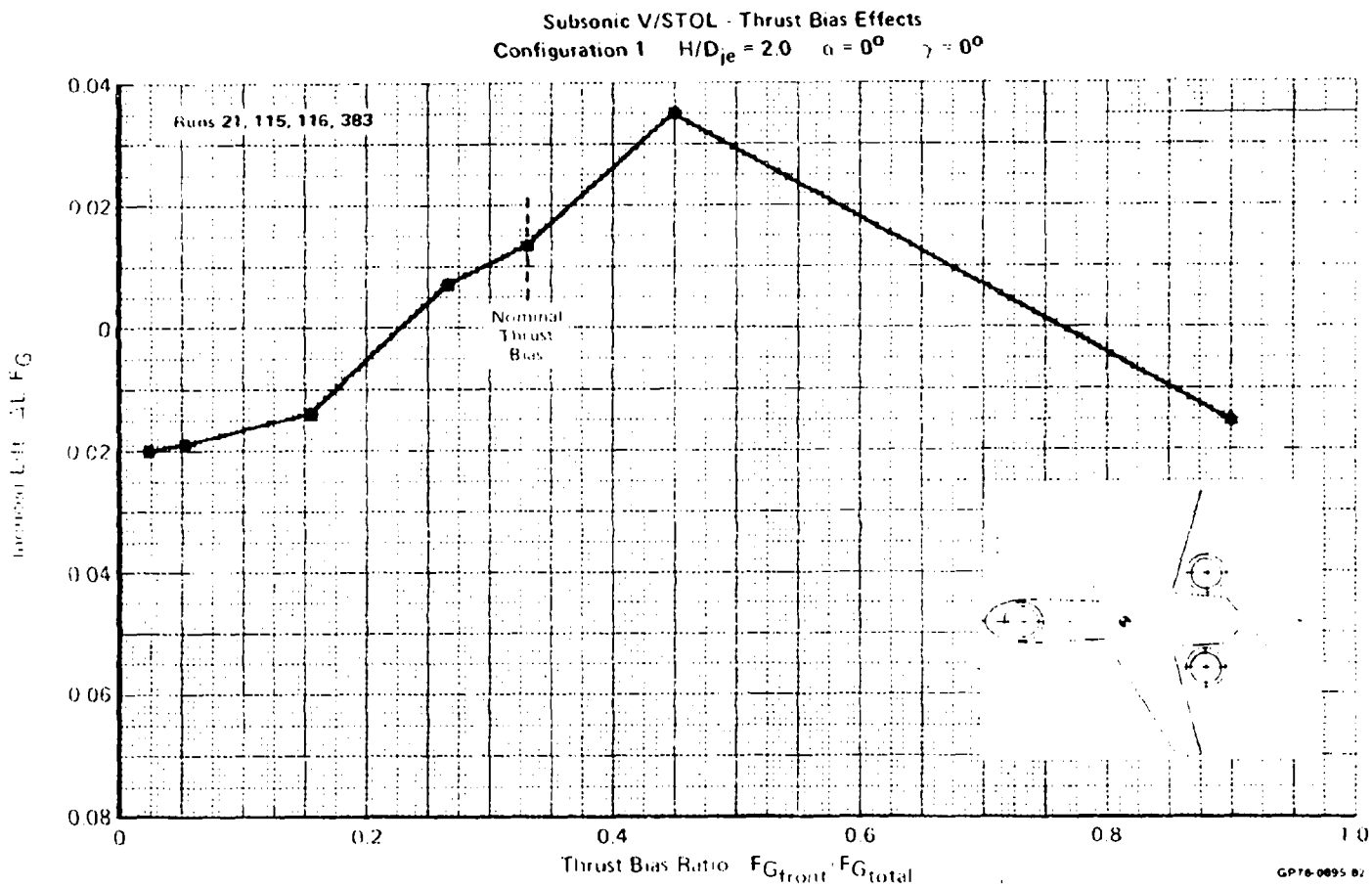

FIGURE 5-14
SUBSONIC V/STOL THRUST BIAS EFFECTS

5.1.2 Supersonic V/STOL Configuration - The supersonic V/STOL configurations investigated (Figure 2-10) represent a variety of advanced designs. The primary configuration represents either a three- or four-nozzle vehicle with either a single or dual forward lift fan(s) and two vectoring aft lift/cruise jets. An alternate configuration represents a two-nozzle vehicle with a single forward lift fan and a single aft lift fan, each driven by a turbofan engine mounted over the wing. The configuration variables included model surface contouring, nozzle arrangement and spacing, LID's and wing height. The test variables included height above the deck, deck pitch and roll angles, and thrust bias. It should be noted that these tests were conducted at the same heights as for the subsonic V/STOL configuration. The heights are nondimensionalized by the equivalent jet diameter, which varies for each configuration.

Effect of Height - Induced lift characteristics at static hover conditions for the three-nozzle supersonic V/STOL model with a contoured lower surface are presented in Figure 5-15. The suckdown is substantially greater than for the subsonic configuration, since the ratio of planform area to total jet exit area was approximately 5 times larger. In addition, the rear jets are much closer together, reducing the fountain strength. Thus, at gear height, the induced lift loss is approximately 20 percent of thrust, and OGE approximately 2 percent. Other data obtained in this program and in MCAIR company funded studies indicate the lift loss for this configuration is highly dependent on nozzle arrangement and geometry, with substantially lower lift loss occurring for certain configurations.

Effect of Deck Pitch and Roll Angles - The induced lift and pitching moment data for the three-nozzle semi-contoured model are presented in Figure 5-16 as a function of deck pitch angle. Induced lift is relatively insensitive to pitch angle, even close to the deck. This occurs since the fountain strength is relatively weak. Pitching moment on the other hand is sensitive to pitch angle at an H/D_{je} of 1.7 (7 ft. or 2.1m full scale) or less.

The deck roll angle has only a slight effect on induced lift and rolling moment IGE as shown in Figure 5-17, also due to the weak fountain. The induced rolling moment tends to be destabilizing, since increasing the roll angle increases the rolling moment. Rolling the deck pushes the fountain to the opposite side of the fuselage, thus inducing more roll on the airframe.

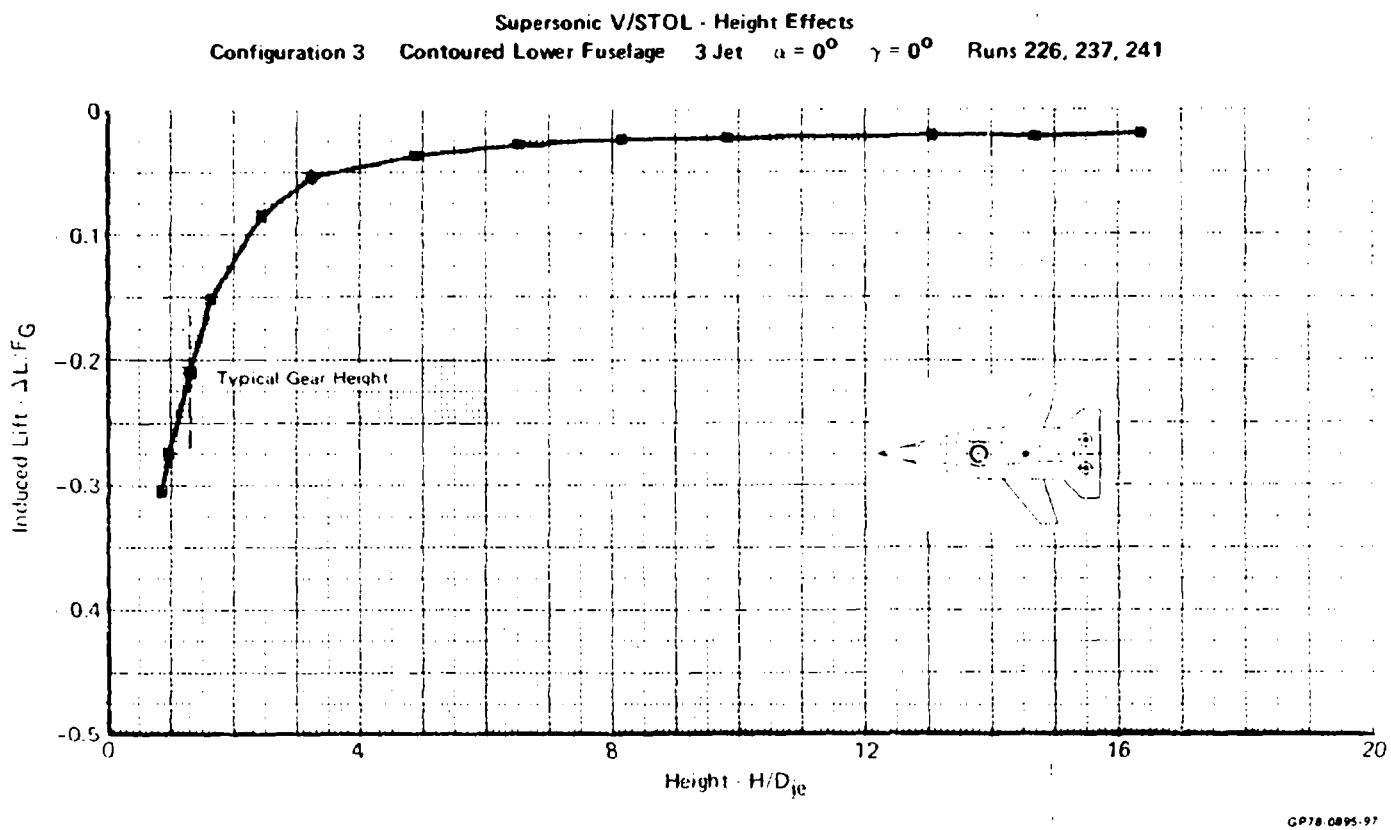

FIGURE 5-15
3 JET SUPERSONIC V/STOL STATIC HEIGHT EFFECTS

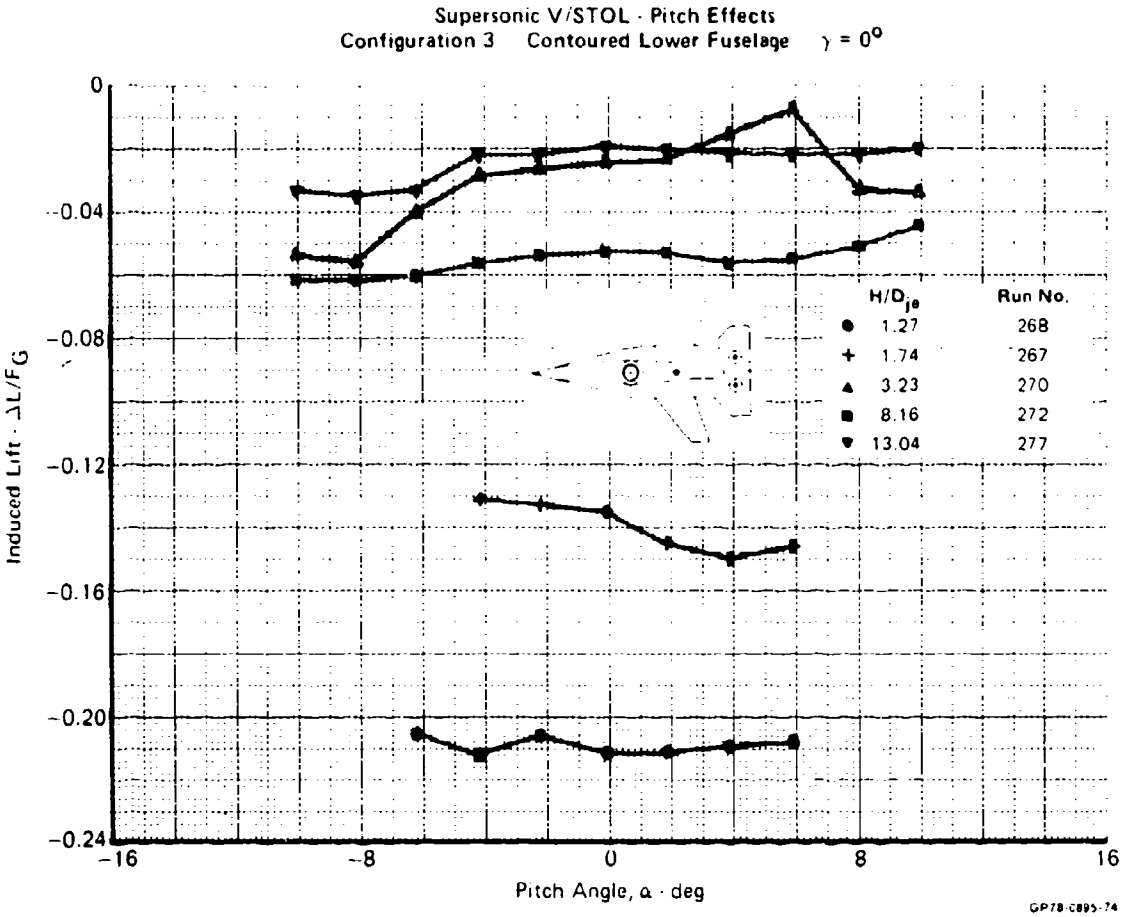

a) Induced Lift

FIGURE 5-16
3 JET SUPERSONIC V/STOL STATIC PITCH EFFECTS

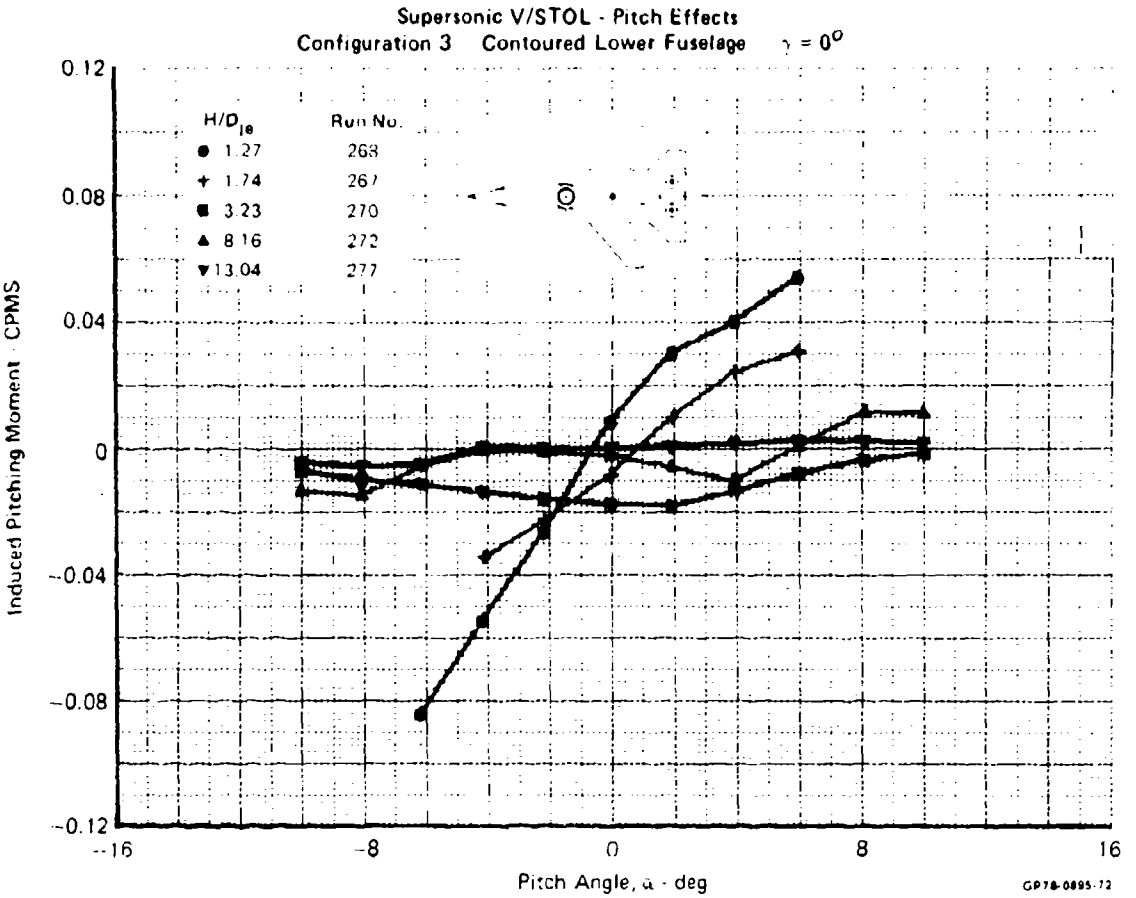

b) Induced Pitching Moment

FIGURE 5-16 (Concluded)
3 JET SUPERSONIC V/STOL STATIC PITCH EFFECTS

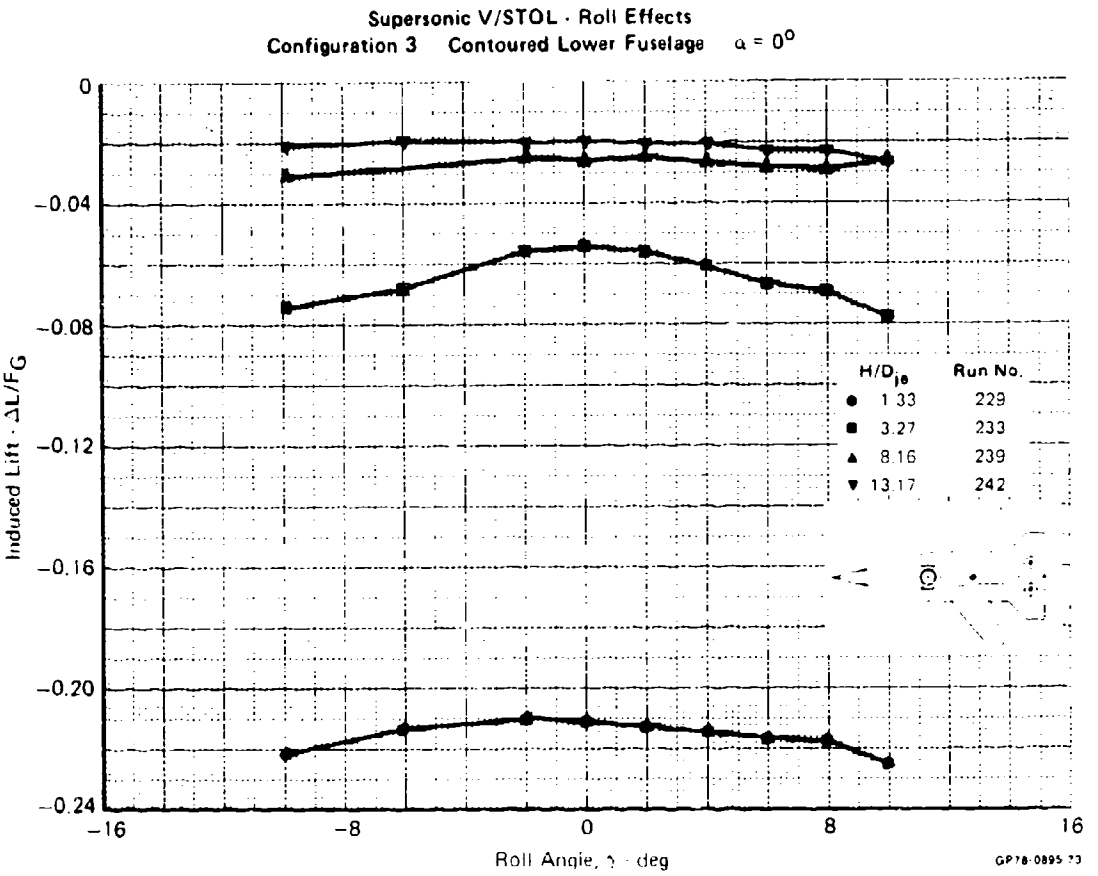

a) Induced Lift

FIGURE 5-17
3 JET SUPERSONIC V/STOL STATIC ROLL EFFECTS

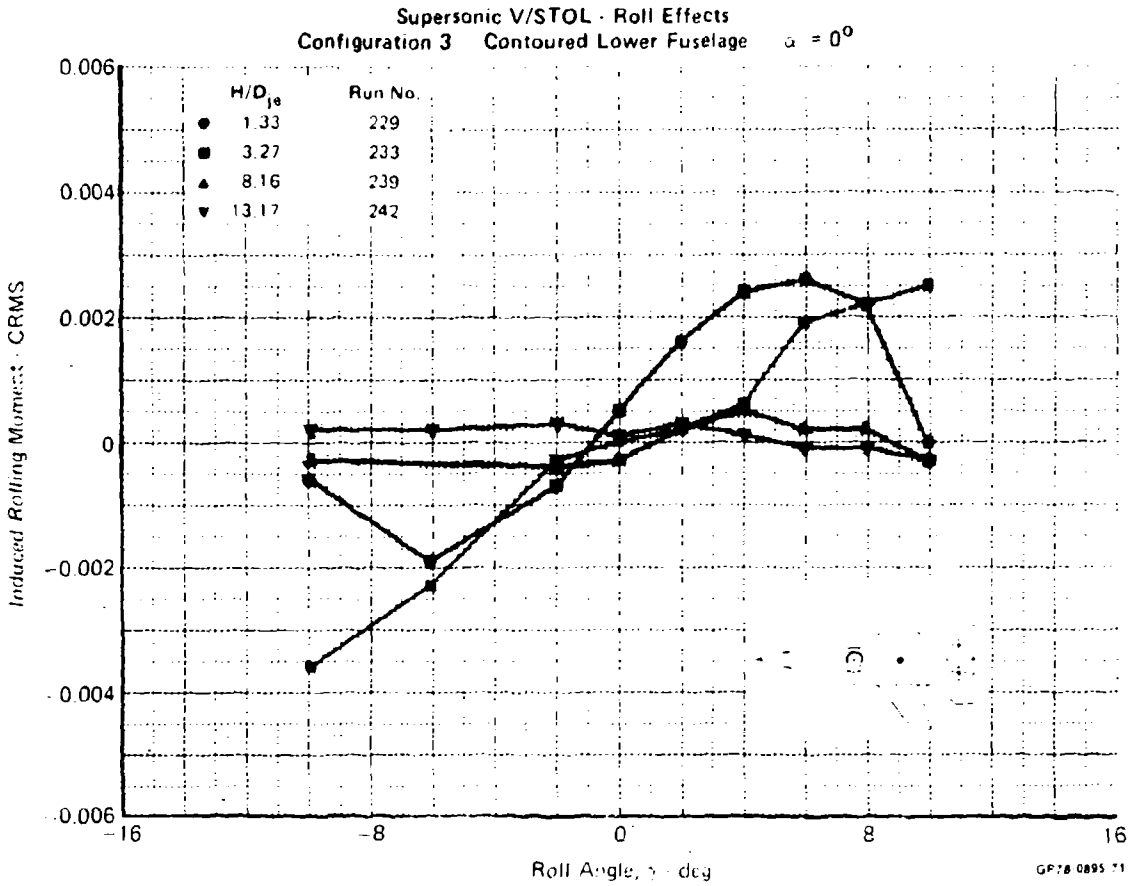

b) Induced Rolling Moment

FIGURE 5-17 (Concluded)
3 JET SUPERSONIC V/STOL STATIC ROLL EFFECTS

Effect of Model Surface Contouring - The effects of adding the contoured lower fuselage to the model are shown in Figure 5-18. The lower fuselage contouring increases the induced lift at gear height approximately 10 percent, primarily because the lift fan exit is further away from the large wing and fuselage, thereby reducing the suckdown. As with the subsonic V/STOL configuration, the same trends are indicated by both the planform and semi-contoured models, but the force levels are sensitive to body contouring and the placement of the nozzle exits relative to the airframe.

Effect of Thrust Bias - The effect of thrust bias between the lift fan nozzle and the aft lift/cruise nozzles was investigated at static hover conditions. These results, shown in Figure 5-19, indicate that the induced lift is sensitive to thrust bias. The optimum split IGE is to have about 39 percent of the thrust provided by the front lift fan as opposed to the nominal design thrust split of 69 percent for this configuration. Induced lift is insensitive to thrust bias OGE.

With only the forward fan operating, no fountain forms and the induced lift consists entirely of suckdown. These data are compared with the three-nozzle data in Figure 5-20. Although there is an increase in suckdown with the two rear nozzles operating, the induced lift is only about 3 percent higher at typical gear height indicating that a relatively weak fountain is formed.

Effect of LID's - The effect of adding LID's to the three-jet supersonic planform model is shown in Figure 5-21. The LID's increase the induced lift by 8 percent at gear height, which is a substantial increase, but the suckdown still dominates. Recent company funded tests on a similar configuration indicated that careful tailering of the width, length, depth, and placement of the LID's can increase the induced lift by as much as 20 percent of thrust. Thus, the design of the lower fuselage and the incorporation of LID's should be given careful attention early in the design of a V/STOL aircraft. As on the subsonic configuration, the LID's are effective at roll, as shown by the increases in lift in Figure 5-22. No adverse effects on the rolling moment are apparent in Figure 5-23.

Effect of Wing Height - Raising the wing on the planform model was found to improve the induced lift by 6 percent of the thrust at gear height, as shown in Figure 5-24. As with the subsonic configuration, this is due to the reduction in suckdown on the wing. Wing height had no effect OGE.

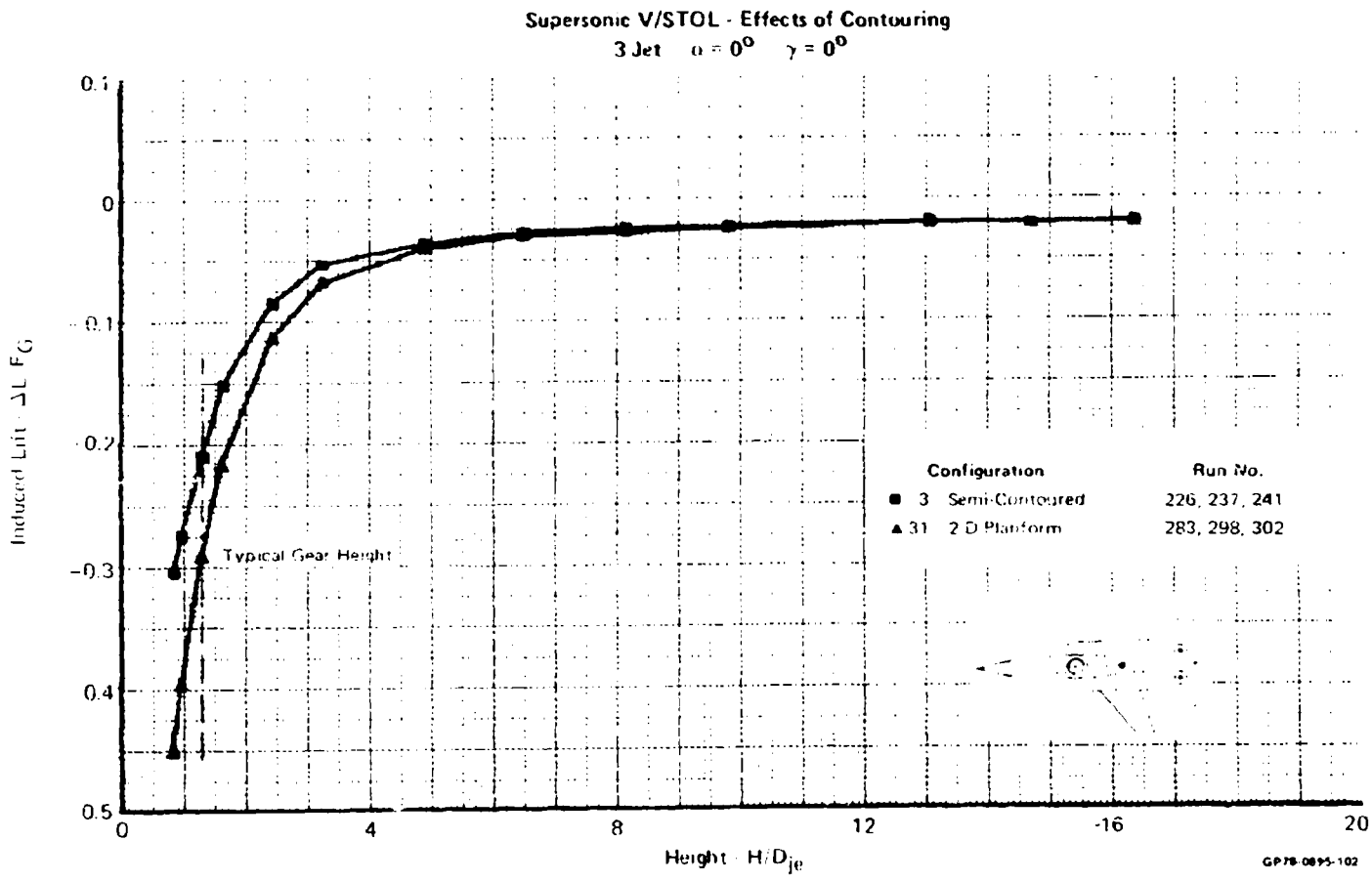

FIGURE 5-18
SUPERSONIC V/STOL CONTOURING EFFECTS

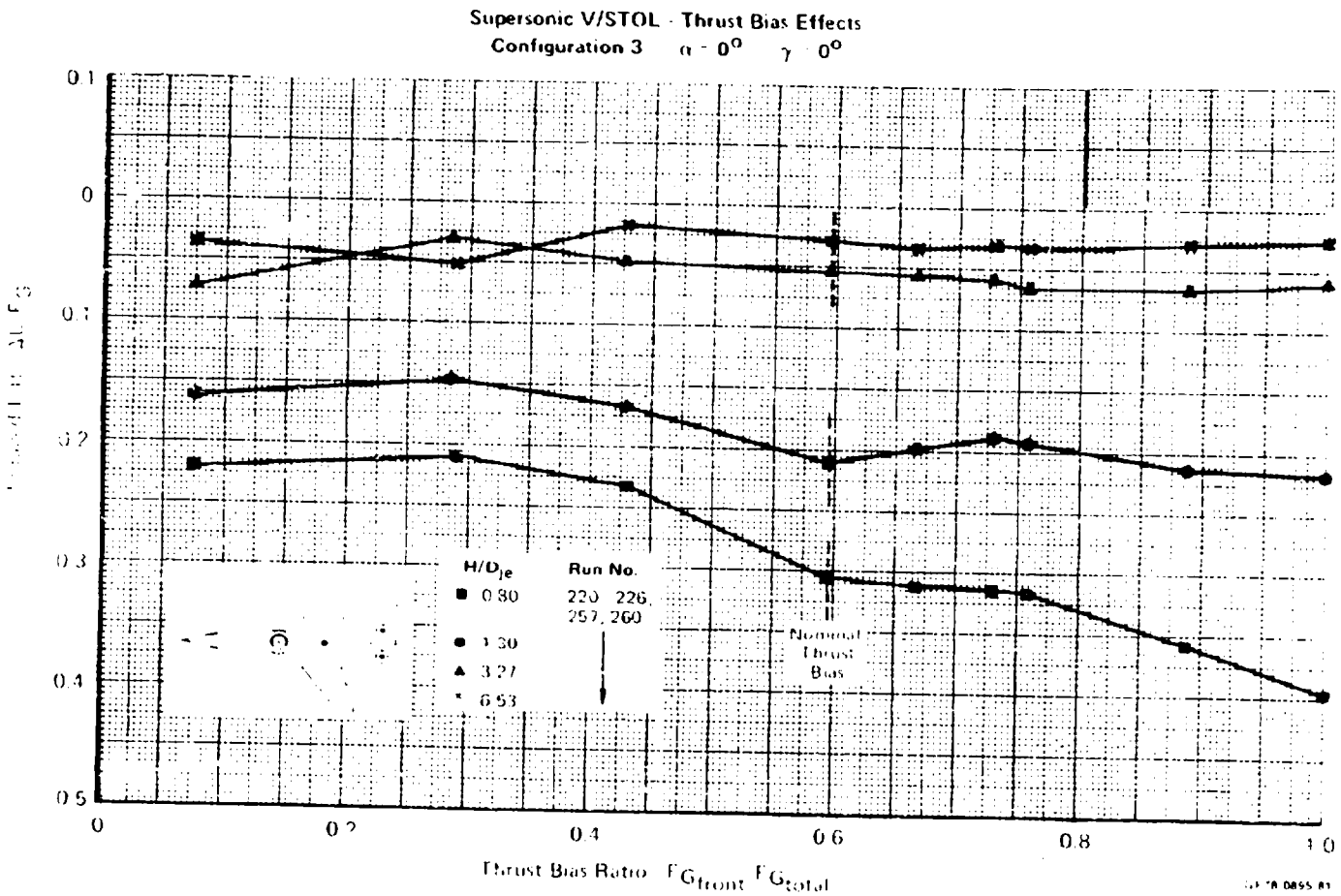

FIGURE 5-19
3 JET SUPERSONIC V/STOL THRUST BIAS EFFECTS

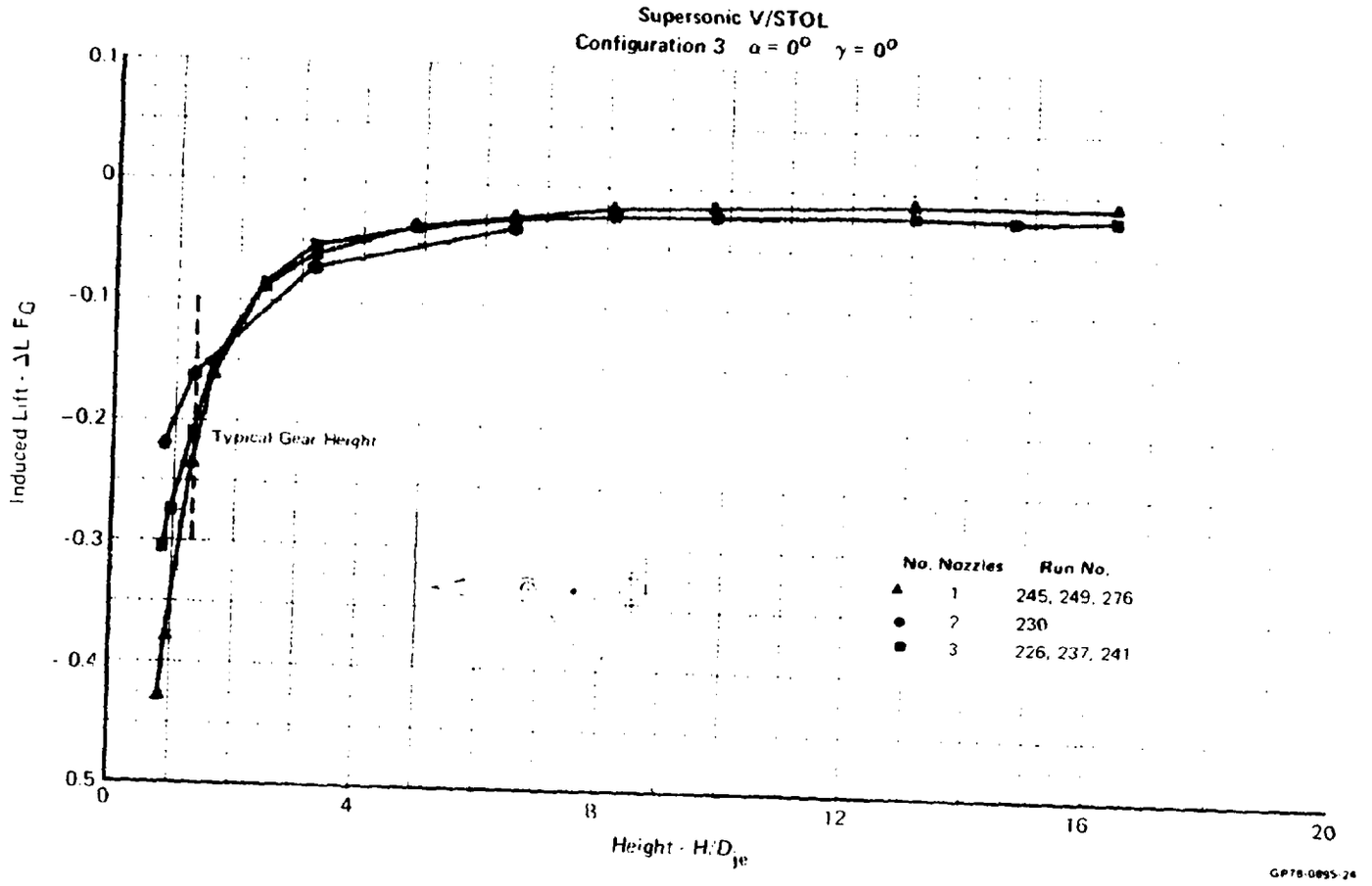

FIGURE 5-20
SUPERSONIC V/STOL NUMBER OF NOZZLES EFFECT

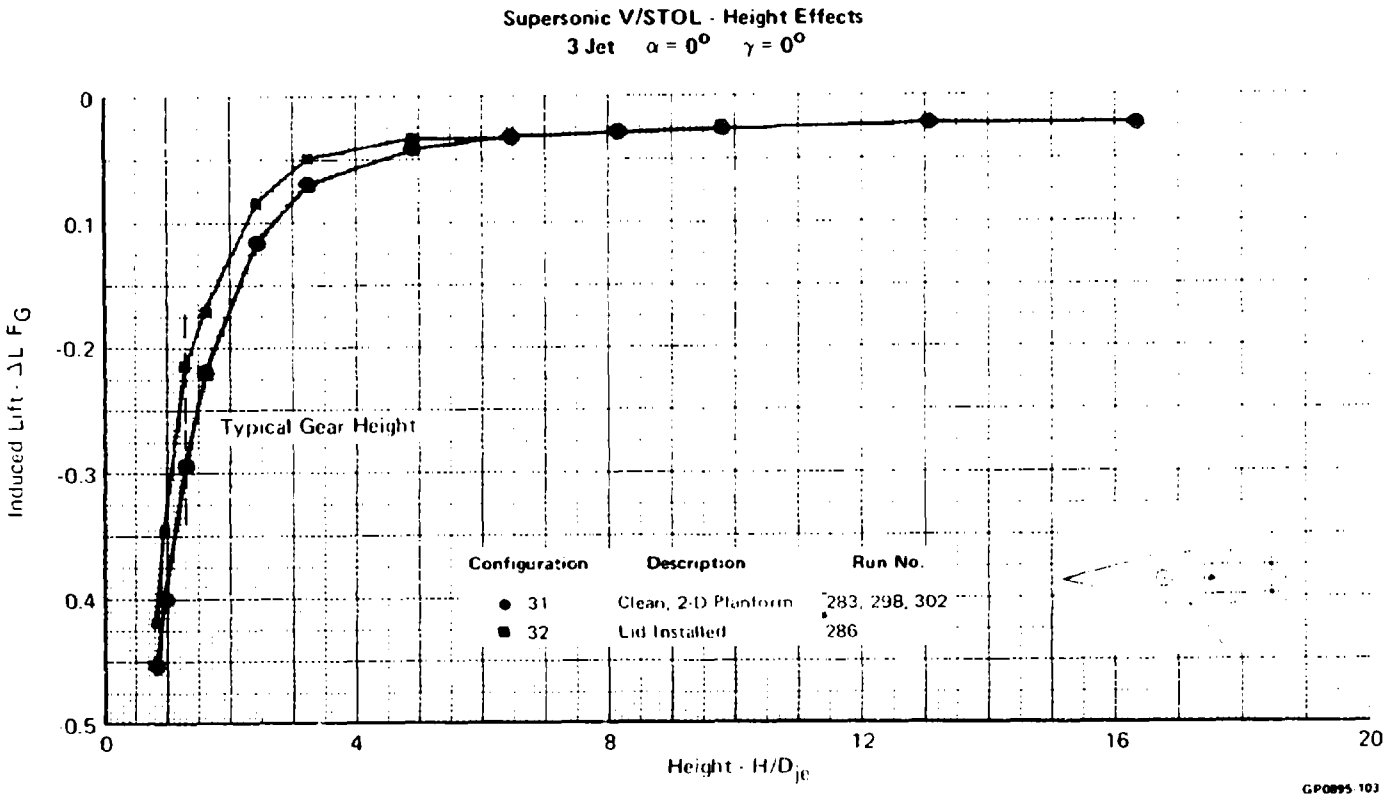

FIGURE 5-21
SUPERSONIC V/STOL WITH LIFT IMPROVEMENT DEVICES

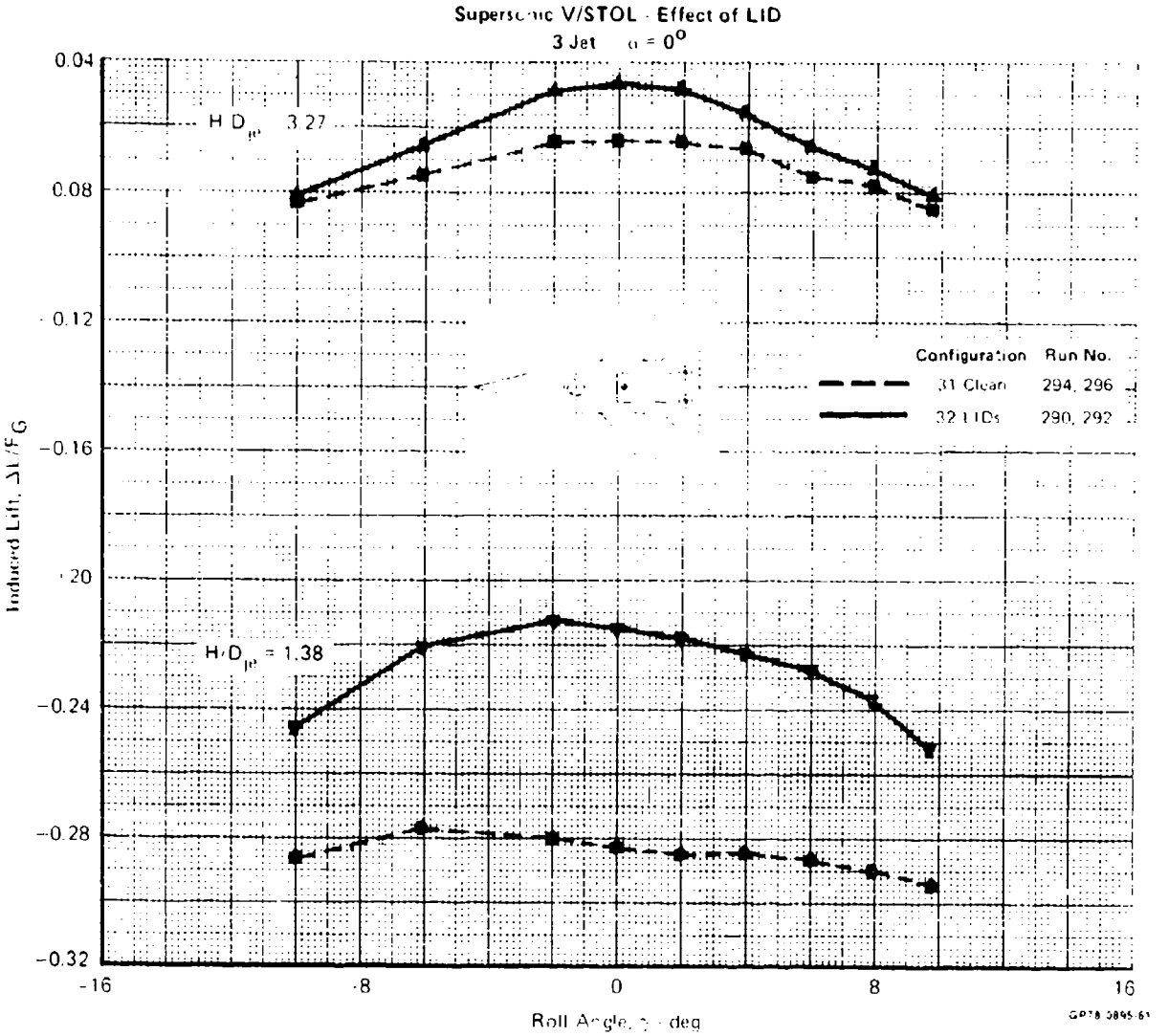

FIGURE 5-22
SUPERSONIC V/STOL ROLL EFFECTS ON INDUCED LIFT WITH LIFT IMPROVEMENT DEVICES INSTALLED

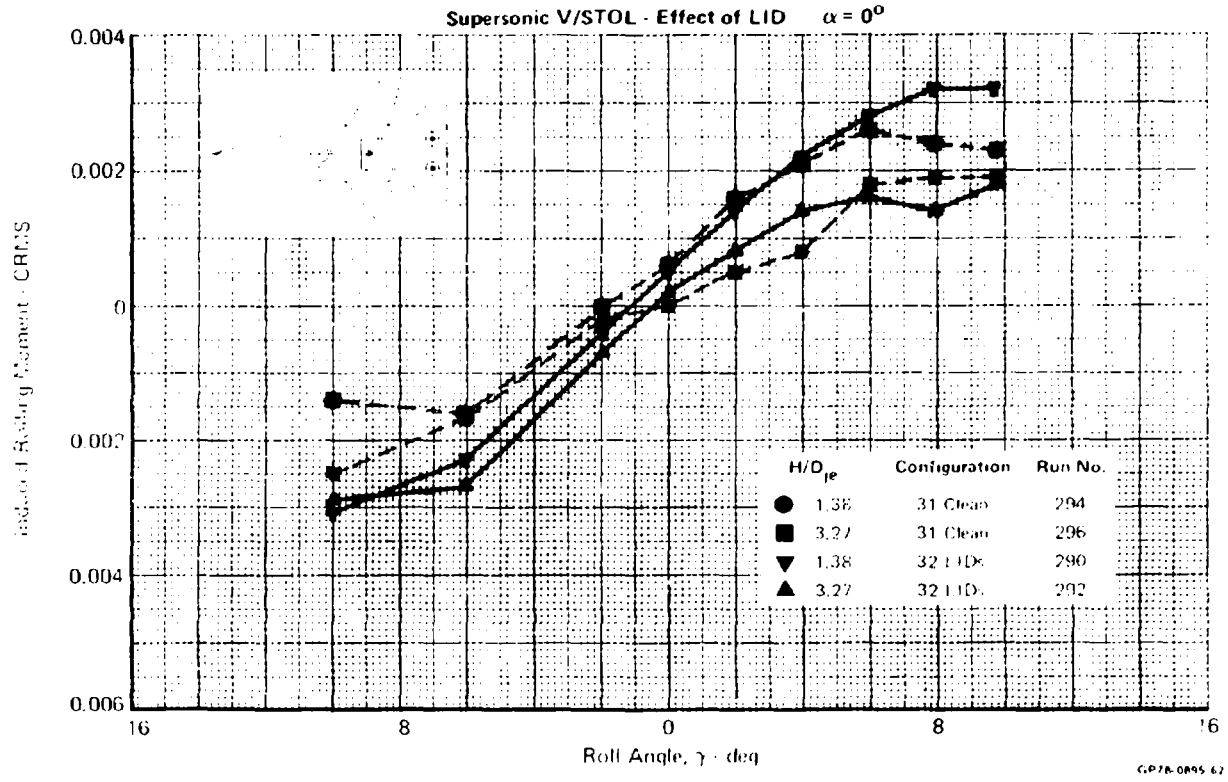

FIGURE 5-23

SUPERSONIC V/STOL ROLL EFFECTS ON INDUCED ROLLING MOMENT WITH LIFT IMPROVEMENT DEVICES INSTALLED

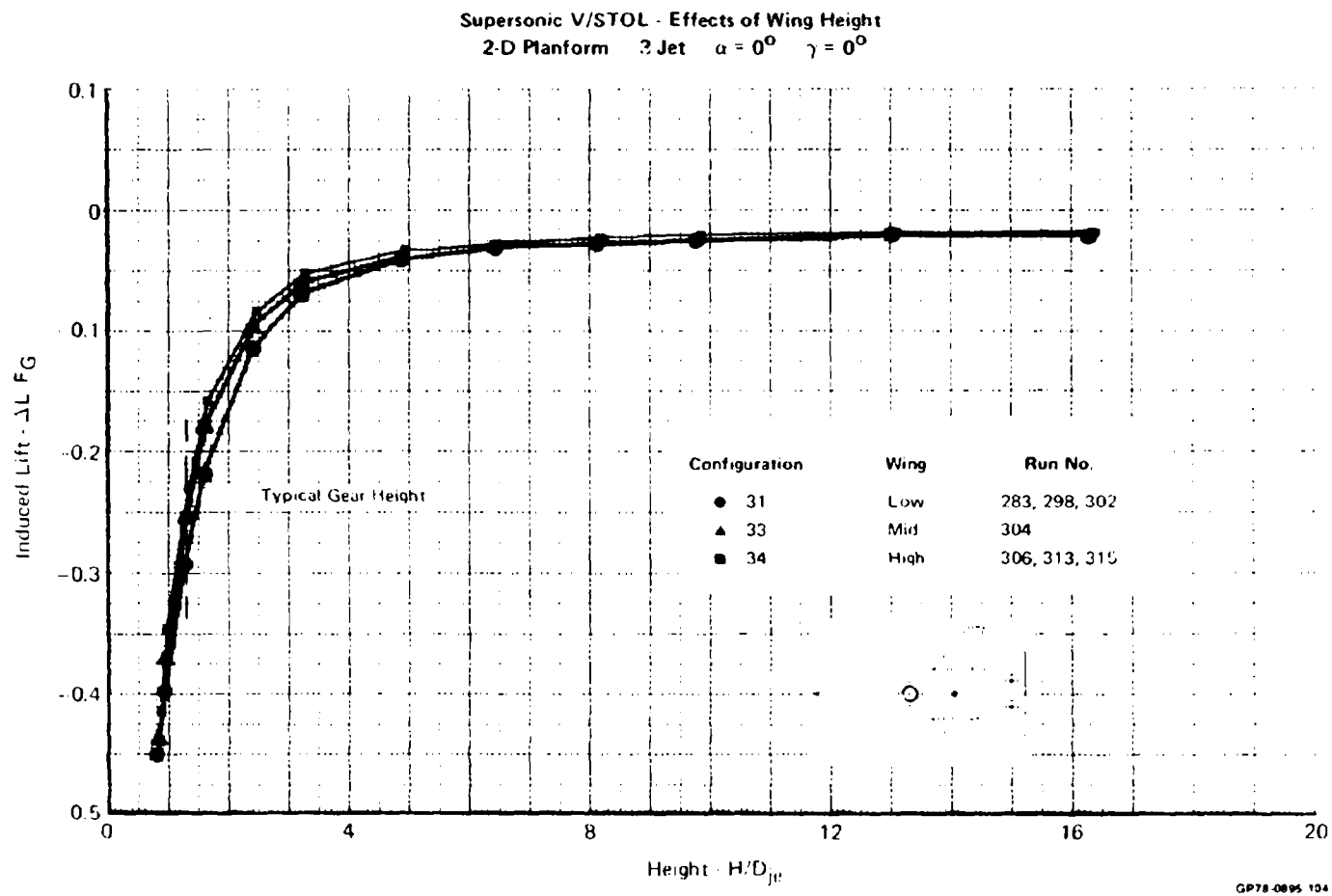

FIGURE 5-24
SUPERSONIC V/STOL WING HEIGHT EFFECTS

Effect of Nozzle Arrangement and Spacing - Nozzle arrangement and spacing has a significant influence on the induced aerodynamics. In addition to the three-nozzle configuration discussed above, a four-nozzle design (Figure 2-11g) and a two-nozzle design (Figure 2-11f) were investigated.

Increased induced lift is evident for the four-nozzle planform configuration in Figure 5-25. The increase is attributed to less suckdown and a stronger fountain. The suckdown is lower because the nozzles are nearer the edge of the planform, causing less area to be affected from entrainment by the ground jet flows. In addition, moving the front lift fans forward to increase the spacing results in a 2 to 5 percent higher induced lift IGE at the same nominal thrust split. No variations in thrust bias were investigated on the four-jet configuration.

The induced lift and pitching moment data for the four-jet supersonic planform model with the front lift fans in the mid location are shown in Figure 5-26 as a function of deck pitch angle. Close to the deck, lift and pitching moment vary significantly with the pitch angle, due to the stronger fountain compared to the three-jet configuration. Pitch angle has little effect OGE. Similarly, induced lift and rolling moment vary significantly with deck roll angle IGE, but not OGE, as shown in Figure 5-27.

The induced lift IGE, presented in Figure 5-28, for the two-nozzle configuration are similar to those for the four-jet configuration, even though the four-jet configuration has a stronger fountain. Increasing the spacing between the two nozzles increases the induced lift by nearly 2 percent. However, even OGE the induced lift is approximately 1.5 percent higher than for the three- and four-jet configurations. A 50/50 thrust split appears to be optimum as shown in Figure 5-29.

Induced lift and pitching moment of the two-jet model are sensitive to pitch angle near the deck, as shown in Figure 5-30. Induced lift and rolling moment are less sensitive to deck roll angle IGE than on the four-jet configuration but are more sensitive than on the three-jet model as shown in Figure 5-31.

5.2 DYNAMIC DECK MOTION EFFECTS - The primary objective of this program was to investigate the effects of the heaving, pitching, and rolling motion of a simulated landing platform on the jet-induced aerodynamics of both subsonic and supersonic V/STOL aircraft designs. Dynamic tests were performed with simple one degree of freedom motions, such as heave, and with combined motions, such as heave and roll. The response of the aircraft models to the

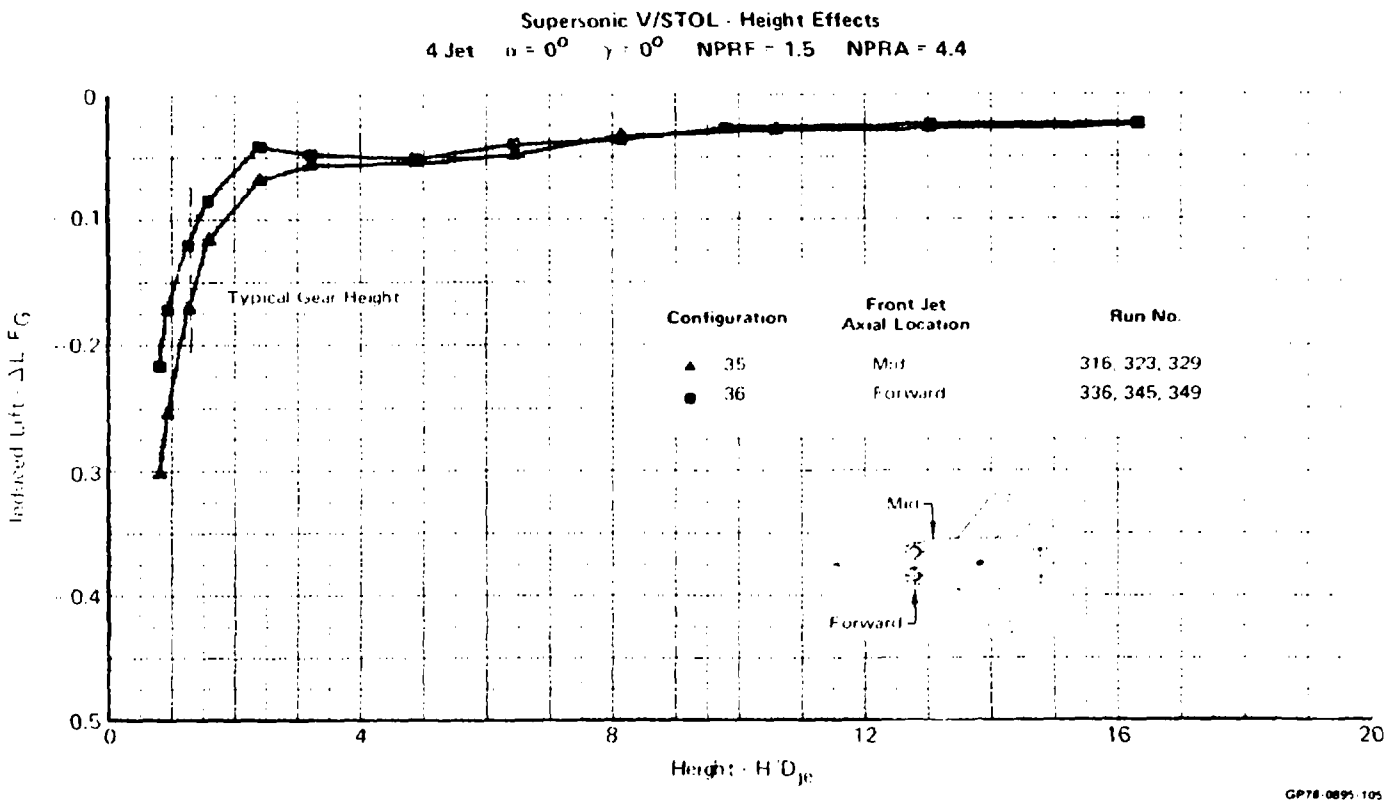

FIGURE 5-25

4 JET SUPERSONIC V/STOL STATIC HEIGHT EFFECTS

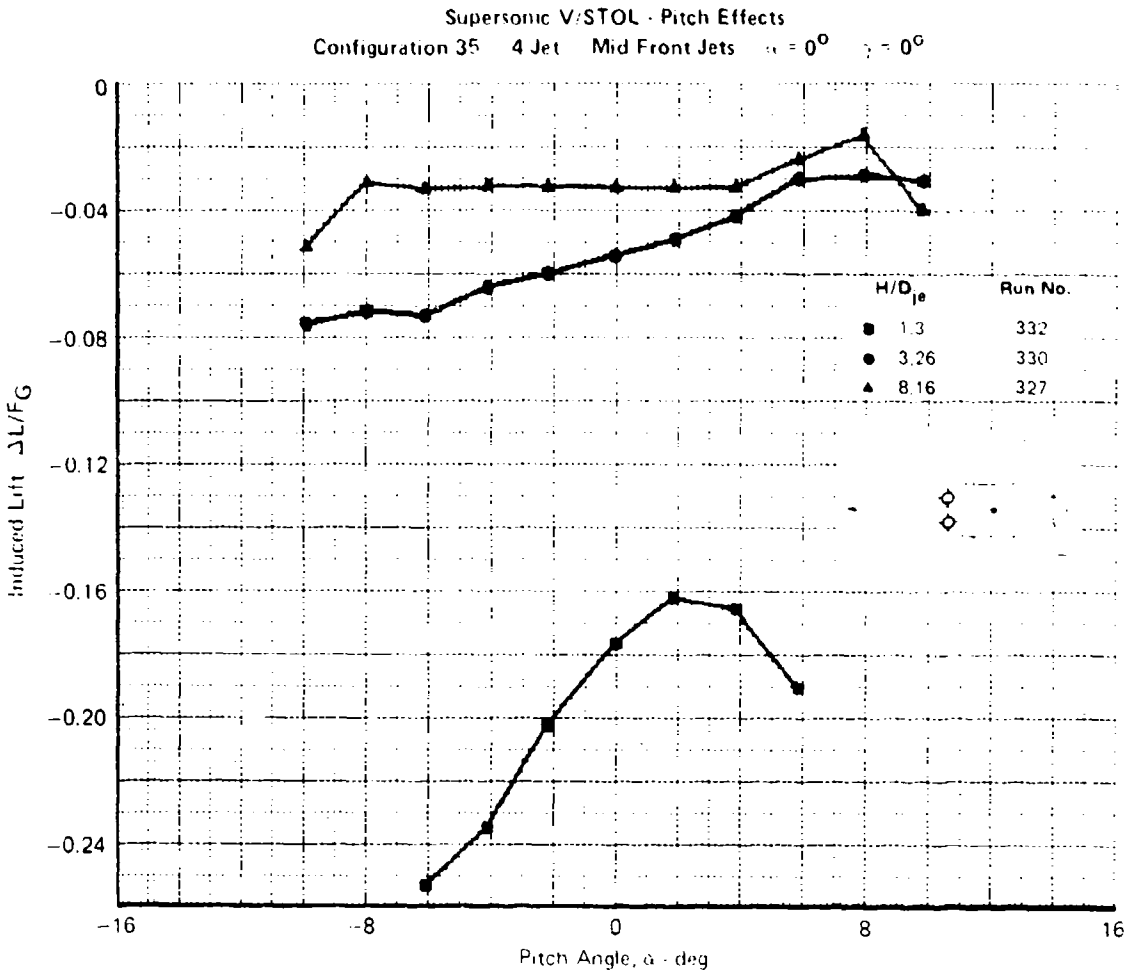

a) Induced Lift

FIGURE 5-26
4 JET SUPERSONIC V/STOL STATIC PITCH EFFECTS

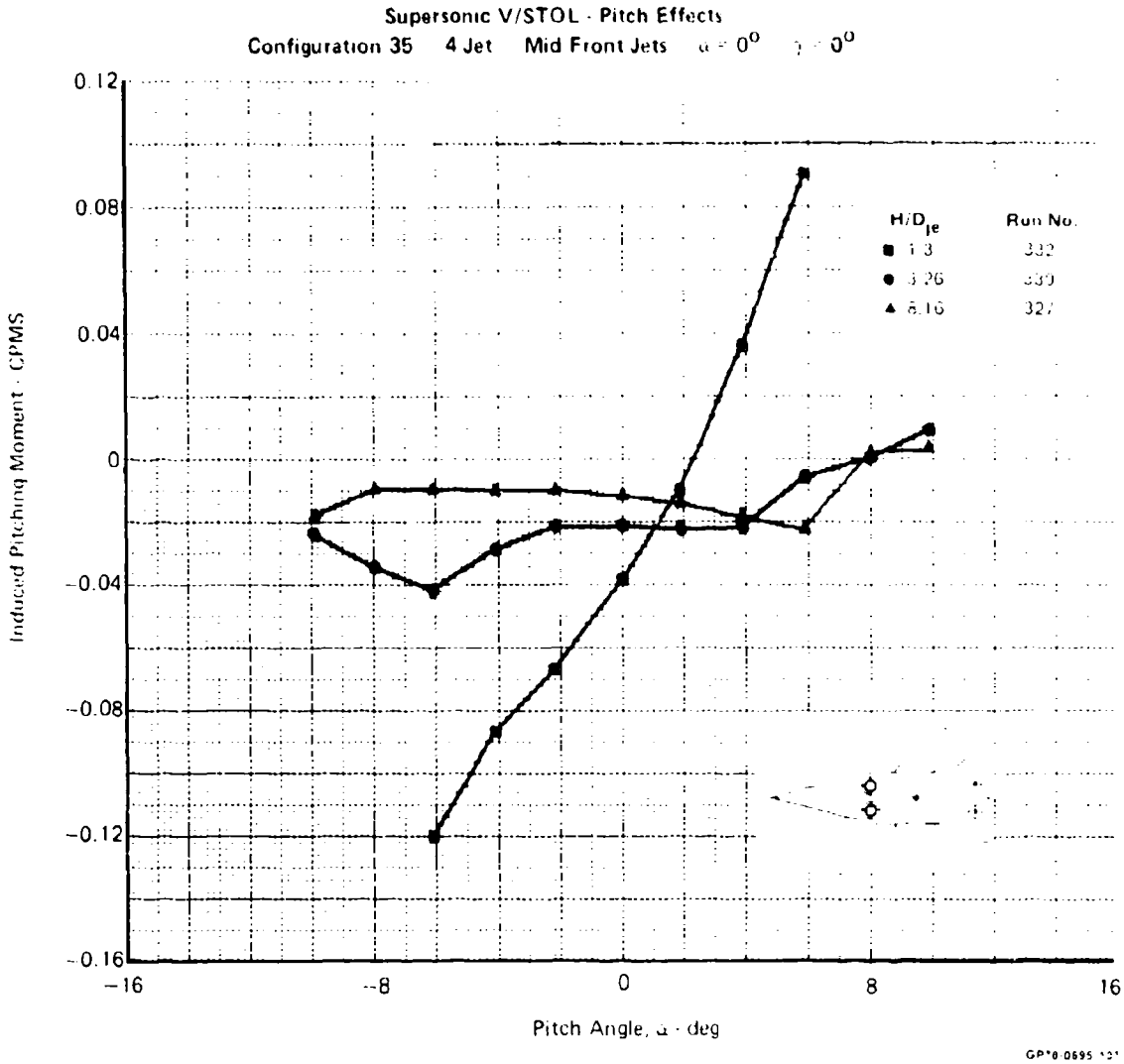

b) Induced Pitching Moment

FIGURE 5-26 (Concluded)
4 JET SUPERSONIC V/STOL STATIC PITCH EFFECTS

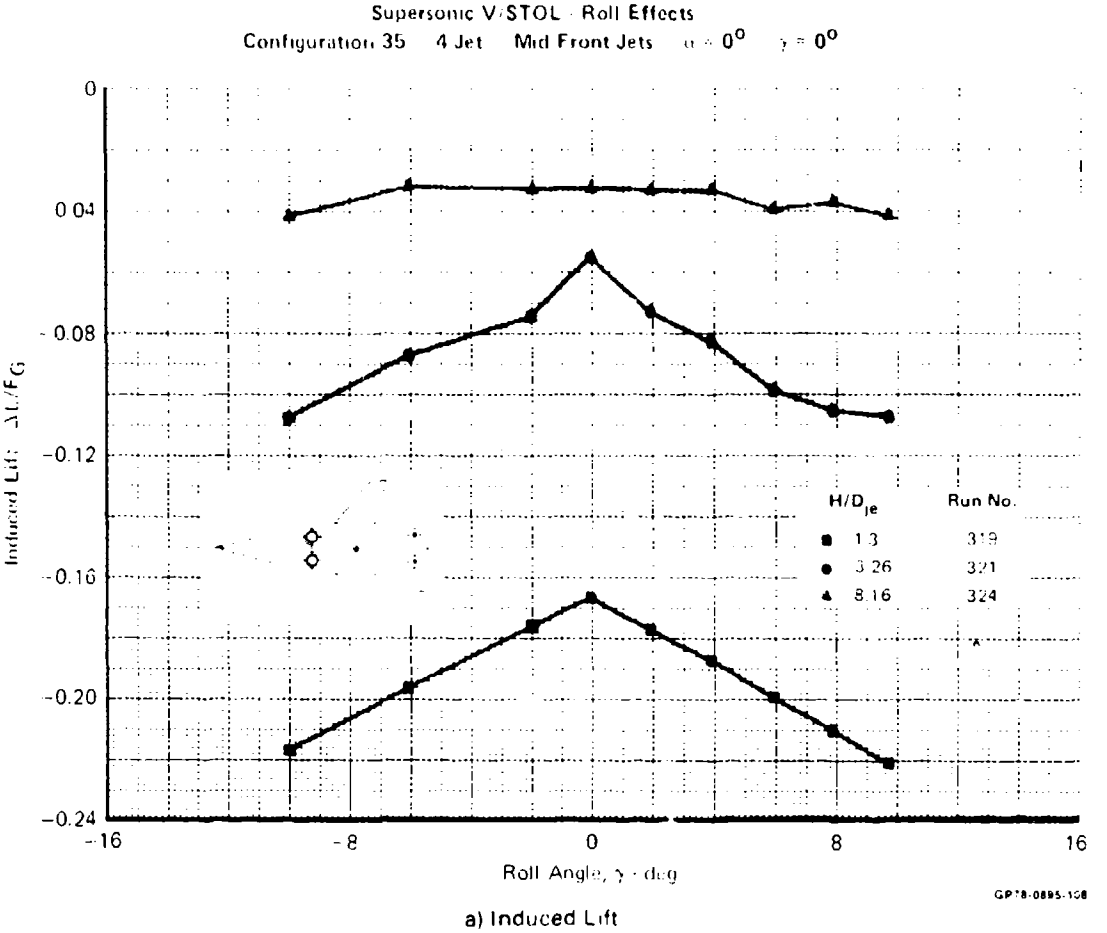

a) Induced Lift

FIGURE 5-27
4 JET SUPERSONIC V/STOL STATIC ROLL EFFECTS

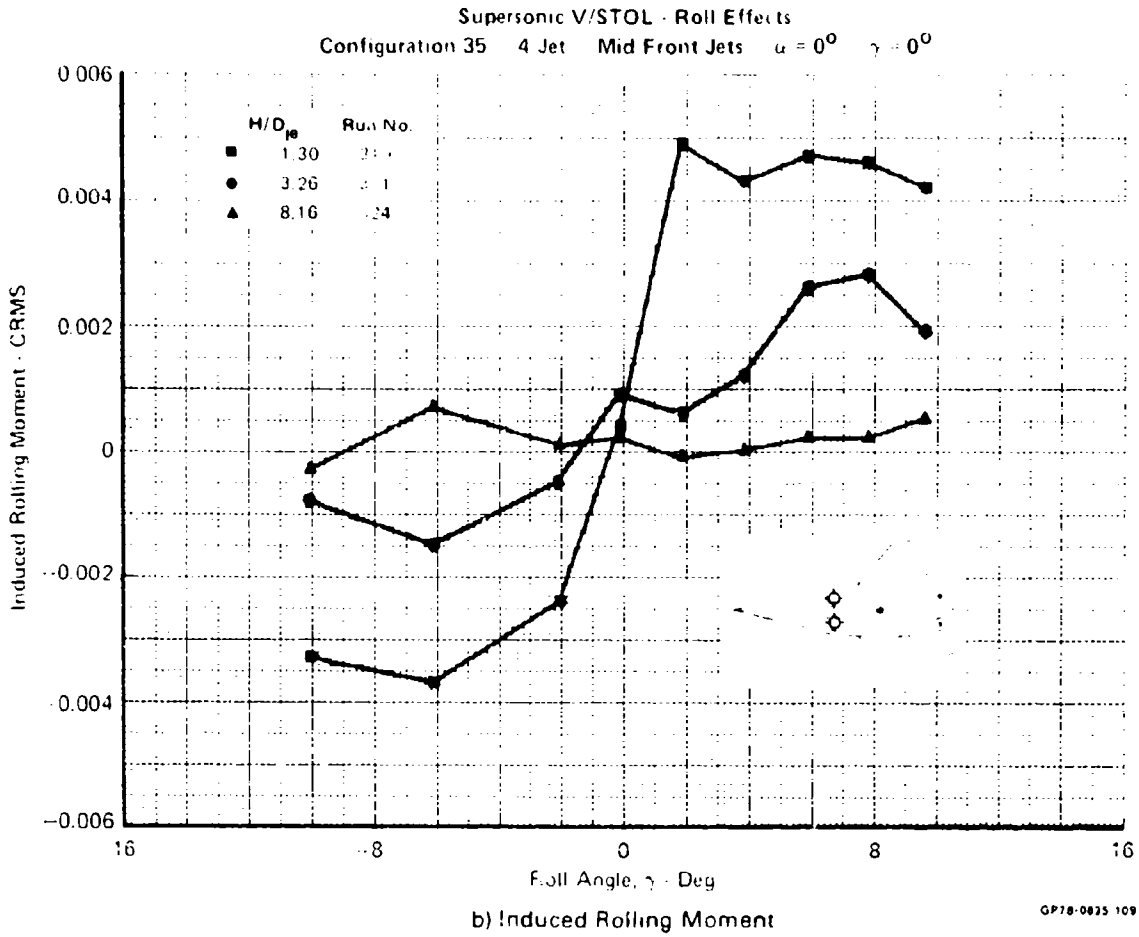

b) Induced Rolling Moment

FIGURE 5-27 (Concluded)
4 JET SUPERSONIC V/STOL STATIC ROLL EFFECTS

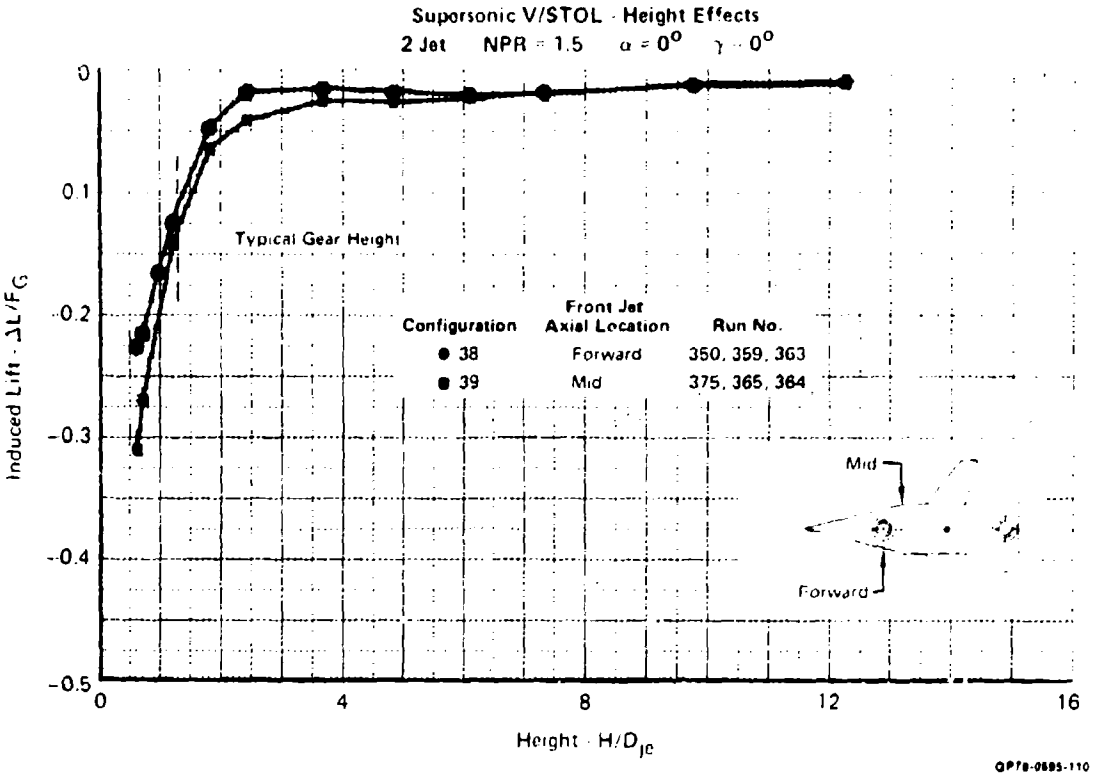

FIGURE 5-28
2 JET SUPERSONIC V/STOL STATIC HEIGHT EFFECTS

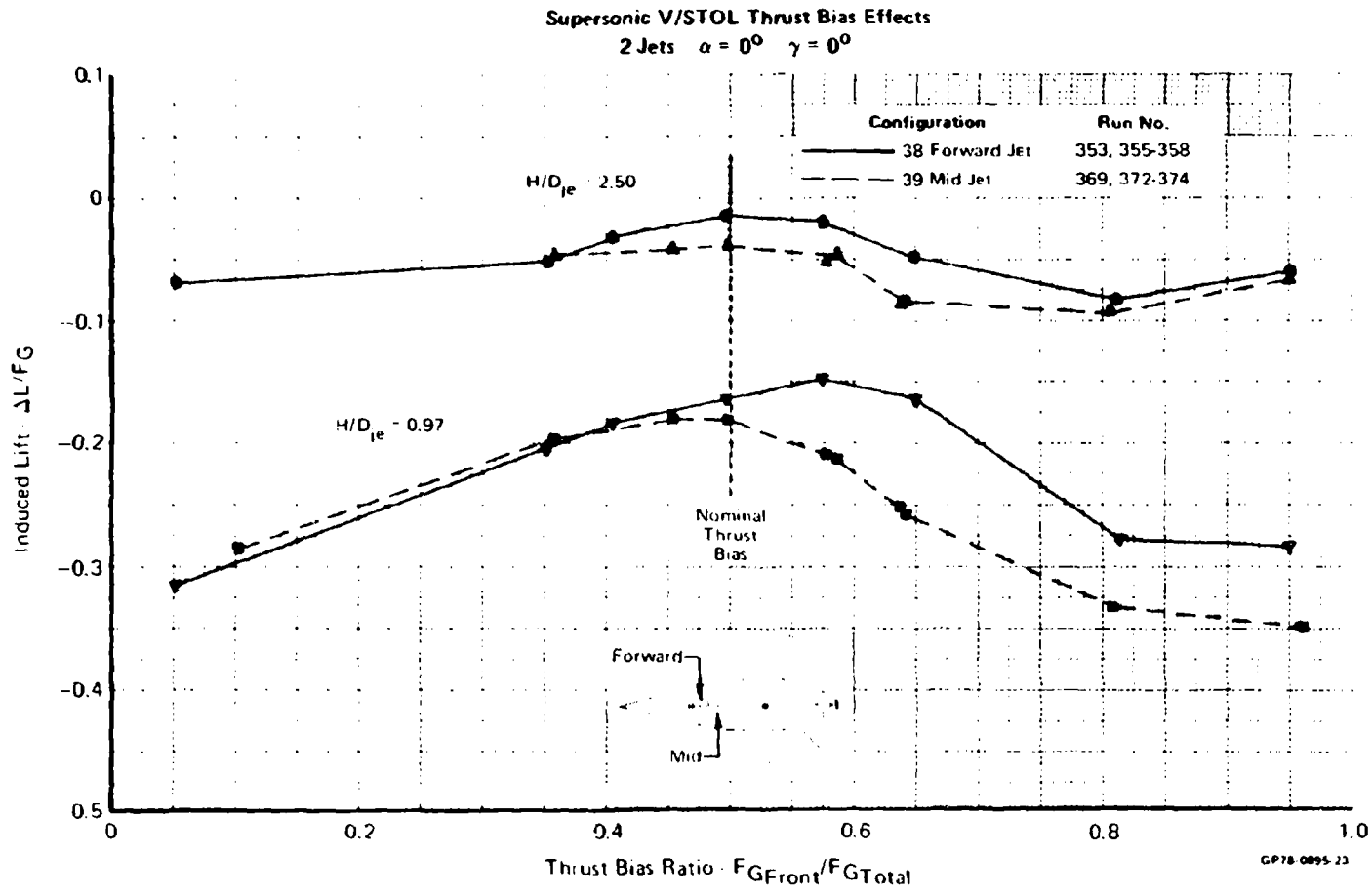

FIGURE 5-29
2 JET SUPERSONIC V/STOL THRUST BIAS EFFECTS

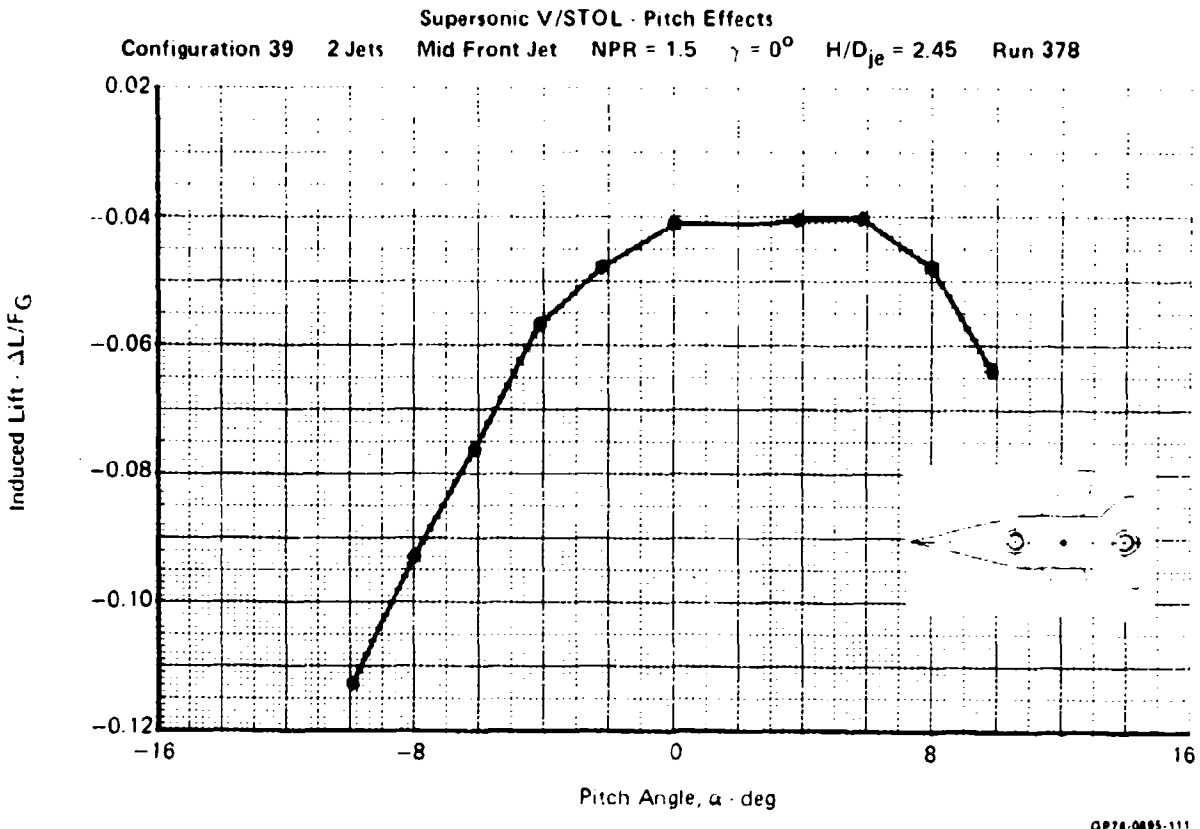

a) Induced Lift

FIGURE 5-30

2 JET SUPERSONIC V/STOL STATIC PITCH EFFECTS

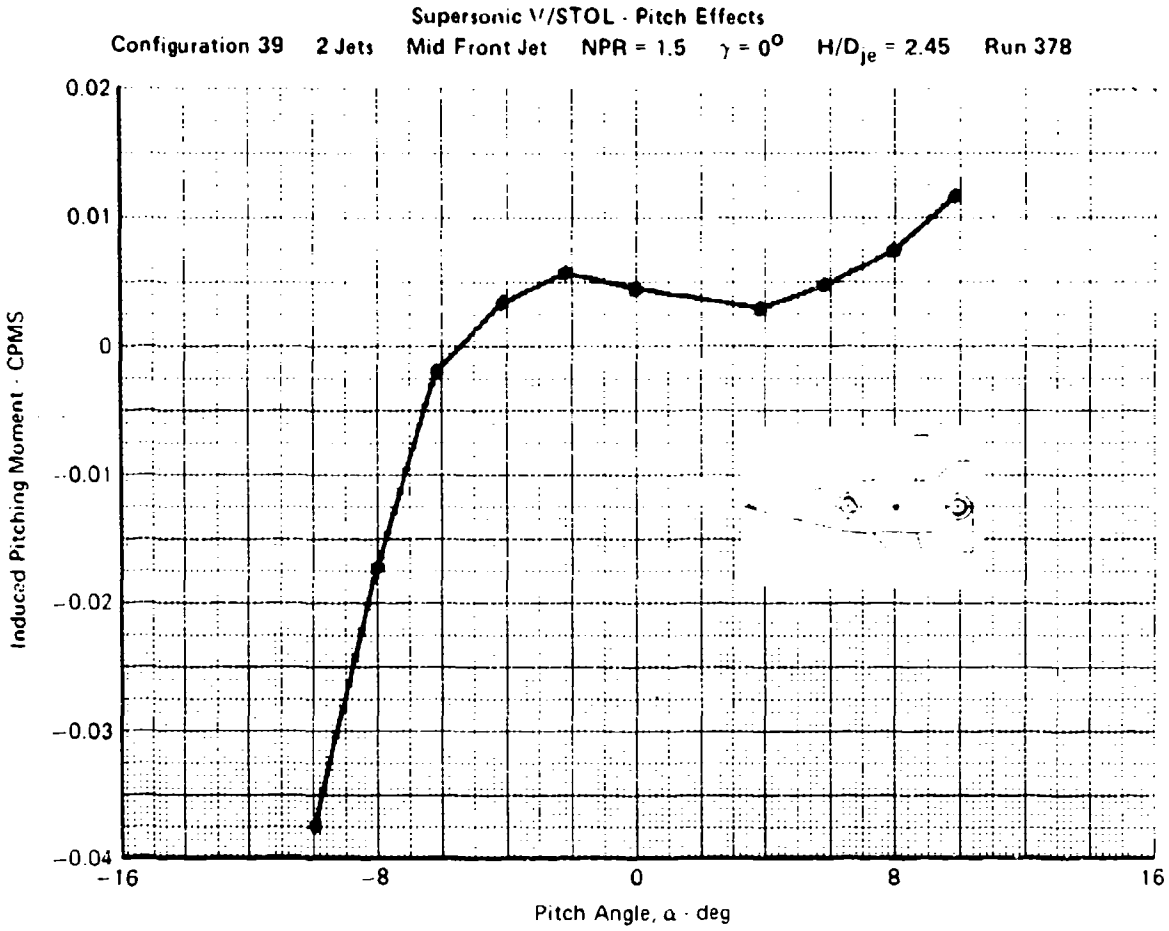

b) Induced Pitching Moment

GP78-0895-112

FIGURE 5-30 (CONCLUDED)
2 JET SUPERSONIC V/STOL STATIC PITCH EFFECTS

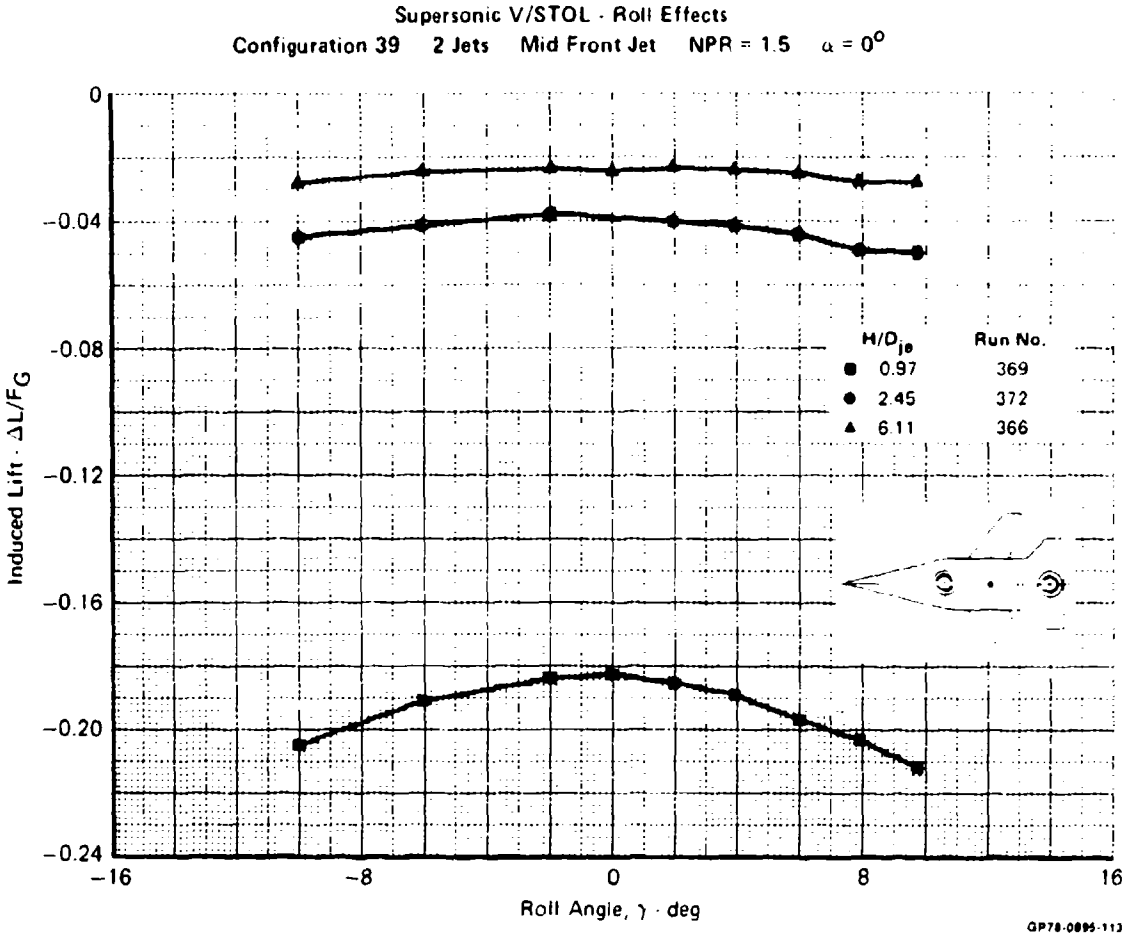

a) Induced Lift

FIGURE 5-31

2 JET SUPERSONIC V/STOL STATIC ROLL EFFECTS

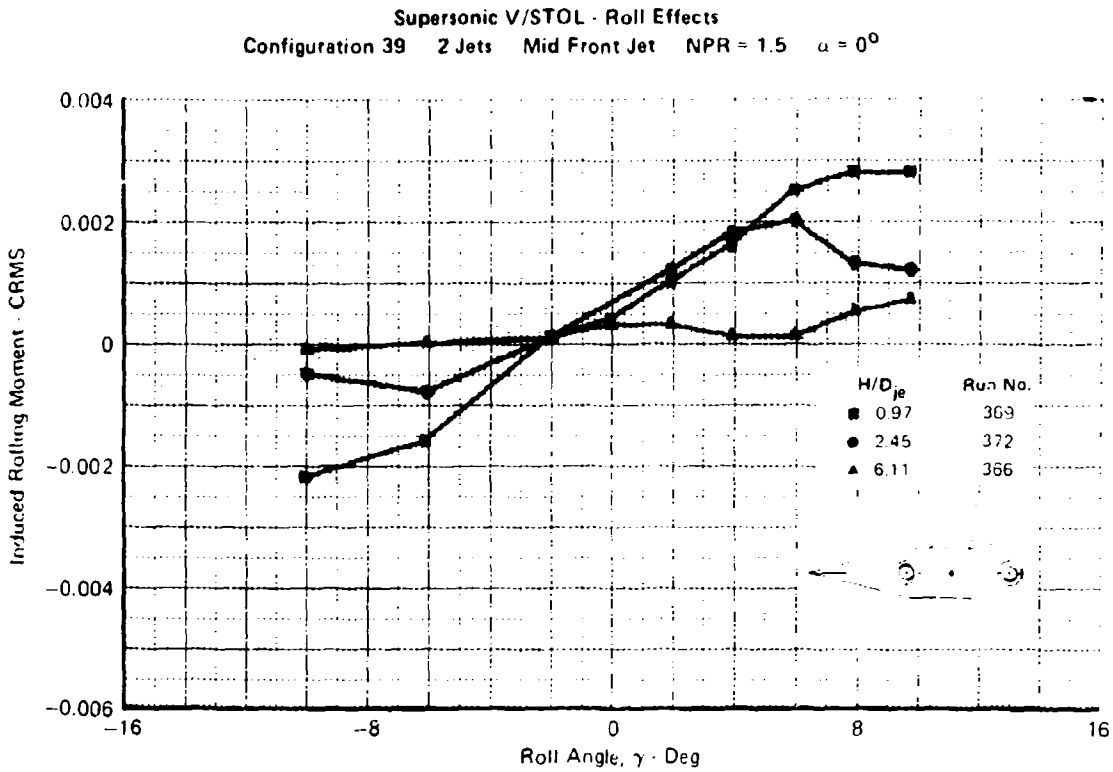

b) Induced Rolling Moment

FIGURE 5-31 (Concluded)
2 JET SUPERSONIC V/STOL STATIC ROLL EFFECTS

deck motion was used to establish the frequency content of the data and the phase relationship between the motion and the response. The effects of selected configuration variables on the dynamic responses were also investigated. The dynamic jet-induced force and moment data are presented in their entirety in Appendix C in Volume II of this report.

5.2.1 Dynamic Jet-Induced Force and Moment Data - Tests were performed at scaled deck motion frequencies and amplitudes which bracketed values predicted from Reference 2. For example, for a DD963 class destroyer in a rough sea the scaled frequency is about 1.5 Hz and the scaled amplitude is about one equivalent nozzle diameter (about 7 ft or 2.1m full scale).

In this study, induced force and moment data were examined for five second time segments randomly selected from the dynamic data records, which were nominally two minutes in length to allow statistical analyses as described in Section 5.2.2. As with the static hover data, discussed in Section 5.1, emphasis is placed on presenting induced lift. However, the effects of the deck pitch and roll angles on the induced moment data as well as the induced lift are presented. In addition, most of the data presented are for the subsonic configuration.

Response to Deck Heave - The influence of deck heave on the induced lift of the fully-contoured subsonic model is shown in Figure 5-32. The heave amplitude was 1.5 D_{je} at 2 Hz, with the neutral point set at the height for maximum induced lift (H/D_{je} = 2). Thus, the height of the model above the deck varies sinusoidally from an H/D_{je} of 0.5 to 3.5. The induced lift response is of a complex periodic nature, but is fairly repeatable, considering the highly turbulent nature of the flowfield. It should be noted that for each of the dynamic data presentations, the deck motion is shown properly aligned with the aerodynamic response.

At a typical gear height, H/D_{je} of 0.7, the lift loss is about 3 percent of the net thrust. As the deck moves away from the model, the induced lift reaches a peak level near H/D_{je} of 2.0 and then begins to decrease as H/D_{je} approaches 3.5. However, when the deck approaches the model, peak lift is higher at an H/D_{je} of 2. This increase in lift (approximately 2 percent) is attributed to a compression or increased cushioning effect in the fountain region due to the velocity of the deck (approximately 6.3 fps or 1.9 m/sec. max).

The inner region plate model described in Section 5.1.1 enables the separate evaluation of the heaving motion on the fountain forces. In dynamic tests with the inner region plate model, the same incremental increase in the fountain force occurs with approaching deck motion as with the complete

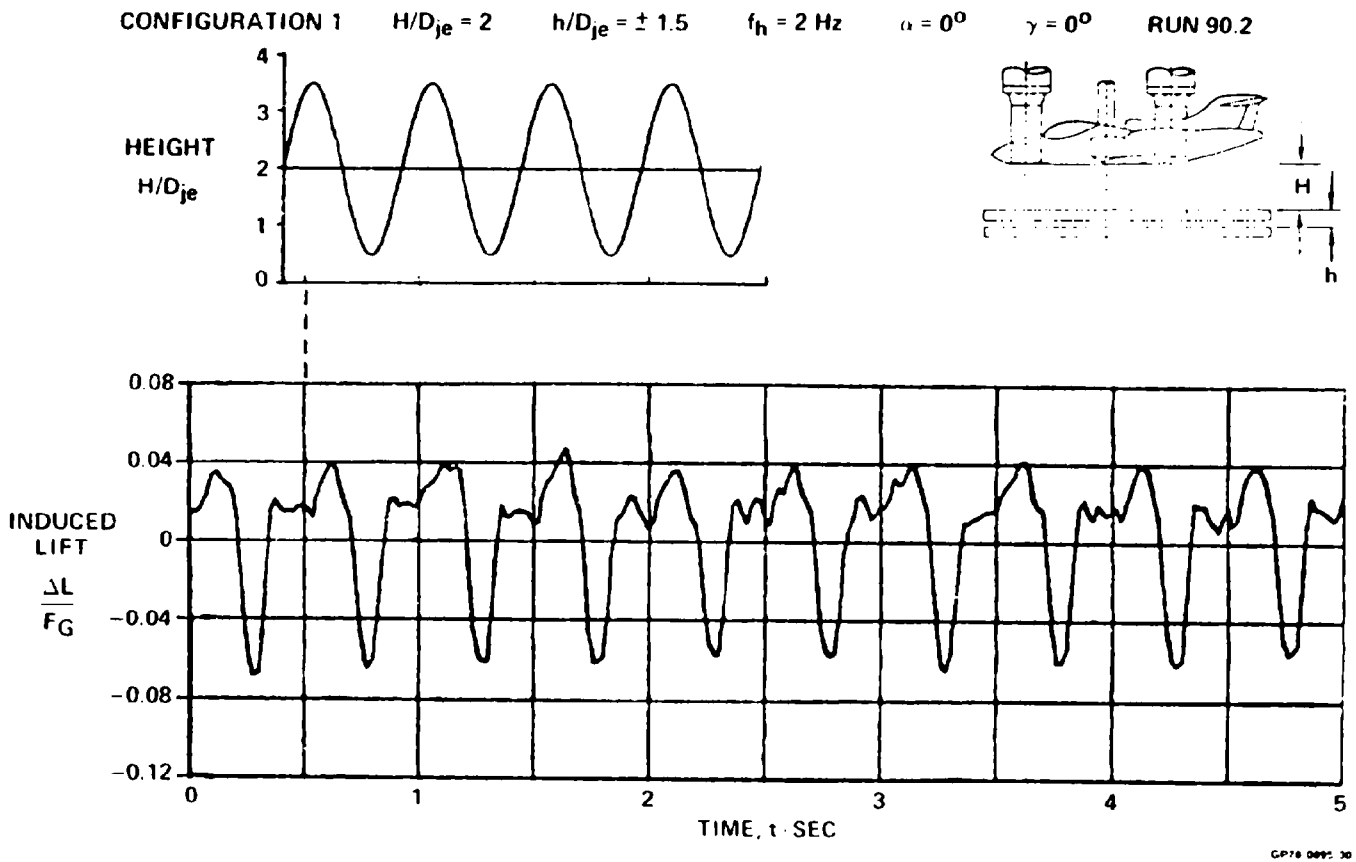

FIGURE 5-32
INDUCED LIFT ON FULLY-CONTOURED SUBSONIC V/STOL FOR HEAVING DECK

model. These results, shown in Figure 5-33, support the conclusion that the increased lift effect with approaching deck motion is associated primarily with the fountain.

The induced lift is influenced at certain heights to a slight degree by the frequency of the deck motion, as seen in Figure 5-34, where data are presented for both 1, 2, and 3 Hz. A larger difference is apparent at 3 Hz between the induced lift values for heave toward and away from the model. This is attributed to the change in peak deck velocity and the modified compression effect in the fountain.

The decrease in the induced lift variation with heave amplitude is shown in Figure 5-35 for an H/D_{je} of 2. The reduced response is apparent at a heave amplitude of 0.5 D_{je}.

Response to Deck Pitch and Roll - For small ships, the roll is generally the motion having the highest frequency and amplitude, and thus, may have the most impact on V/STOL aircraft operations. For example, the DD963 class ship can respond to a rough sea condition with a roll of approximately $\pm 10°$ and a full scale period of about 8 seconds (Reference 2). The deck pitch is of much smaller magnitude, generally around $\pm 2°$. However, for this study equal pitch and roll amplitudes were investigated, since it was assumed that the V/STOL aircraft could land or take-off at any orientation relative to the deck.

The induced lift and rolling moment variations for $\pm 2°$, $\pm 6°$, and $\pm 10°$ of deck roll are presented in Figures 5-36 and 5-37 for the subsonic configuration at an H/D_{je} of 2. A significant induced lift loss occurs for roll angles greater than $\pm 2°$. This is attributed to a loss in the fountain lift as the impingement point moves off the centerline toward the side further away from the deck and to the upward slope of the fuselage relative to the deck. The lift loss is accompanied by a destabilizing rolling moment, which is primarily caused by fountain impingement on the wing. With dynamic motion, the impingement oscillates back and forth from one wing to the other.

The effects of deck roll are highly sensitive to height as shown in Figure 5-38, where the induced lift and rolling moment data are presented for $\pm 10°$ roll at H/D_{je} values of 0.8 and 5. Adverse effects are negligible at an H/D_{je} of 5.

The induced lift and pitching moment variations for $\pm 2°$, $\pm 6°$, and $\pm 10°$ of deck pitch are presented in Figures 5-39 and 5-40 at an H/D_{je} of 2. Induced lift losses are apparent primarily at the positive, or nose up, pitch

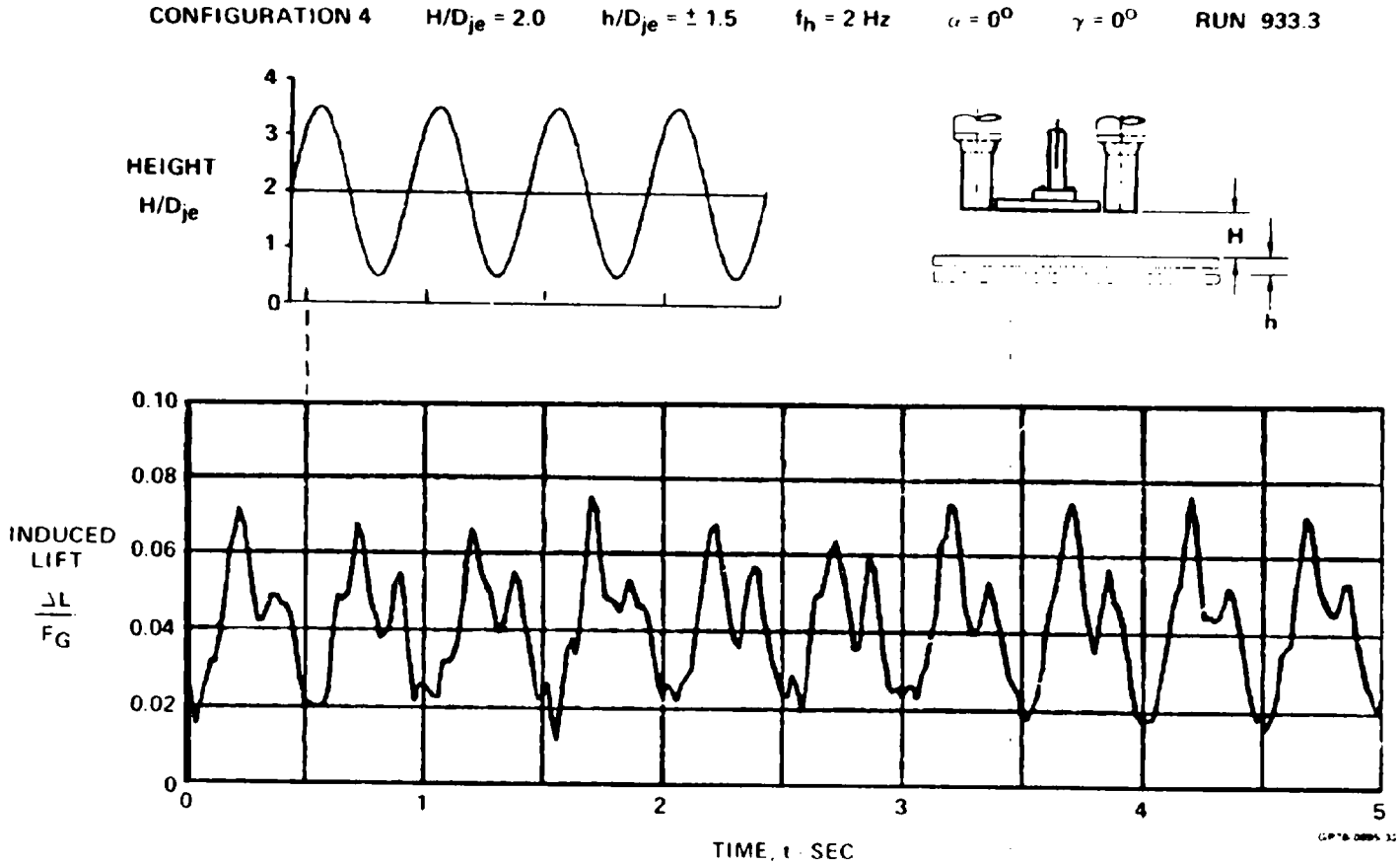

FIGURE 5-33
INDUCED LIFT ON INNER REGION PLATE FOR HEAVING DECK

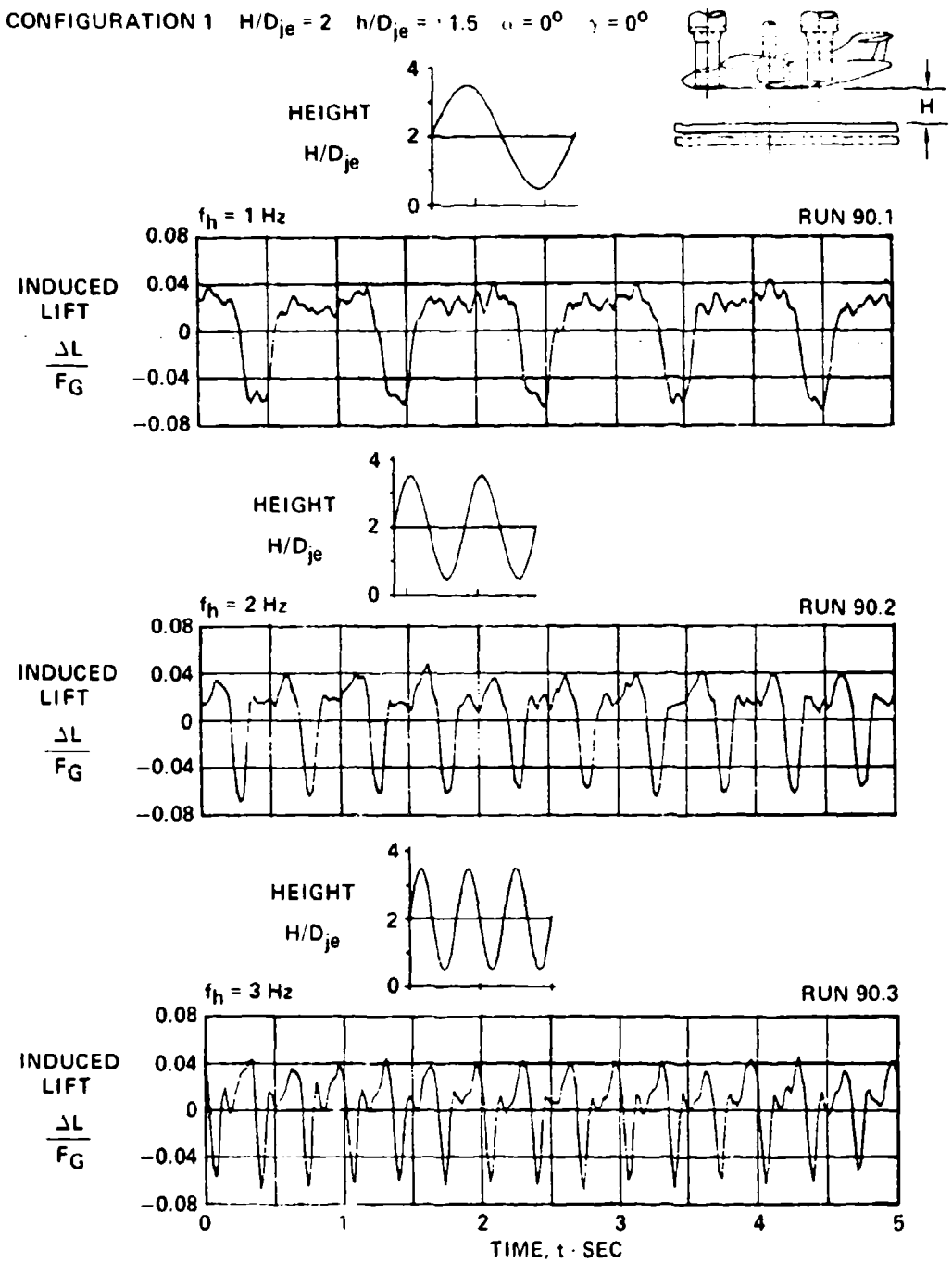

FIGURE 5-34

SUBSONIC V/STOL HEAVE FREQUENCY EFFECTS

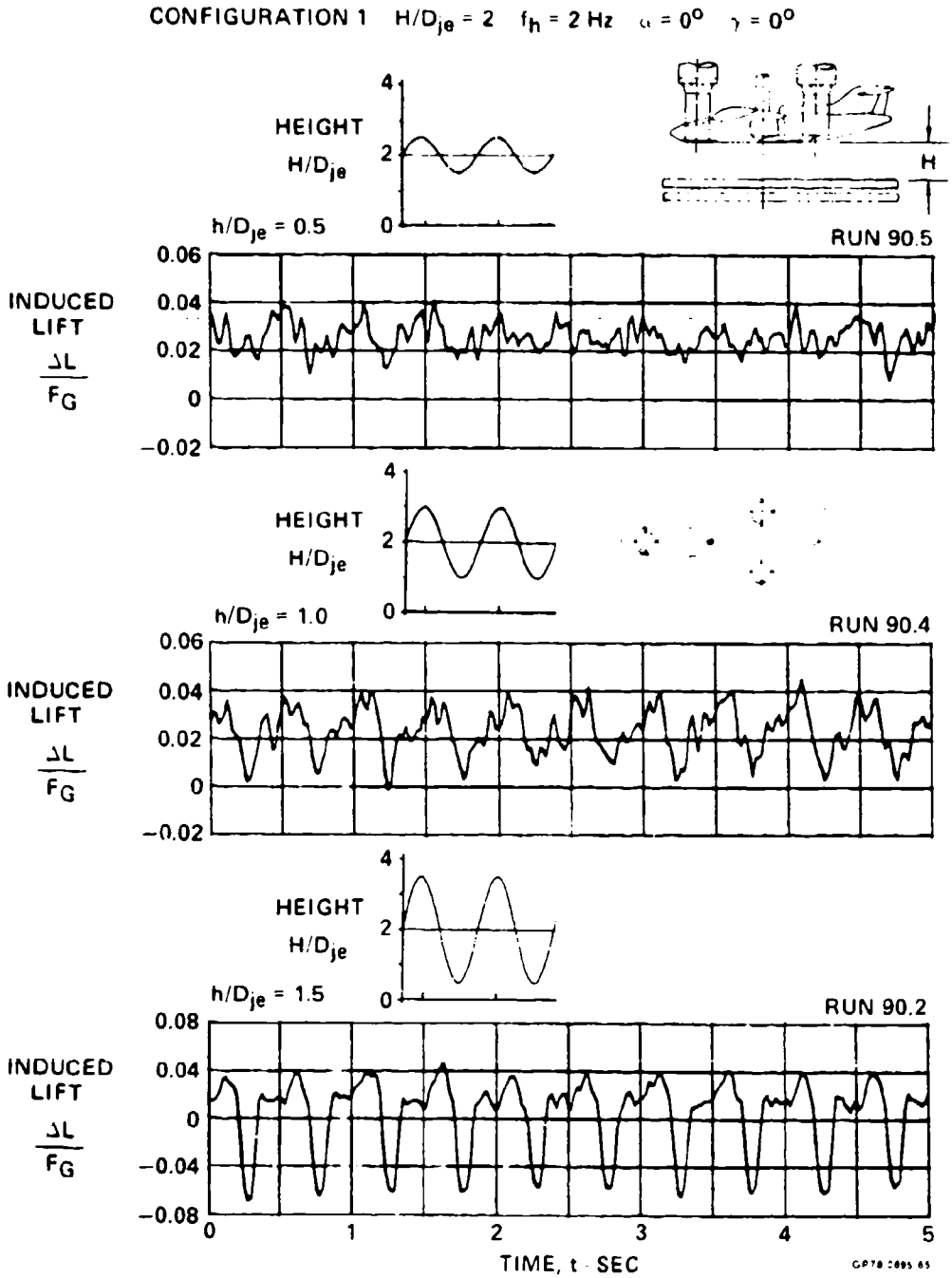

FIGURE 5-35
SUBSONIC V/STOL HEAVE AMPLITUDE EFFECTS

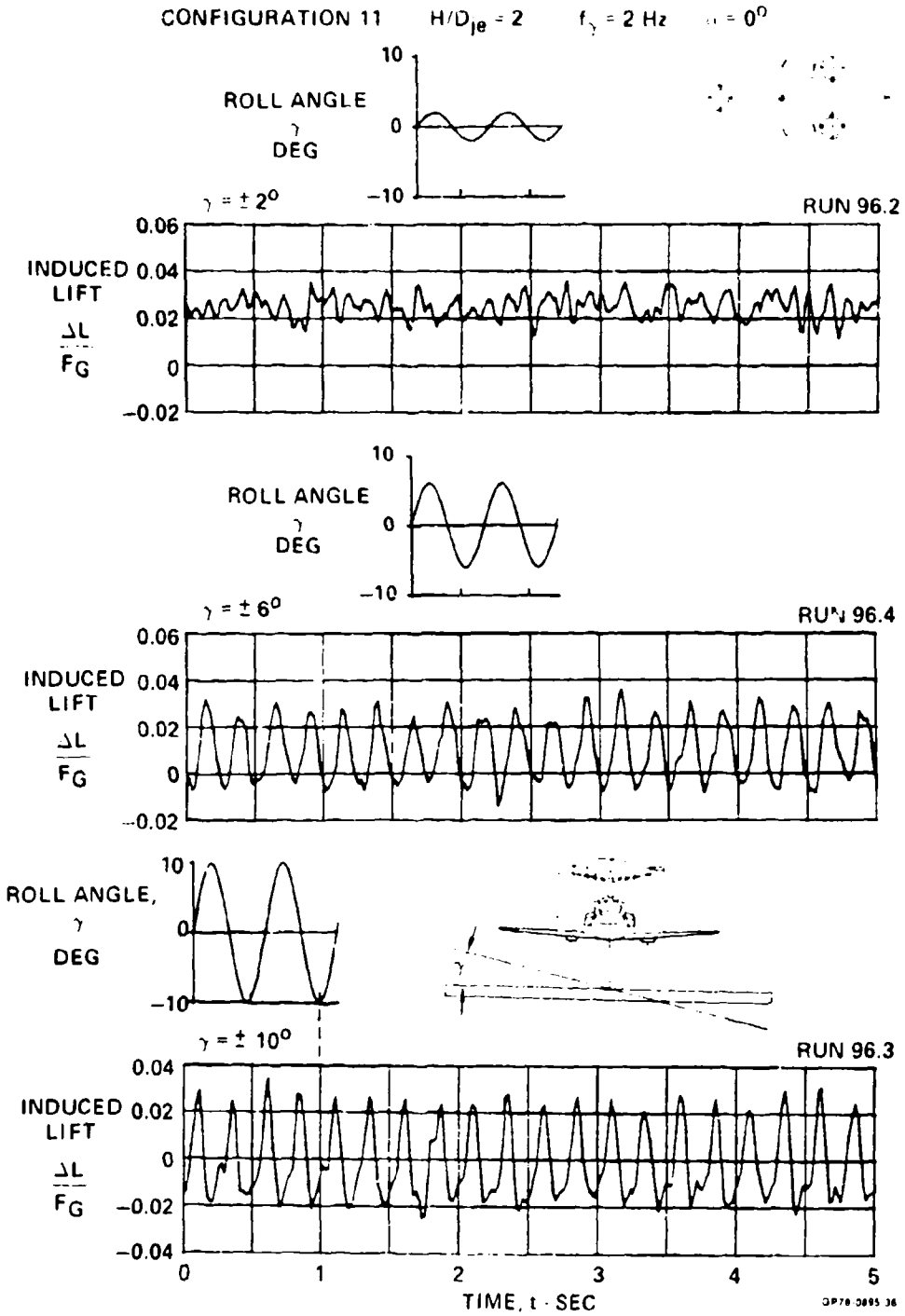

FIGURE 5-36
SUBSONIC V/STOL INDUCED LIFT FOR ROLLING DECK

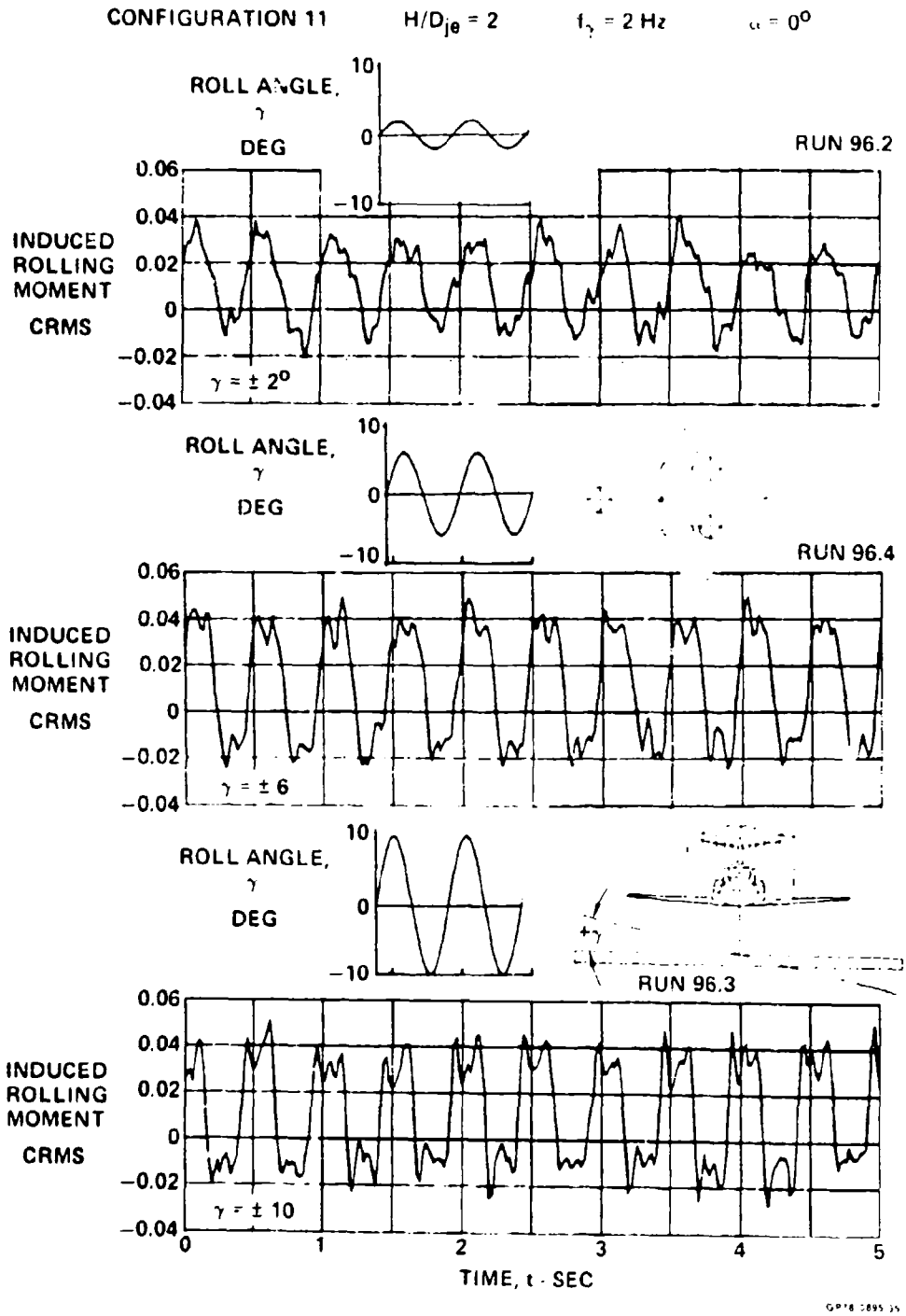

FIGURE 5-37
SUBSONIC V/STOL INDUCED ROLLING MOMENT FOR ROLLING DECK

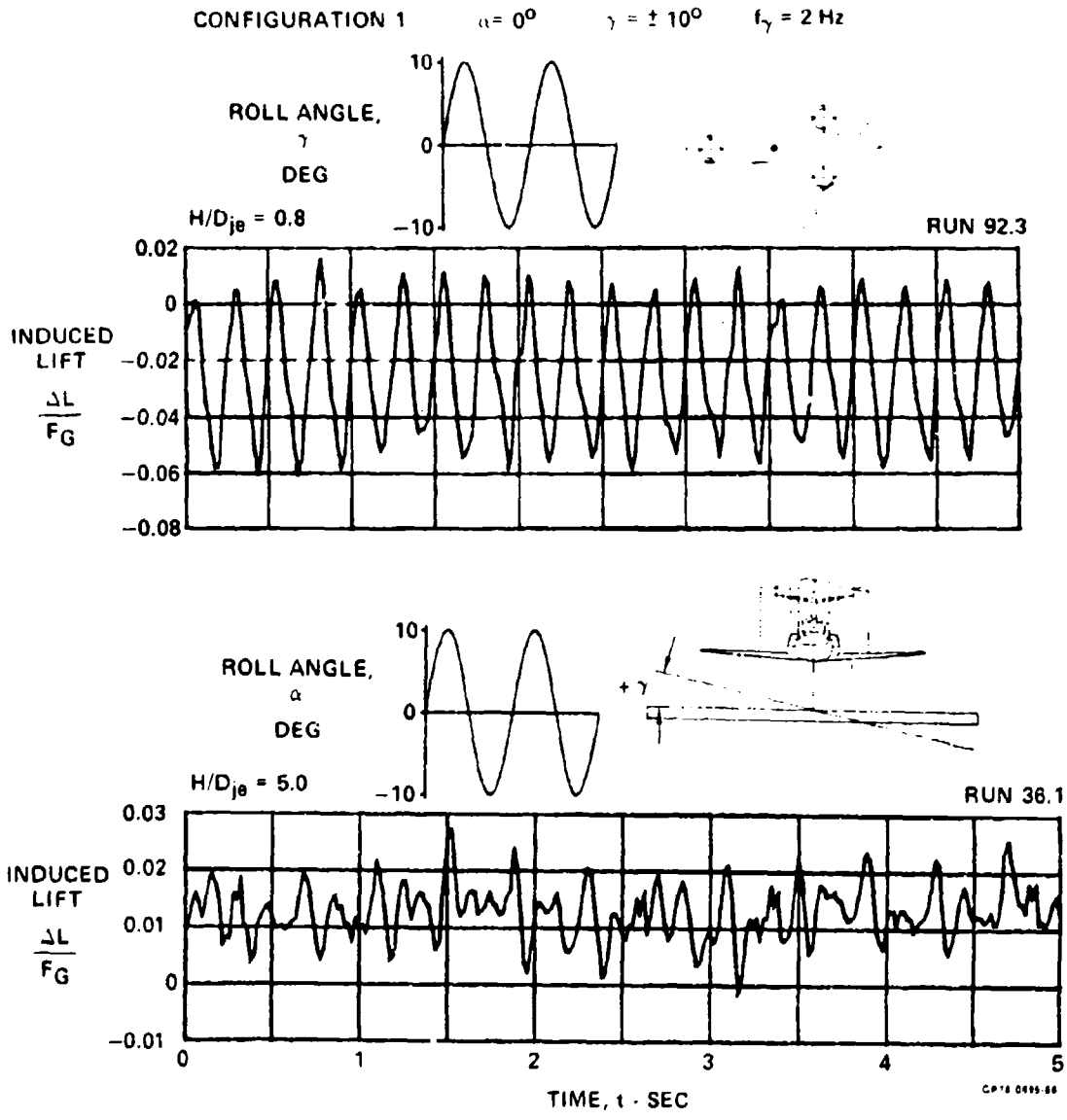

FIGURE 5-38
SUBSONIC V/STOL HEIGHT EFFECTS FOR ROLLING DECK

attitudes relative to the deck. This is attributed to increased suckdown near the two rear nozzles and aft-end, which are nearer the deck at positive pitch angles.

The induced pitching moment tends to become more negative (nose down) with negative pitch angle, probably due to an increase in suckdown on the forebody and movement of the fountain impingement point aft.

As with deck roll, the adverse effects of deck pitch are negligible at an H/D_{je} of 5. This is illustrated in Figure 5-41 where the induced lift and pitching moment are presented for $\pm 10°$ pitch at H/D_{je} values of 0.8, 2 and 5.

Based on the effects of deck pitch and roll discussed above, a preferred aircraft orientation, particularly during recovery operations, may be derived. Since deck motion in the roll axis of the aircraft has more impact on the lift and stability, alignment of the aircraft roll axis with the ship pitch axis would appear to be favorable due to the lower amplitude pitching motion of ships.

Response to Combined Motions - Tests were performed with various combinations of heave, pitch and roll motions to measure the jet-induced aerodynamic response of the aircraft to the complex flowfields established under these conditions. The effect of the phase angle between the motions was also investigated (e.g., the roll and pitch motions were tested in phase and 90° out of phase). Most of the tests were made on the subsonic configuration at an H/D_{je} of 2.

The lift response to combined heave and roll motions is presented in Figure 5-42. The heave amplitude was $1.5\ D_{je}$ and the roll amplitude $\pm 10°$, both at 2 Hz. A lift loss of approximately 6 percent occurs near a typical gear height.

Responses to combined heave and pitch; pitch and roll; and heave, pitch, and roll are presented in Figures 5-43 through 5-45. Each set of data indicates a fairly well defined, repeatable, complex periodic response to the combined motion. Thus, the response to complex motions is not random, but follows a consistent pattern.

Limited tests were performed with heaving motion superimposed on a height variation to simulate vertical take-off and landing maneuvers. The height variation (or variation of the deck neutral point) was accomplished using a ramp function generator for the height, plus a sine function generator for the heave. A partial trace of the induced lift response taken in a height range from H/D_{je}

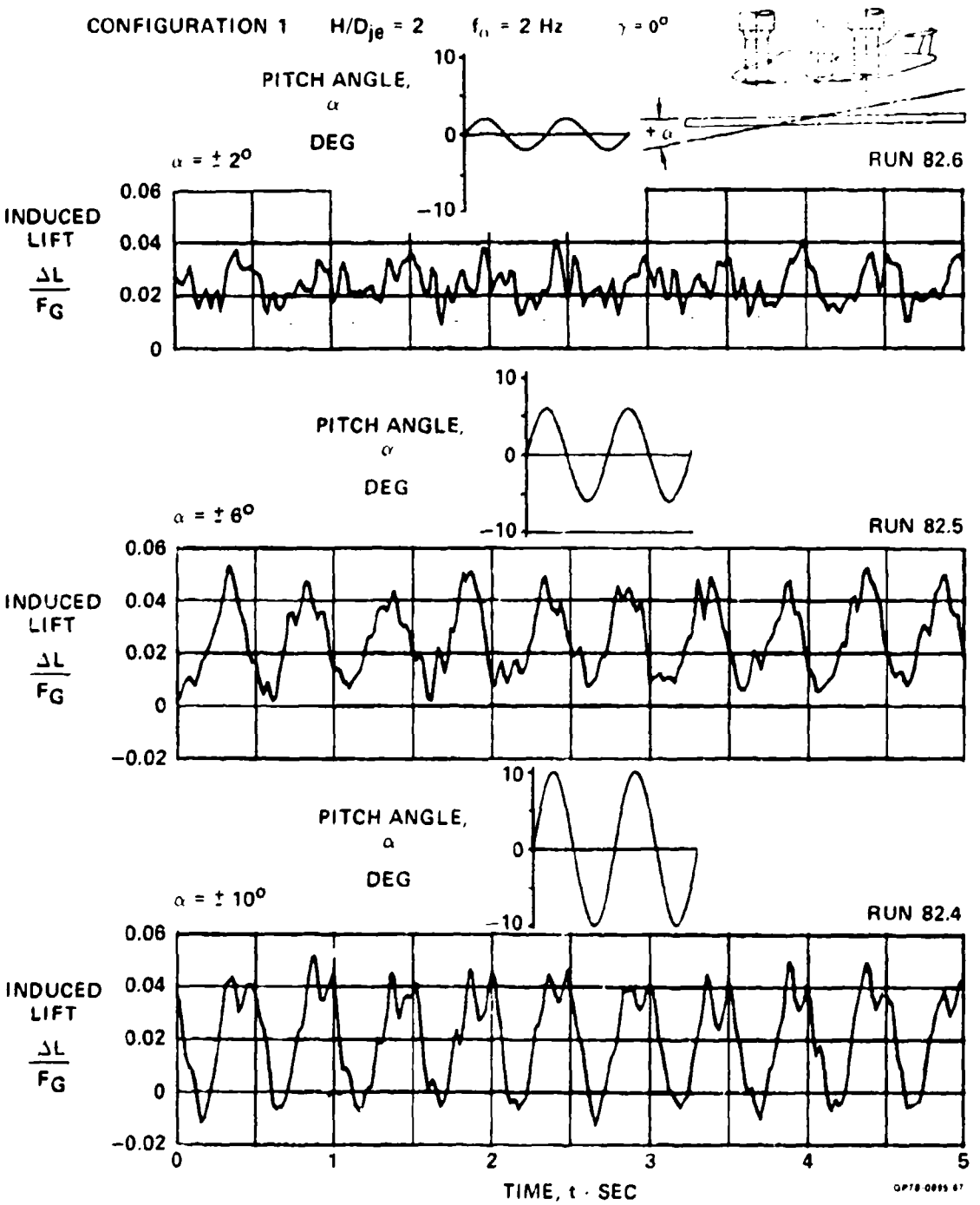

FIGURE 5-39
SUBSONIC V/STOL INDUCED LIFT FOR PITCHING DECK

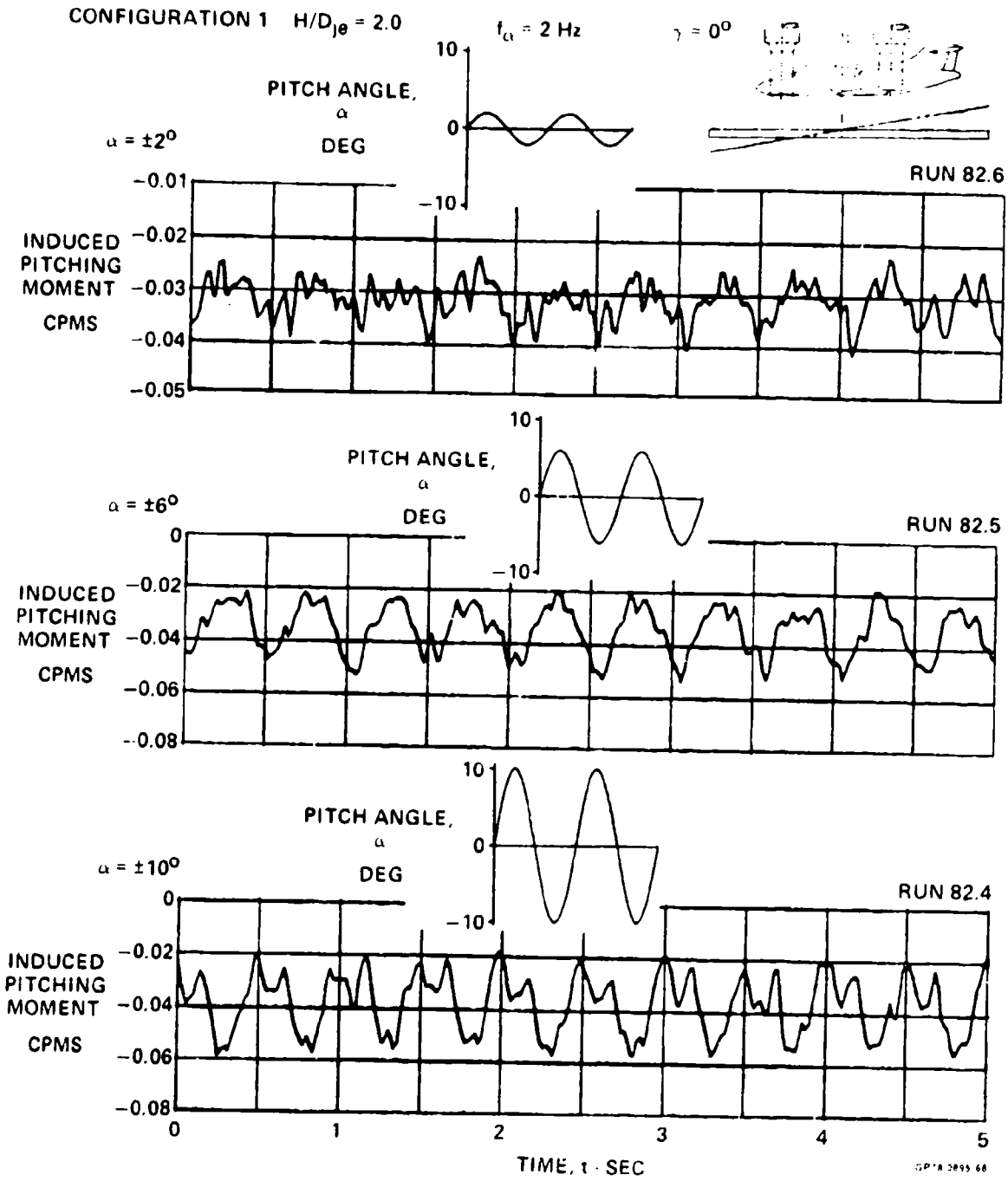

FIGURE 5-40

SUBSONIC V STOL INDUCED PITCHING MOMENT FOR PITCHING DECK

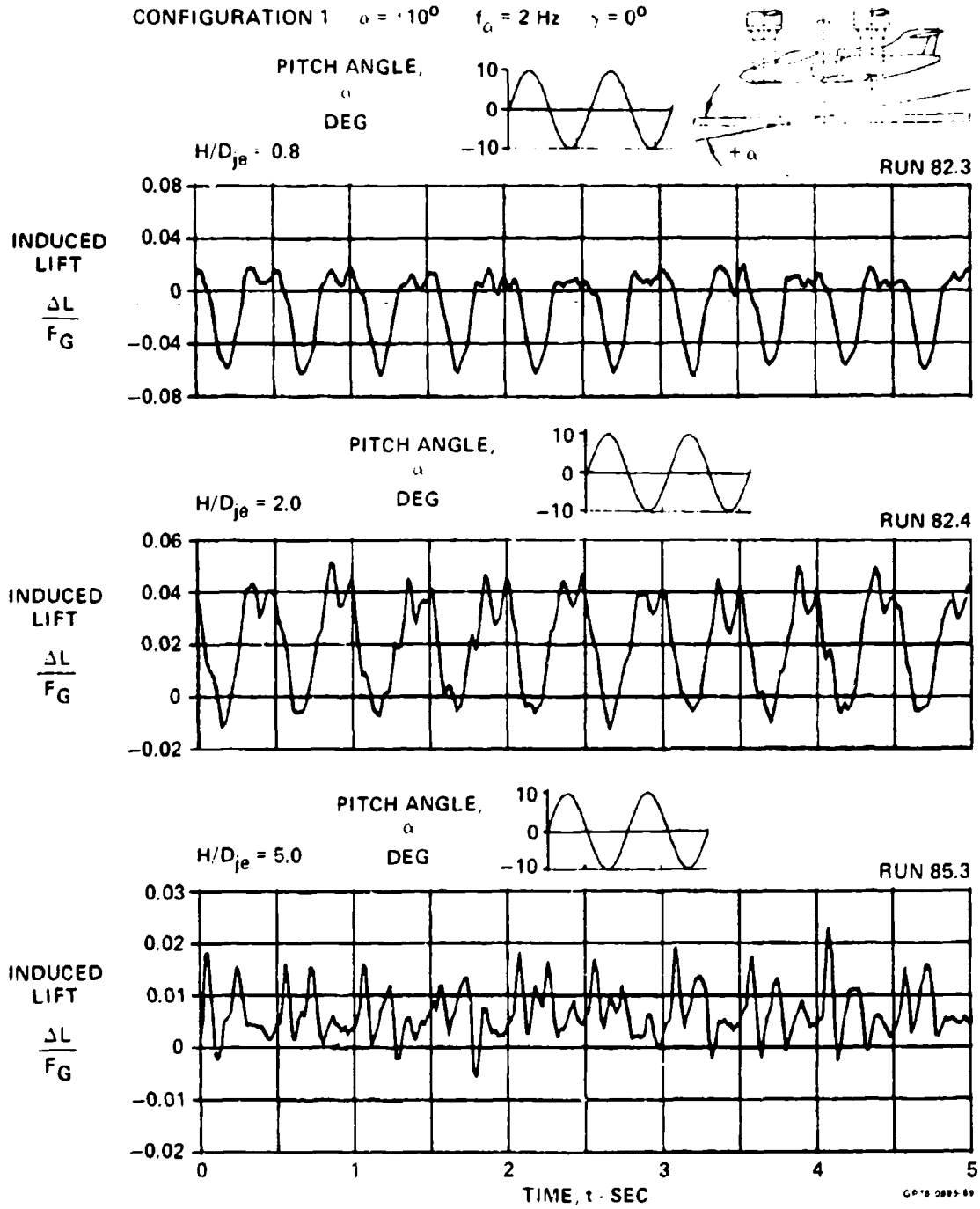

a) Induced Lift

FIGURE 5-41
SUBSONIC V/STOL HEIGHT EFFECTS FOR PITCHING DECK

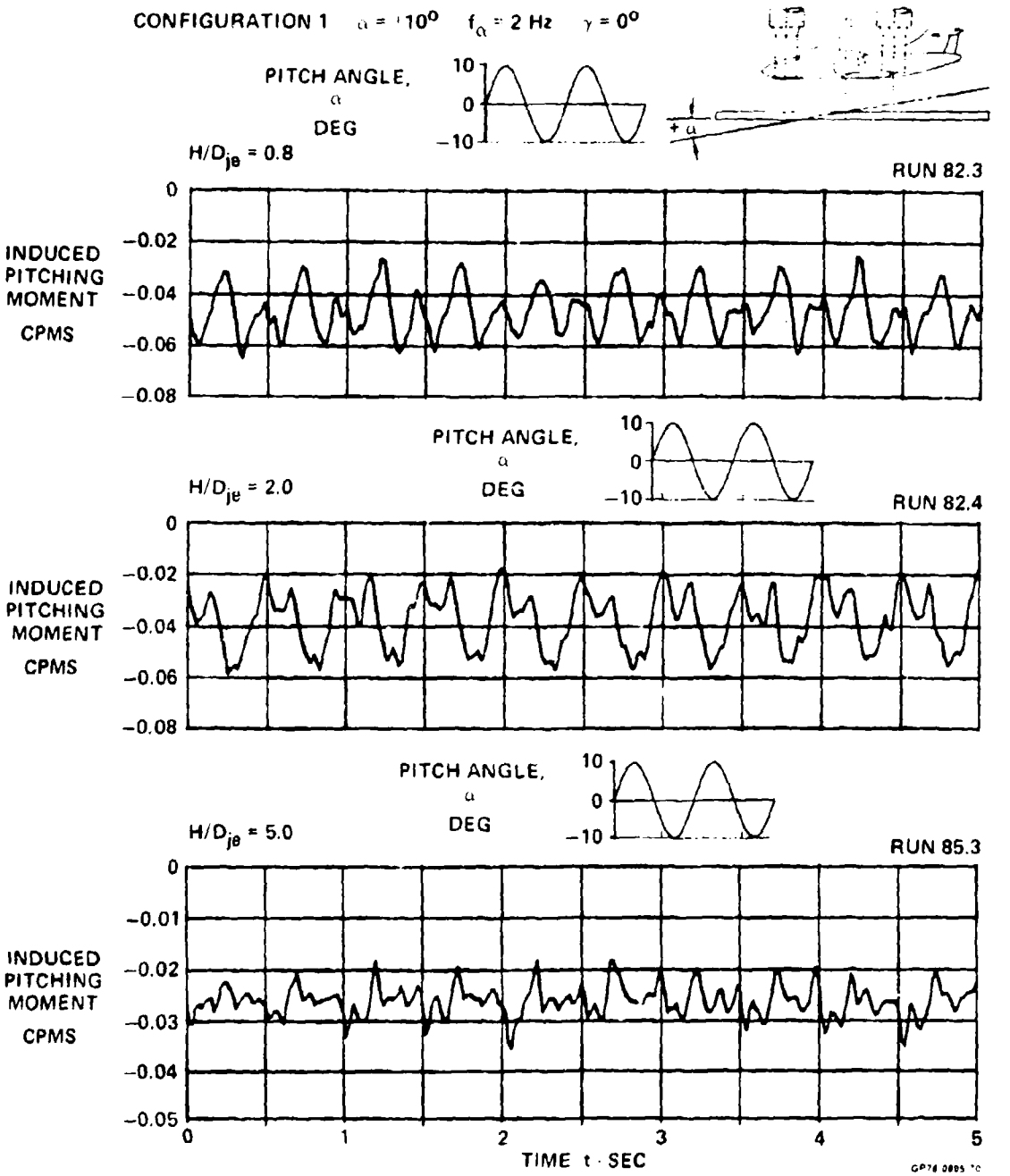

b) Induced Pitching Moment

FIGURE 5-41 (Concluded)
SUBSONIC V/STOL HEIGHT EFFECTS FOR PITCHING DECK

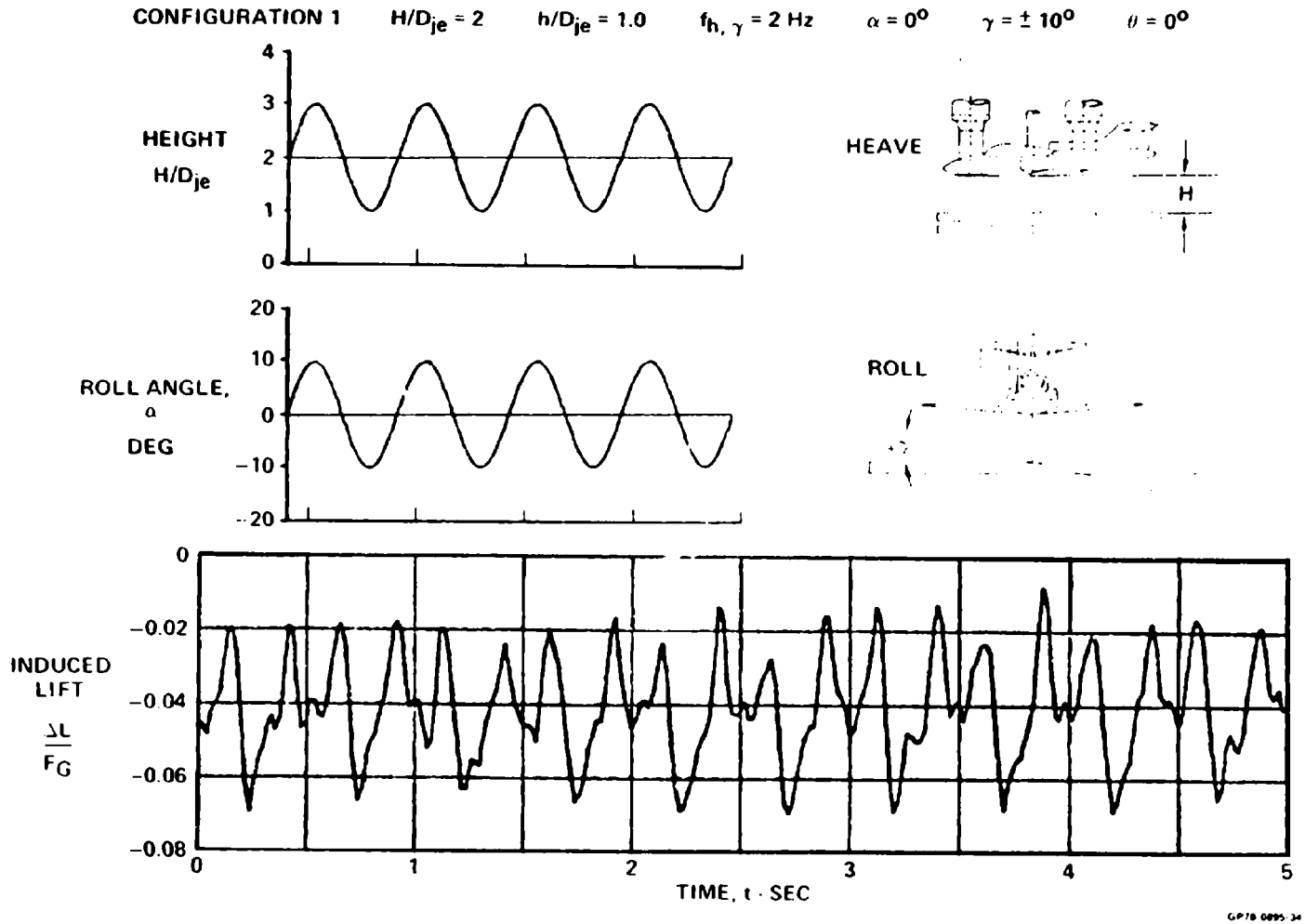

FIGURE 5-42
SUBSONIC V/STOL INDUCED LIFT FOR HEAVING AND ROLLING DECK

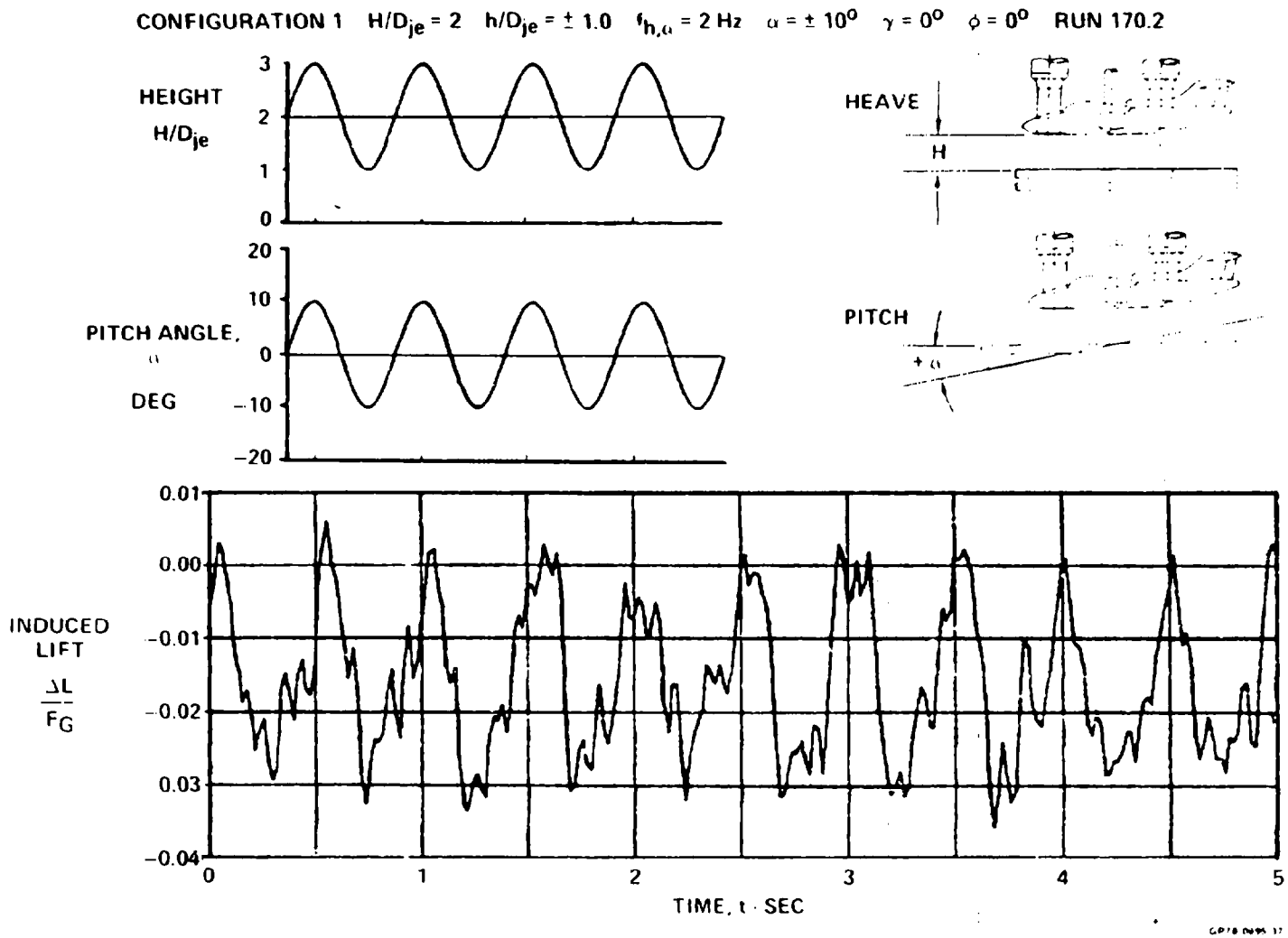

FIGURE 5-43
SUBSONIC V/STOL INDUCED LIFT FOR HEAVING AND PITCHING DECK

CONFIGURATION 1 $H/D_{je} = 2$ $\alpha = \pm 10^{o}$ $\gamma = \pm 10^{o}$ $f_{\alpha,\gamma} = 2$ Hz RUN 165.1
$\varphi = 0^{o}$

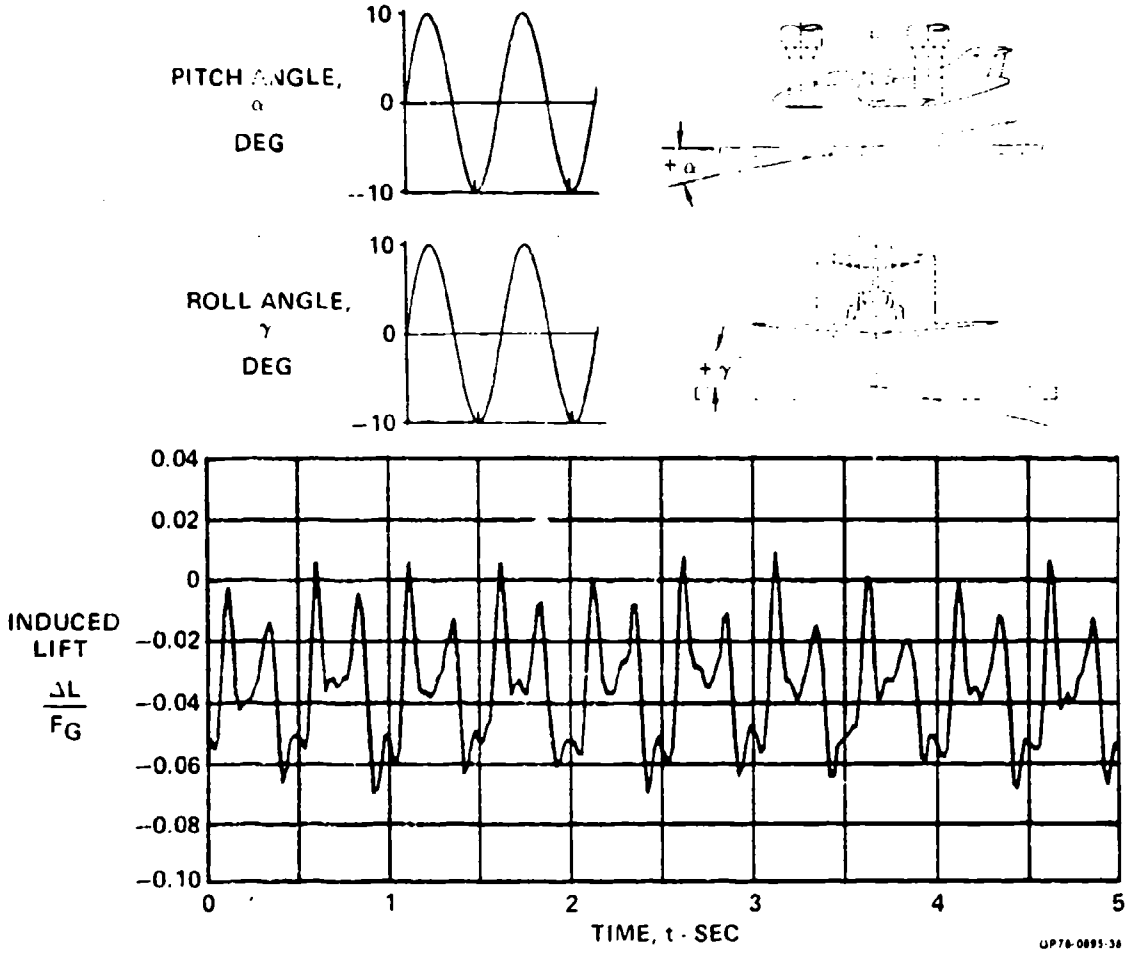

FIGURE 5-44
SUBSONIC V/STOL INDUCED LIFT FOR PITCHING AND ROLLING DECK

CONFIGURATION 1 $H/D_{je} = 2$ $h/D_{je} = +1.0$ $\alpha = \pm 10^{o}$ $\gamma = \pm 10^{o}$ RUN 171.1

$f_{h,\alpha,\gamma} = 2$ Hz

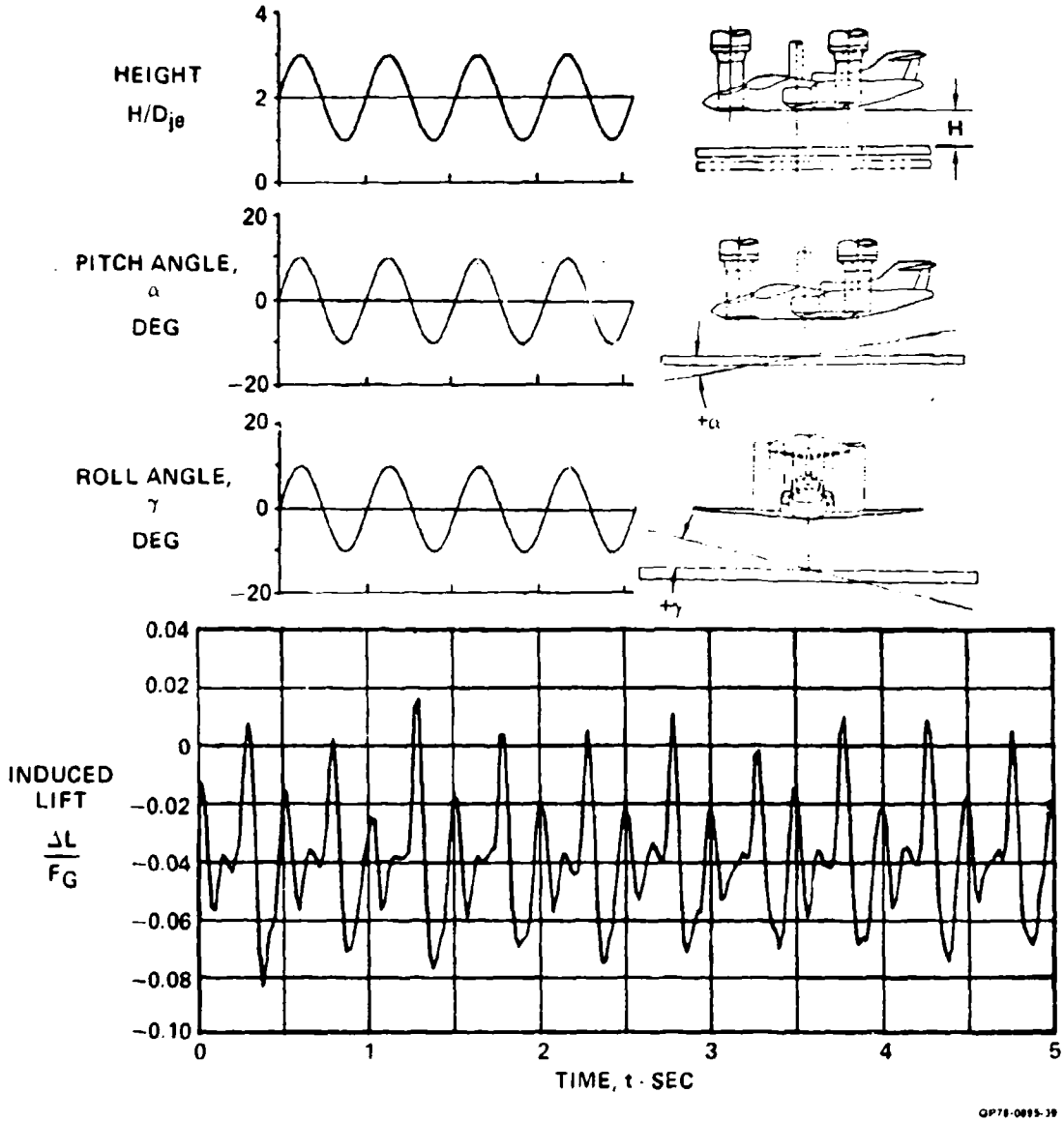

FIGURE 5-45
SUBSONIC V/STOL INDUCED LIFT FOR HEAVING, PITCHING, AND ROLLING DECK

of 2 to 5 with a heave amplitude of approximately 1.0 D_{je} is shown in Figure 5-46. The results simulate a vertical landing at a descent rate of 0.06 fps (or 0.018 m/sec), which is considerably less than actual descent rates (about 3 fps or 0.9 m/sec). However, the results are more clearly indicated at this rate. Data for higher rates are also available in Appendix C. The induced lift variation shown in Figure 5-46 indicates an increase in lift as the deck height approaches an H/D_{je} of 2, and is generally consistent with the data obtained for motions about fixed points.

Configuration Effects - The effects of overall aircraft design (subsonic versus supersonic), nozzle arrangement, lift improvement devices, and fuselage contouring were also examined. Induced lift data are presented for a heave amplitude of 1.5 D_{je} at an H/D_{je} of 2. The effects of the selected configuration variables are generally consistent with those observed in the static hover data at a given height.

The three-nozzle subsonic planform configuration is compared to the three-nozzle supersonic planform configuration in Figure 5-47. Substantially different induced lift variations are apparent since the subsonic configuration has a relatively strong fountain and low suckdown whereas the suckdown dominates the supersonic configuration.

The effectiveness of the LID's in improving the lift characteristics of the subsonic configuration IGE can be readily seen in Figure 5-48. The maximum induced lift of approximately 12 percent is even larger than that measured in static hover tests due to the increase in the cushioning effect when the deck is approaching the model. The results for rolling motion indicate that the LID's are effective even at high roll angles, consistent with the static data results. These data are given in Appendix C.

The fuselage contouring effects on the induced lift can be readily seen in Figure 5-49 for the subsonic configuration. The largest difference is near the deck neutral point, H/D_{je} of 2, and as explained in Section 5.1, is attributed to the difference in curvature in the region between the two rear nozzles. This is the region of the strongest fountain momentum and the resulting net lift on the fully-contoured model is reduced due to the upward curvature of the lower fuselage.

5.2.2 Frequency Content and Phase Relationship of the Dynamic Data - The frequency content of the aerodynamic response to the deck motion was assessed statistically by performing a power spectral density analysis. Since the induced force and moment data were found to be stochastic complex periodic

CONFIGURATION 1 H/D_{je} = 2 TO 5 h/D_{je} = ± 1.0 f_h = 2 Hz VTOL RATE = 0.06 FT/SEC $\alpha = 0^o$ $\gamma = 0^o$ RUN 182.1

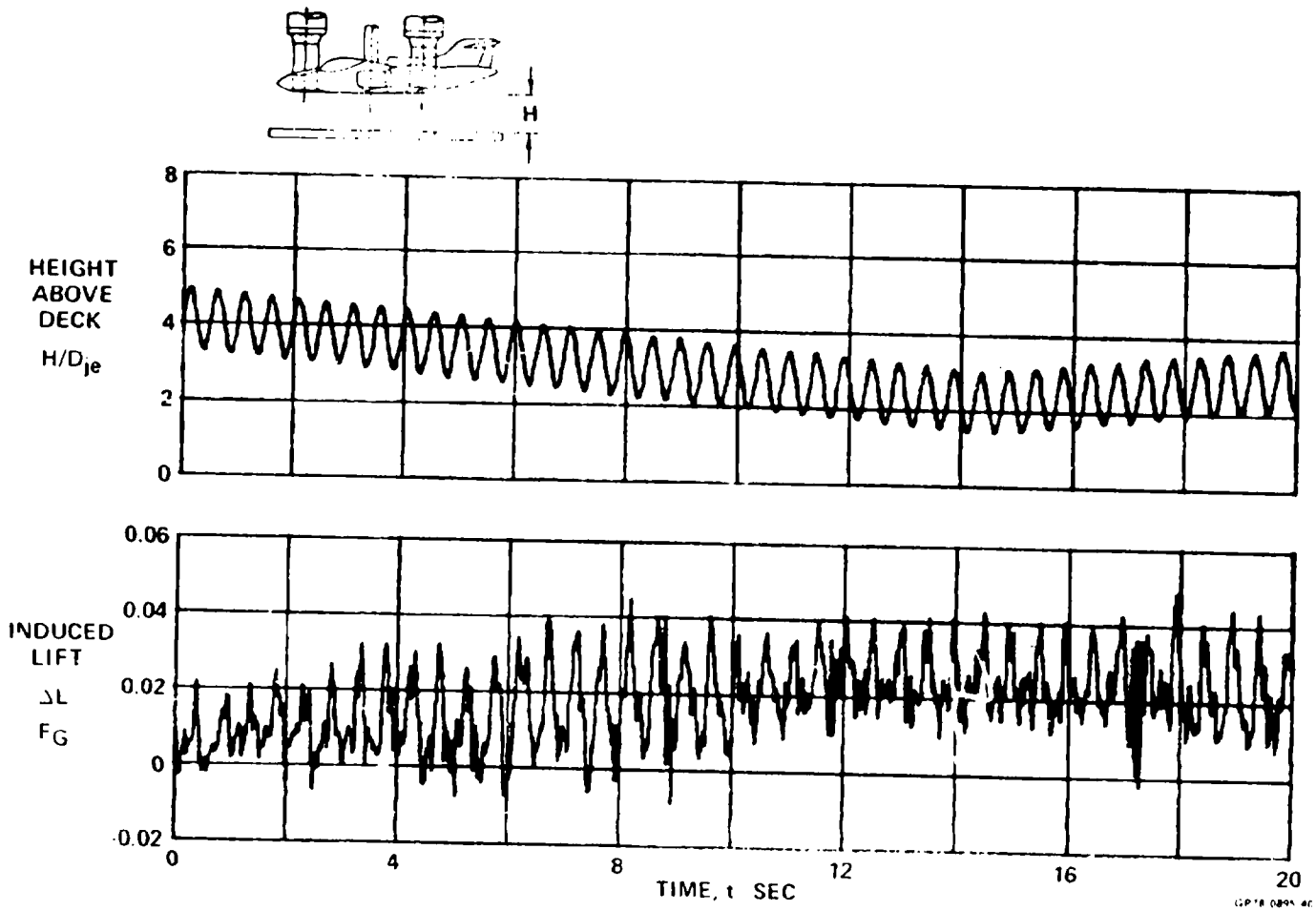

FIGURE 5-46
SUBSONIC V/STOL INDUCED LIFT FOR DYNAMIC VERTICAL TAKEOFF AND LANDING SIMULATION

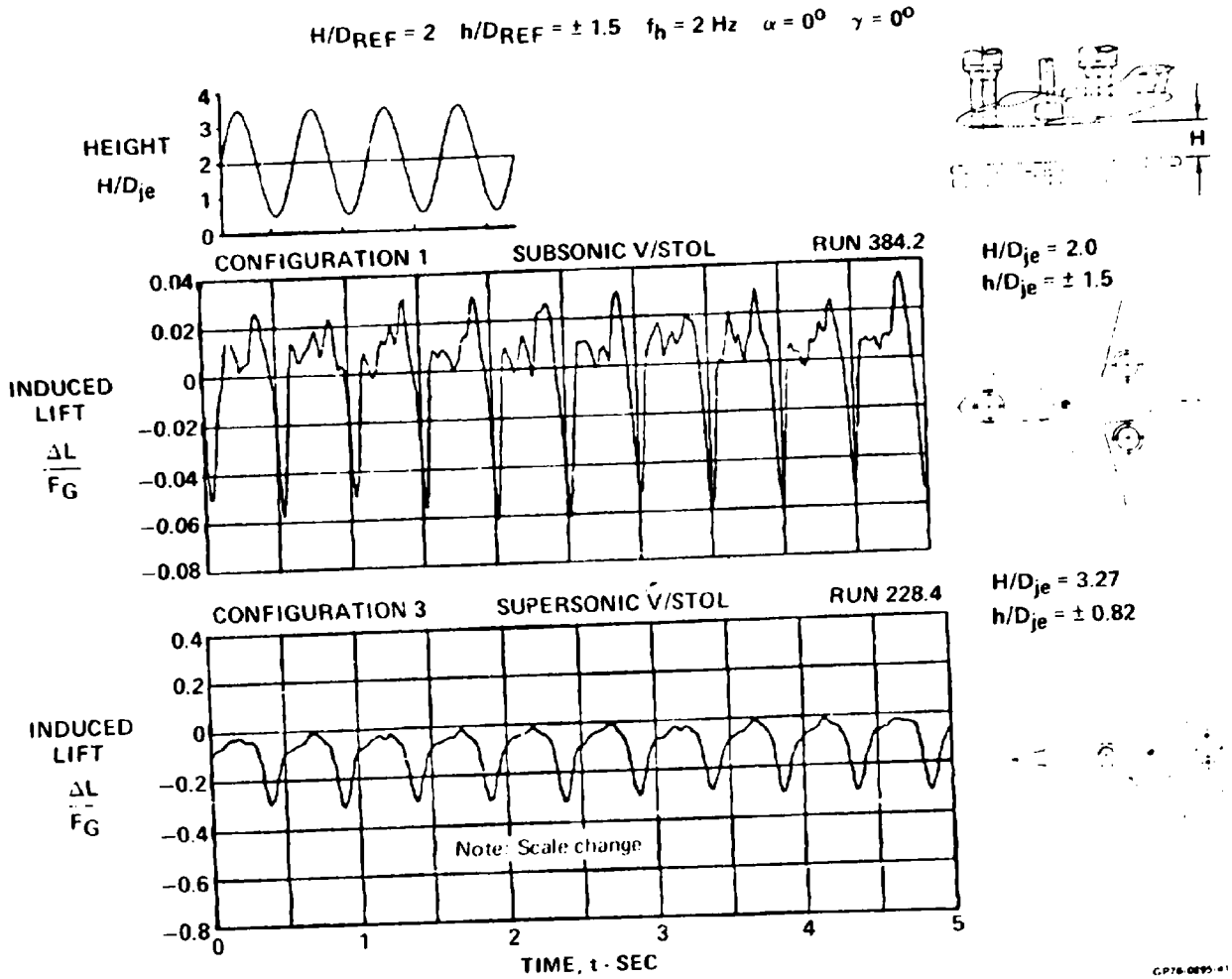

FIGURE 5-47
PLANFORM CONFIGURATION EFFECTS FOR HEAVING DECK

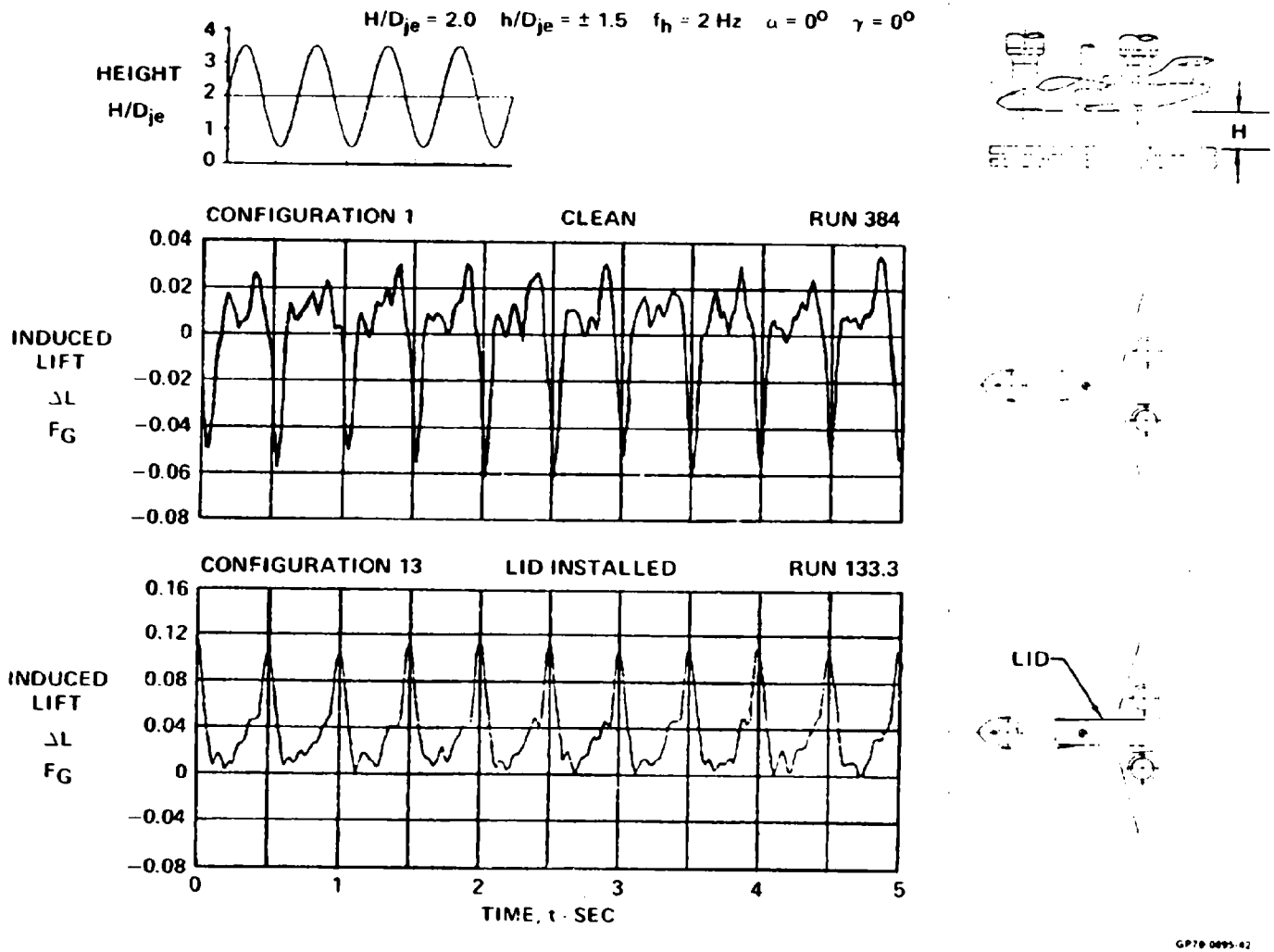

FIGURE 5-48
SUBSONIC V/STOL LID EFFECTS FOR HEAVING DECK

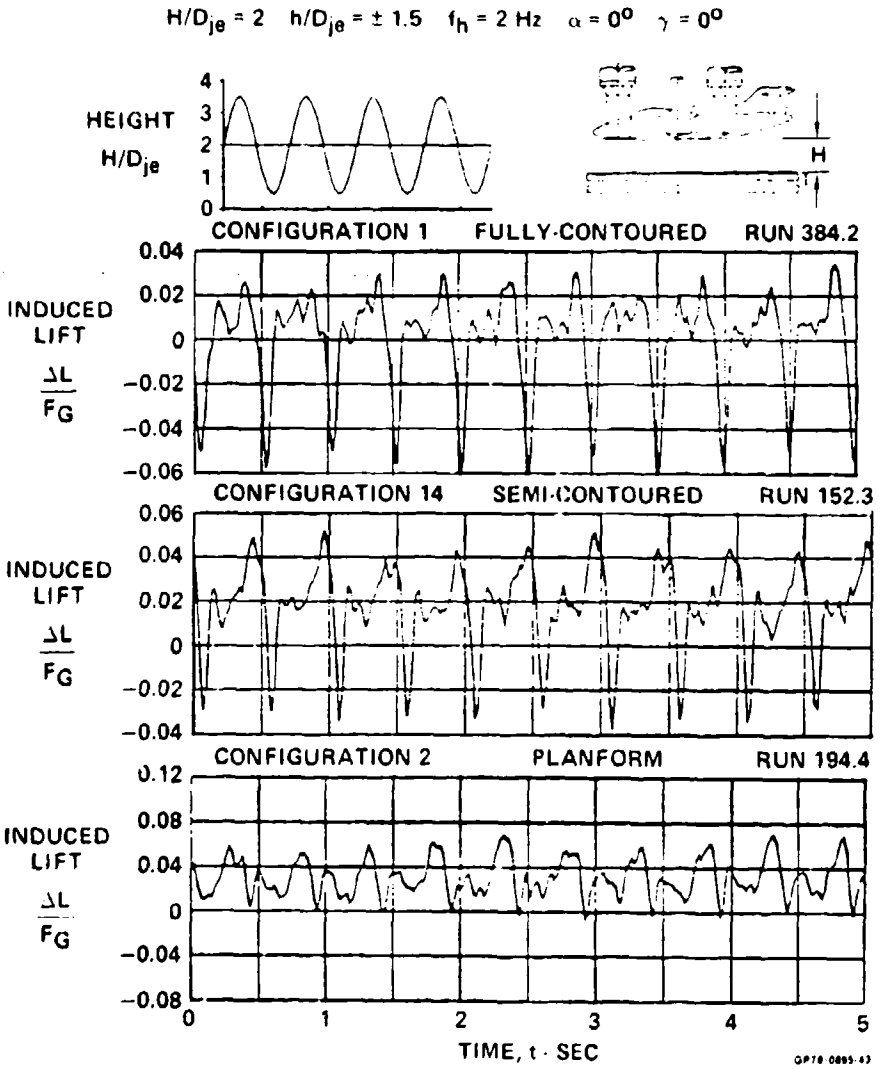

FIGURE 5-49
SUBSONIC V/STOL FUSELAGE CONTOURING EFFECTS FOR HEAVING DECK

data and not non-stationary random data, substantially less than the two minutes of data acquired are actually necessary to assess the frequency content.

The phase relationship or lag time between the input deck motion and the output aerodynamic response was obtained from the cross power spectral density. Limited auto correlations and cross correlations verified that the major aerodynamic responses measured were of a periodic nature similar to the input motion and that the responses correlated with the motion.

A power spectral density (PSD) analysis of the induced lift data is presented in Figure 5-50, reflecting responses to heaving motion (amplitude of 1.5 D_{je}) with the neutral point at an H/D_{je} of 2 on the fully contoured subsonic model. The PSD indicates that the major response is at the frequency of the deck motion, in this case 2 Hz (about 0.1 Hz full scale). Lesser responses are apparent at multiples of this frequency.

PSD's for deck motion frequencies of 1 Hz and 3 Hz, shown in Figure 5-51, indicate the same results. Depending on the shape of the lift loss curve and the neutral point setting, a response at higher frequencies can result from a given motion. For example, about a certain neutral point, a configuration may have an induced lift variation with height which has a local maximum point in addition to different end point values. For heaving motion, responses will be at the primary frequency (heave frequency) and also at twice the primary frequency. Examination of lift loss characteristics measured at static hover conditions verifies this observation.

The lower deck heave amplitudes at an H/D_{je} of 2 result in less variation in lift, as shown in Figure 5-52. Integration under the PSD curve provides the root mean square value of the induced lift. Responses at higher frequencies are not as apparent as in Figure 5-50, due to the height range covered.

The phase relationships between the input motion and the responses were analyzed statistically using the imaginary portion of the cross power spectral density (CSD) function, which is expressed in terms of phase angles. These phase angles were correlated with aircraft height to illustrate the change in phase angle with distance. Results are shown in Figure 5-53.

As expected, the phase angle lags increasingly with the height above the deck. The phase angles can be expressed in terms of a lag time as well. The results indicate essentially an instantaneous response to the deck motion when the model is near the deck. The slope of phase angle versus height remains nearly constant for heaving motion with different configurations. However,

CONFIGURATION 1 $H/D_{je} = 2.0$ $h/D_{je} = \pm 1.5$ $f_h = 2$ Hz $\alpha = 0^o$ $\gamma = 0^o$ RUN 90.2

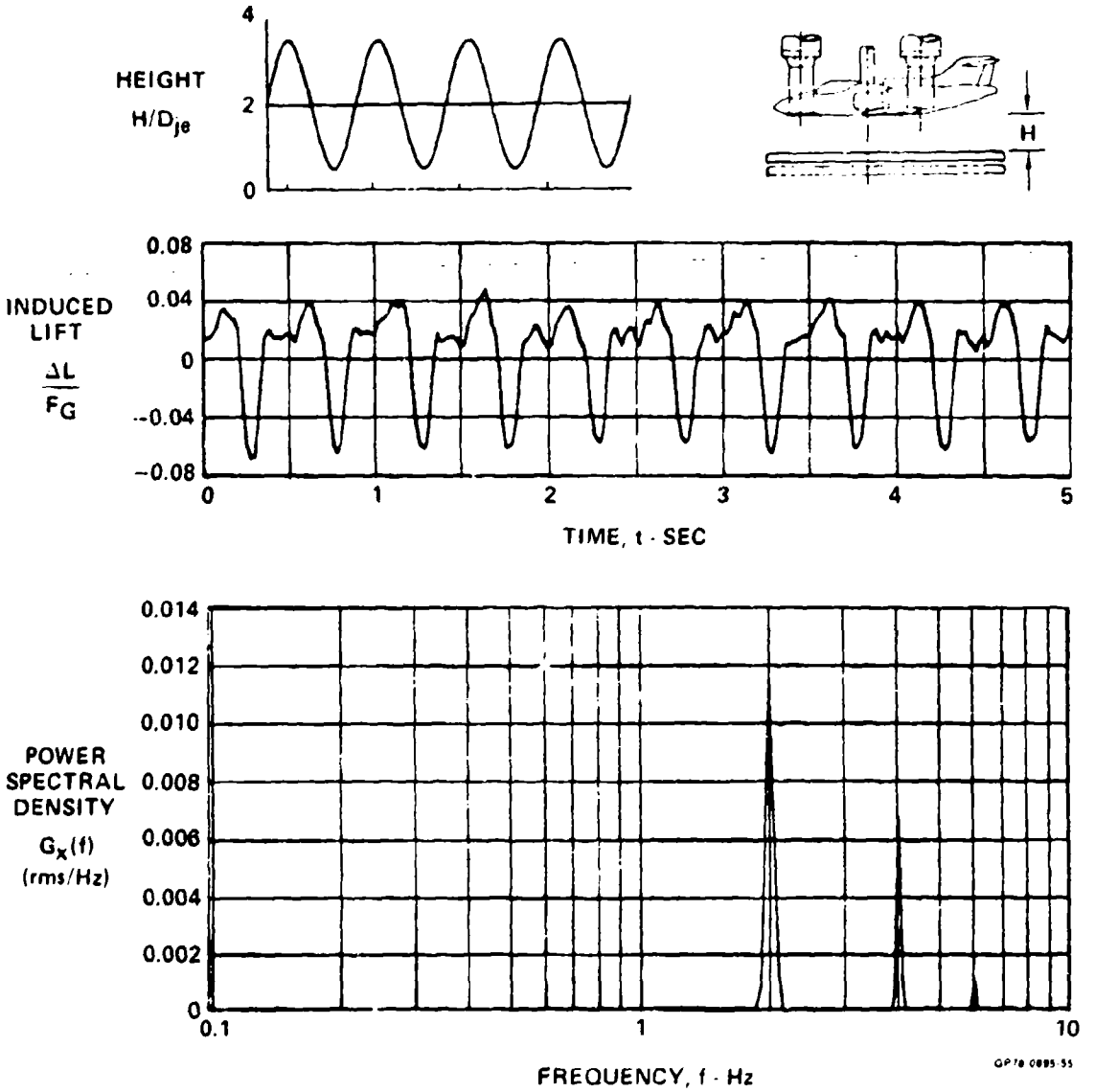

FIGURE 5-50
SUBSONIC V/STOL INDUCED LIFT PSD RESPONSE TO HEAVING DECK

CONFIGURATION 1 $H/D_{je} = 2$ $h/D_{je} = \pm 1.5$ $f_h = 1$ Hz $\alpha = 0^o$ $\gamma = 0^o$ RUN 90.1

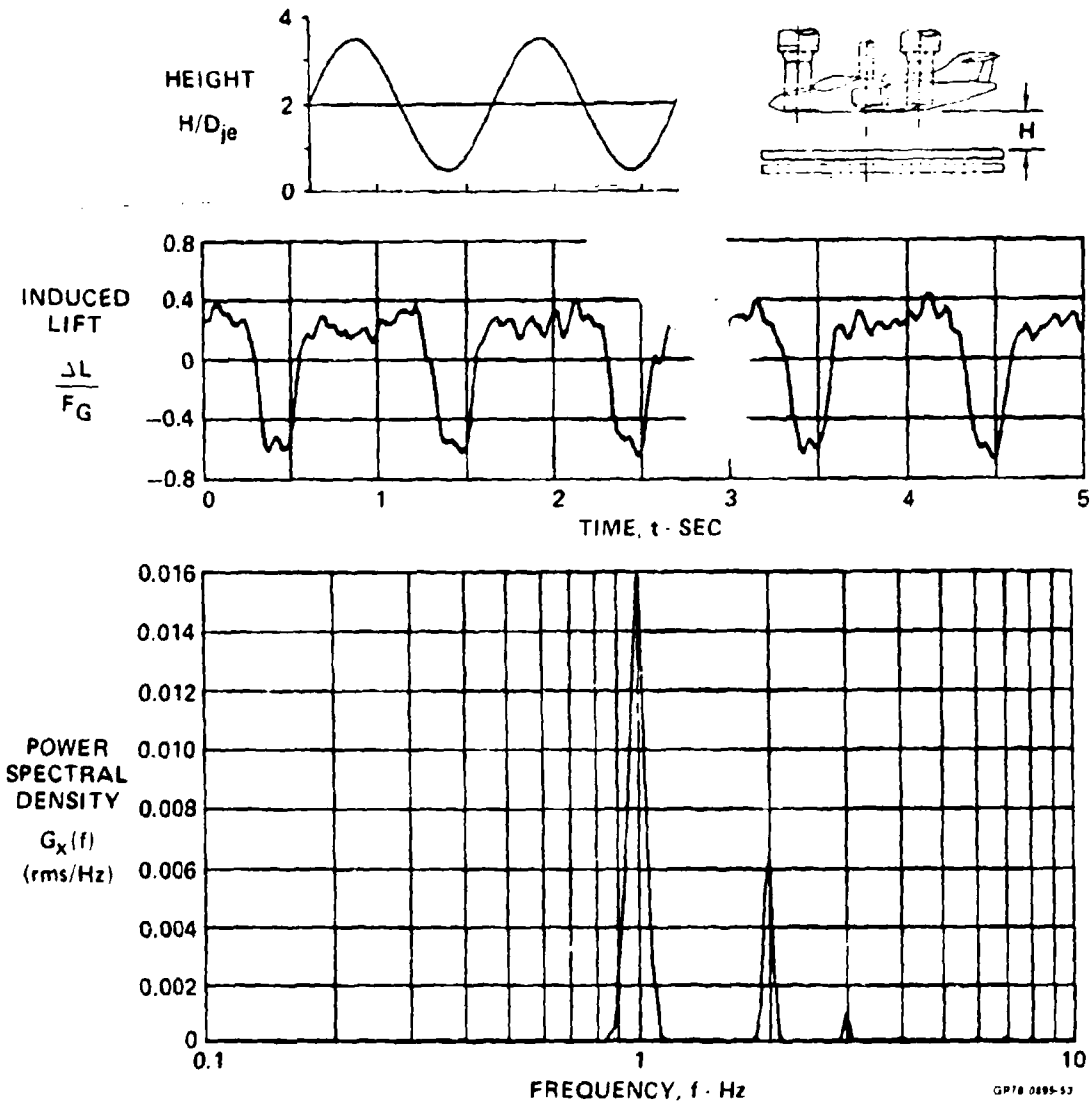

a) $f_h = 1$ Hz

FIGURE 5-51

SUBSONIC V/STOL INDUCED LIFT PSD RESPONSE WITH FREQUENCY VARIATIONS

CONFIGURATION 1 $H/D_{je} = 2$ $h/D_{je} = \pm 1.5$ $f_h = 3$ Hz $\alpha = 0^o$ $\gamma = 0^o$ RUN 90.3

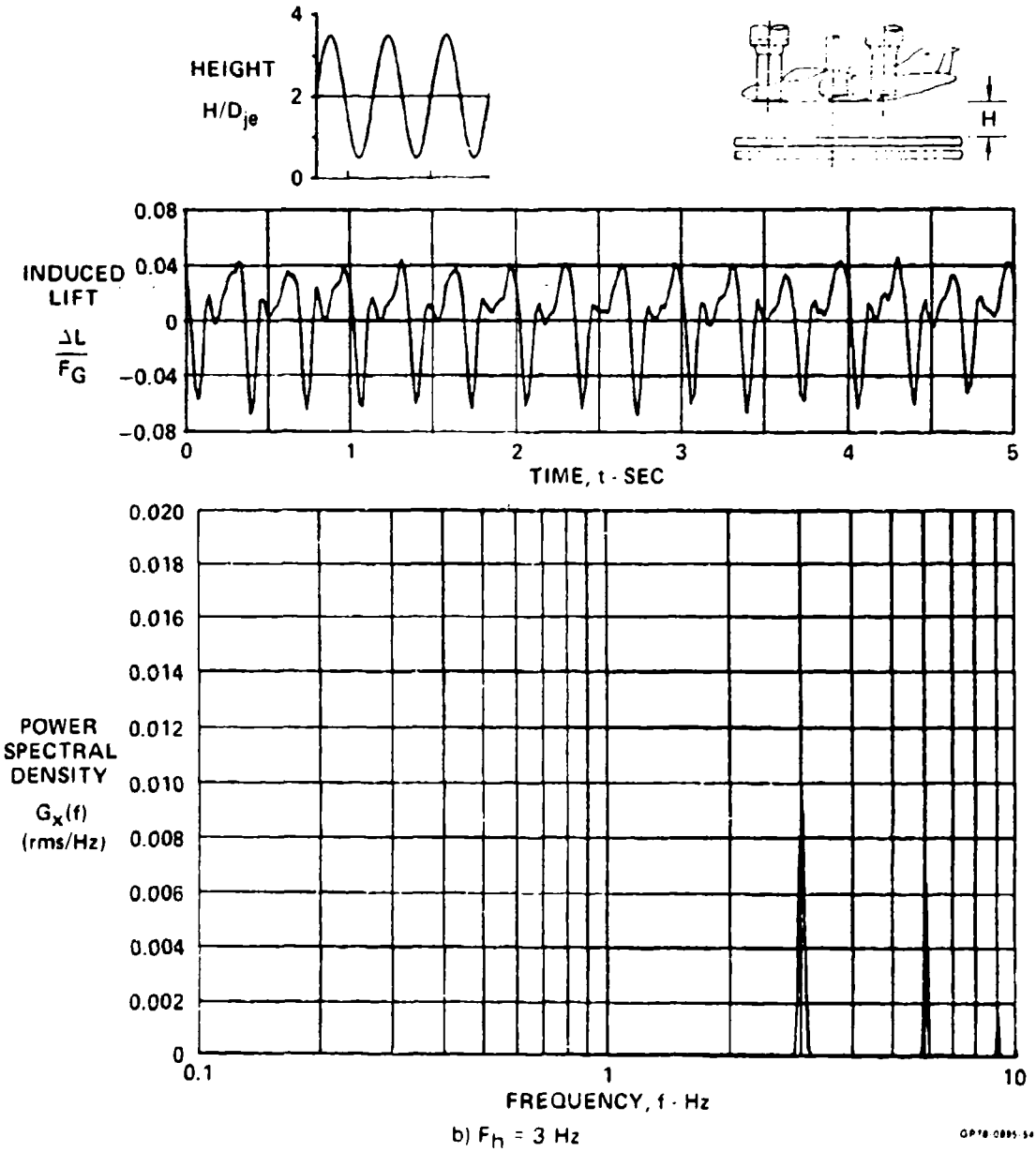

b) $F_h = 3$ Hz

FIGURE 5-51 (Concluded)
SUBSONIC V/STOL INDUCED LIFT PSD RESPONSE WITH FREQUENCY VARIATIONS

CONFIGURATION 1 $H/D_{je} = 2$ $h/D_{je} = 0.5$ $f_h = 2$ Hz $\alpha = 0^o$ $\gamma = 0^o$ RUN 90.5

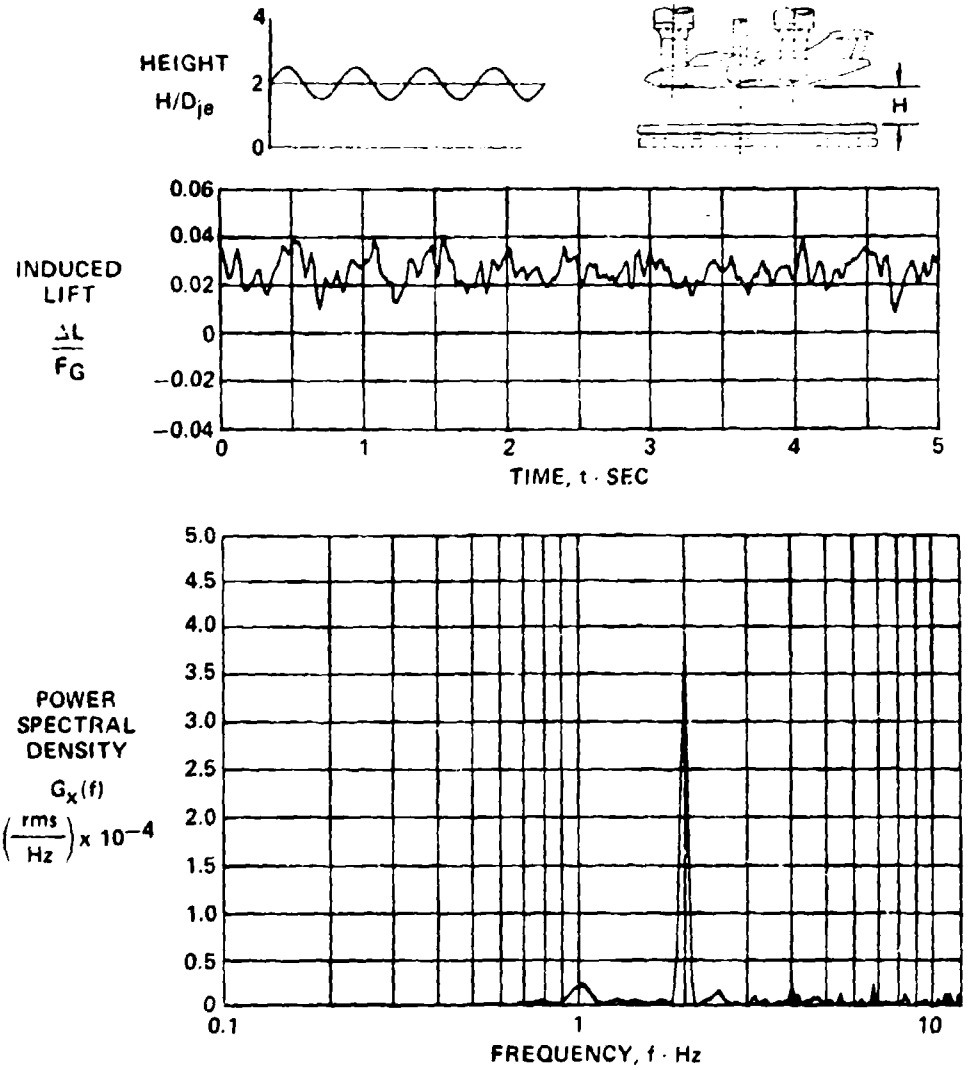

a) $h/D_{je} = 0.5$

FIGURE 5-52
SUBSONIC V/STOL INDUCED LIFT PSD RESPONSE WITH AMPLITUDE VARIATIONS

CONFIGURATION 1 $H/D_{je} = 2$ $h/D_{je} = 1.0$ $f_h = 2$ Hz $\alpha = 0^o$ $\gamma = 0^o$ RUN 90.4

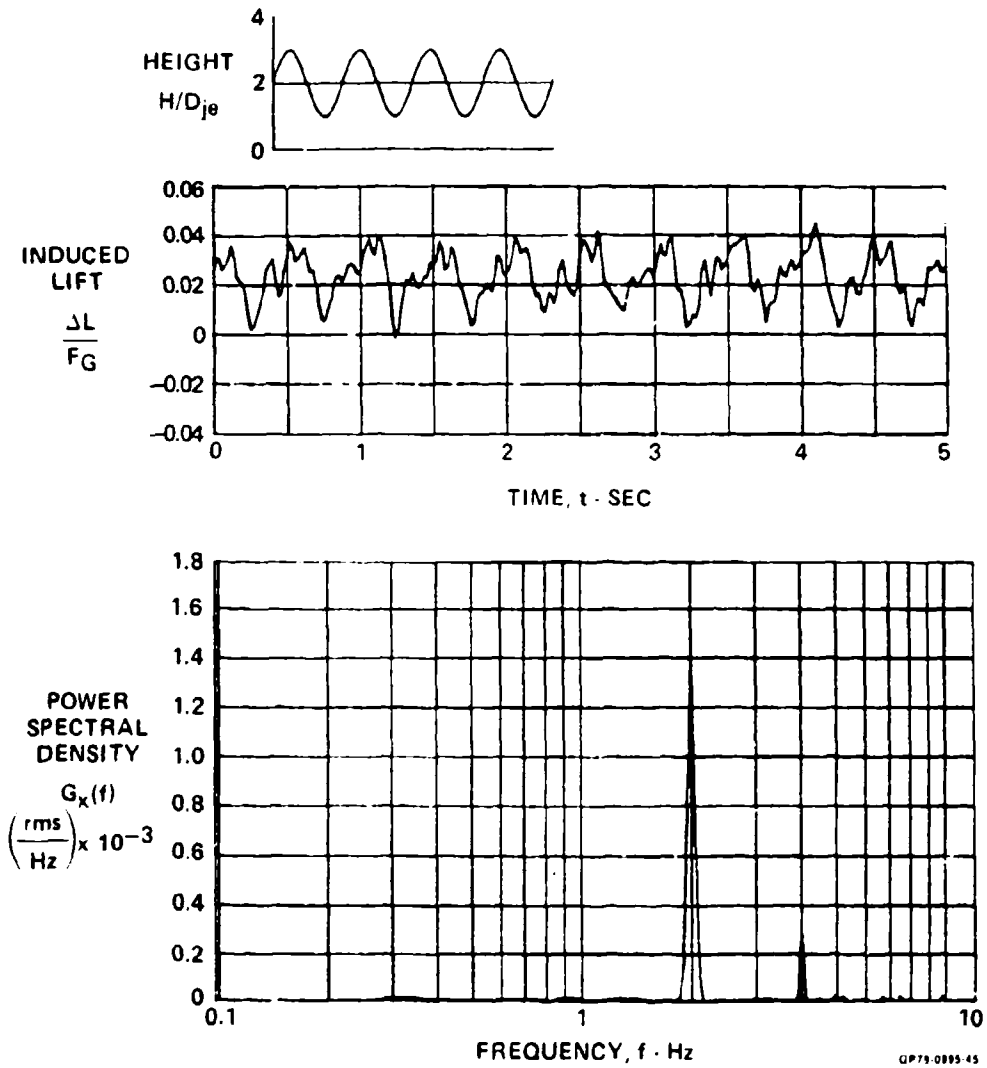

b) $h/D_{je} = 1.0$

FIGURE 5-52 (Concluded)
SUBSONIC V/STOL INDUCED LIFT PSD RESPONSE WITH AMPLITUDE VARIATIONS

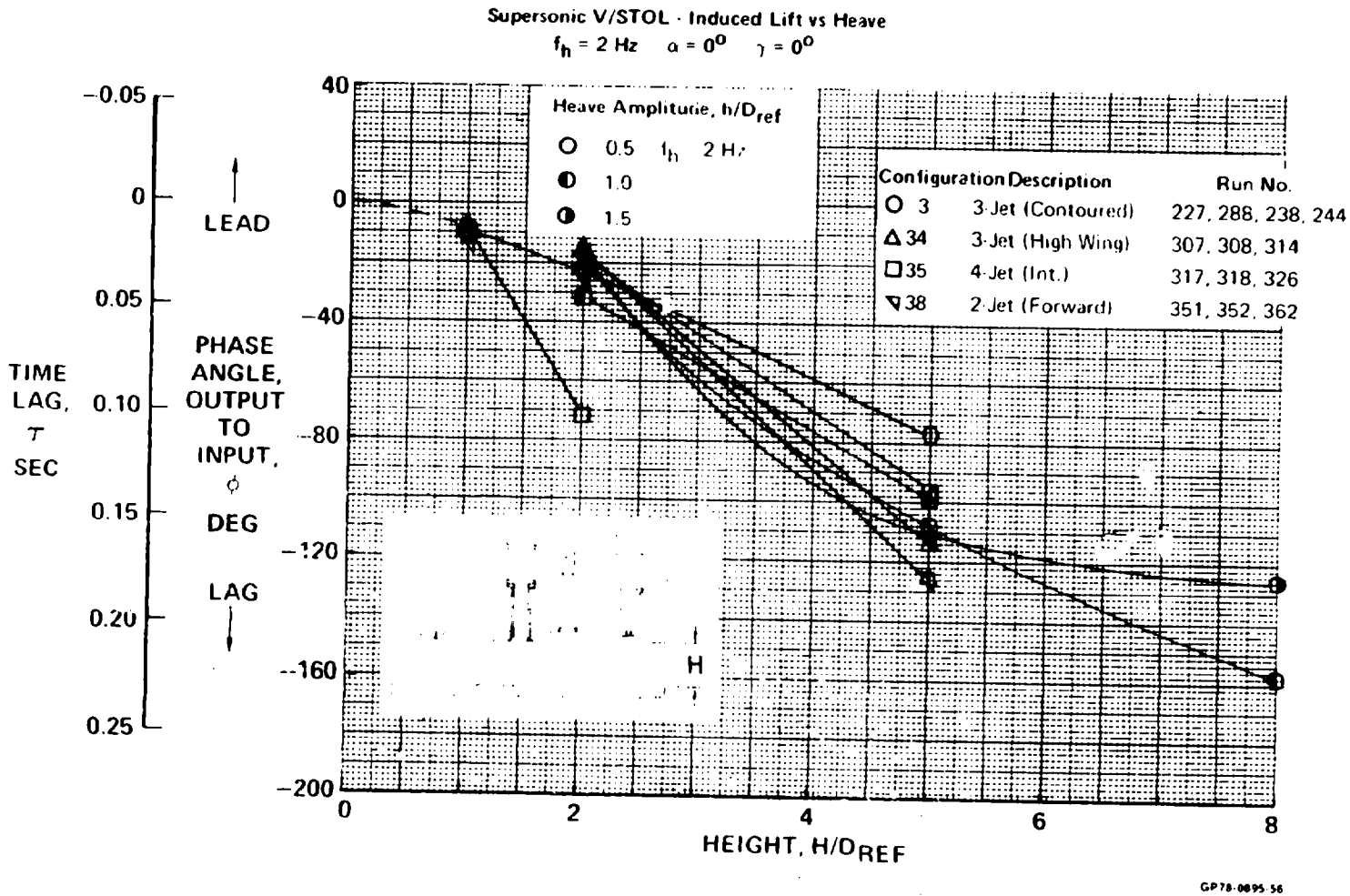

FIGURE 5-53
RESPONSE PHASE ANGLE WITH HEIGHT VARIATIONS FOR HEAVING DECK

configuration dependence is seen for deck rolling motion at different heights, as shown in Figure 5-54.

To further examine the frequency content and phase relationship of the data, classical linear frequency-response methods were applied. The deck frequencies were varied from 1 to 3 Hz at several heights for sinusoidal heaving motions representing full scale periods of about 6 to 20 seconds. The resulting amplitudes and phase angles of the induced aerodynamic response are presented for the subsonic configuration in Figure 5-55 in a conventional Bode diagram format. The ratio of response to deck motion, given in decibels, has a constant gain factor as shown by the data. The phase angle, given in degrees, changes only slightly over the frequency range indicating a transportation lag.

The transfer function of the aerodynamically coupled system is nearly constant, thus indicating that this is a simple proportional system and that varying the frequency from 1 to 3 Hz has little effect on the response. It should be noted, however, that the transfer function is generated from a statistical value of the response, and thus may not reflect frequency effects at certain instances in time. This would include the frequency effect observed due to heave in Figure 5-34. The gain factor for the amplitude does change with height (Figure 5-55) and is configuration dependent. Similar results also apply to deck rolling motions as shown in Figure 5-56 for the supersonic V/STOL configuration.

It should be noted that the frequencies tested are relatively low, and that an amplitude roll off could be expected at higher frequencies, but such frequencies would be well beyond the range of realistic ship motions.

5.3 EMPIRICAL PREDICTION PROCEDURES - An objective of this program was to develop empirical procedures for the prediction of the induced force and moment variations with deck motion. Past efforts, both analytical and experimental, have been directed toward development of procedures for static hover conditions. One such analytical study, performed under contract to NADC by MCAIR, involved the development of methodology for the prediction of the jet-induced aerodynamics of multi-jet V/STOL aircraft both in and out of ground effect. The results of this program are reported in Reference 4. Currently, the methodology provides reasonable results for the suckdown forces but the fountain impingement model overpredicts the resultant lift force.

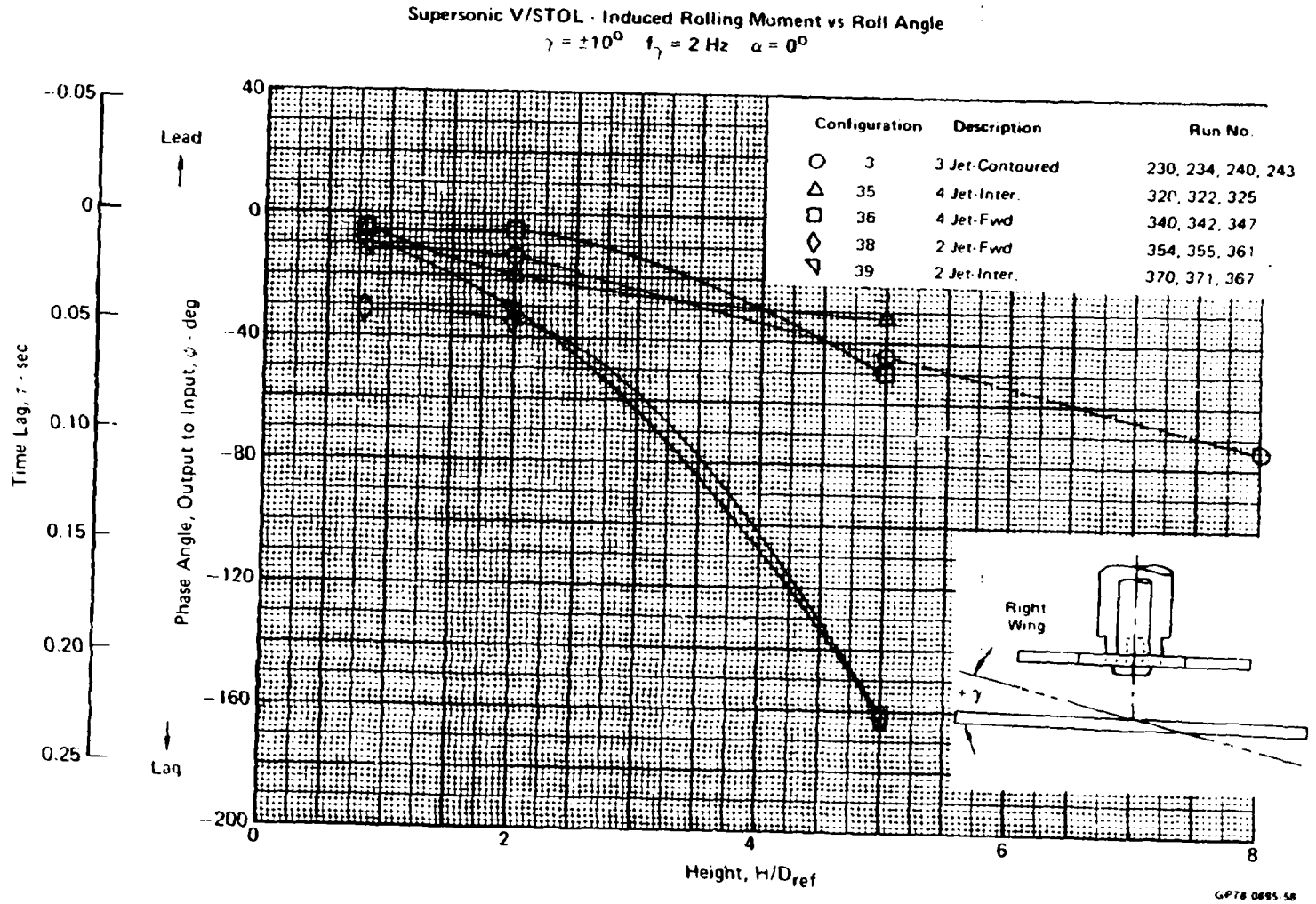

FIGURE 5-54
RESPONSE PHASE ANGLE WITH HEIGHT VARIATIONS FOR ROLLING DECK

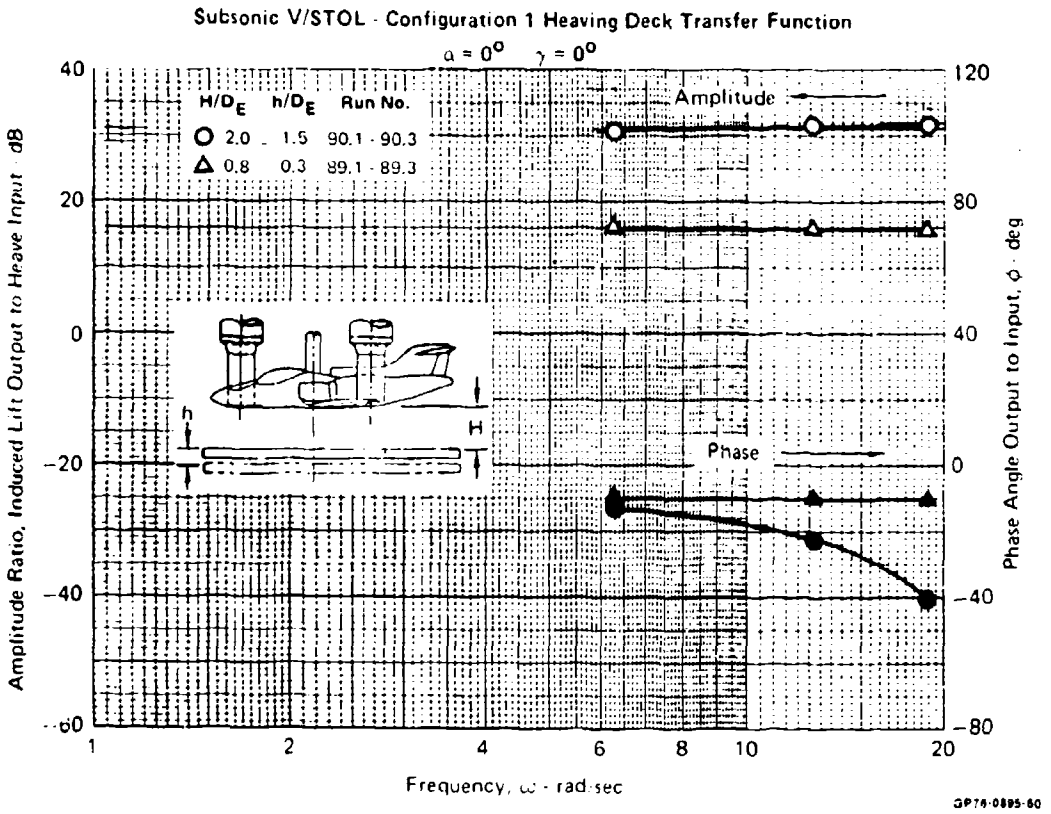

FIGURE 5-55
AMPLITUDE AND PHASE ANGLE FREQUENCY RESPONSE TO HEAVING DECK

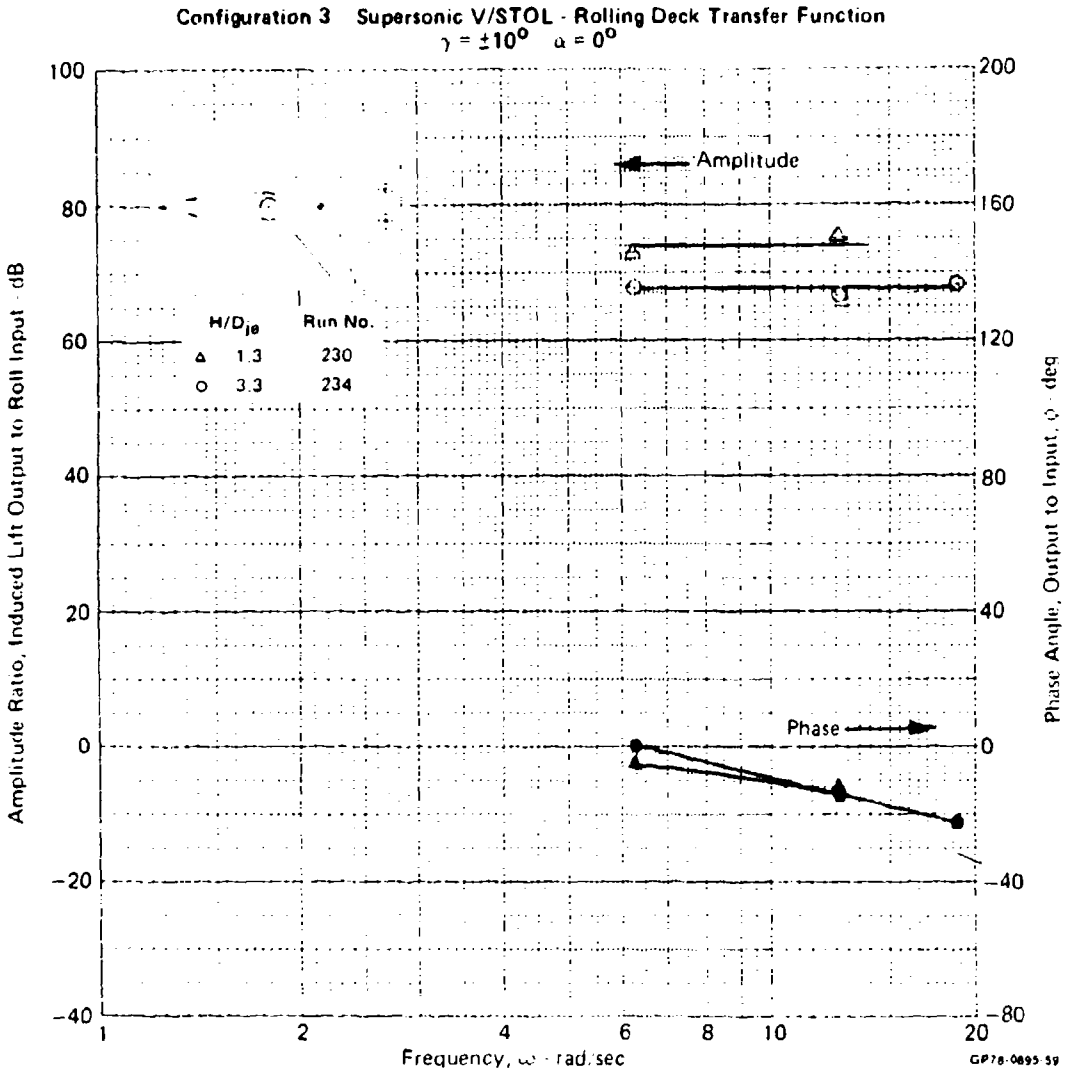

FIGURE 5-56
AMPLITUDE AND PHASE ANGLE FREQUENCY RESPONSE TO ROLLING DECK

A significant quantity of empirical information was required to develop the Reference 4 methodology, particularly relative to the entrainment of the jets and the fountain formation. Areas where additional data are needed to improve the procedures are indicated in Reference 4. It is further noted that the comprehensive theoretical prediction of the complex flowfields and the resulting induced aerodynamic forces for arbitrary V/STOL configurations is several years off, even for static hover conditions. Such a method would be invaluable as a screening tool and efforts are continuing in this area at MCAIR under both contracted and company funded programs. However, complementary efforts, relying more heavily on experimental induced aerodynamic data are necessary at this time to develop rapid prediction procedures for static hover conditions and to address additional factors such as the effects of deck motion, wind, and superstructure. This program supplied substantial data for both static hover conditions and deck motion.

5.3.1 Prediction of Deck Motion Effects from Static Hover Data - The parametric induced aerodynamic data given in Section 5.1 provide the capability of predicting the induced forces and moments acting on configurations similar to those investigated for static hover conditions. The data can be used to predict the effects of height, pitch, and roll, nozzle arrangement and spacing, LID's, and many other V/STOL aircraft design variables applicable to both subsonic and supersonic configurations. Further, the static data can be used to predict the induced aerodynamic response to deck motions by assuming that the motion is quasi-steady state. This can be accomplished for a given deck motion, which may be complex periodic in nature, by determining the deck height, pitch, or roll angle variation with time and obtaining from the static hover data, the corresponding variation in the induced aerodynamic characteristics of interest.

Since the deck motion was well defined in this program, the attitude or position of the deck at any particular time can be determined. Thus, the motion can be defined by a series of discrete points. The induced force and moment variations can then be evaluated from plots of the static hover data. Comparisons of the induced lift were made for heave, pitch, and roll at a neutral point, H/D_{je} of 2, for both the subsonic and supersonic configurations. In addition, comparisons were made of the induced rolling and pitching moments for the angular deck motions.

Based on the static hover data obtained, it was also possible to generate comparative predictions for some of the combined motions. These comparisons were made for combined heave and roll and combined pitch and roll both in phase and out of phase. The combined motions particularly indicate some rather significant differences from the static predictions.

Heave, Pitch, and Roll - Subsonic V/STOL Configuration - The comparison of the static hover prediction with dynamic data for heaving motion is presented in the time domain in Figure 5-57. The results are in fair agreement, with the exception of the increased fountain cushion effect which occurs as the deck approaches the model from the maximum height of 3.5 D_{je}. The difference is more clearly shown by presenting the comparison as a function of height as in Figure 5-58. This comparison was made by fairing a curve through a series of discrete points selected from the time history.

The static to dynamic comparison for the induced lift variation with deck pitch is shown in Figure 5-59. Fairly good agreement is indicated, but an increase in lift from the fountain (approximately 1 percent) with dynamic deck motion is apparent. This is attributed to the increased cushioning effect in the fountain due to the deck pitching motion.

In Figure 5-60, a fairly large difference is seen between the static prediction and the dynamic data for induced pitching moment, the dynamic data indicating a more negative or nose down pitching moment. The negative pitching moment with positive pitch (nose-up relative to the deck) is attributed in part to an increase in the fountain impingement force between the two rear nozzles due to the compression effect. This has been shown to be the region of highest fountain strength in Reference 3 and is aft of the c.g., thus the force on this region provides a negative pitching moment contribution. This overcomes the positive pitching moment contribution caused by the increase in suckdown on the aft fuselage. The negative pitching moment with negative pitch (nose-down relative to the deck) is attributed primarily to movement of the fountain further aft of the c.g. than occurs at fixed deck pitch angles.

The static to dynamic comparison for deck roll is shown in Figure 5-61. As with pitch angle, the dynamic induced lift variation is approximately 1 percent higher. The induced rolling moment variation is also shown in Figure 5-61. The dynamic data are not symmetric about the zero level as is the static hover prediction. This may have been due to a slight offset (about 0.5°) in the angle, since the rolling moment is very sensitive to roll angle near zero degrees (see Figure 5-3b).

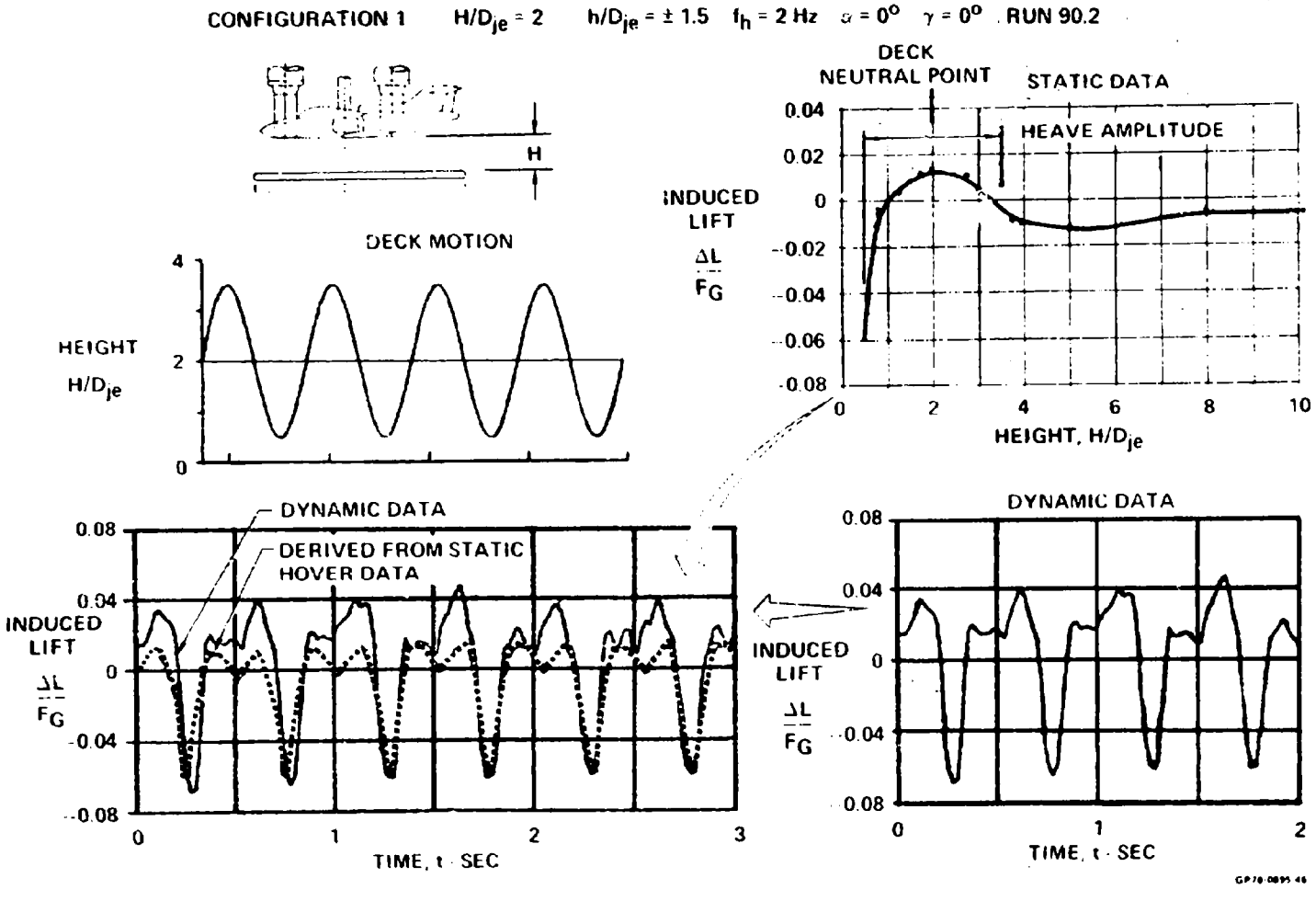

FIGURE 5-57
SUBSONIC V/STOL STATIC TO DYNAMIC DATA COMPARISON IN TIME DOMAIN FOR HEAVING DECK

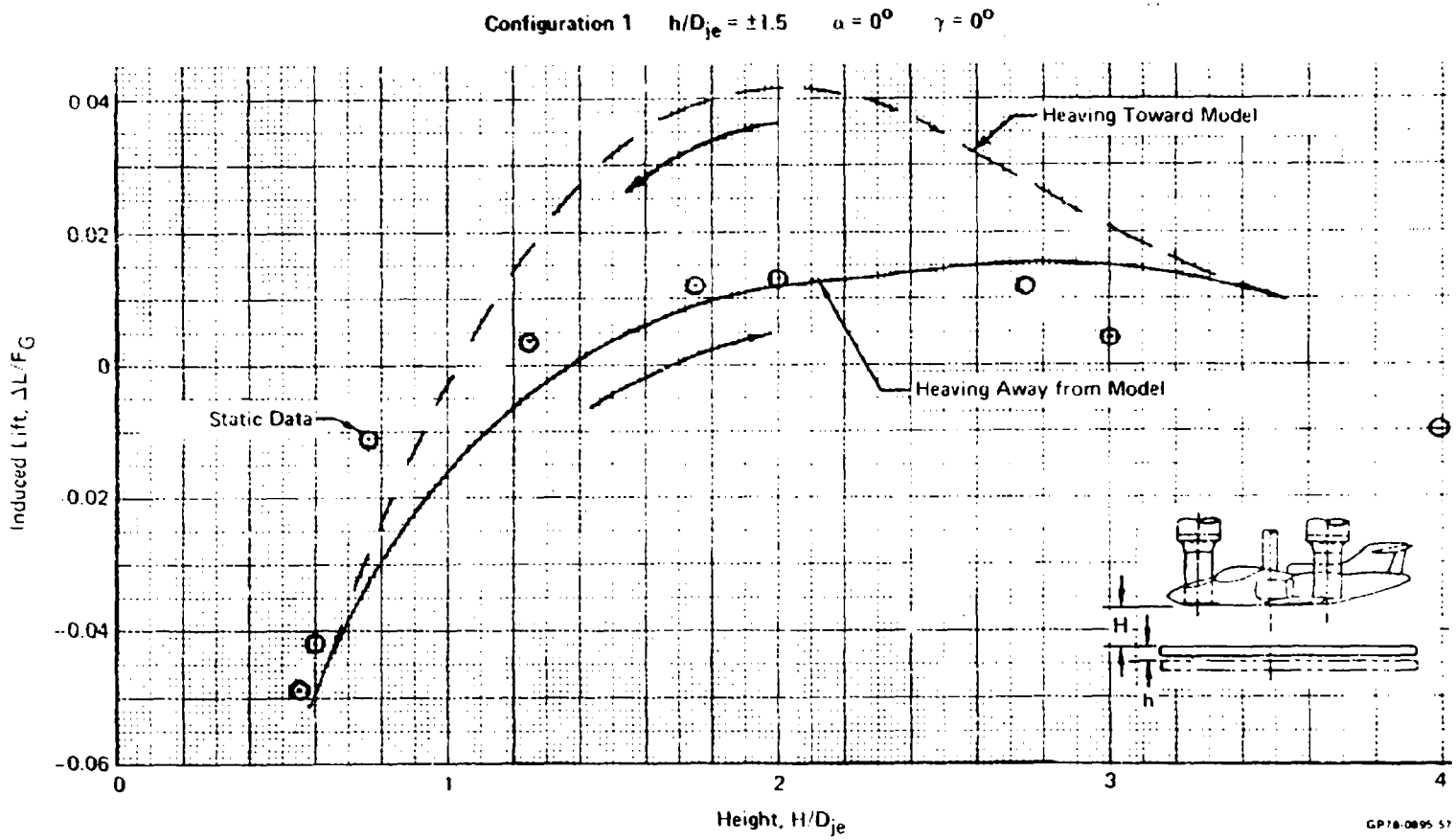

FIGURE 5-58
SUBSONIC V/STOL STATIC TO DYNAMIC DATA COMPARISON IN PHYSICAL DOMAIN FOR HEAVING DECK

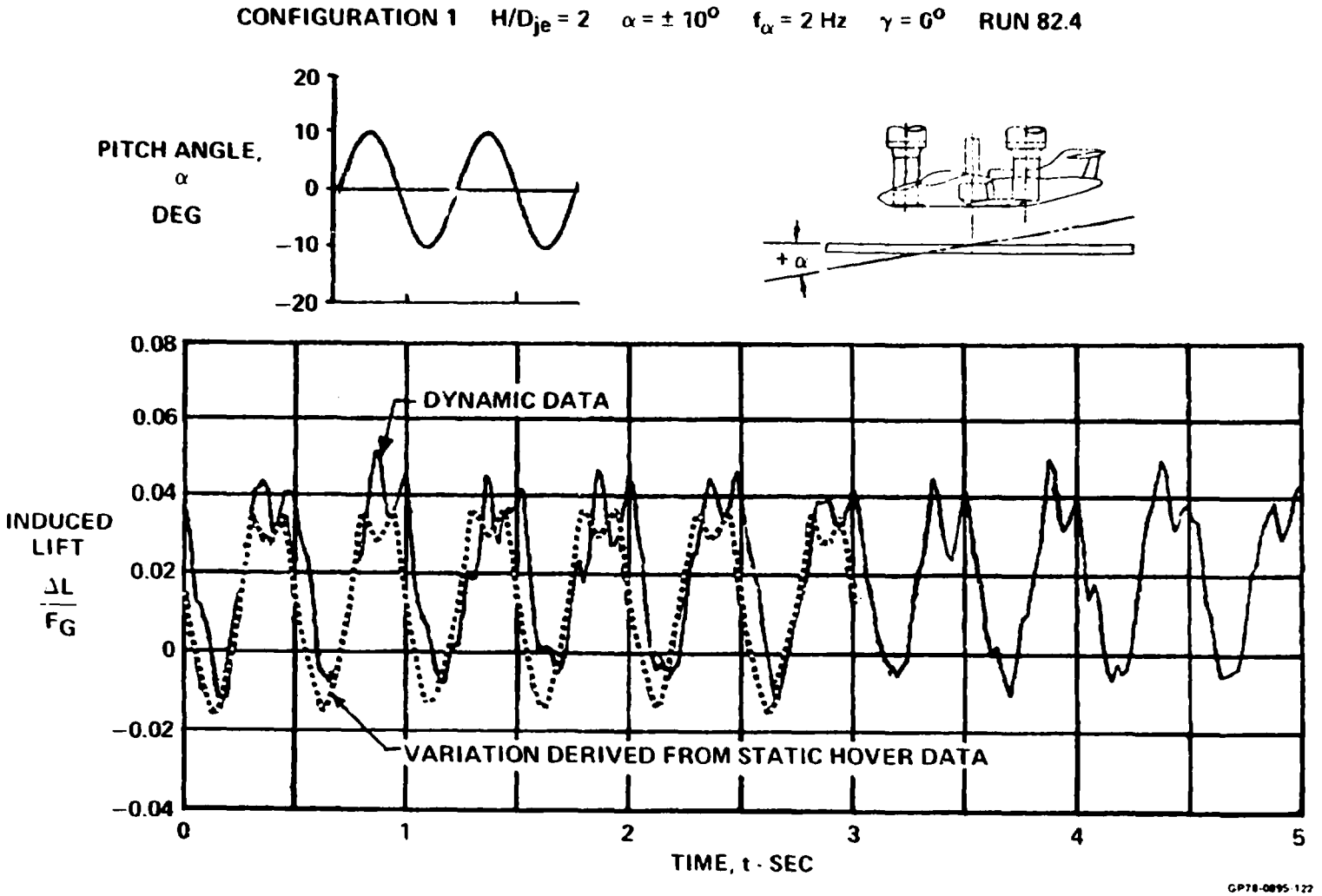

FIGURE 5-59
SUBSONIC V/STOL STATIC TO DYNAMIC INDUCED LIFT DATA COMPARISON FOR PITCHING DECK

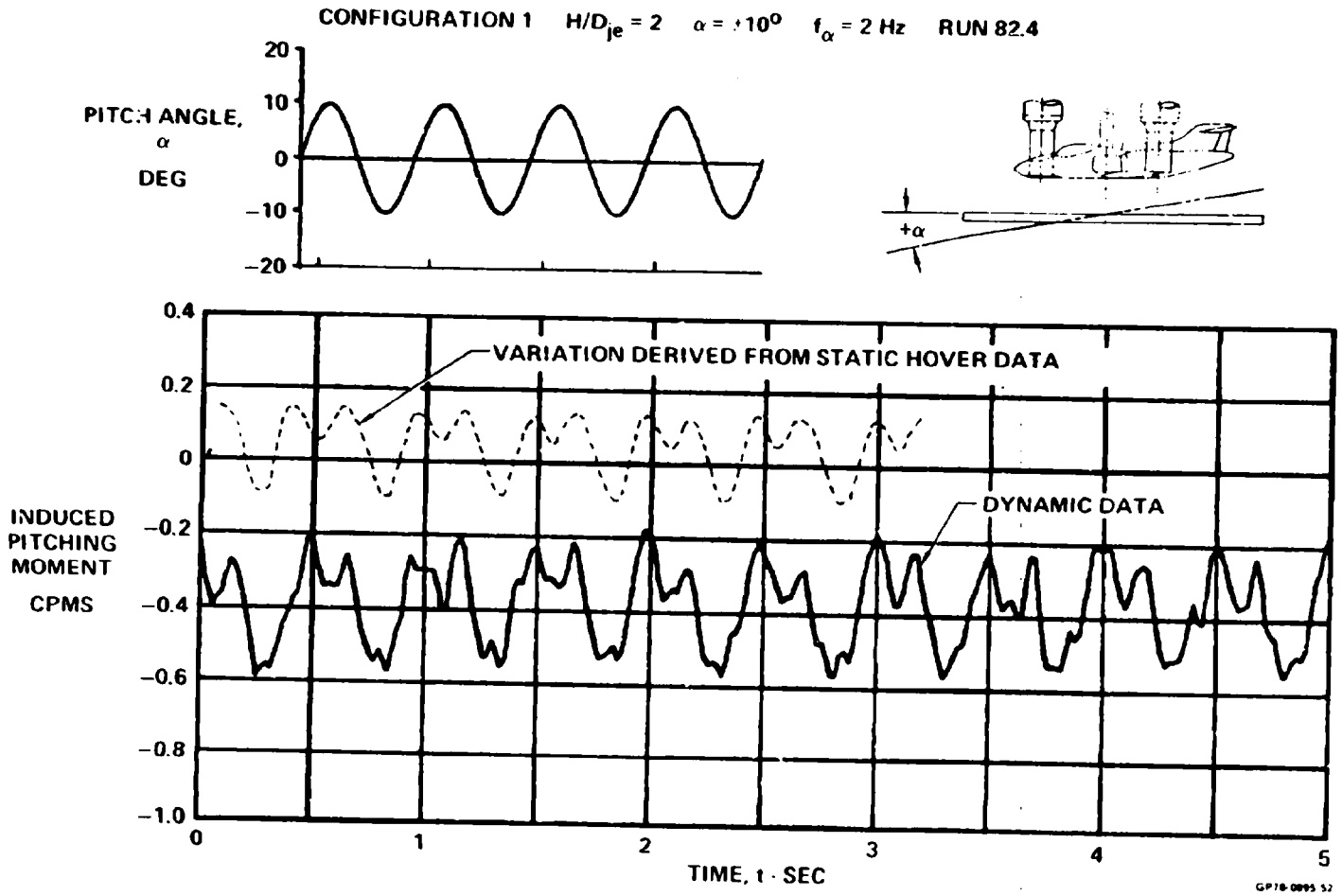

FIGURE 5-60
SUBSONIC V/STOL STATIC TO DYNAMIC INDUCED PITCHING MOMENT DATA COMPARISON FOR PITCHING DECK

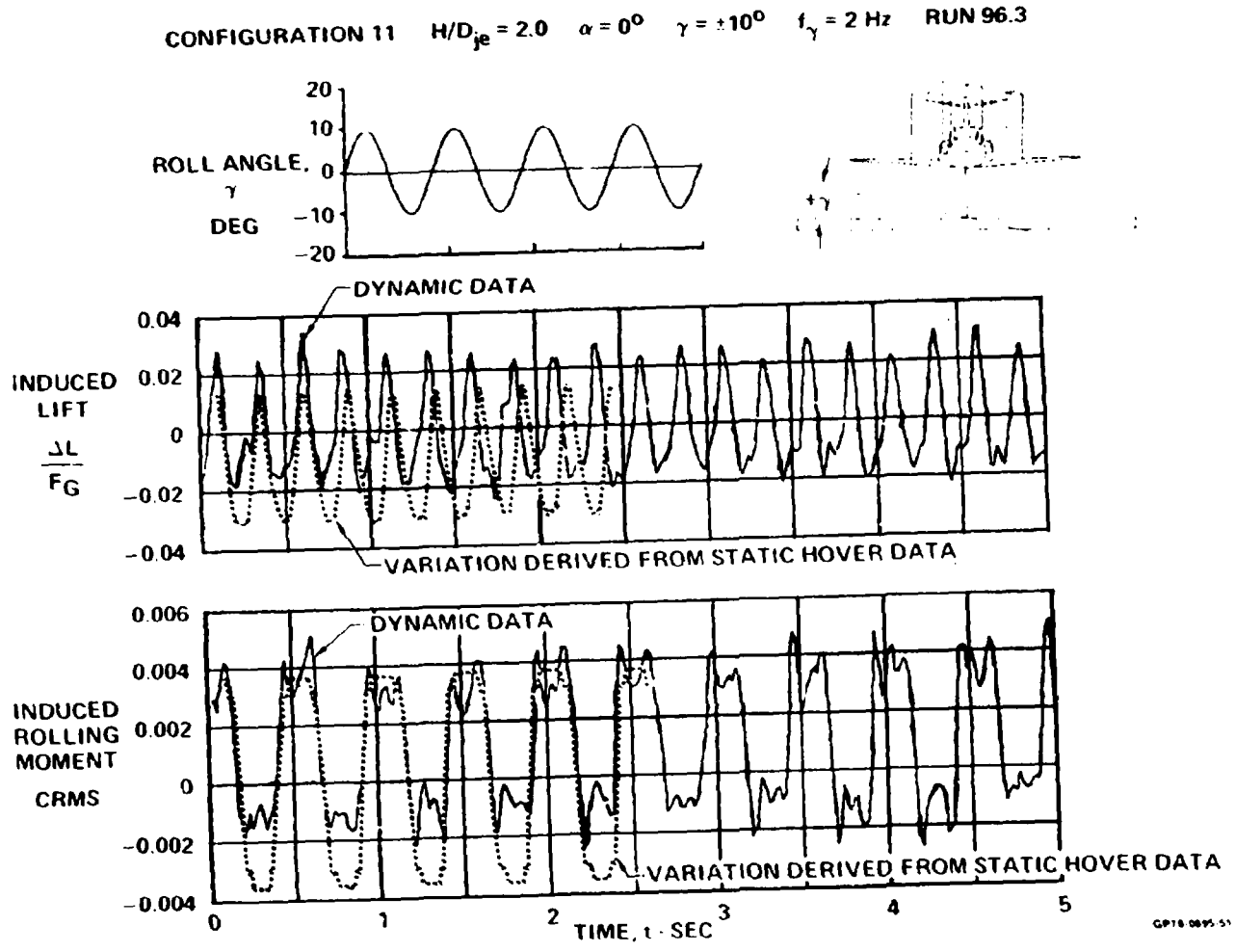

FIGURE 5-61

SUBSONIC V/STOL STATIC TO DYNAMIC INDUCED LIFT AND INDUCED ROLLING MOMENT DATA COMPARISON FOR ROLLING DECK

Heave, Pitch and Roll - Supersonic V/STOL Configuration - The comparison of the static prediction and the dynamic data for heaving motion is shown in Figure 5-62. The induced lift is dominated by a large suckdown. Although the minimum induced lift levels compare well at an H/D_{je} of about 0.8, the dynamic data reflect a lift loss significantly higher than the predictions (as much as 8 percent) at H/D_{je} values above 1.6. This is attributed to an increase in suckdown effect resulting from the rapid movement of the deck away from the model. This adverse effect is not apparent on the subsonic configuration, probably due to its rather low suckdown and strong fountain. Since there is consistent evidence that there is an increase in the fountain lift with deck motion toward the model, it is logical to expect that there will be some decrease in lift when the deck moves away from the model, particularly when the suckdown dominates the induced lift.

The static to dynamic comparison for the induced lift variation with deck pitch is shown in Figure 5-63. The induced lift variation is more noticeable in the dynamic data than in the static hover data. Likewise, the pitching moment variation increased with deck motion as shown in Figure 5-64. As observed on the subsonic V/STOL model, the induced lift is higher and is accompanied by an increase in the nose down pitching moment. The change in pitching moment with deck motion is attributed to the same reasons as discussed for the subsonic model.

The static to dynamic comparison with deck roll is shown in Figure 5-65. As with the heaving motion, the deck rolling motion has an adverse effect on the induced lift. An adverse effect on the induced rolling moment also occurs, as indicated in Figure 5-65.

Combined Motions - Actual sea state conditions, being of a complex periodic nature, cause a complex response from ships, as indicated in Reference 2. To evaluate the effects on induced lift, several combinations of heave, pitch, and roll motions were investigated, primarily with the subsonic configuration. Predictions of the induced forces and moments could be made for some cases.

The comparison for a combination of heave and roll is shown in Figure 5-66 for an H/D_{je} of 2. The static hover prediction was obtained from a parametric plot of induced lift as a function of roll angle for several heights (Figure 5-3a). For discrete roll angles, the induced lift was determined by interpolation. It can be seen that the actual induced lift with combined motion was lower than predicted. The extremely complex, turbulent flowfield created under such combined motions is believed to increase the mixing and entrainment and therefore, increase the lift loss. For this case, the heave

CONFIGURATION 3 $H/D_{je} = 3.27$ $h/D_{je} = +2.45$ $f = 2$ Hz $\alpha = 0^o$ $\gamma = 0^o$ RUN 228.4

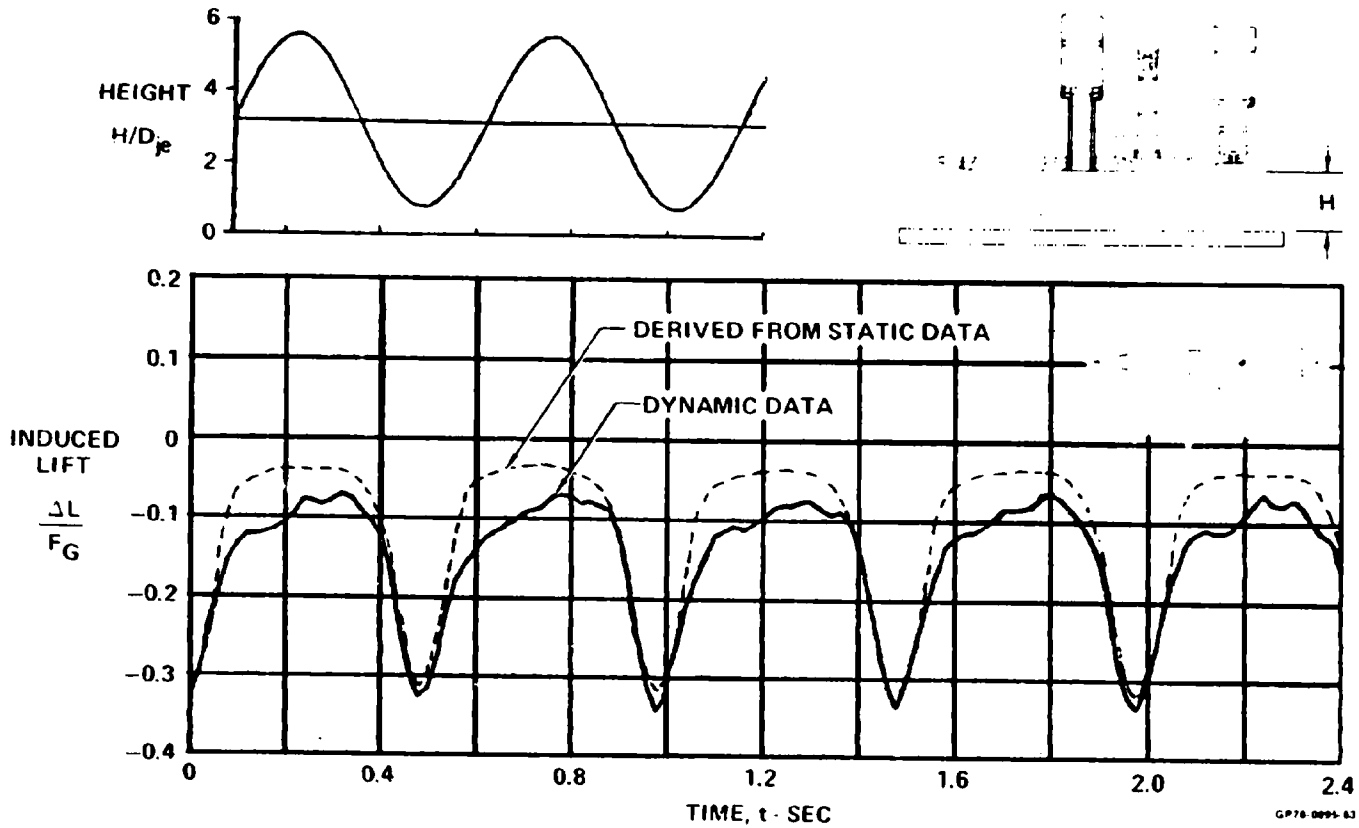

FIGURE 5-62
SUPERSONIC V/STOL STATIC TO DYNAMIC INDUCED LIFT DATA COMPARISON FOR HEAVING DECK

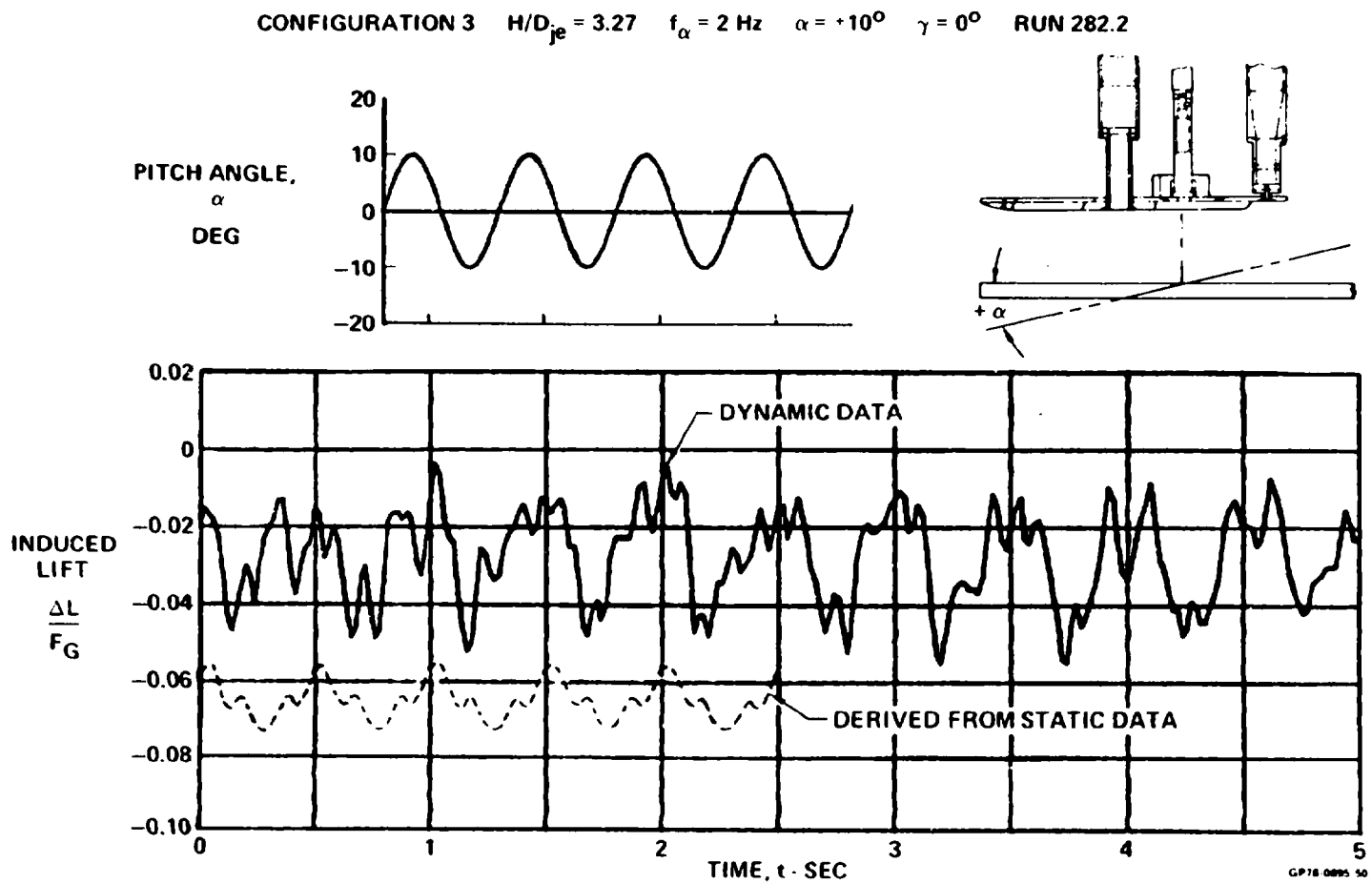

FIGURE 5-63
SUPERSONIC V/STOL STATIC TO DYNAMIC INDUCED LIFT DATA COMPARISON FOR PITCHING DECK

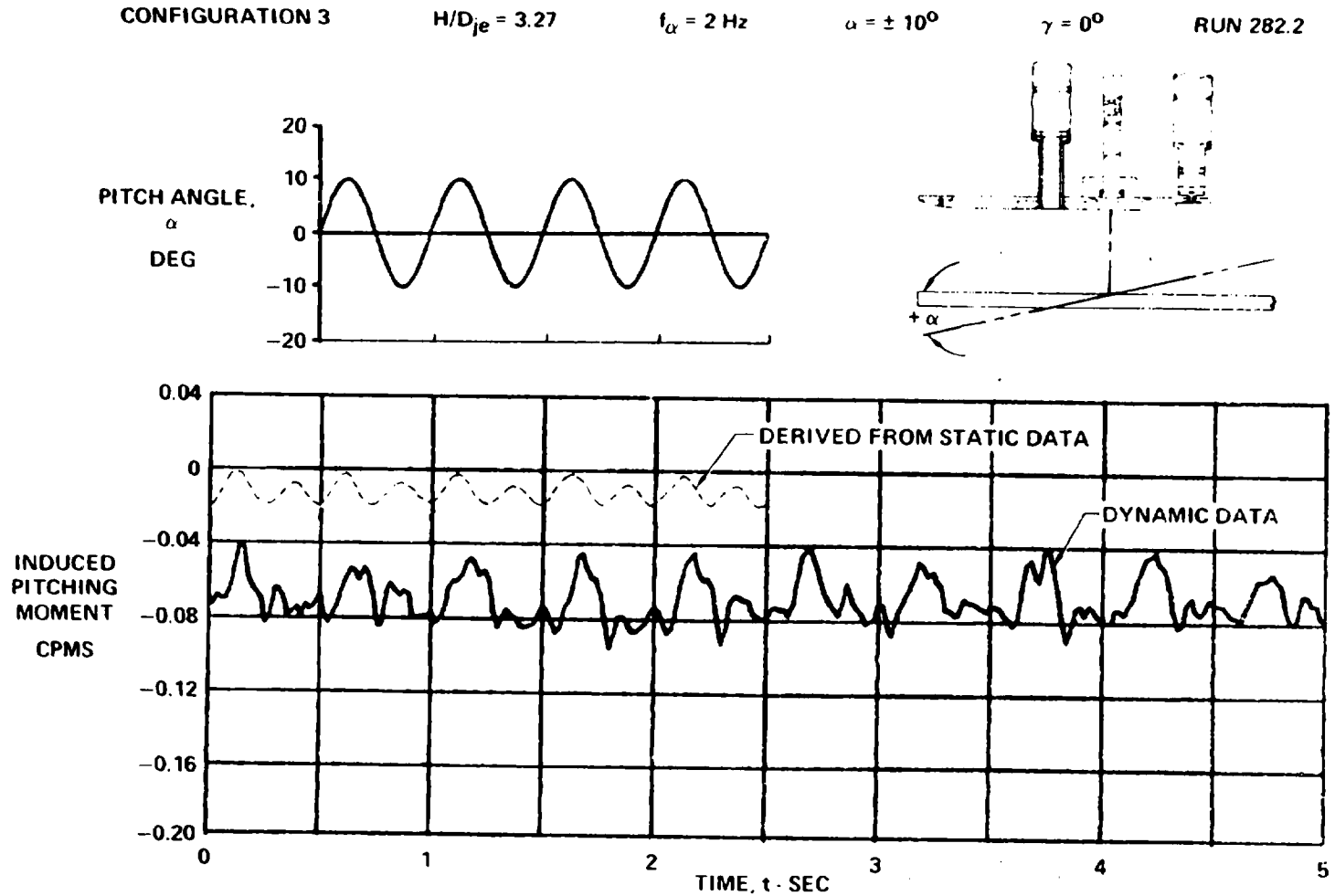

FIGURE 5-64
SUPERSONIC V/STOL STATIC TO DYNAMIC INDUCED PITCHING MOMENT DATA COMPARISON FOR PITCHING DECK

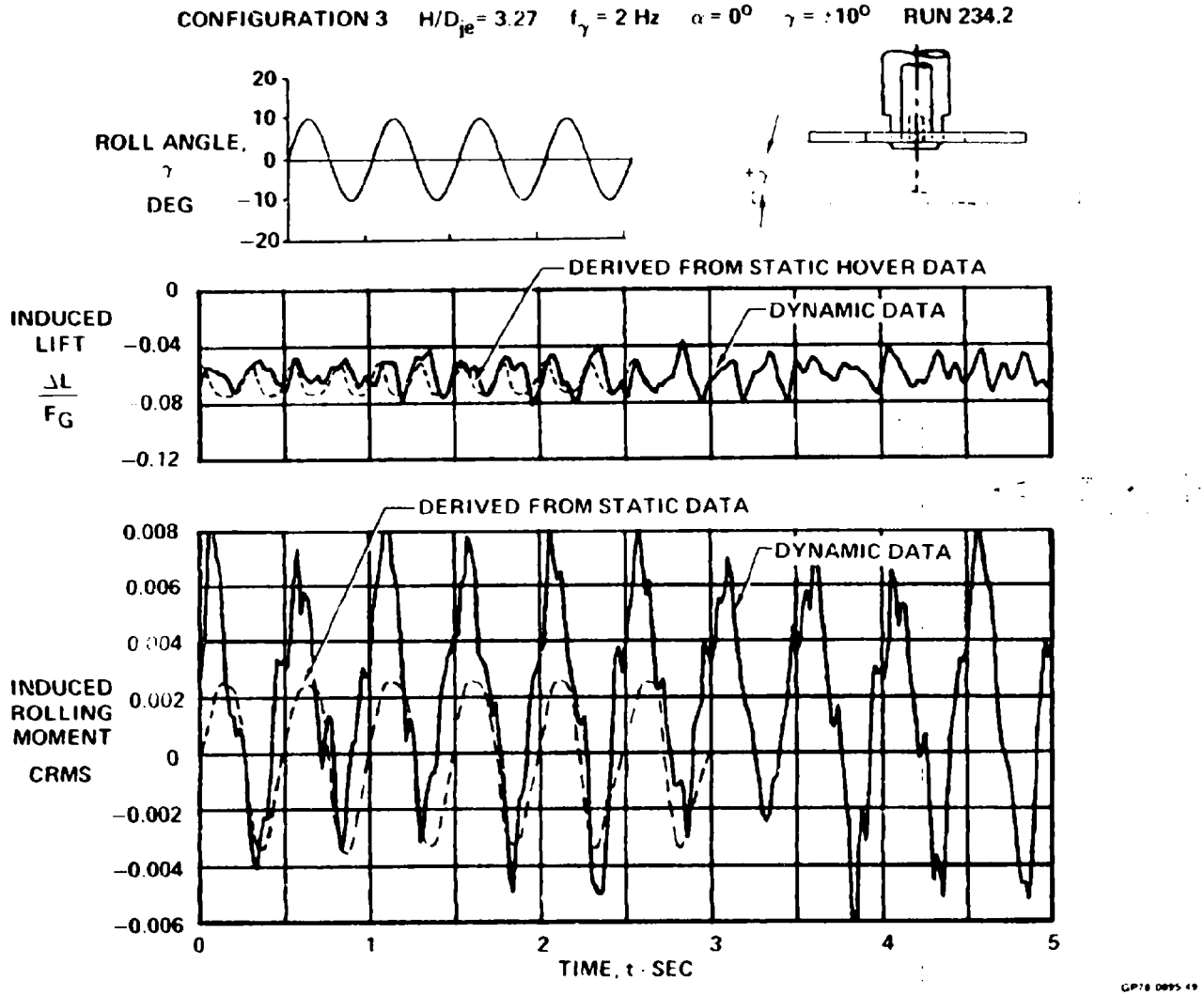

FIGURE 5-65
SUPERSONIC V/STOL STATIC TO DYNAMIC INDUCED LIFT AND INDUCED ROLLING MOMENT DATA COMPARISON FOR ROLLING DECK

CONFIGURATION 1 $H/D_{je} = 2$ $h/D_{je} = \cdot 1.0$ $f_{h,\gamma} = 2$ Hz $\alpha = 0^o$ $\gamma = \cdot 10^o$ $\varphi = 0^o$ RUN 172.2

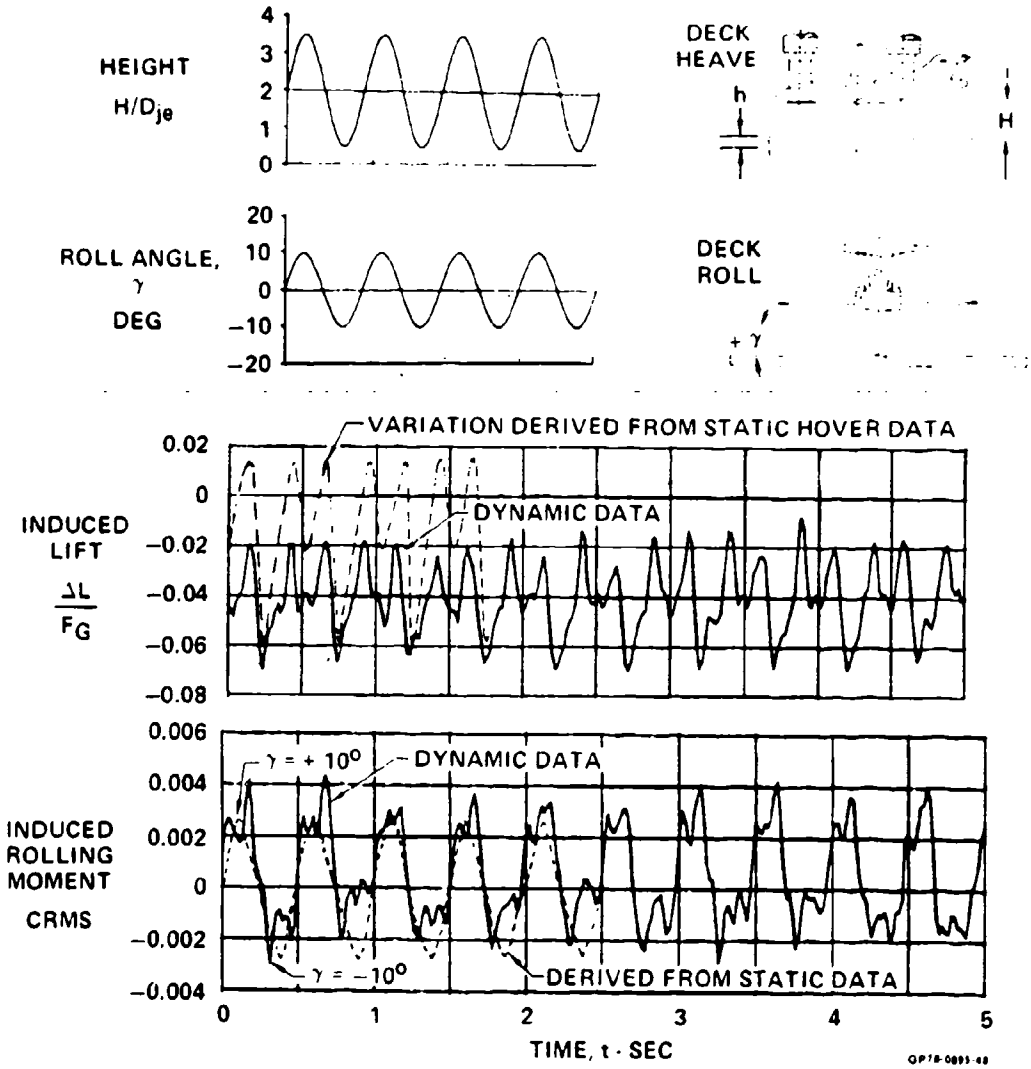

FIGURE 5-66
SUBSONIC V/STOL STATIC TO DYNAMIC INDUCED LIFT AND INDUCED ROLLING MOMENT DATA COMPARISON FOR HEAVING AND ROLLING DECK

and the roll were in phase such that the deck motion resembled a swinging door. To supplement the induced lift comparison, a comparison of rolling moments is also shown in Figure 5-66. A fairly good comparison is seen.

The static to dynamic comparison for a combination of deck pitch and roll in phase is given in Figure 5-67. In this case, the deck rocks diagonally from corner to corner and the values of the pitch and roll angles are equal at all times. Static tests were performed by setting the deck pitch and roll angles at equivalent values. As with the combined heave and roll motions, the combined pitch and roll motions have a more adverse effect on the induced lift than indicated by the static hover data.

Tests were also made with the pitch and roll angles 90° out of phase, thus giving the deck a wobbling motion. For this motion, the values of the pitch and roll angles are always different, but when either the pitch or roll angle is a maximum, the other angle is zero. Thus, an induced lift prediction can be made by using the static data obtained at the maximum values of both pitch and roll. As shown in Figure 5-68, the dynamic induced lift is substantially lower than the static prediction. These results further substantiate the adverse effects caused by the increased turbulent mixing action during combined motions.

To summarize the above comparisons of the dynamic and static data, it appears that predictions based on the static hover data can indicate the general trends of the dynamic response to deck motion and would probably be adequate for trade studies early in the design. However, the static hover predictions are often optimistic, particularly for the more complex combined deck motions. Consequently, the static hover data do not provide the degree of accuracy desired for aircraft design development.

5.3.2 Prediction Procedures for the Three Jet Subsonic Configuration - The development of generalized prediction procedures of the jet-induced aerodynamics, even for static hover conditions, is complicated by the high degree of configuration dependence which has been observed in this and many other programs. Due to this strong configuration dependence and the many significant test variables (i.e. height, roll, aircraft position relative to the deck, etc.), the development of a generalized procedure for the prediction of the effects of deck motion is believed to require additional data at

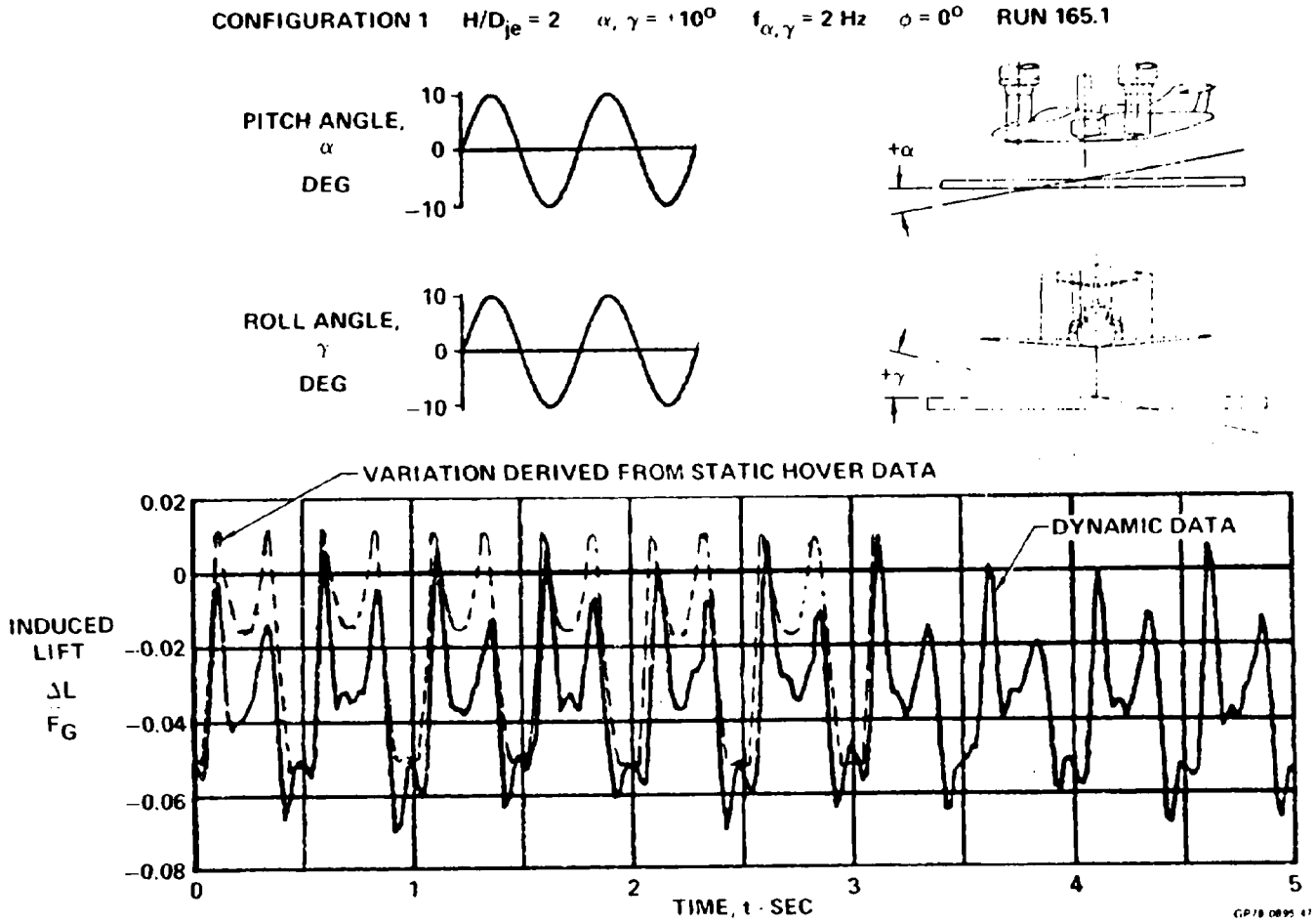

FIGURE 5-67
SUBSONIC V/STOL STATIC TO DYNAMIC INDUCED LIFT DATA COMPARISON FOR PITCHING AND ROLLING DECK

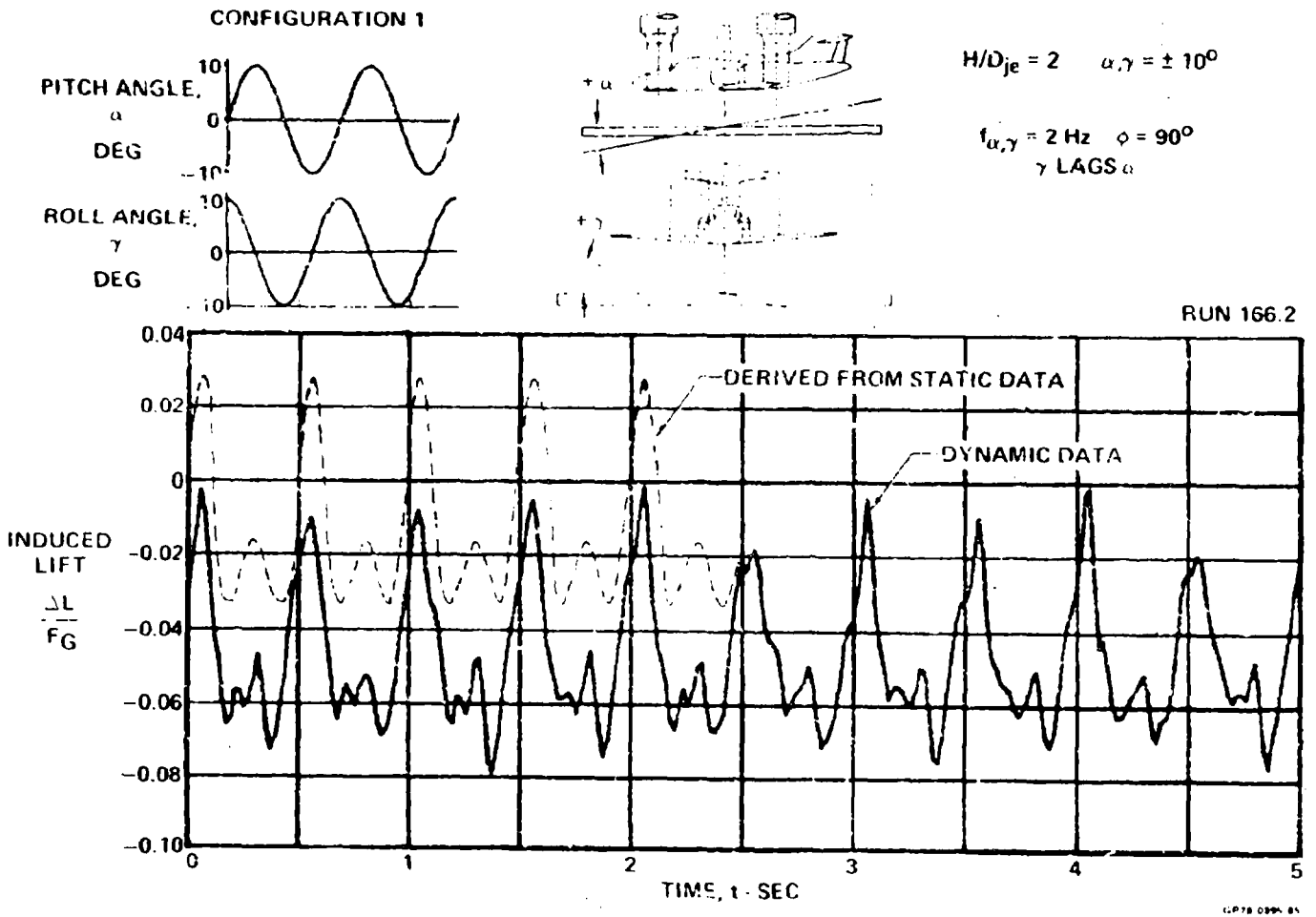

FIGURE 5-68
SUBSONIC V STOL STATIC TO DYNAMIC INDUCED LIFT DATA COMPARISON
FOR PITCHING AND ROLLING DECK OUT OF PHASE

more amplitudes, frequencies, and neutral point settings as well as more fundamental data (see Section 5.3.3). However, based on the dynamic data obtained for the fully-contoured subsonic model, expressions of the induced aerodynamics have been developed for selected deck motions.

Since the induced aerodynamic responses to deck motion are generally of a complex periodic nature, a potential expression for the variations involves a Fourier series. For example, the induced lift expression would be of the form:

$$\Delta L/F_G = A_o + \sum_{n=1}^{k} A_n \cos\frac{2n\pi t}{T} + B_n \sin\frac{2n\pi t}{T}$$

where T is the fundamental period, n is the component frequency, K is the highest numbered coefficient selected, and A_n and B_n are the Fourier series coefficients.

As indicated by the power spectral densities in Section 5.2.2, the induced aerodynamic re[illegible]ses to deck motion generally occur at the frequency of the motion and [illegible]multiples of this frequency. Use of a Fourier series would include terms for these frequency components.

Fourier series curve fits for the induced lift variation with a heave amplitude of 0.5 D_{je} at an H/D_{je} of 0.8 and of 1.5 D_{je} at an H/D_{je} of 2 are given in Figure 5-69. An accurate fit of the dynamic data is apparent in both cases. The Fourier series expressions include only those terms corresponding to the frequencies of the response indicated by the PSD's. In addition, the relative value of each term is proportional to the respective amplitude in the PSD, indicating that the Fourier series reflects the correct power at each frequency.

Fourier series curve fits are shown in Figures 5-70 and 5-71 for the induced lift and pitching moment variations with pitch angle at H/D_{je} values of 0.8 and 2.0. Similar curves are provided in Figures 5-72 and 5-73 for the induced lift and rolling moment variations with roll angle. Additional plots are provided in Figure 5-74 for frequencies of 1 and 3 Hz. Good fits of the data are seen in each case, using the terms in the Fourier series which correspond to the response frequencies indicated in the PSD's.

Correlations were made of the Fourier series coefficients with the amplitudes and frequencies of the motions. However, these correlations were not well behaved either due to the highly turbulent nature of the phenomena

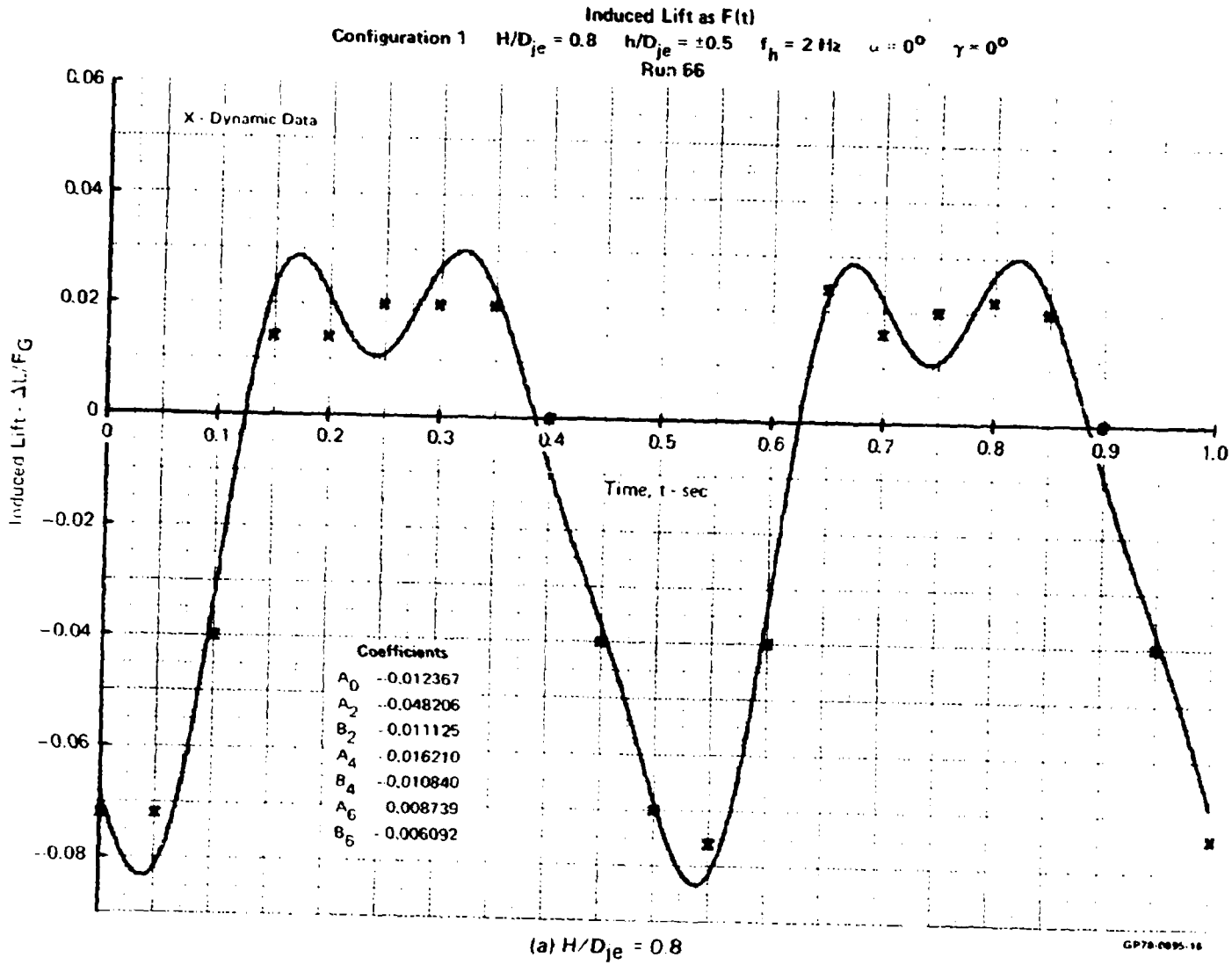

(a) $H/D_{je} = 0.8$

FIGURE 5-69
FOURIER SERIES FIT OF INDUCED LIFT VARIATIONS FOR HEAVING DECK

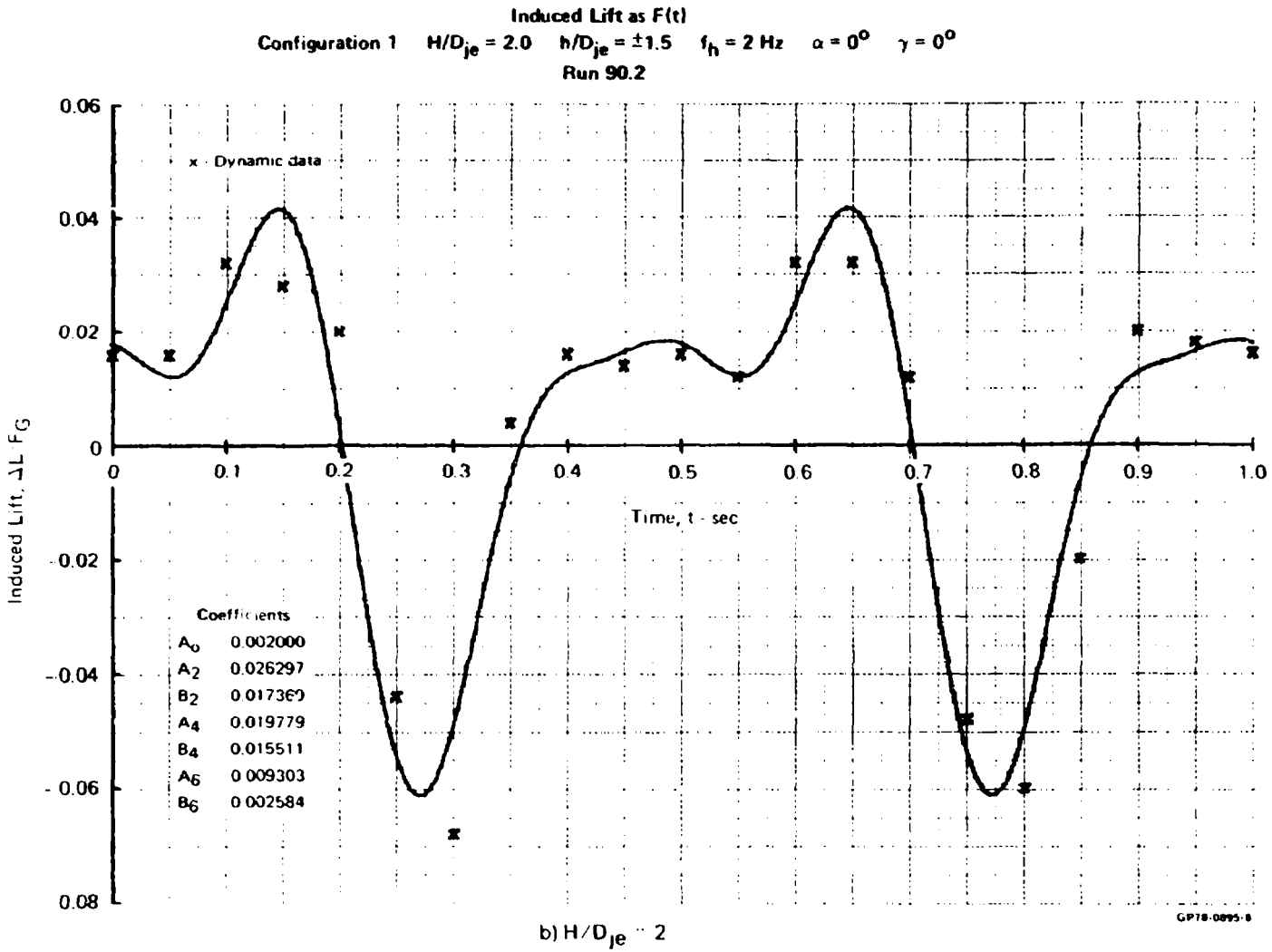

b) $H/D_{je} = 2$

FIGURE 5-69 (Concluded)
FOURIER SERIES FIT OF INDUCED LIFT VARIATIONS FOR HEAVING DECK

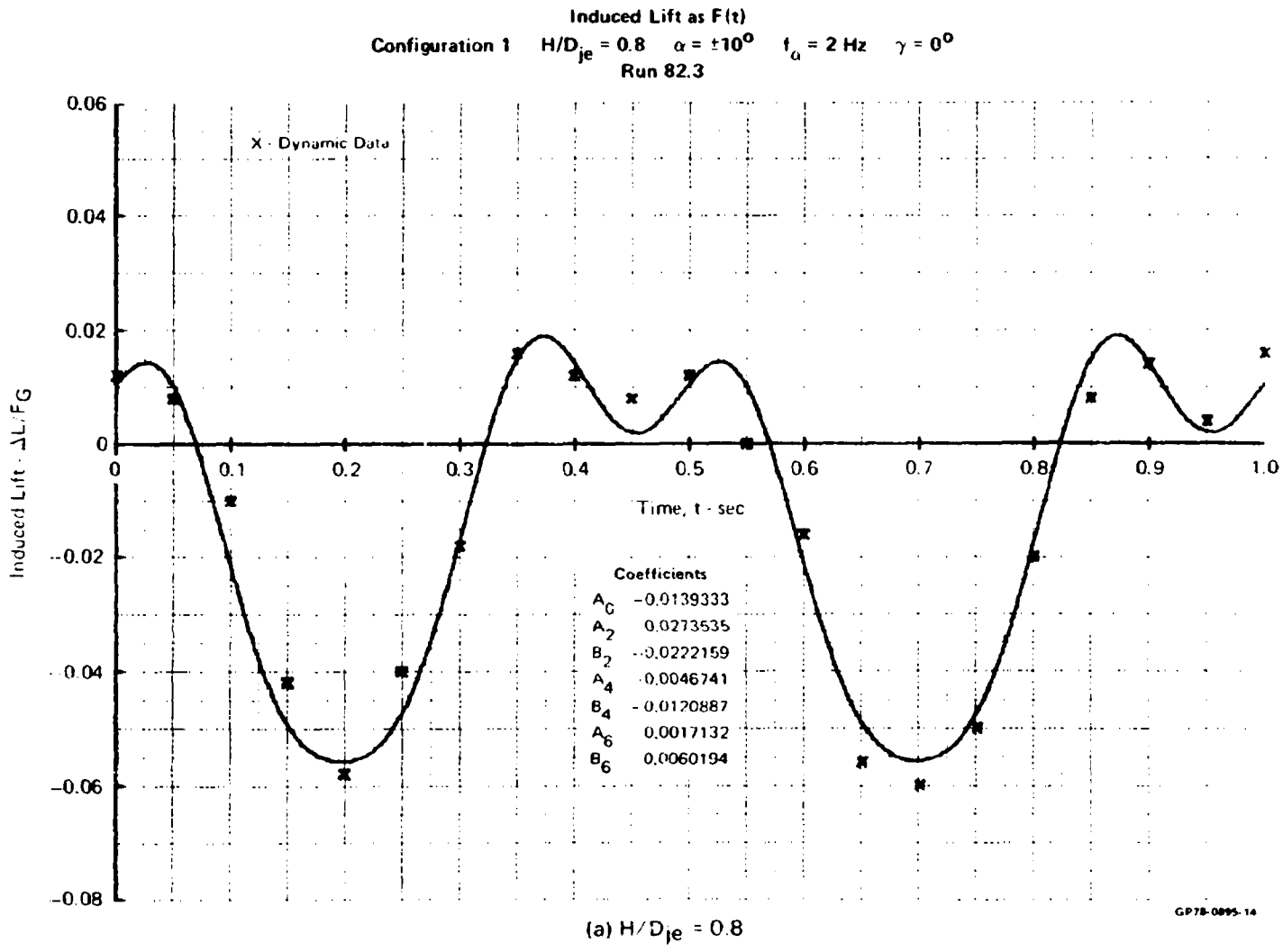

(a) $H/D_{je} = 0.8$

FIGURE 5-70
FOURIER SERIES FIT OF INDUCED LIFT VARIATIONS FOR PITCHING DECK

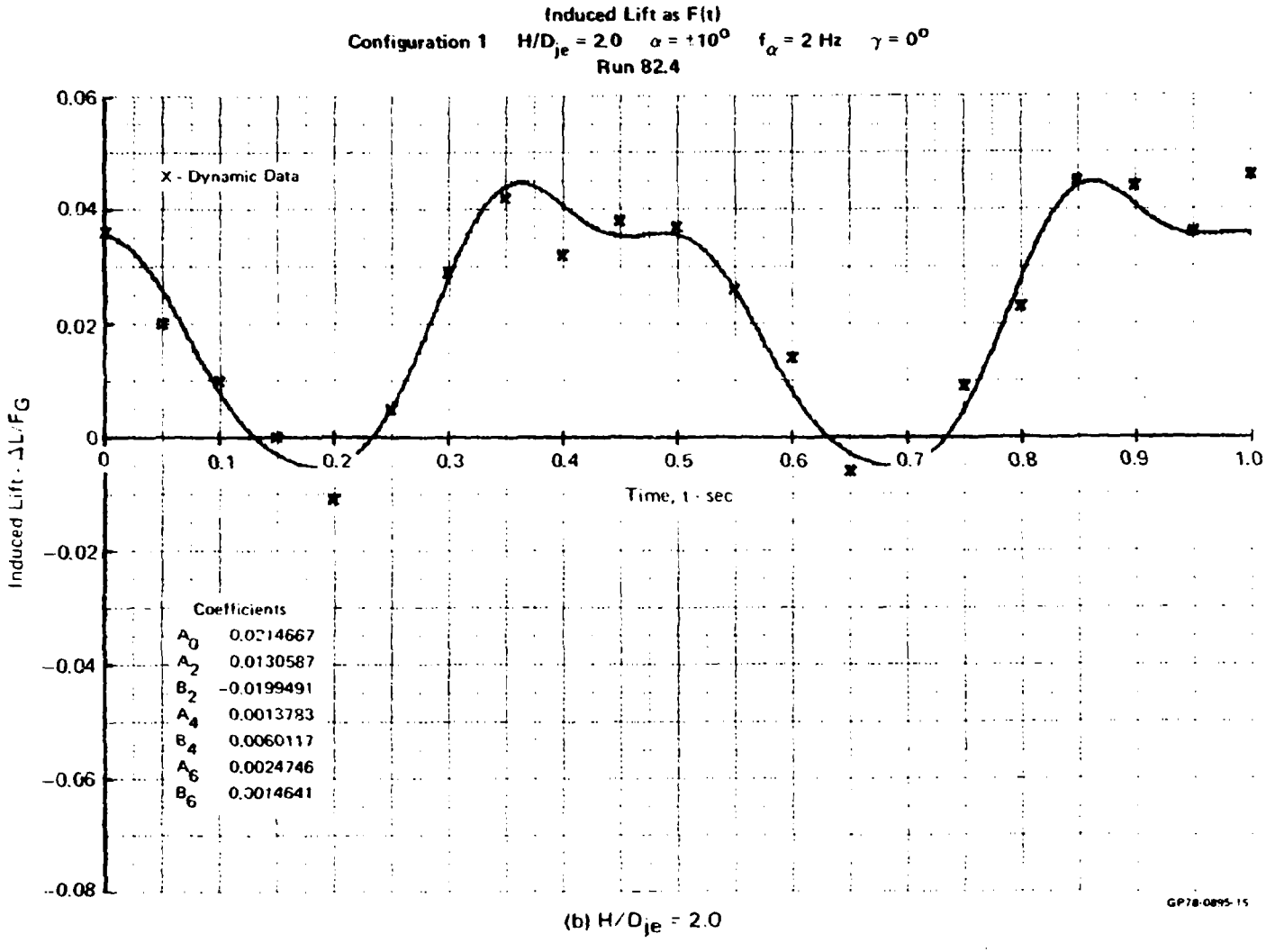

(b) $H/D_{je} = 2.0$

FIGURE 5-70 (Concluded)
FOURIER SERIES FIT OF INDUCED LIFT VARIATIONS FOR PITCHING DECK

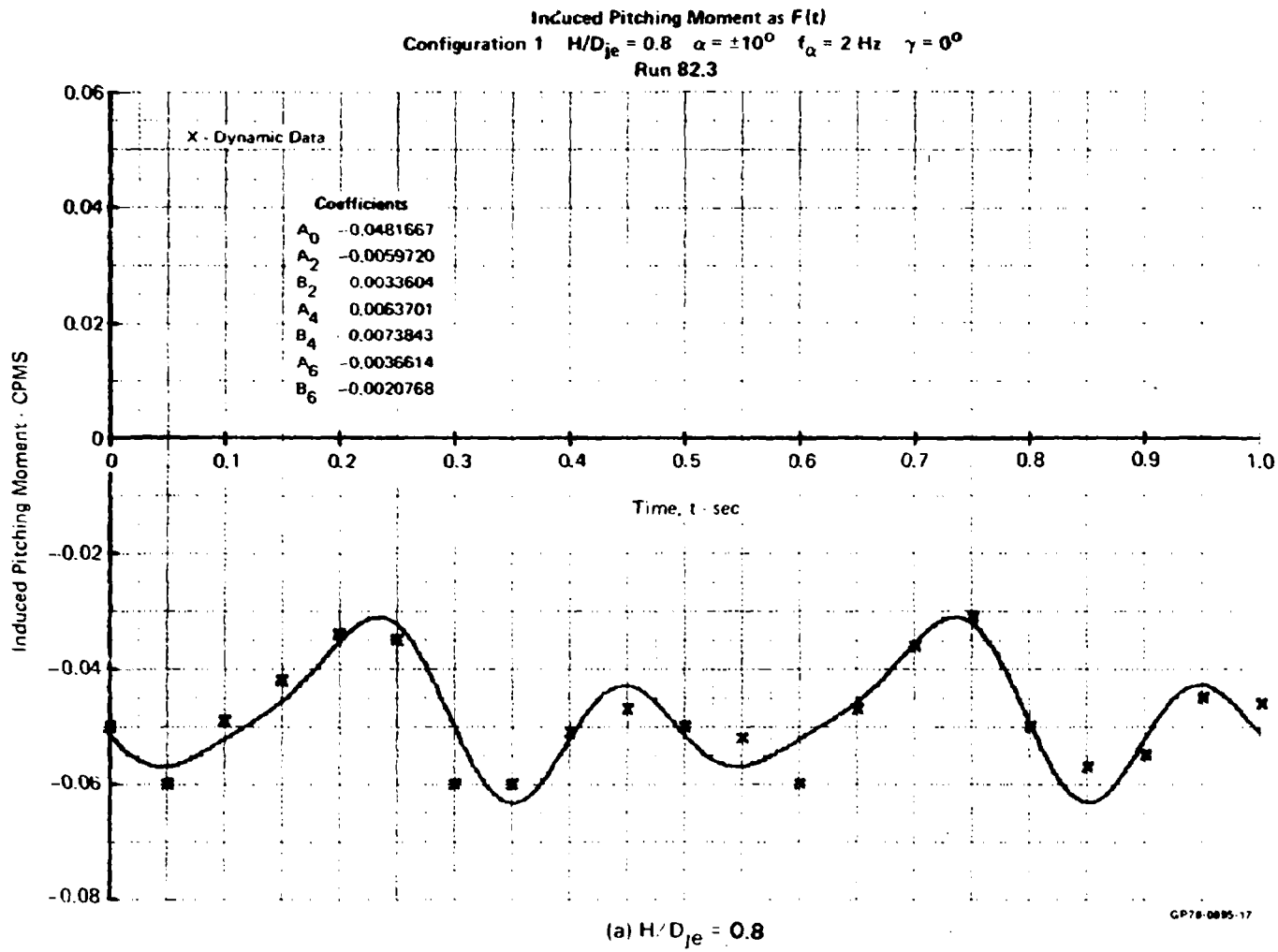

(a) $H/D_{je} = 0.8$

FIGURE 5-71
FOURIER SERIES FIT OF INDUCED PITCHING MOMENT VARIATIONS FOR PITCHING DECK

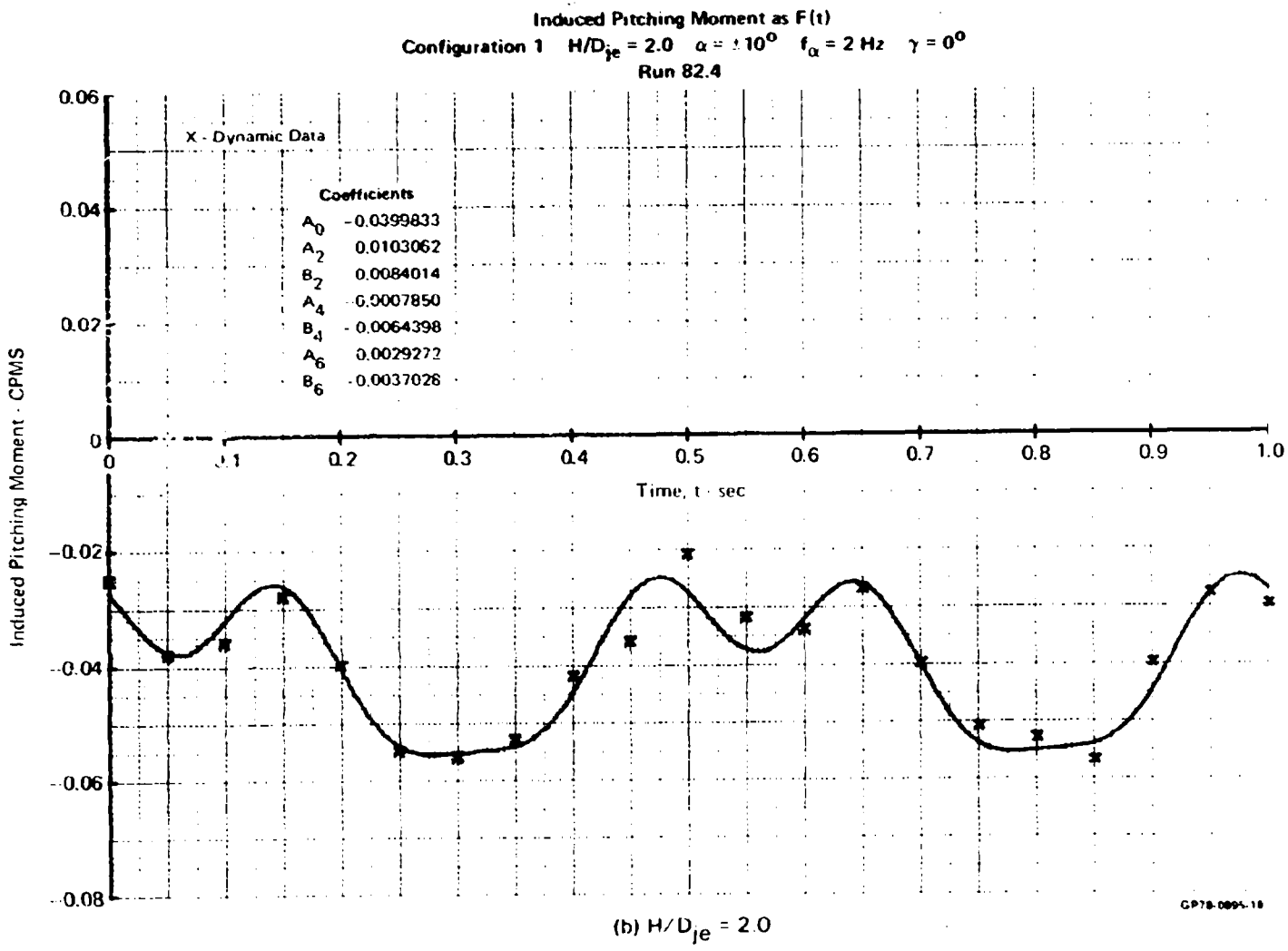

(b) $H/D_{je} = 2.0$

FIGURE 5-71 (Concluded)
FOURIER SERIES FIT OF INDUCED PITCHING MOMENT VARIATIONS FOR PITCHING DECK

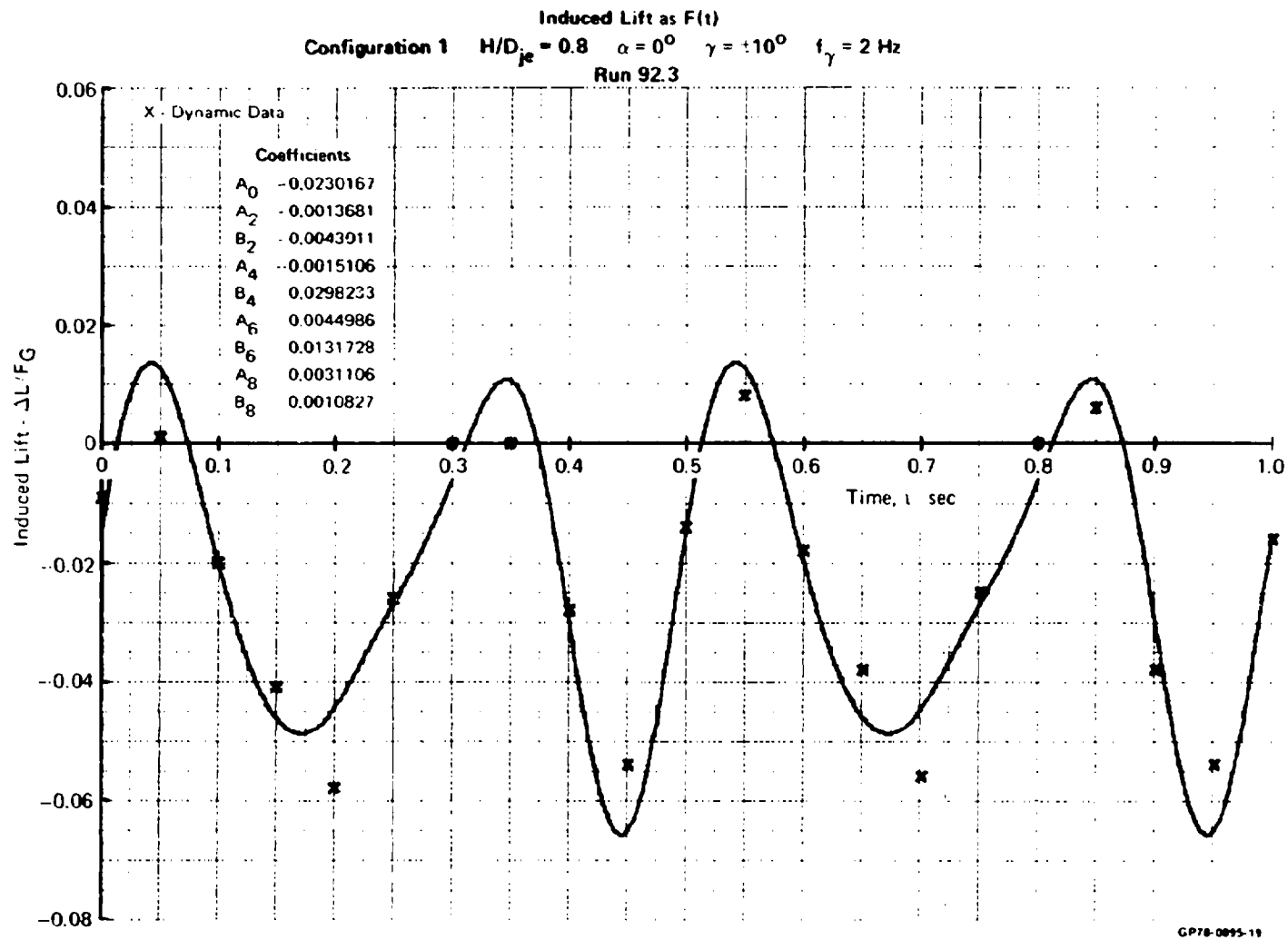

(a) $H/D_{je} = 0.8$

FIGURE 5-72
FOURIER SERIES FIT OF INDUCED LIFT VARIATIONS FOR ROLLING DECK

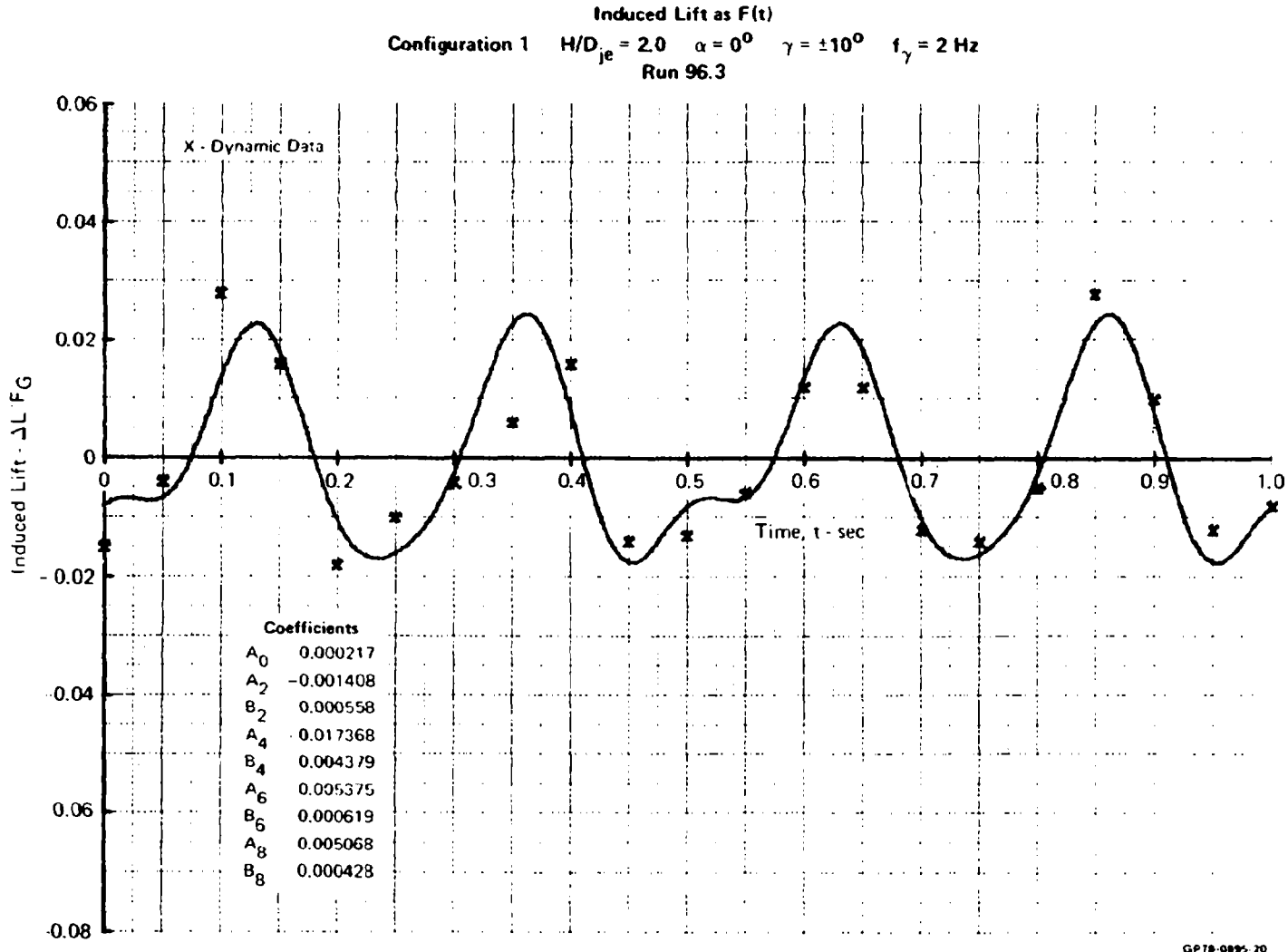

(b) $H/D_{je} = 2.0$

FIGURE 5-72 (Concluded)
FOURIER SERIES FIT OF INDUCED LIFT VARIATIONS FOR ROLLING DECK

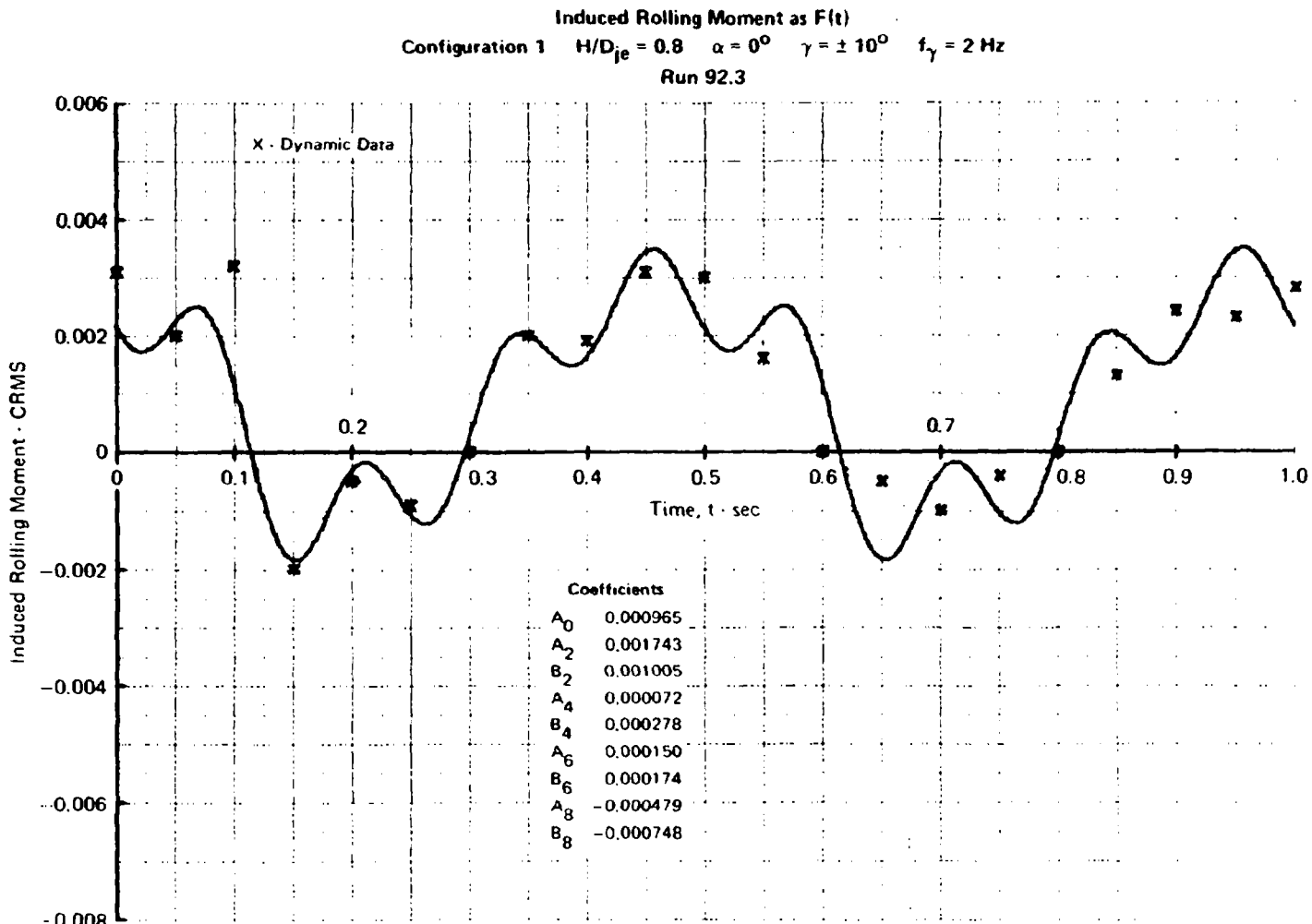

(a) $H/D_{je} = 0.8$

FIGURE 5-73

FOURIER SERIES FIT OF INDUCED ROLLING MOMENT VARIATIONS FOR ROLLING DECK

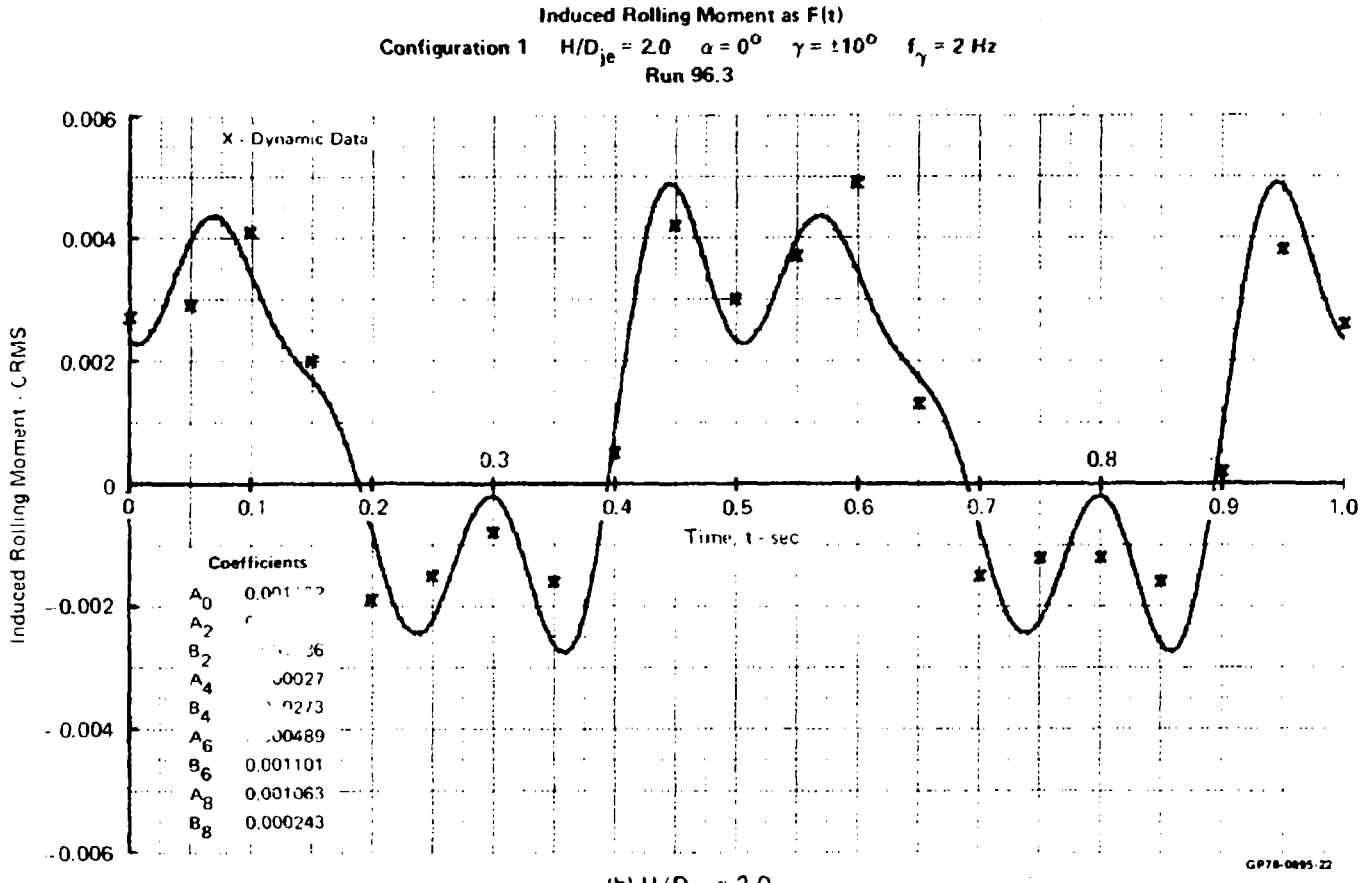

(b) $H/D_{je} = 2.0$

FIGURE 5-73 (Concluded)
FOURIER SERIES FIT OF INDUCED ROLLING MOMENT VARIATIONS FOR ROLLING DECK

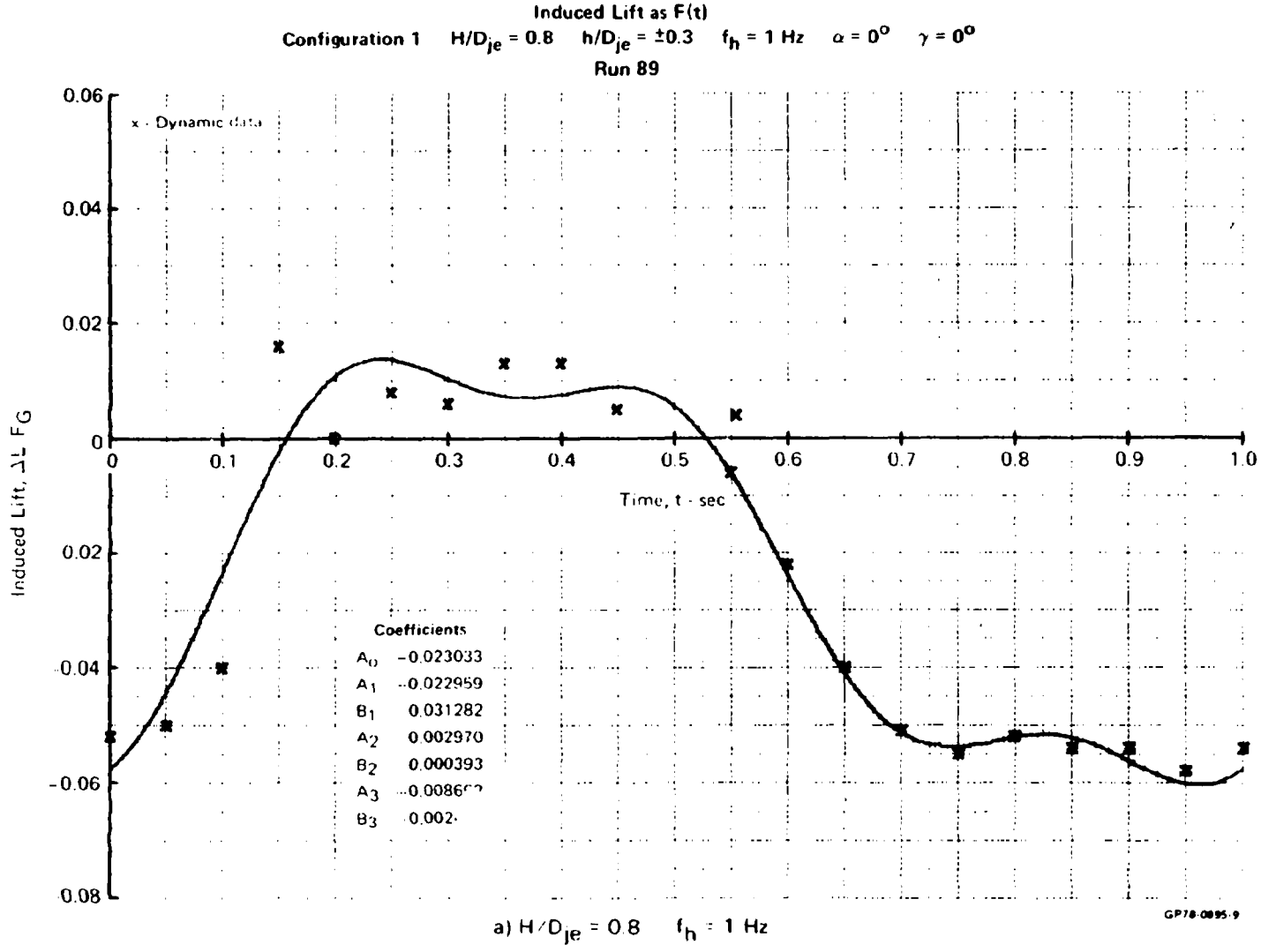

a) $H/D_{je} = 0.8$ $f_h = 1$ Hz

FIGURE 5-74
FOURIER SERIES FIT OF INDUCED LIFT VARIATIONS FOR HEAVING DECK AT VARIOUS FREQUENCIES

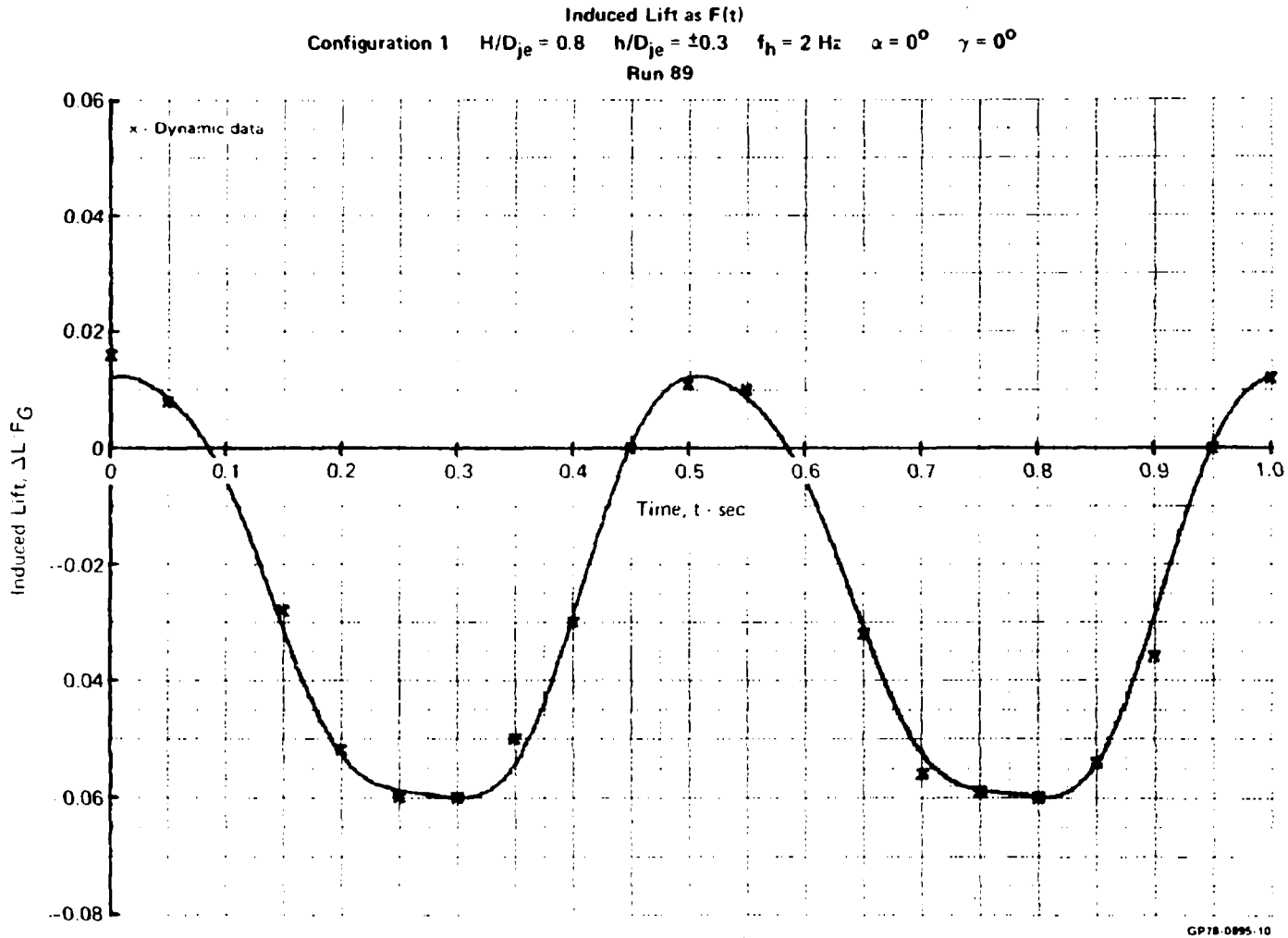

b) $H/D_{je} = 0.8$ $f_h = 2$ Hz

FIGURE 5-74 (Continued)
FOURIER SERIES FIT OF INDUCED LIFT VARIATIONS FOR HEAVING DECK AT VARIOUS FREQUENCIES

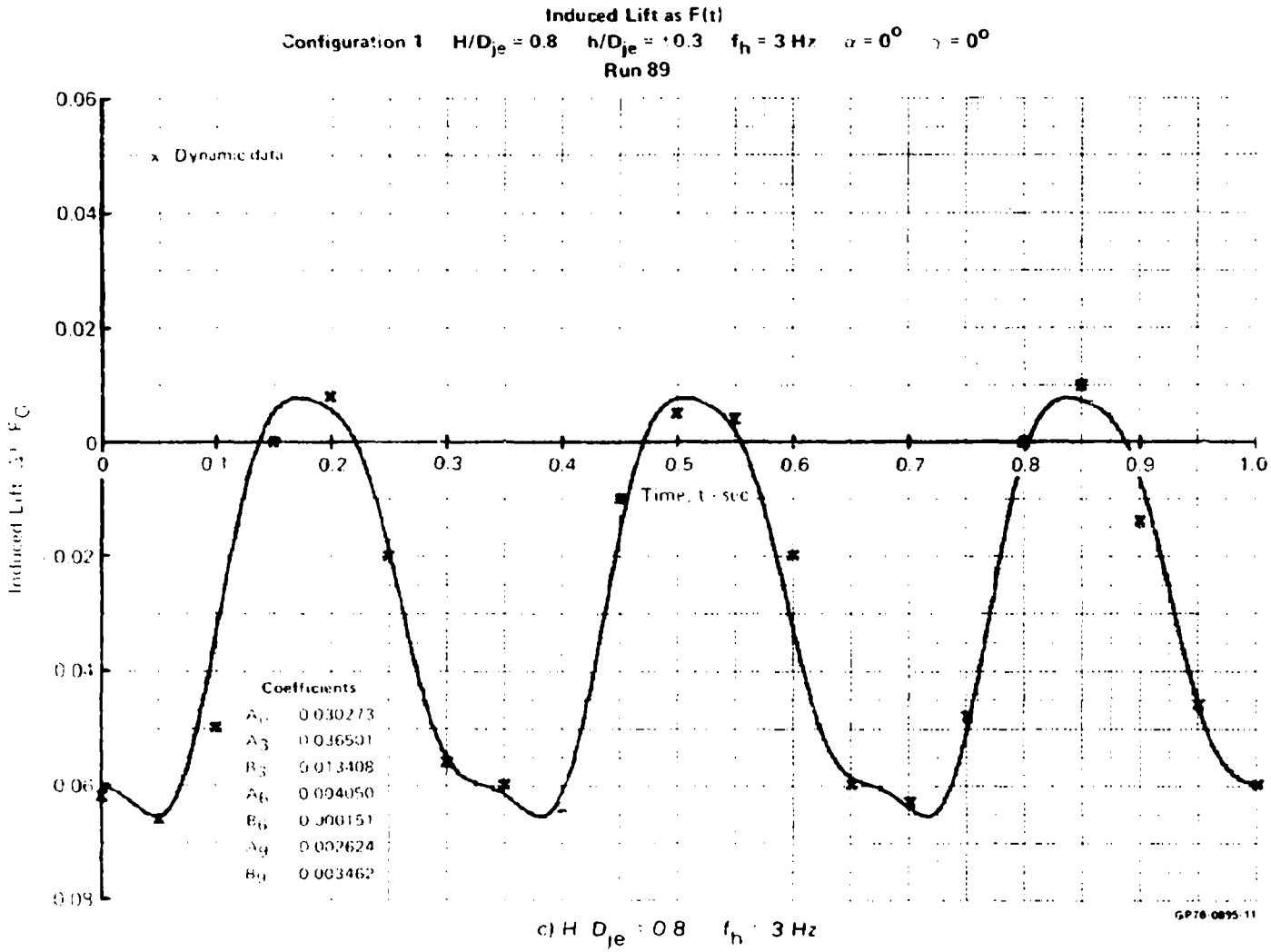

c) H/D_je = 0.8 f_h = 3 Hz

FIGURE 5-74 (Continued)
FOURIER SERIES FIT OF INDUCED LIFT VARIATIONS FOR HEAVING DECK AT VARIOUS FREQUENCIES

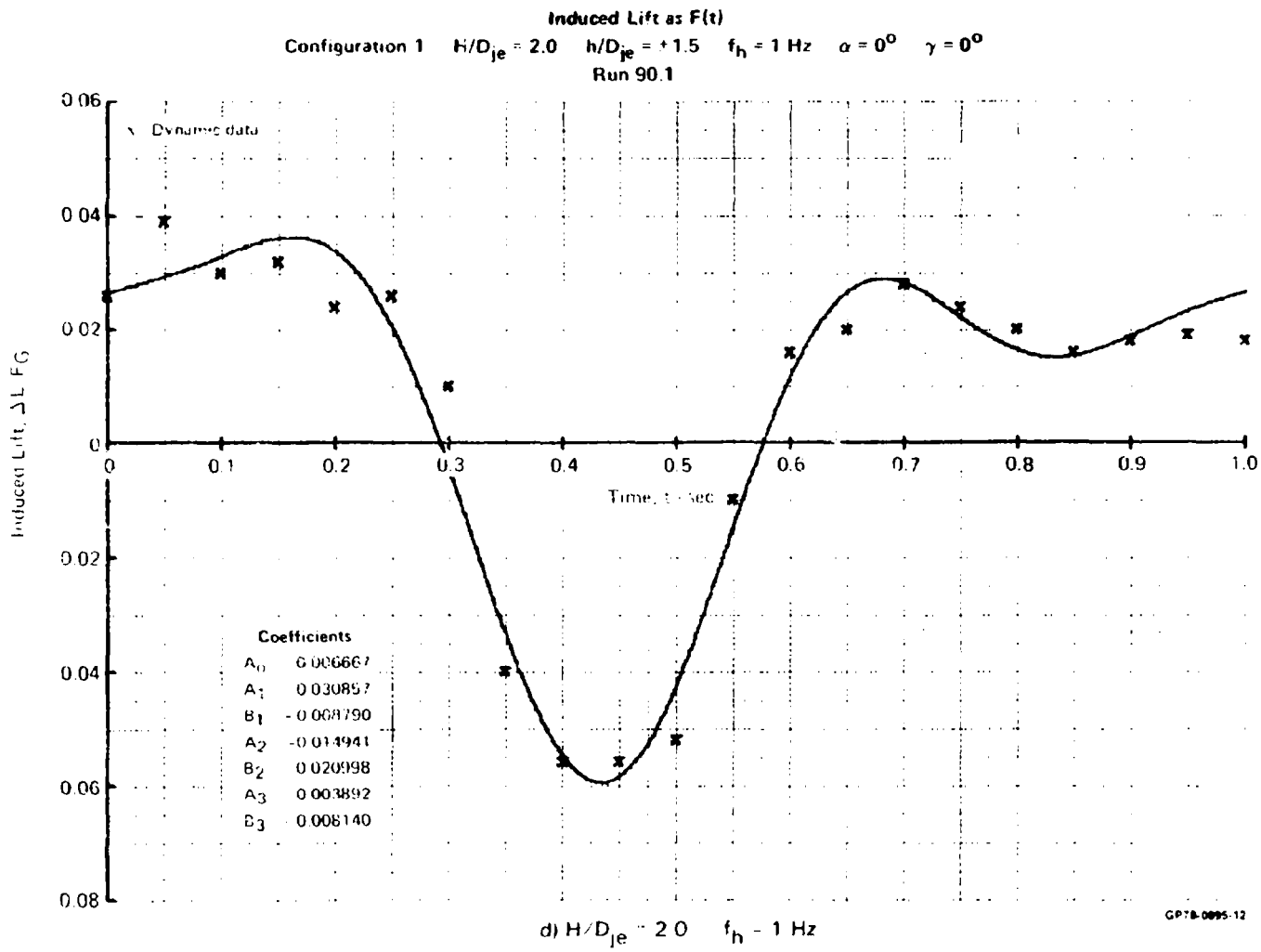

d) $H/D_{je} = 2.0$ $f_h = 1$ Hz

FIGURE 5-74 (Continued)
FOURIER SERIES FIT OF INDUCED LIFT VARIATIONS FOR HEAVING DECK AT VARIOUS FREQUENCIES

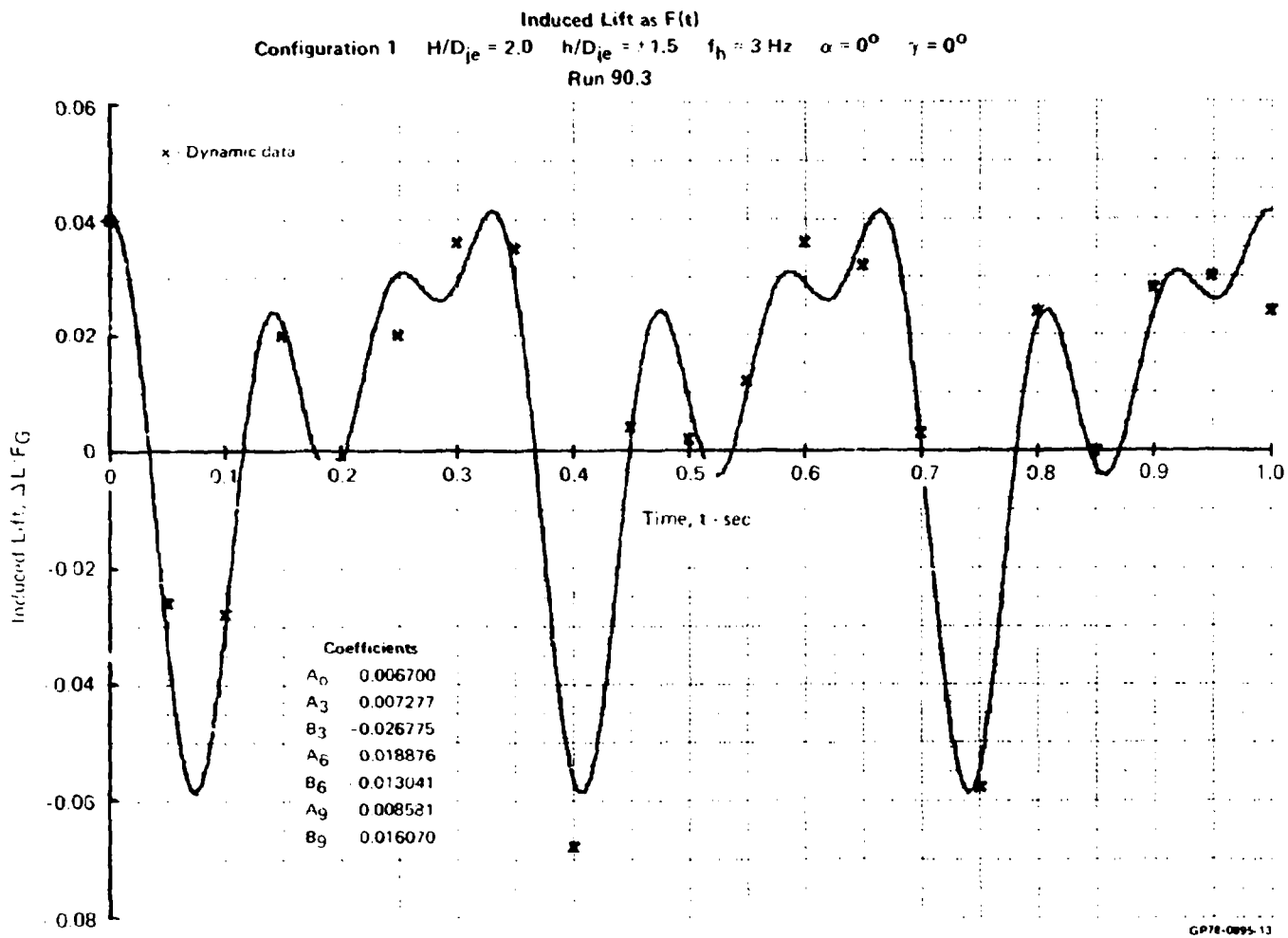

e) $H/D_{je} = 2.0$ $f_h = 3$ Hz

FIGURE 5-74 (Concluded)
FOURIER SERIES FIT OF INDUCED LIFT VARIATIONS FOR HEAVING DECK AT VARIOUS FREQUENCIES

or the inability to adequately define the correlation. It is believed that data at more amplitudes, frequencies, and neutral point settings would provide consistent correlations and thus, would allow the definition of the dynamic response to any given amplitude of motion. Potential applications for these formulations of the dynamic responses to deck motion for a representative V/STOL configuration are in the hover control system design and in piloted computer-based simulations of the take-off and recovery operations aboard ship.

5.3.3 Suggested Approach to the Development of Improved Prediction Procedures - One area requiring improvement in the above approach, as far as general applicability, is to relate the Fourier expressions to the significant configuration variables such as the nozzle spacing, the inner region area, and the total planform area. A more fundamental, less configuration dependent experimental program would supply much needed additional information relating to the separate effects of the important configuration variables and test conditions on the fountain and suckdown forces.

In the Reference 4 study, it was concluded that the fountain flowfield is an area that requires much further investigation to improve the resultant force and moment predictions IGE at static hover conditions. In addition, it has been shown in this program that the fountain may well have the largest impact on the induced force and moment variations with deck motion.

The predominant impact of the fountain can be demonstrated by combining the dynamic lift variation measured on the inner region plate model (representing the inner region of the subsonic model) with the suckdown prediction based on static hover data described in Section 5.1. Reasonably good agreement between this induced lift variation and the dynamic data for the complete model is shown in Figure 5-75 for heaving deck motion.

A similar procedure was applied to the induced lift variation with roll angle, again combining the dynamic data from the inner region model with the suckdown variation with roll angle predicted from static hover data. Again, fairly good agreement with the dynamic data for the complete model can be seen in Figure 5-76.

These comparisons imply that the jet-induced aerodynamic variations which occur with deck motion primarily result from the modified fountain cushion effect and the fountain movement with angular motions. Thus, a parametric test program utilizing 2, 3, and 4 nozzle arrangements with corresponding

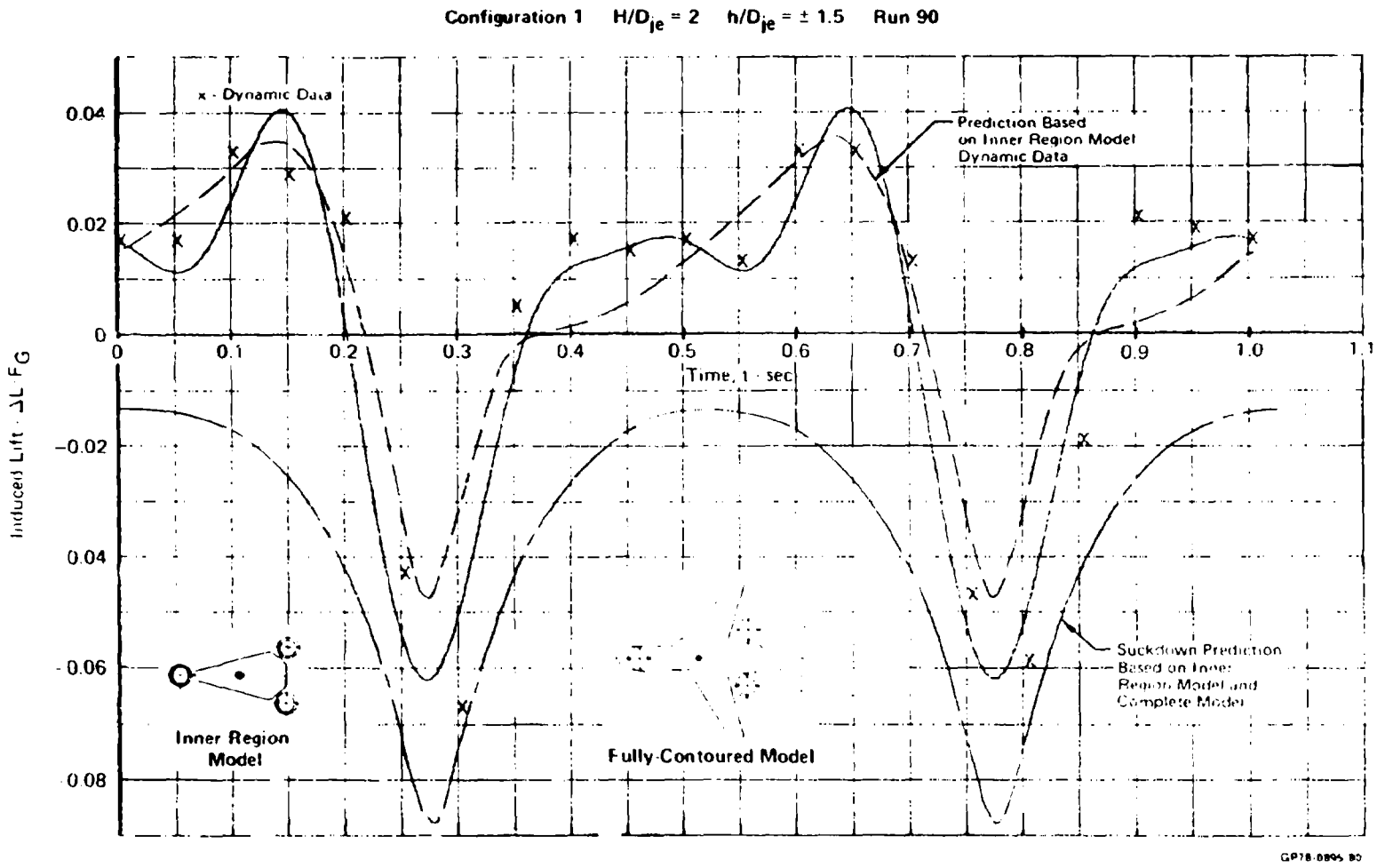

FIGURE 5-75

INDUCED LIFT VARIATION FOR HEAVING DECK BASED ON INNER REGION MODEL

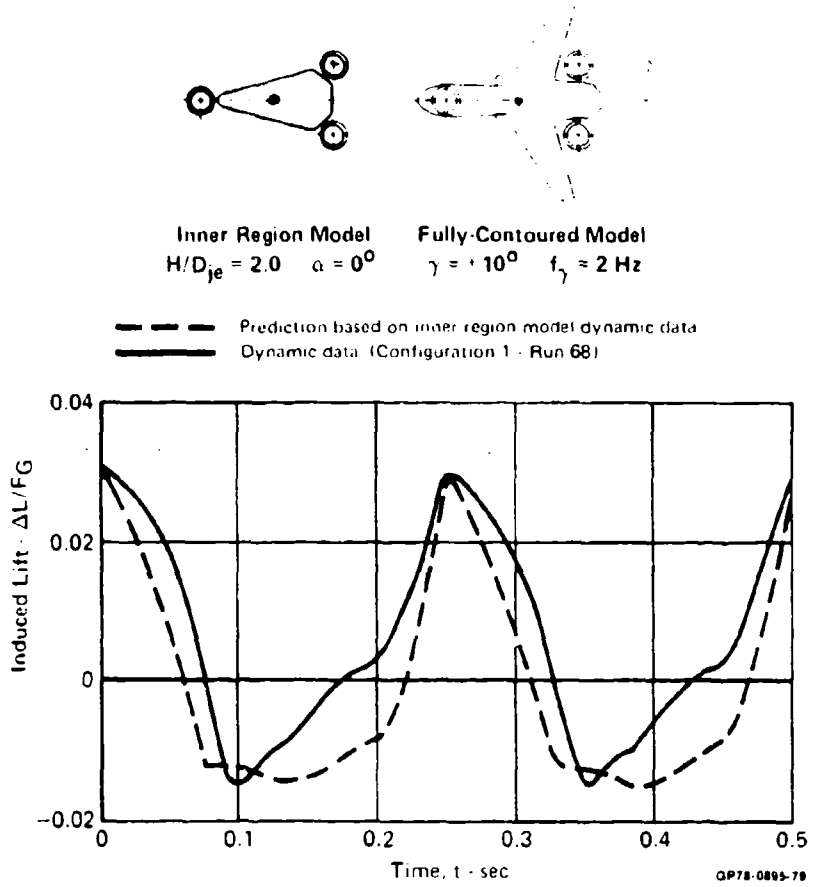

FIGURE 5-78
INDUCED LIFT VARIATION FOR ROLLING DECK BASED ON INNER REGION MODEL

inner region plate models would supply significant information to relate the dynamic force and moment variations with the important configuration variables. By limiting the investigation to the inner region, a truly parametric test can be performed without being unduly restricted by the aircraft planform shape. A corresponding investigation on suckdown would also be beneficial by determining the conditions for which dynamic deck motion affects suckdown.

These suggested experimental efforts, combined with the results of this program, would provide the parametric data base to allow the formulation of generalized empirical procedures for predicting the jet-induced force and moment variations with deck motion. Particular emphasis should be placed on combined motions, which would normally exist aboard ship.

6. CONCLUSIONS AND RECOMMENDATIONS

Several significant conclusions were derived from this program regarding the propulsive lift system induced aerodynamics of V/STOL aircraft at both static hover conditions and with deck motion. These conclusions are given below along with recommendations for future studies.

6.1 CONCLUSIONS - The conclusions relate to the effects of model configuration variables and deck motion.

Planform Configuration

- The three-jet subsonic configuration has significantly lower induced lift loss than the three-jet supersonic configuration primarily due to a lower planform to jet area ratio and a stronger fountain.
- The induced aerodynamics of a configuration having a strong fountain are sensitive to deck pitch and roll in ground effect (IGE).

Nozzle Arrangement

- Increasing the number and the fore to aft spacing of nozzles increases the fountain strength and reduces the net lift loss.
- Locating the nozzles close to the planform edge or in a region where the adjacent planform area is small, reduces suckdown.

Nozzle Simulation/Operation

- Nozzle vectoring vanes and other flow control devices can increase suckdown and reduce the fountain strength which is attributed to a more rapid free jet decay rate.
- Testing at the full scale nozzle pressure ratio is required to provide the most accurate flowfield simulation.
- The induced aerodynamics are very sensitive to the thrust bias between the fore and aft nozzles.

Airframe Simulation

- Simulation of the model lower surface contouring, particularly in the fountain impingement region, can significantly affect the induced aerodynamics IGE.
- Upper surface contouring appears to be unimportant without crosswind, but placement of the airframe surfaces in the proper plane relative to the nozzles is advisable.

- Simple flat plate planform models provide reasonable data trends and incremental configuration effects, and thus can be used for economical preliminary configuration studies.
- Near typical gear heights, the induced lift increases with wing height.

Lift Improvement Devices (LID's)

- Properly designed LID's can significantly enhance the induced lift IGE and can be effective even at high roll angles

Deck Size

- The deck size has no appreciable effect provided the model is centered over the deck and no superstructure is present.

Deck Motion

- The responses of the induced aerodynamics to deck motion are of a complex periodic nature at the same and/or multiples of the deck motion frequency.
- The responses are essentially instantaneous IGE due to the high velocity jets.
- Up to 3 Hz, the motion frequency has little effect on the statistical response as indicated by a nearly constant transfer function. However, frequency can affect the instantaneous response characteristics.
- The induced lift resulting from fountain impingement increases as the deck heaves toward the model.
- For a configuration with high suckdown, a significantly higher lift loss occurs when the deck heaves away from the model.
- Deck roll produces a destabilizing rolling moment due to the movement of the fountain.
- Based on tests with an inner region model, the fountain appears to have the largest impact on the force and moment variations with deck motion.

Prediction Procedures

- Predictions based on static hover data can differ significantly from actual dynamic data and often indicate lower lift loss and higher moment variations, particularly for combined motions.

- The differences between the static predictions and the dynamic data are attributed primarily to increased turbulent mixing and modification of the fountain impingement forces due to deck motion.
- The induced aerodynamic variations can be accurately expressed with Fourier series.

6.2 RECOMMENDATIONS - Based on the results of this program, the following recommendations are given to guide future efforts.

- In the near term, further detailed analyses of the established data base (e.g., examination of the individual force components comprising the pitching and rolling moments) and supporting analytical efforts would supply useful information for defining additional test and analysis efforts. Potential results of such an effort could be a method for correcting static data for single degree and possibly multiple degree of freedom deck motions.
- A parametric test program utilizing 2, 3, and 4 nozzle arrangements with corresponding inner region plate models is recommended to isolate the deck motion and configuration effects on the fountain forces.
- Parametric data at additional amplitudes, frequencies, and neutral point settings are required to develop data correlations with greater statistical confidence.
- Testing is recommended on a single representative V/STOL configuration with exact random ship motions generated from Reference 2. This testing should be conducted for more combined motions and should include predicted aircraft motions superimposed on the deck motion.
- Investigations should be performed to more clearly define the effects of planform to nozzle area ratio.
- Scale effects should be investigated by comparing small scale data with large scale data on a configuration such as the Harrier.
- An investigation of the effects of ship superstructure and the associated turbulence due to crosswind is recommended.
- Effort should be directed toward assessing the effects of aircraft position relative to the deck, which results in different jet impingement locations.

- A computer simulation is recommended which would include six degree-of-freedom equations of motion, a ship motion model, dynamic ground effects, a ship superstructure turbulence model, and mathematical pilot model or autoland guidance equations.

7. REFERENCES

1. Meyers, J. J., editor, "Handbook of Ocean and Underwater Engineering," McGraw-Hill Book Co., 1967.
2. Baitis, A. E., Meyers, W. G., and Applebee, T. R., "A Non-Aviation Ship Motion Data Base for the DD-963, CG-26, FF-1052, FFG-7, and the FF-1040 Ship Classes," DTNSRDC Report No. SPD-738-01, December 1976.
3. Schuster, E. P. and Flood, J. D., "Important Simulation Parameters for the Experimental Testing of Propulsion Induced Lift Effects," AIAA Paper No. 78-1078, July 25-27, 1978.
4. Kotansky, D. R., et al., "Multi-Jet Induced Forces and Moments on VTOL Aircraft Hovering In and Out of Ground Effect," Report No. NADC-77-229-30, 19 June 1977.

DISTRIBUTION LIST

Naval Air Development Center (16)*(6)
Warminster, PA 18974
Attn: Code 6053

Commander (1)*(1)
Naval Weapons Center
China Lake, CA 93555

Commanding Officer (1)*(1)
Naval Air Propulsion Test Center
Trenton, NJ 98628

Commander (1)*(1)
David Taylor Naval Ship Research
and Development Center
Bethesda, MD 20034
Attn: P. Schevrich

Chief (1)*(1)
Office of Naval Research
800 N. Quincy Street
Arlington, VA 22217
Attn: D. Siegel

Superintendent (1)*(1)
Naval Postgraduate School
Monterey, CA 93940
Attn: L. Schmidt

Director (1)*(1)
National Aeronautics and
Space Administration
Ames Research Center
Moffett Field, CA 94035
Attn: D. Hickey

Director (1)*(1)
National Aeronautics and
Space Administration
Langley Research Center
Hampton, VA 23365
Attn: R. Margason

Director (1)*(1)
National Aeronautics and
Space Administration
21000 Brooke Park Road
Cleveland, OH 44135

Director (1)*(1)
Air Force Flight Dynamics
Laboratory (ASD/ENFDH)
Wright-Patterson AFB
Dayton, OH 45433

Commander (1)*(1)
Air Force Aeronautical Systems
Division
Wright-Patterson AFB
Dayton, OH 45433

Adminstrator (12)*(2)
Defense Documentation Center
for Scientific and Technical
Information (DDC)
Bldg #5, Cameron Station
Alexandria, VA 22314

Commanding General (1)*(1)
Army Aviation Systems Command
St. Louis, MO 63102

Boeing Company (2)
Seattle, WA 98101
Attn: E. Omar
G. Lampard

LTV Aerospace Corporation (3)
Dallas, TX 75221
Attn: T. Beatty
W. Simpkin
G. Booth

Rockwell International (1)
Columbus, OH 43216
Attn: W. Palmer

General Dynamics Corporation (1)
Ft. Worth, TX 76108
Attn: W. Folley

Commander (4)*(1)
Naval Air Systems Command (AIR-954)
Department of the Navy
Washington, DC 20361
Attn: AIR-320D 2 copies for
AIR-5301 retention

*Volume II - Limited Distribution

DISTRIBUTION LIST
(Continued)

Nielson Engineering (1)
510 Clyde Avenue
Mountain View, CA 94043

Duvvuri Research Company (1)
641 Windsor Circle
Chula Vista, CA 92112

Lockheed-California Company (1)
P.O. Box 551
Burbank, CA 91503
Attn: A. Yackle

Northrop Corporation (1)
Hawthorne, CA 90250
Attn: P. T. Wooler

Grumman Aerospace Corporation (2)
Bethpage Long Island, NY 11714
Attn: F. Wohllebe
D. Bigdal

Royal Aeronautical Establishment (1)
Bedford, England
Attn: A. Woodfield

Fairchild-Republic Corporation (1)
Farmingdale, Long Island, NY 11735

Calspan (1)
4455 Genesee Street
Buffalo, NY 14221

McDonnell Douglas Corporation (1)
P.O. Box 516
St. Louis, MO 63166
Attn: C. W. Miller

Computational Mechanics (1)
3601A Chapman Highway
Knoxville, TN 37920

Lockheed-Georgia Co. (1)
Marietta, GA 30061

SUPPLEMENTAL

INFORMATION

29 September 1978

NADC-77-107-30 - Vol 1

AD-A060 206

ERRATA-March 1979

The following corrections are applicable to NADC-77-107-30, "Lift System Induced Aerodynamics of V/STOL Aircraft in a Moving Deck Environment", 29 September 1978:

page 63

Reverse the symbols in the legend.

page 107

Change the ordinate values for the rolling moment from 0.02, 0.04, etc. to 0.002, 0.004, etc.

page 114

Change $\Theta = 0°$ to $\phi = 0°$ in the description of the test conditions.

page 139

Change the ordinate values for the pitching moment from 0.2, 0.4, etc. to 0.02. 0.04, etc.

page 146

Reduce the amplitude shown for the sinusoidal height variation (H/D_{je}) from ± 1.5 to ± 1.0 equivalent nozzle diameters.

page 149

Reverse the sinusoidal roll angle variation from leading the pitch angle to lagging the pitch angle. The roll angle variation

should begin at $\gamma = -10°$ instead of $+10°$.

page 162

Add the following Fourier coefficients to the figure.

	Coefficients
A_o	-0.026967
A_2	0.036964
B_2	0.011011
A_4	0.003634
B_4	0.000268
A_6	-0.001497
B_6	-0.002599

page 167

Add following label for solid line: Fourier Series Curve Fit.